NASA CONTRACTOR REPORT

NASA CR-250

NASA CR-250

MANUAL SPACE NAVIGATION COMPUTER PROGRAM

by W. Blair

Prepared under Contract No. NAS 2-1477 *by*
AMERICAN BOSCH ARMA CORPORATION
Garden City, N. Y.
for

NATIONAL AERONAUTICS AND SPACE ADMINISTRATION • WASHINGTON, D. C. • JULY 1965

NASA CR-250

MANUAL SPACE NAVIGATION COMPUTER STUDY

By W. Blair

Prepared under Contract No. NAS 2-1477 by
AMERICAN BOSCH ARMA CORPORATION
Garden City, N.Y.

for

NATIONAL AERONAUTICS AND SPACE ADMINISTRATION

For sale by the Clearinghouse for Federal Scientific and Technical Information
Springfield, Virginia 22151 – Price $4.00

TABLE OF CONTENTS

LIST OF ILLUSTRATIONS

LIST OF ILLUSTRATIONS (Continued)

ABSTRACT

28778

This report describes and evaluates the design and use of a simple manual space navigation computer. This computer is intended to provide backup guidance capability under abort conditions during an advanced manned space mission.

A design study with an evaluation of the accuracy of the various components used in the computer is presented. A detailed accuracy analysis has been performed by simulation techniques. The overall accuracy of the manual space navigation computer is presented showing the results of the study for various abort trajectories.

Significant relationships between accuracy and the operational usage of the manual computer have been developed.

Author

1. INTRODUCTION

1.1 General

Advanced manned space missions impose ever increasing demands for complexity of the primary navigation and guidance systems such as the need for highly versatile digital computers. This, together with the use of longer duration mission times, imposes perhaps an unrealistically severe reliability requirement on the space navigation and guidance equipment.

One approach to solving this reliability problem is the use of simple and highly reliable backup equipment to supplement the primary navigation system. The philosophy that permits the backup system to be very simple is (1) to make use of manual operations as opposed to more complex automatic techniques and (2) limiting the function of the backup equipment to only what is necessary to achieve recovery of the crew.

The manual space navigation computer which has been studied under this contract incorporates this philosophy. The inputs to the computer are vehicle position data obtained by sextant observations. These are manually obtained and inserted into the computer. The computer determines the "vacuum perigee" of the space vehicle trajectory which establishes whether or not a safe recovery back to earth will be achieved. If the vacuum perigee is outside the allowable "reentry corridor", the computer is then used to determine the corrective maneuver necessary for safe reentry.

1.2 Scope of the Study

The scope of the work performed under this contract and which is presented in this report is as follows:

A design study of the manual computer was performed to arrive at a functional configuration of components and overall design. The components were studied to specify reasonable performance tolerances.

A detailed error analysis program was prepared for high-speed digital computation. Twenty-four cases were examined based upon:

1. The performance capability of the components in the manual computer developed from the design studies.

2. Abort trajectories furnished Arma by Ames Research Center, N.A.S.A.

3. Various locations for taking the space vehicle position data along the abort trajectories.

The error analysis also included the effects of errors in the manual sextant observations and the theoretical errors inherent in the approach used in the computer. The theoretical errors are (1) the two body vs. four body and earth oblateness assumption used in computing the vacuum perigee and (2) the assumption of a parabolic trajectory in computing the corrective maneuver.

The results of the simulations were evaluated to establish the overall accuracy capability of the manual space navigation computer and to generally relate locations along the trajectory where sextant observations are made. All the accuracy results are presented as R.M.S. or 1 σ errors.

1.3 Summary of the Accuracy Analysis Results

The results of the accuracy analysis of the manual space navigation computer are as follows:

1. The overall total error (1 σ) in achieving perigee varies from 16 km for an early abort trajectory ($e = 0.8$) to 35 km for a near parabolic trajectory. These results are based on the following assumptions:

   a. Three sextant observations of position have been obtained. The use of additional redundant, readings should statistically improve the accuracy. However, this has not been included in the analysis.

   b. The first observation is taken shortly after abort or, in the case of a near parabolic abort trajectory, at 260,000 km from the earth.

   c. The corrective maneuver is performed about 1/2 hour before perigee.

   d. The last observation is taken about 1/2 hour before the corrective maneuver.

e. The second or middle observation is taken at a sweep angle roughly halfway between the first and third observation.

2. The accuracy degrades significantly if the first observation is taken later or if the third observation is taken earlier.

3. The major causes of error are instrumentation errors of the manual computer. These contribute about eight times as much error in perigee radius as do the input data errors from the sextant observations.

4. The theoretical errors from the two body assumption in computing perigee and the parabolic assumption in computing the corrective maneuver are much less than the hardware errors.

5. The incremental error contributed from computing the corrective maneuver is less than the error in computing perigee without a maneuver. The total error with a maneuver is generally only slightly greater than the error without a maneuver.

1.4 Organization of the Report

The balance of this report is organized as follows:

Section 2 gives the theory of operation of the manual space navigation computer, its role as a backup computer during an abort condition and the operational usage of the computer to achieve a safe reentry.

Section 3 presents the design approach developed under the study. The expected accuracy capabilities of the various components used in this configuration are indicated and form the basis for the specific design features which have been adopted.

Section 4 describes in detail the method of analysis used to perform a complete overall accuracy analysis of the manual computer. A special computational program for the IBM 7094 using Fortran II was developed for this purpose.

Section 5 presents the results of the accuracy analysis performed on the IBM 7094 computer. There are 24 tables of data, each table being a complete error breakdown for a particular case of using the manual computer.

Four abort trajectories provided by Ames, N. A. S. A. were used and with each trajectory various sets of observational data were chosen.

Section 6 is a discussion of the results of the accuracy analysis. The results are evaluated to arrive at the overall capability of the manual space navigation computer. In addition, the general relationships between the location of the observation points and accuracy have been established.

The actual Fortran II statement used to perform the accuracy analysis is given in the Appendix at the end of the report.

2. THEORY OF OPERATION AND FUNCTIONAL APPROACH

2.1 Theoretical Basis of the Data Processing Computer

For operation of this manual space navigation computer, it is assumed that suitable observation data from an Astro-Sextant or an equivalent instrument is available. The basic purposes of the space navigation data processing computer are the following:

... To enable the operator to predict future points on the vehicle trajectory on the basis of observed sextant observations.

... To enable the operator to predict whether a safe reentry will be accomplished if the vehicle continues on its present trajectory.

... To enable the operator to determine the required corrective maneuver, if necessary, to insure safe reentry.

The theoretical approach utilizes a single mathematical equation as the basis for satisfying all the above requirements. Thus, the data processing computer only requires the capability of solving this single equation.

The rigorous mathematical theory of space vehicle trajectories must take into account earth oblateness as well as the gravitational effect on the vehicle of the moon and sun. However, for earth-moon trajectories these effects are small compared with the basic inverse-square gravitational field of the earth. Therefore, the theoretical approach makes the two following simplifying assumptions:

... It is assumed that only the earth exerts a gravitational pull on the vehicle (i. e. the gravitational effects of the moon and sun are ignored.)

... It is assumed that the earth is spherical (i. e. earth oblateness effects are ignored).

Once these assumptions have been made, all of the theory associated with Kepler trajectories can be applied. These trajectories can be represented by the following equation: (See Figure 2-1)

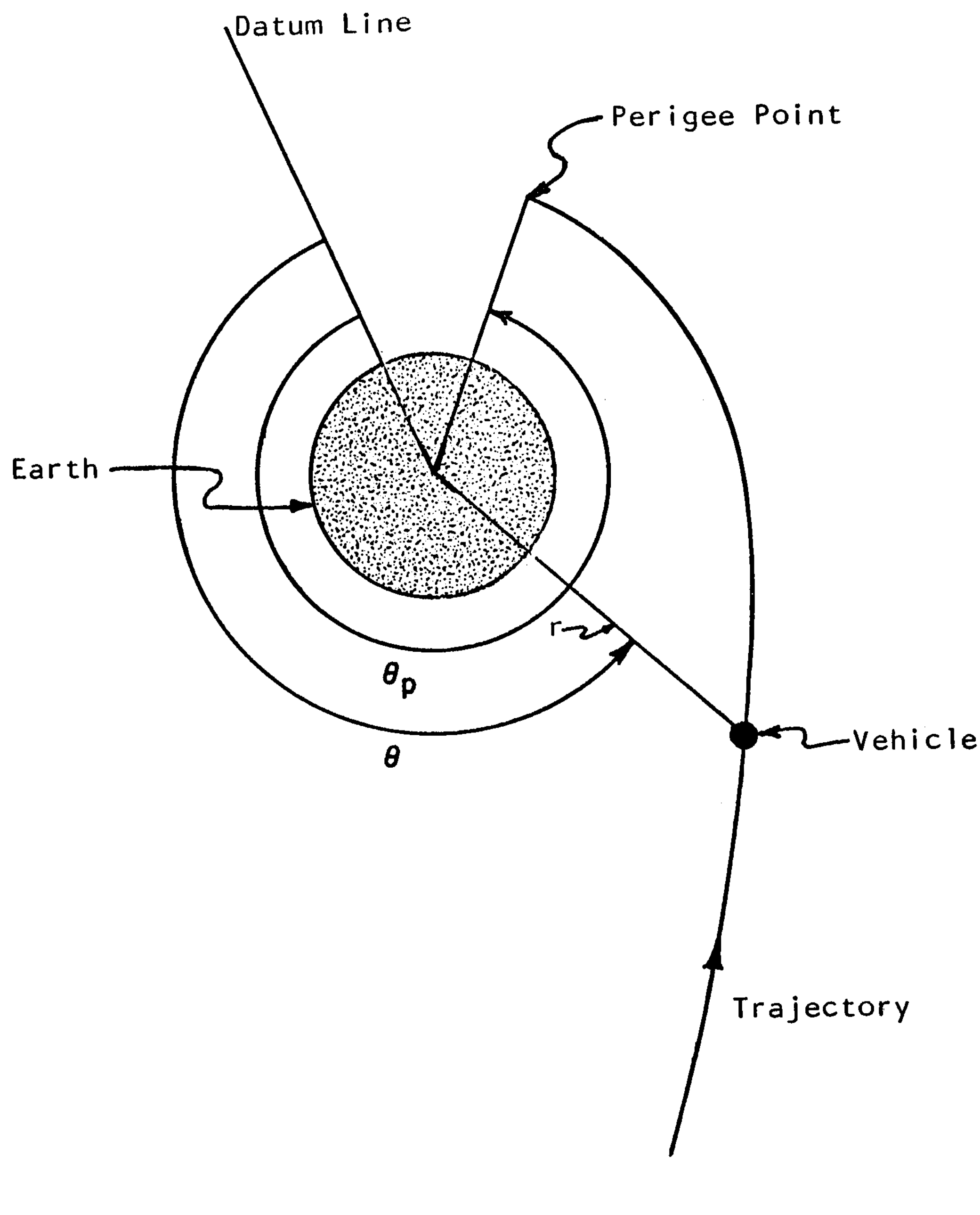

FIGURE 2-1 TYPICAL SPACE VEHICLE TRAJECTORY

$$r = \frac{h^2}{\mu} \left(\frac{1}{1 + e \cos(\theta - \theta_p)} \right) = \frac{\ell}{1 + e \cos(\theta - \theta_p)} \qquad \text{(II-1)}$$

where:

θ_p = the angle from an arbitrary datum line to the perigee point

θ = the angle from the arbitrary datum line to the space vehicle

r = the distance from the space vehicle to the center of the earth

$\ell = \frac{h^2}{\mu}$ = the semi-latus rectum

h = the specific angular momentum of the vehicle

μ = the gravitational constant of the earth

e = the eccentricity of the orbit

where if:

$e > 1$, trajectory is hyperbolic,

$e = 1$, trajectory is parabolic,

$e < 1$, trajectory is elliptical.

The quantities ℓ, h, μ and e are all constants on a Kepler trajectory.

Equation II-1 can be rewritten

$$\frac{\dfrac{1 + e \cos(\theta - \theta_p)}{\ell}}{\dfrac{1}{r}} = 1 \qquad \text{(II-2)}$$

Then, in general, for any one conic

$$\frac{1 + e \cos(\theta_3 - \theta_p)}{\dfrac{1}{r_3}} = \frac{1 + e \cos(\theta_2 - \theta_p)}{\dfrac{1}{r_2}} = \frac{1 + e \cos(\theta_1 - \theta_p)}{\dfrac{1}{r_1}} \qquad \text{(II-3)}$$

where r_1, θ_1, r_2, θ_2, r_3, θ_3 are the coordinates of three points on the trajectory.

CR-250

From proportion theory:

$$\frac{a}{b} = \frac{c}{d} = \frac{e}{f} = \frac{a-e}{b-f} = \frac{c-e}{d-f}$$

Therefore

$$\frac{1 + \varepsilon\cos(\theta_3-\theta_p) - 1 - \varepsilon\cos(\theta_1-\theta_p)}{\frac{1}{r_3} - \frac{1}{r_1}} = \frac{1 + \varepsilon\cos(\theta_2-\theta_p) - 1 - \varepsilon\cos(\theta_1-\theta_p)}{\frac{1}{r_2} - \frac{1}{r_1}} \qquad \text{(II-4)}$$

or

$$\frac{\cos(\theta_3 - \theta_p) - \cos(\theta_1 - \theta_p)}{\frac{1}{r_3} - \frac{1}{r_1}} = \frac{\cos(\theta_2 - \theta_p) - \cos(\theta_1 - \theta_p)}{\frac{1}{r_2} - \frac{1}{r_1}} \qquad \text{(II-4)}$$

where:

$\theta_{1,\ 2,\ 3}$ = Observed geocentric angles between the vehicle and a reference star in the plane of the vehicle's trajectory.

$r_{1,\ 2,\ 3}$ = Stadiametrically derived distances between the vehicle and the earth's center, corresponding to the angles $\theta_{1, 2, 3}$.

θ_p = Geocentric angle between the reference star and perigee point of the present trajectory.

2.2 Functional Description of the Computer

A block diagram of the computer which solves equation (II-4) is shown on Figure 2.-2. Seven quantities are involved in the equation, and the computer contains a control knob and counter for each. If any six of these are set into the computer (by means of handcranks and counters) the seventh can be found by rotating the corresponding crank until the bridge is balanced, as indicated by a zero reading on the "NULL INDICATOR". The associated counter is then read to find the value of the unknown quantity which satisfies equation (II-4).

Internally, motion of any handcrank drives the associated counter through appropriate gearing and provides one input to a mechanical differential. (Light frictional drags are placed on all input shafts to keep the motion of any

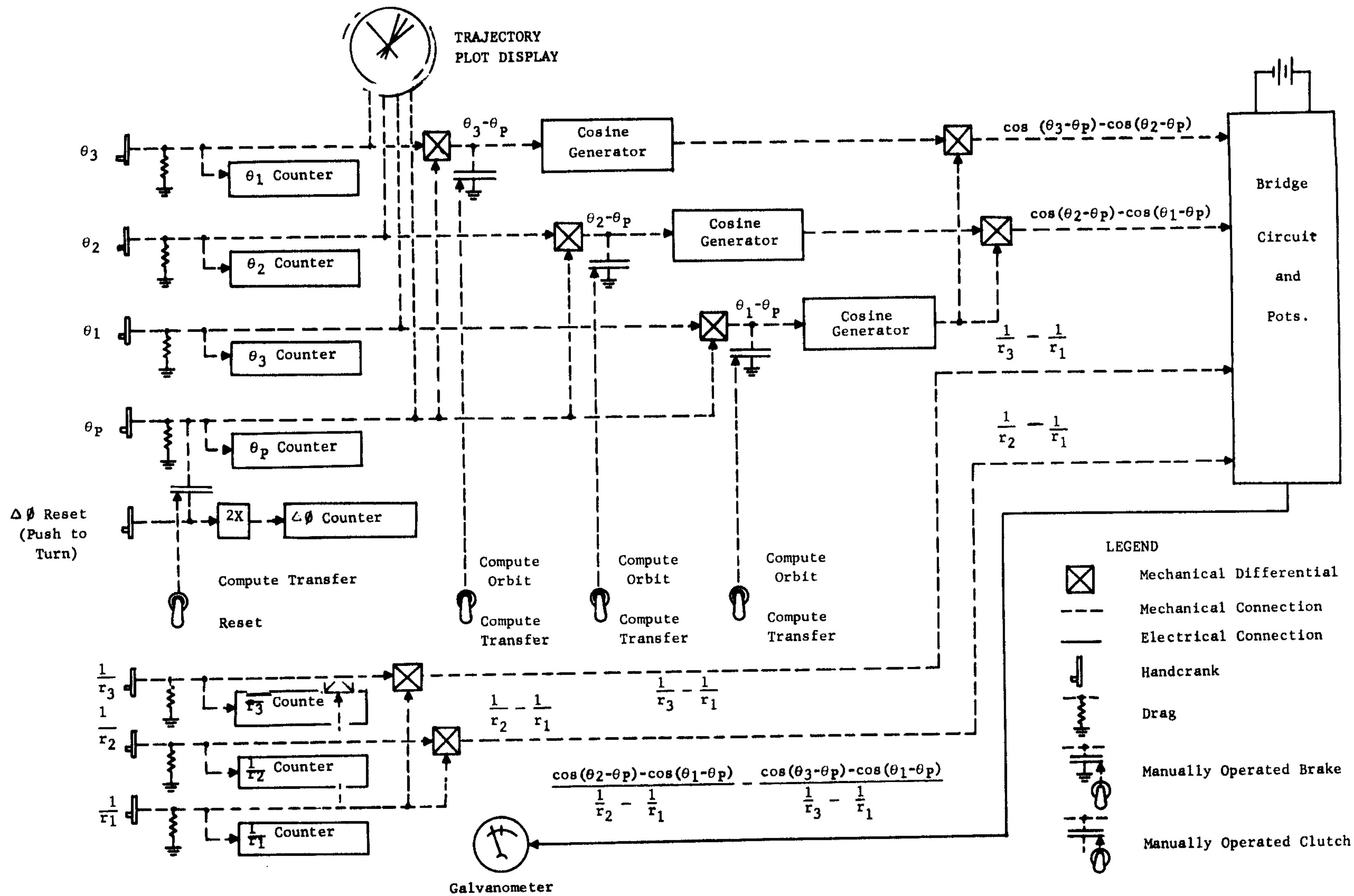

FIGURE 2-2.- COMPUTER FUNCTIONAL BLOCK DIAGRAM.

one from rotating any of the others through the differentials.) As shown in Figure 2-2, the outputs of the differentials are: $(\theta_3 - \theta_p)$, $(\theta_2 - \theta_p)$, $(\theta_1 - \theta_p)$, $\left(\frac{1}{r_3} - \frac{1}{r_1}\right)$ and $\left(\frac{1}{r_2} - \frac{1}{r_1}\right)$. The output shafts of the angle differentials are then used to drive mechanical cosine generators whose output shafts are, in turn, used as inputs to mechanical differentials. There are, finally, four shaft positions, representing the quantities:

(1) $\cos(\theta_3 - \theta_p) - \cos(\theta_1 - \theta_p)$

(2) $\cos(\theta_2 - \theta_p) - \cos(\theta_1 - \theta_p)$

(3) $\left(\frac{1}{r_3} - \frac{1}{r_1}\right)$

(4) $\left(\frac{1}{r_2} - \frac{1}{r_1}\right)$

These are the numerators and denominators of the left and right sides of equation (II-4), and are the inputs to the electrical portion of the computer. Specifically, these shaft angles position the wipers of four potentiometers arranged in a modified bridge circuit. The output of this circuit is proportional to the difference between the two sides of equation (II-4). When this quantity is zero (as indicated by the galvanometer), the equation is satisfied; i.e. the "unknown" quantity has been adjusted to correspond to the trajectory parameters which were set into the other six inputs.

In addition, the computer incorporates a manually operated roller chart which is simply a form of table giving the relationship between the observed angle subtended by the earth's disk and the corresponding range and reciprocal range. The mechanism consists of a long tape with corresponding values of variables printed on it side by side (somewhat in the manner of the scales on the body of a slide rule), a pair of drums to receive the tape, and a knurled wheel to drive it. In use, the operator simply rotates the knob until the correct value of the known variable (say, subtense angle) is under the hairline. The corresponding values of the range and its reciprocal also appear under the hairline and are read out directly.

2.3 Operational Usage of the Computer

The manual space navigation computer performs four functions as follows:

... Assistance in the determination of present vehicle position

... Prediction of future vehicle position

... Determination of whether reentry will be accomplished safely if vehicle continues on present trajectory

... Determination of corrective maneuver, if necessary, to assure that safe reentry will occur.

The present position of the vehicle will be specified in terms of distance from earth (r) and vehicle angular position (θ) measured in the plane of the trajectory from a known datum line through the center of the earth. Figure (2-3) illustrates the method by which the coordinates r and θ are determined. The known datum line is taken as the line from the center of the earth to a reference star in the plane of the trajectory. The angles A and B are measured with the sextant. A is the angle from the reference star to the edge of the earth's disk. B is the angle subtended by the disk of the earth. Knowing the angle B, the operator easily determines the distance r by use of the roller chart. The angle θ is determined by

$$\theta = 180 - \left(A \pm \frac{B}{2}\right) \qquad \text{(II-5)}$$

The choice of sign in Equation (II-5) is governed by whether A is measured to the near or far edge of the earth.

One of the important applications of the proposed manually operated computer is to predict future points along the vehicle's trajectory on the basis of present position. The basis of the method (see Figure 2-4) is the use of three present position fixes. The entire position prediction problem is solved through using the expression (Equation (II-4)) which is mechanized in the manual computer. Future position prediction is accomplished as follows:

The angles θ_1, θ_2, θ_3 corresponding to the three present position fixes, are manually set into the corresponding counters on the face of the computer (Figure 2-5). The three observed ranges r_1, r_2, r_3 are converted to corresponding reciprocal ranges by use of the roller chart. These reciprocal ranges are set into the appropriate counters. Every quantity entering the basic equation (II-4) has now been set into the computer, except for the perigee angle, θ_p. Therefore, the angular position of the perigee point can be found by turning the perigee angle crank until the null meter indicates zero. The angular position of the perigee point can be now read from the appropriate counter. To

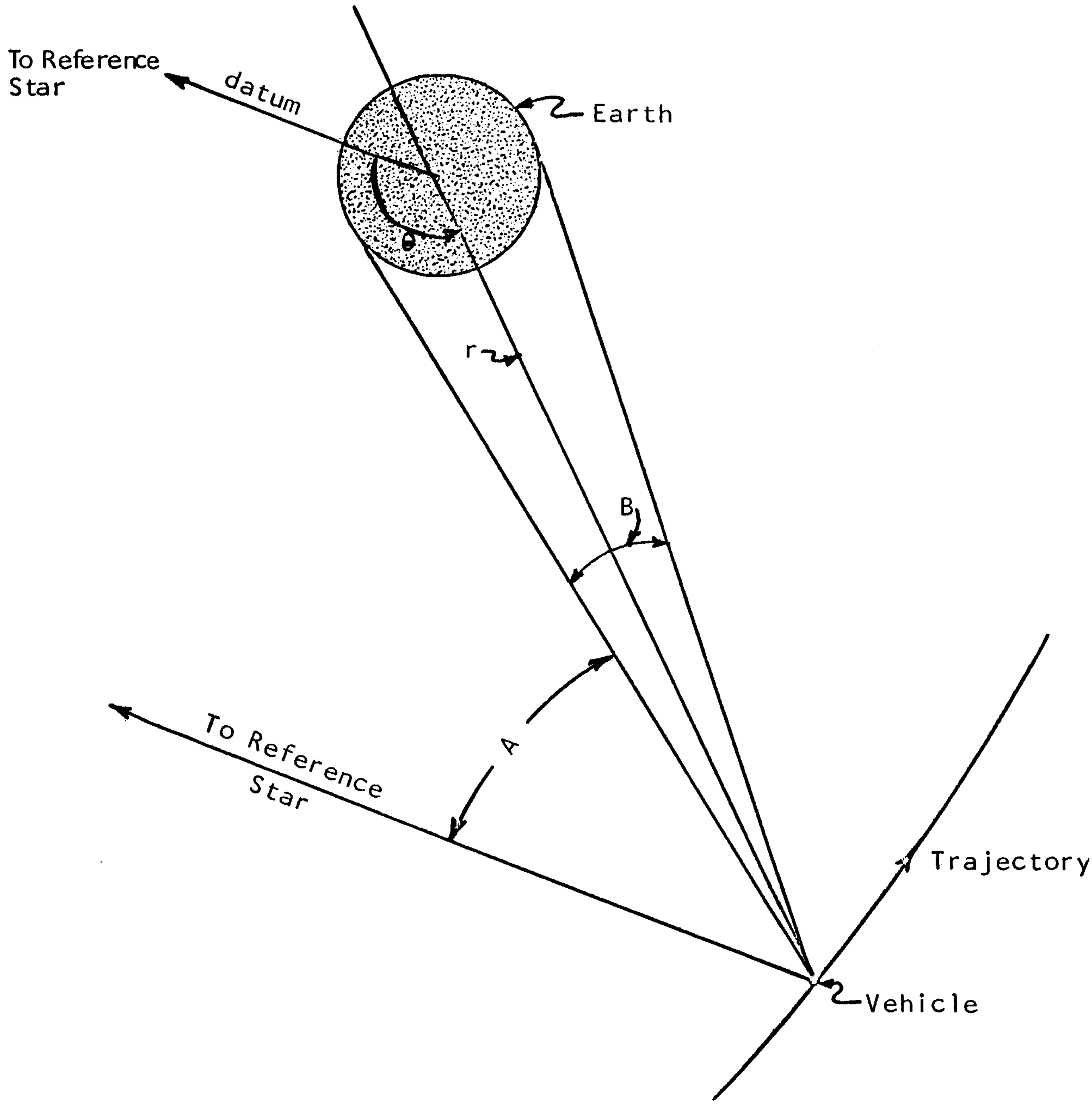

FIGURE 2-3 METHOD OF FIXING PRESENT VEHICLE POSITION

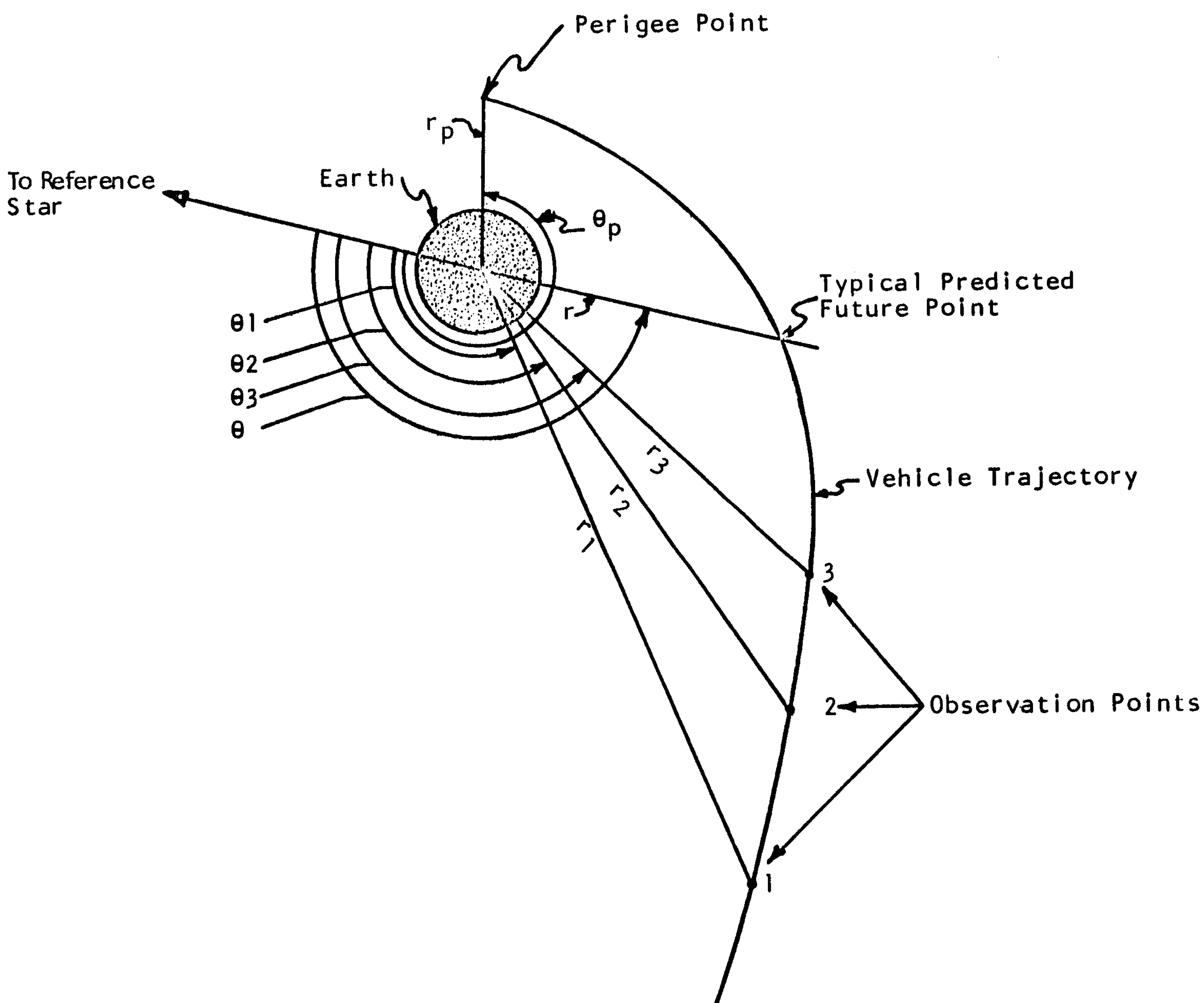

FIGURE 2-4 PROPOSED METHOD OF PREDICTING FUTURE POINTS ALONG THE VEHICLE TRAJECTORY

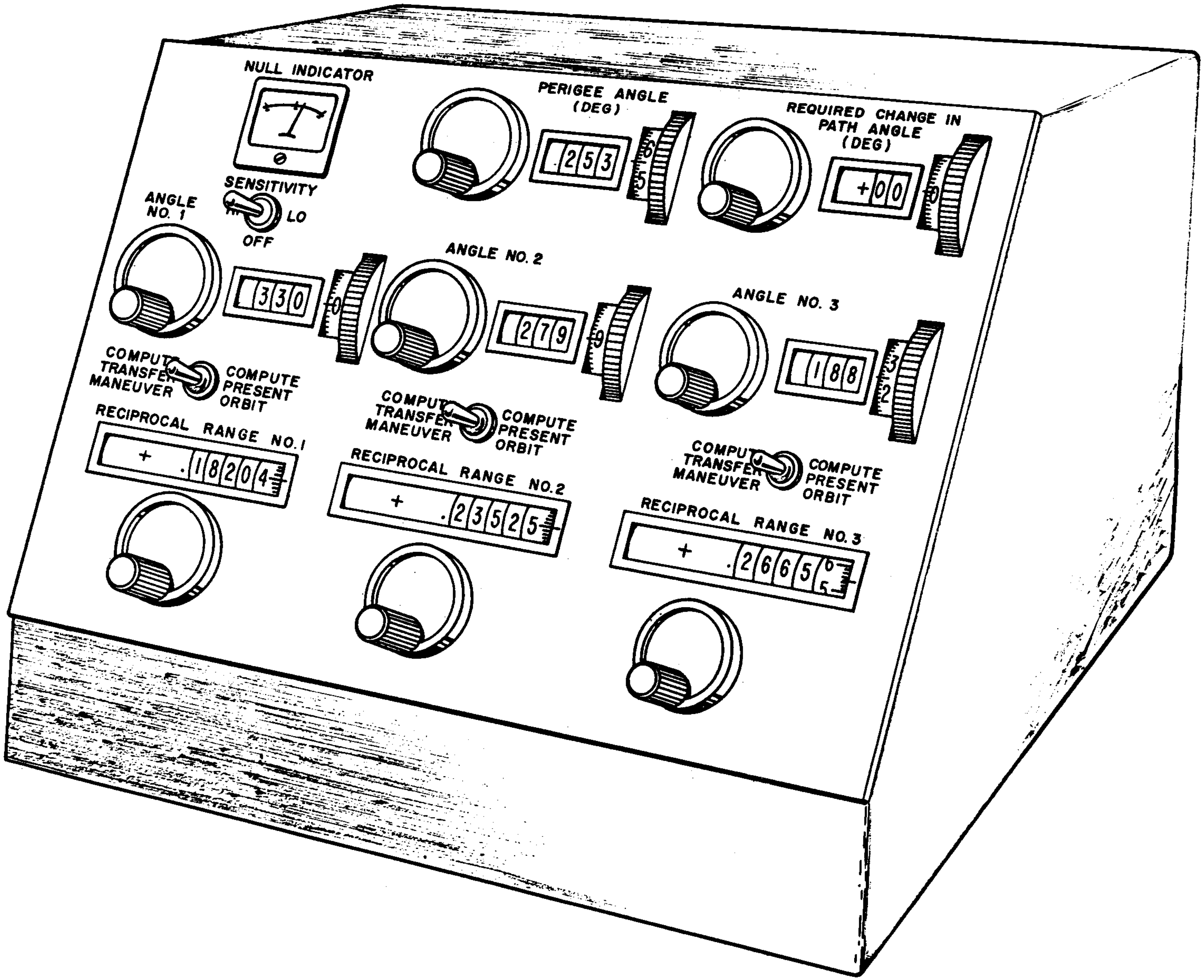

FIGURE 2-5 MANUAL SPACE COMPUTER PACKAGE (Preliminary)

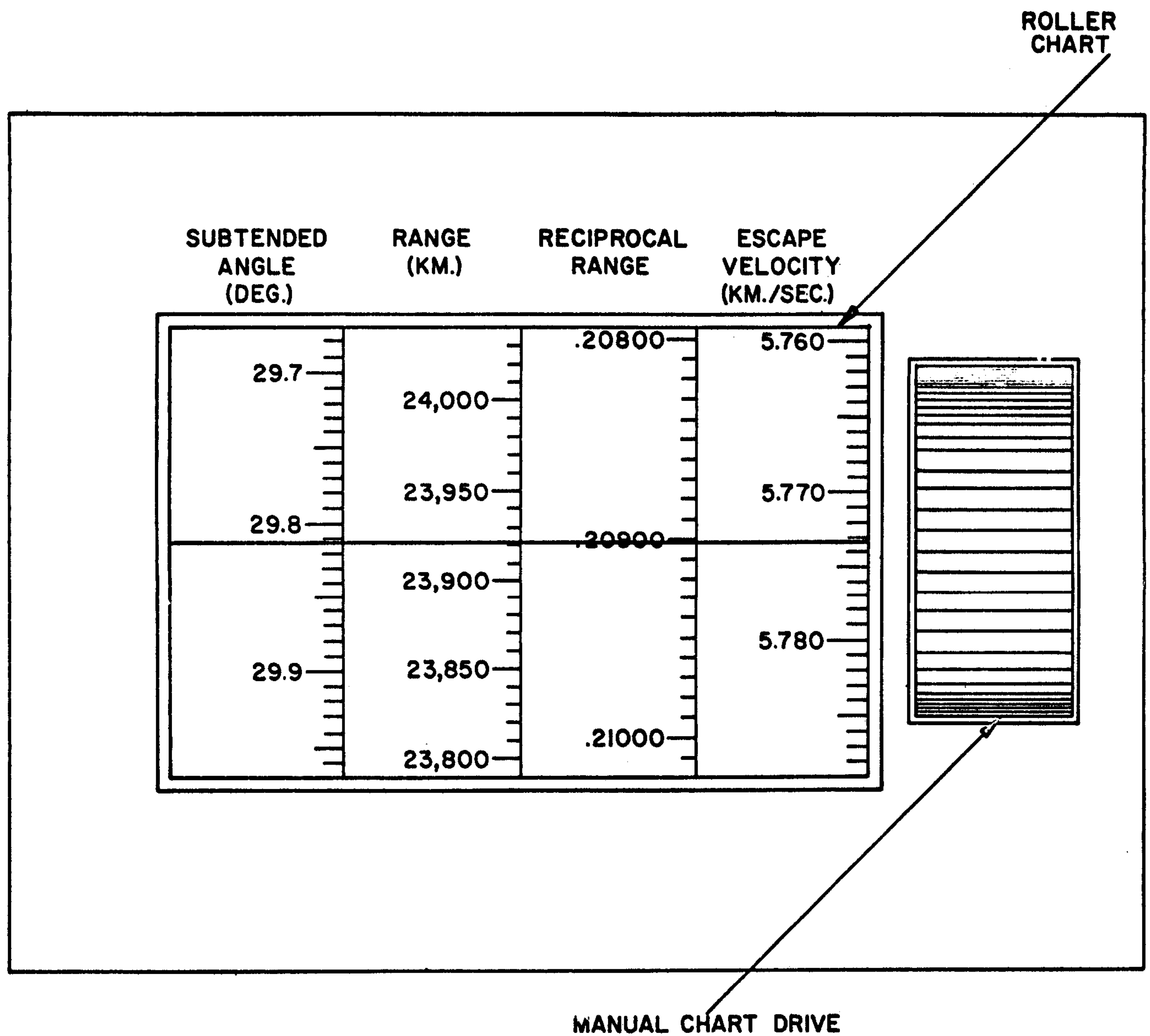

FIGURE 2-6 - ROLLER CHART

predict where the vehicle will be when it reaches some distance, r, from earth, (indicated as "typical predicted future point" on Figure 2-4), the reciprocal range corresponding to r is set in on the "reciprocal range No. 3" counter. This causes the bridge to become unbalanced. The bridge is rebalanced by turning the "angle No. 3" handcrank until the null meter once again reads zero. The angular position of the vehicle at the predicted point is then read from the "angle No. 3" counter.

An extremely important application of the proposed system is to determine whether the vehicle will reenter the earth's atmosphere safely if it is allowed to continue on its present trajectory. Insuring safe reentry is particularly important on deep space missions, since in this case too steep a reentry angle will cause the vehicle to burn up in the atmosphere, and too shallow a reentry angle will cause the vehicle to skip back into outer space.

It is convenient, in performing reentry analysis, to employ the concept "vacuum perigee", which is equivalent in significance to reentry path angle. When the vehicle enters the atmosphere the aerodynamic forces cause the vehicle to follow a trajectory which cannot any longer be described in terms of Keplerian theory. Conceptually, however, one can consider what would happen if there were no atmosphere. In that case the vehicle would continue on a Kepler trajectory and would reach a certain perigee distance from the center of the earth; i. e. a "vacuum perigee". Clearly, reentry path angle is related to vacuum perigee, since a steeper reentry path angle will result in a smaller vacuum perigee distance. Thus, a certain allowable spread in reentry path angle is equivalent to an allowable spread in vacuum perigee. The allowable spread in vacuum perigee is referred to as the safe reentry corridor. On a space mission the limits of the safe reentry corridor will be known in advance. The basic method of using the computer to ascertain whether reentry will be safe is to predict the vacuum perigee, and see whether it lies within the limits of the safe reentry corridor.

This is accomplished as follows: Three position fixes are obtained. The resulting angles and reciprocal ranges (as determined from the roller chart on the computer) are inserted manually into the appropriate counters in the computer. Next, the angular position of perigee is determined by turning the perigee crank until the null meter reads zero. The "angle No. 3" crank is turned until the "angle No. 3" counter shows the same reading as the "perigee angle" counter. This will cause the bridge to become unbalanced. The "reciprocal range No. 3" crank is now turned until the bridge is once again balanced, as indicated by a zero reading of the null indicator. The value read from "reciprocal range No. 3" counter is converted to range in kilometers by using the roller chart. This value of range is the vacuum perigee distance. Since the operator knows the allowable limits of the safe reentry corridor, he immediately can tell whether or not a safe reentry will occur.

If the above procedure leads to the conclusion that the vehicle will not reenter safely, then it is necessary that the proposed system be capable of determining a corrective maneuver which will modify the trajectory so that safe reentry will occur. The basic problem is illustrated in Figure 2-7. The vehicle is shown on a present trajectory which will result in an unsafe reentry because the vacuum perigee falls below the safe reentry corridor (i.e., the vehicle would burn up in the atmosphere). It is desired to find the direction and magnitude of the incremental velocity, Δv, which should be inserted during a corrective maneuver.

In executing a maneuver to correct vacuum perigee there is always an optimum direction in which thrust should be applied to minimize rocket fuel expenditure. In general, this optimum maneuver causes both the magnitude and the direction of the velocity vector to change. However, determination of this truly optimum maneuver would complicate the computational requirements to an extent which would be incompatible with equipment simplicity. Therefore, a compromise has been adopted which insures accomplishment of the desired corrective maneuver with a reasonable (although not truly minimized) expenditure of fuel. This has been achieved by assuming that the corrective maneuver incremental velocity, Δv, will always be inserted perpendicular to the present velocity v, and will thus produce a pure direction change, with no change in magnitude. This is the situation pictured in Figure 2.7. Thus the required corrective maneuver can be expressed completely as a required change, $\Delta\phi$, in the flight path angle.

Furthermore, from Keplerian orbit theory, if two orbits have equal major axes (as shown in Figure 2.-8) then their specific energies are equal. Thus, for example, if a maneuver changes the perigee distance by +10 miles leaving specific energy constant (i.e., not changing velocity magnitude) then the apogee distance changes by -10 miles.

The above considerations are all quite clear for elliptic orbits, since the apogee distance has a clear physical significance. One can, however, always mathematically define an apogee distance, even for non-elliptic orbits, being zero for a parabola and negative for hyperbolic trajectories. The significance of this generalized definition of apogee distance is that the relationship discussed in connection with Figure 2-8, (namely that the sum of the $r_{perigee}$ and r_{apogee} remain the same after a maneuver) can be shown to be valid for all Keplerian orbits.

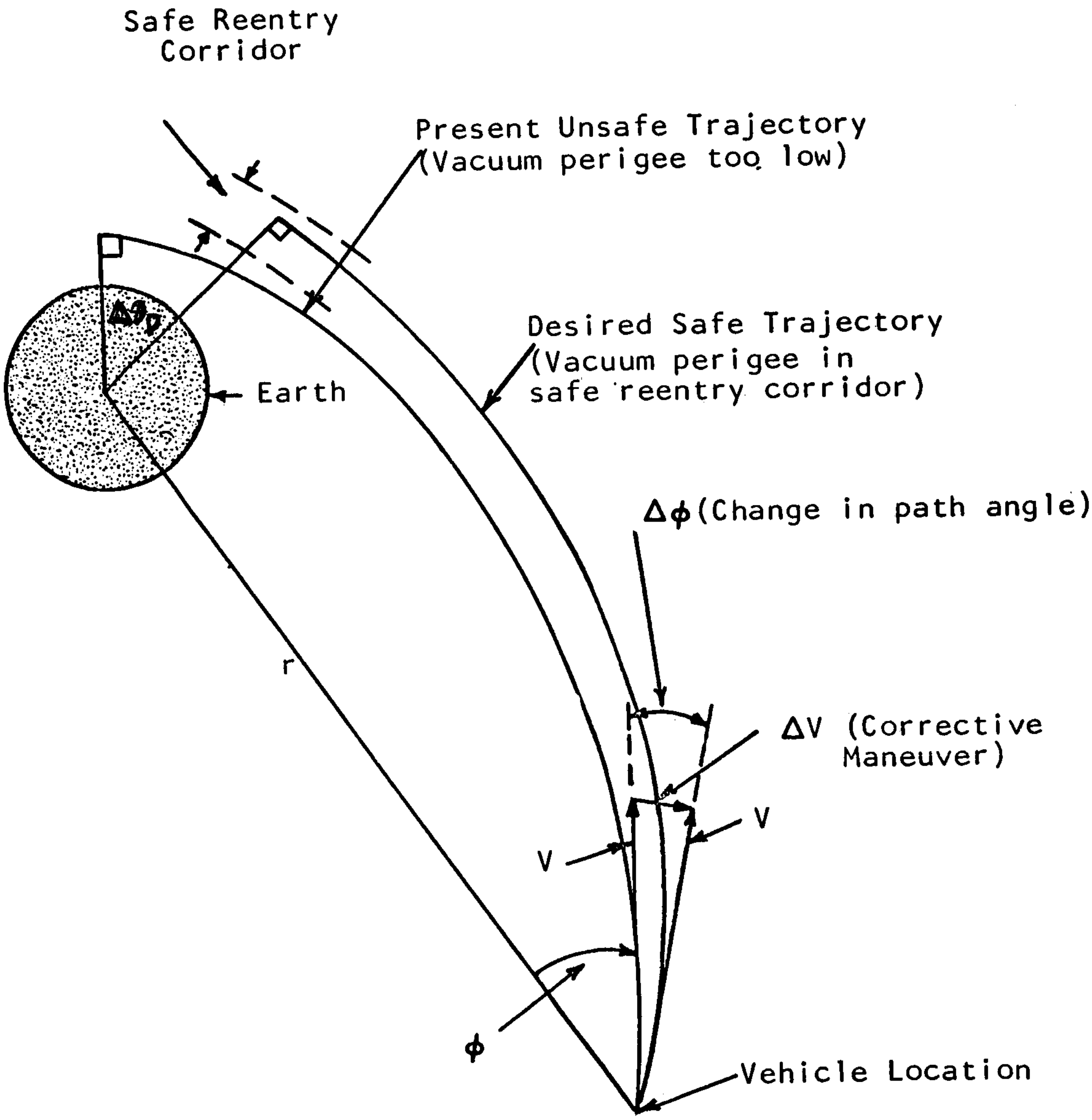

FIGURE 2-7 INSERTION OF CORRECTIVE MANEUVER TO INSURE SAFE REENTRY

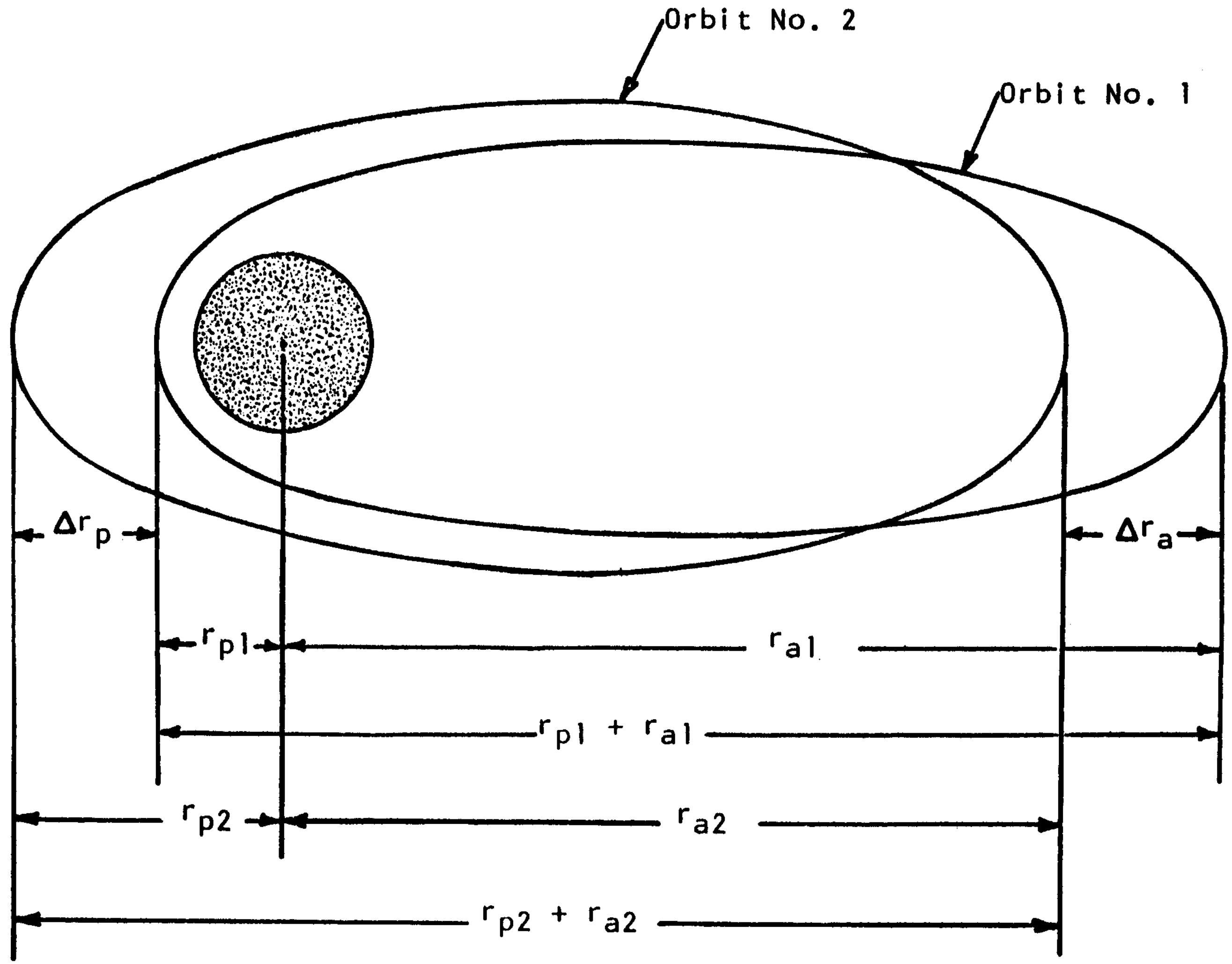

$$r_{p1} + r_{a1} = r_{p2} + r_{a2}$$

since

$$\Delta r_p = \Delta r_a$$

FIGURE 2-8 TWO ORBITS HAVING EQUAL SPECIFIC ENERGY

Before proceeding to the actual operation of the computer in determining corrective maneuvers, it is necessary to discuss one other assumption which is made. It is assumed, in computing corrective maneuvers, that on deep space missions, the vehicle will reenter at a velocity very close to escape velocity which is equivalent to assuming that the vehicle is on a parabolic orbit. It should be stressed that this parabolic assumption is used only for determining corrective maneuvers, and not in computing the vehicle's trajectory. Figure 2-9 illustrates why the parabolic assumption leads to system concept simplification. From geometry and the properties of a parabola it can be seen that the path angle, ϕ, is given by

$$\phi = \frac{(\theta - \theta_p) - 180}{2} \qquad \text{(II-6)}$$

Therefore at vehicle angular position, θ, if a maneuver results in a new trajectory whose perigee angular position differs by $\Delta\theta_p$ from the original perigee angular position, then the maneuver will have a path angle change $\Delta\phi$ given by

$$\Delta\phi = \frac{\Delta\theta_p}{2} \qquad \text{(II-7)}$$

This is an extremely important result, since it says that the required path angle change is determined by simply knowing the angular shift in the perigee which results from changing trajectories via a corrective maneuver of the type being considered.

Having established the above theoretical background we can now proceed to the operational steps required when using the proposed computer to determine a corrective maneuver which will assure safe reentry.

1. The vehicle's present trajectory in the form of three sets of positional fix data is cranked into the appropriate counters and the bridge is balanced by turning the "perigee angle" crank until the null meter reads zero.

2. Next, the perigee distance of the present trajectory is determined. This is accomplished using the "No. 3" input cranks. The "angle No. counter is set so that it reads the same as the "perigee angle" counter. Then the "reciprocal range No. 3" crank is turned until the bridge is balanced. The reading of the "reciprocal range No. 3" crank is converted to range in kilometers through the use of the roller chart. This gives the vacuum perigee of the present

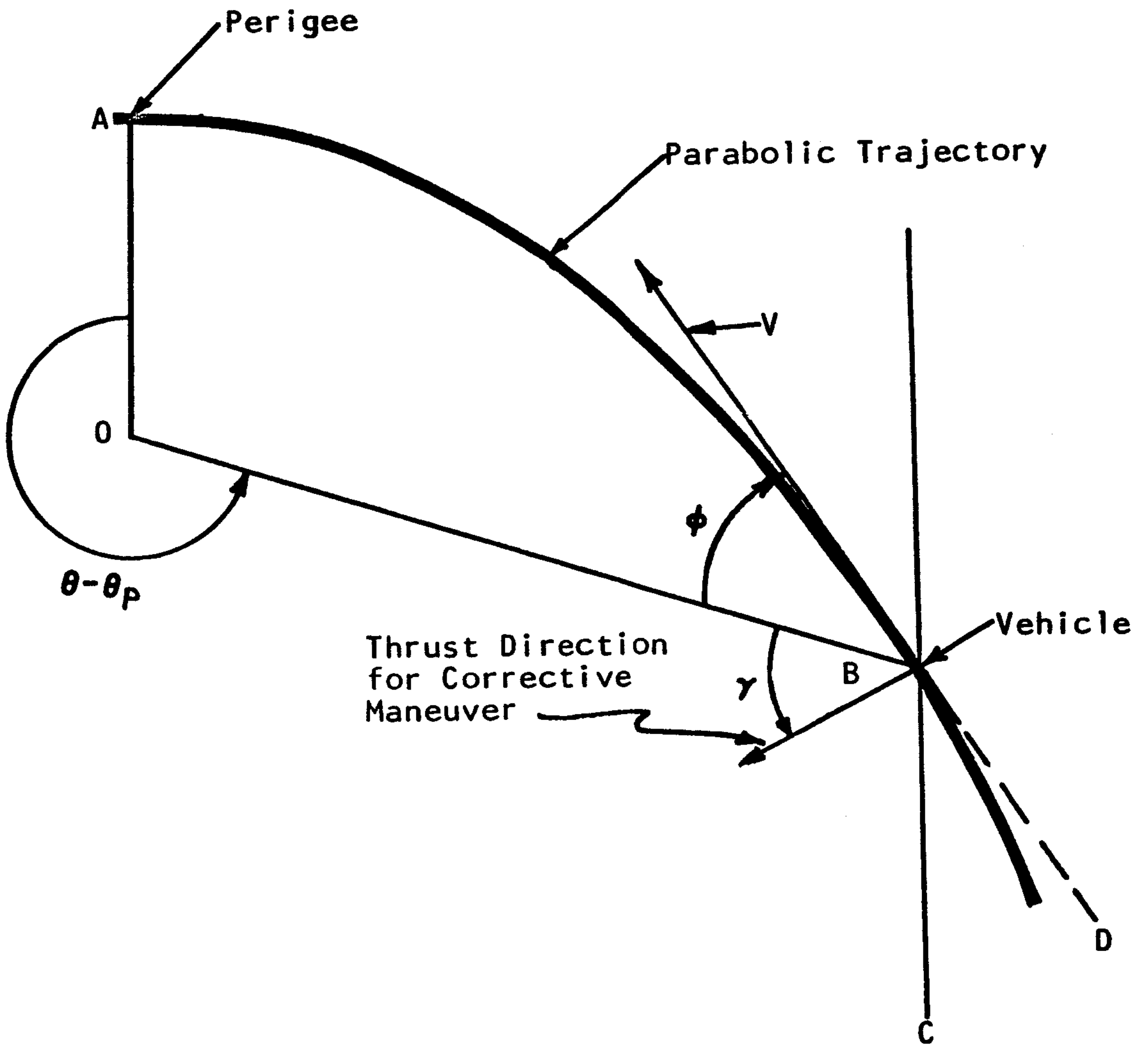

FIGURE 2-9 PARABOLIC TRAJECTORY

trajectory. If it does not fall within the safe reentry corridor, the operator notes this value of vacuum perigee (since it will be needed later in the procedure).

3. The next step is to set in information concerning the point at which the maneuver is to be made. The "No. 2" inputs are used for this purpose. The operator decides on the range distance from earth at which the corrective maneuver is to be made. Through the use of the roller chart this range is converted to reciprocal range and inserted into the "reciprocal range No. 2" counter. This unbalances the bridge. The bridge is rebalanced by turning the "angle No. 2" crank until the bridge is balanced, as indicated by a zero reading on the null indicating meter. The angle reading on the "angle No. 2" counter is then the predicted angular position of the vehicle when it reaches the point at which the maneuver is to be made.

4. The next step is to determine the apogee of the present trajectory. This is done using the No. 1 input cranks. The "angle No. 1" counter is set so that its reading differs by 180 degrees from the "perigee angle" counter. This unbalances the bridge. The bridge is rebalanced by turning the "reciprocal range No. 1" counter. The reading of the "reciprocal range No. 1" counter, converted to range distance in Kms. via the roller chart, is the apogee distance of the present trajectory. It can be either positive or negative depending on whether theorbit is elliptical or hyperbolic as was discussed earlier.

5. The next step is to set in the perigee of the new, desired trajectory. This is accomplished by setting "reciprocal range No. 3" counter to the reciprocal range which corresponds to the new, desired vacuum perigee (usually selected to be in the center of the safe reentry corridor). This operation unbalances the bridge, which now remains unbalanced until the final step in the procedure.

6. The next step is to set in the apogee of the new, desired trajectory. The new apogee distance is determined by algebraically adding to the old apogee distance an amount equal and opposite to the difference between new and old perigee distances. (This is in accordance with our earlier discussion concerning the constancy of apogee plus perigee distance in the face of a maneuver which leaves velocity magnitude unchanged). The reciprocal range corresponding to the new apogee distance is set into the "reciprocal range No. 1" counter.

7. The next step computes the required change in path angle. This operation makes use of the result discussed in connection with equation (II-7). The new trajectory will have a new perigee angular position, and the change in perigee angular position is twice the required change in path angle. (This is the reason for the 2:1 gear ratio interposed between the θ_p shaft and the $\Delta\phi$

counter shown in Figure 2-2). The "angle No. 1" and "angle No. 3" shaft locks are set to the "compute transfer maneuver" position. This locks the outputs of the corresponding differentials shown in Figure 2-2. The "required change in path angle" crank is turned until the bridge is balanced, and the required change in path angle is read from the "required change in path angle" counter. The magnitude of the required incremental velocity is determined by

$$\Delta V = V\Delta\phi \qquad \text{(II-8)}$$

where the symbols are defined with the aid of Figure 2. 7. The value of V to be used in equation (II-8) is known on the basis of the previously discussed parabolic assumption, since V is the parabolic velocity corresponding to the range distance at which the maneuver is made, and therefore can be tabulated in advance. In fact, this information could be included on the roller chart, as shown in Figure 2-6.

8. In addition to knowing the magnitude, v, of the required incremental velocity, it is also necessary to know its direction, since the vehicle thrust vector must be oriented in this direction to properly execute the maneuver. Since the maneuver is to produce a path angle change only, with no change in velocity magnitude, it is clear that the thrust must be directed perpendicular to the velocity vector. Therefore, as is evident from Figure 2-9, the angle, γ, which the vehicle thrust vector makes with the local vertical is given by

$$\gamma = 90 - \phi \qquad \text{(II-9)}$$

which, combined with equation (II-6) yields

$$\gamma = \frac{\theta_p - \theta}{2} \qquad \text{(II-10)}$$

The value of θ (the angular position of the vehicle with respect to the reference star at the predicted maneuver point) is read from the "angle No. 2" counter, and the value of θ_p is read from the "perigee angle" counter. (It would be possible to read γ directly from a counter geared 2:1 with the output of the θ_2 differential in Figure 2-2 although this feature is not shown).

3. DESIGN STUDY AND COMPONENT CAPABILITY

3.1 Summary of Technical Philosophy and Guidelines

The technical philosophy and guidelines governing the design of the manual computer, in summary, are given below.

The proposed manual system will be used for monitoring failures of the more complex primary system, and for performing navigation and guidance on an independent basis.

Hardware ground rules place primary emphasis on manual operation. These rules call for minimization of electric power consumption, use of self-contained unregulated DC where mandatory, and the exclusion of electronic equipment, servos, motor drives, and automatic readout techniques to insure maximum simplicity and reliability.

It is important to recognize that formulation of a system concept which is consistent with the above mentioned simple "hardware ground rules" compels one to pay the price of compromising system flexibility, accuracy, etc. compared with what is achievable with a more complex, less reliable primary navigation and guidance system.

In spite of the above mentioned simple "hardware ground rules" and operational limitations, it is nevertheless mandatory that certain operational requirements be met by the proposed manual system. These include fixing present position, predicting future position, predicting whether safe reentry will be accomplished, determining corrective maneuvers (when necessary) to assure safe reentry.

3.2 Computer Design Considerations

The guiding principles in the design of the data processing system are maximum reliability and minimum power requirements, size and weight consistent with the accuracy required. The design proposed uses a combination of highly accurate manually driven mechanical and electrical computing elements, and a low-voltage, unregulated D.C. source, such as a small dry cell, with linear potentiometers. The circuit is so arranged that the total resistances of these elements need only be nominally correct. No transistors, vacuum tubes, servo motors or other active elements are used anywhere in the computer.

3.3 Description of Computing Elements

The initial design of the proposed system using manually driven mechanical and electrical computing elements, energized by a small self-contained battery source, is shown in Figure 3-1. The packaged unit is illustrated in Figure 2-5.

The Θ input angles are introduced at 72 speed (5 deg/rev.), 0 to 360 degrees of continuous rotation by means of 3 inch crank wheels which permit the operator to spin set the inputs close to the observed values. A thumb wheel and dial is provided to improve input accuracy. Readout is accomplished by means of the counters and thumbwheel dials. Verniers may be installed if extreme accuracy is required. The $\Delta\phi$ counter covers the range -20 to +20 degrees and is equipped with a flagged shutter to indicate sign. It also has a thumbwheel and (±) dials to improve accuracy.

The 1/r counters are zero centered and have a similar flagged shutter to indicate sign. These cover a range of +.99999 to -.99999, although only a small part of the negative range is actually utilized, as explained below. The numbers indicated are not actually the reciprocal of range but, rather, r_{min}/r, the radius of the minimum instrumented range divided by the range observed or computed. This presentation seems preferable since the quantity 1/r itself would contain a minimum of three zeros between the decimal point and the first significant digit. It is felt that this could be a source of confusion to the operator. The value of r_{min} chosen for instrumentation is determined by the earth's radius minus a sufficient allowance to: (1) accommodate computation of initial trajectories which would perigee in the earth, and (2) a sufficient allowance for the phase angle adjustment (to be explained later). In any case r_{min} is selected to cover any possible operational case, plus a margin of safety.

Since the only time a negative range will be encountered is upon computation of radius of apogee for hyperbolic orbits, only a small portion of the 1/r negative range need be instrumented. This lower limit will be determined essentially by the magnitude of eccentricities considered possible for slightly hyperbolic orbits. Limits on the 1/r inputs will be established accordingly by means of mechanical stops.

The Θ and 1/r differentials will be commercial miniature precision types run at high speed to minimize error. Precision 3 or anti-backlash gearing will be utilized at the low speed inputs to the cosine generators, potentiomete and range rheostats since sensitivity to error is obviously greater at these point

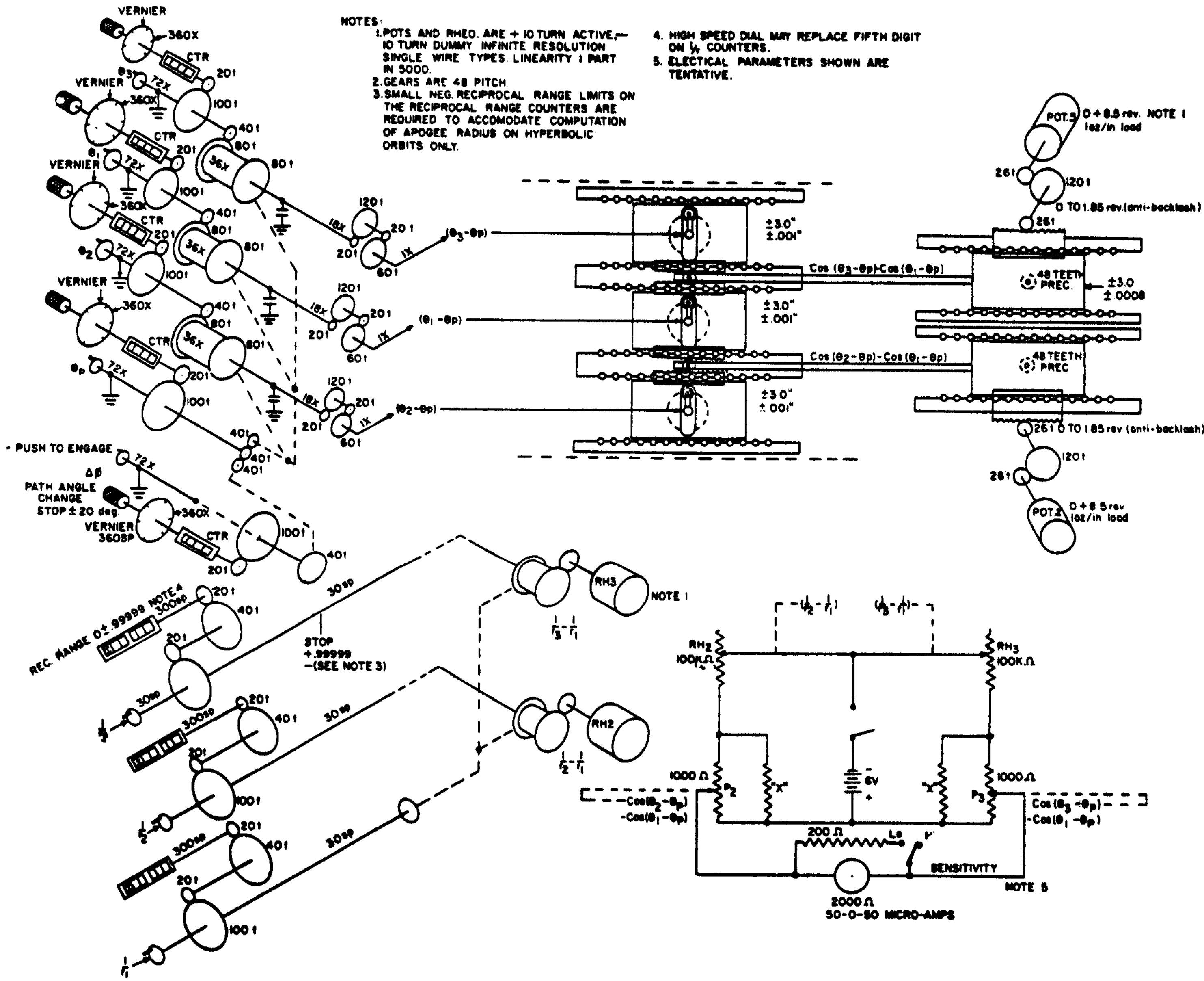

FIGURE 3-1.- MANUAL SPACE COMPUTER GEAR DIAGRAM AND SCHEMATIC DIAGRAM (PRELIMINARY).

It was recognized early in the study that the cosine mechanisms and the low speed cosine differentials would prove to be the critical sources of error. A search for components showed that no available commercial units could provide the accuracy required. As shown in Figure 3-1, the design will be based on the special fabrication of highly accurate scotch yoke angle solvers and linear rack differentials. By increasing the carriage travel to ±3 inches, a factor of four over miniature commercially available units, and by relaxing tolerances only slightly it is believed that the required accuracy can be attained. Rugged construction will be utilized to minimize compliance errors. The improvement to be attained, in effect, puts the cosine generators and rack differentials about on a par, error-wise, with the range rheostats and cosine potentiometers.

In order to obtain the maximum in accuracy from the delta reciprocal range rheostats and the delta cosine potentiometers, a simple operational rule in the designation of the first and third observations will be utilized. This rule is interpreted by the operator to mean that data relating to the observation furthest from earth should be inserted always in the Θ_1, $1/r_1$ channels, while data corresponding to the minimum range is introduced in the Θ_3, $1/r_3$ channels regardless of which observation comes first. This is particularly important on elliptical flight paths where observations might normally cover as many as 3, and theoretically even 4 quadrants. This restricts the cosine differences to a functional range of 2 (from 0 to 2) instead of 4, and the $1/r$ differences to a value of $1/r_{min} + 1/r_{a\ hyperbolic}$ instead of $2/r_{min}$. As noted previously, the $1/r_{a\ hyperbolic}$ term is quite small, making the instrumented range just slightly larger than the selected value of $1/r_{min}$. Use of this simple operational rule enables double accuracy to be obtained from the rheostats and potentiometers.

The zero resistance point on the rheostats will nominally correspond to the maximum value of the reciprocal range, noted above as $1/r_{min} + 1/r_a$ hyperbolic. On the delta cosine potentiometers the minimum resistance point will correspond to the maximum value of the cosine differences, +2. Figure 3-2 shows the scaling to be used for the rheostats and potentiometers. Adjustment of the phase angle ϕ_0 on the rheostat will be discussed later.

Since it is impractical to attempt to use stops at the low speed end of the cosine trains, and since the Θ inputs must be left unrestricted through 360 degrees in any case, some other means of instrumenting the reduced range of the cosine potentiometers must be employed. This will be accomplished by energizing only one-half of a 20 turn center tapped potentiometer

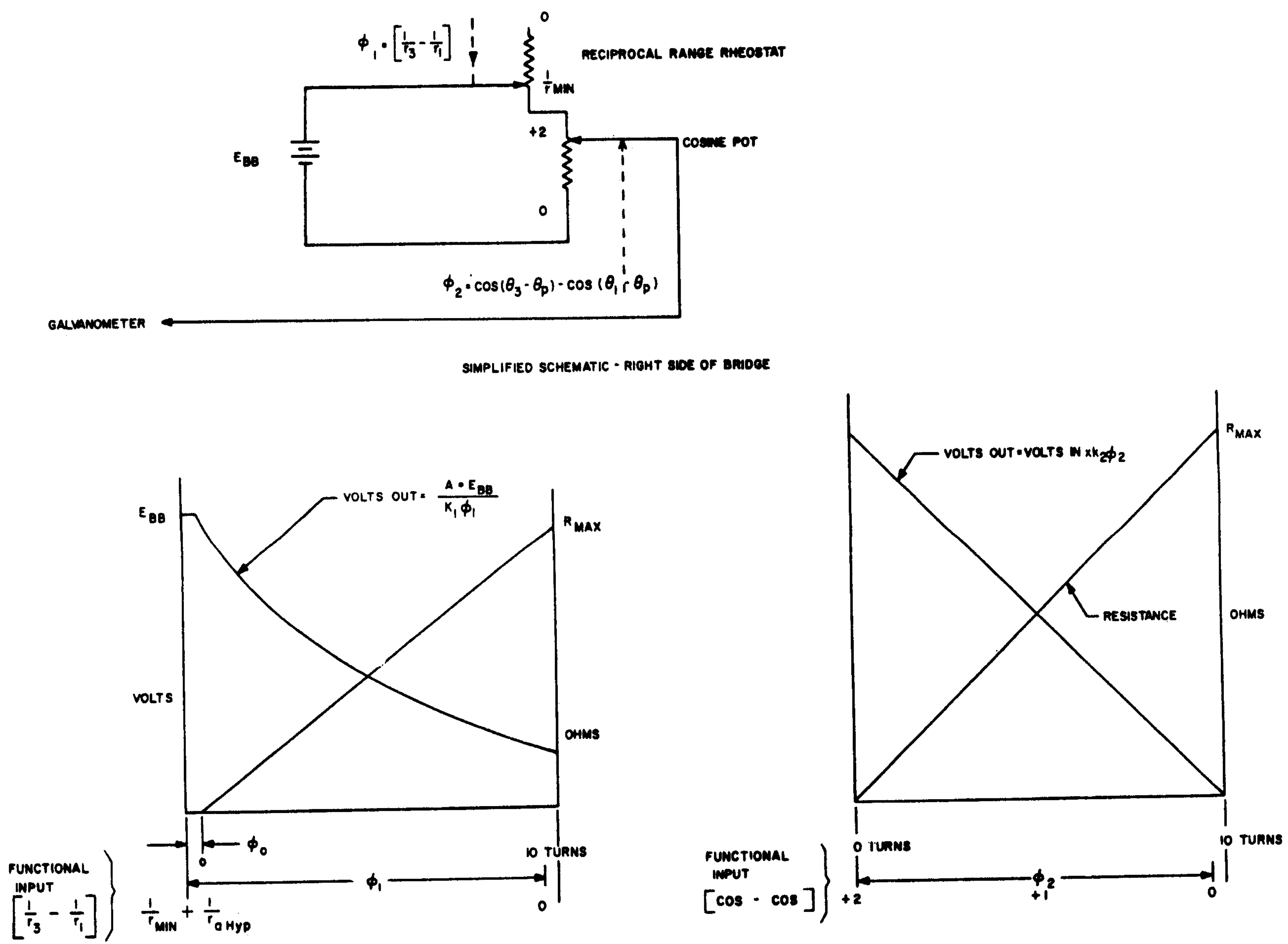

FIGURE 3-2 SCALING FOR THE RECIPROCAL RANGE RHEOSTAT AND COSINE POTS

or utilizing dummy windings on 10 of the turns. It will be necessary to specify and procure units which can meet the same linearity requirements over one-half of their range (i.e., 10 turns) as would be needed on a 10 turn potentiometer. This should impose no great difficulty since the manufacturer needs to maintain the tight linearity only on one half of the center-tapped potentiometer. This scheme enables the Θ inputs to cover any selected angle, 0 to 360 degrees while use of the operational rule insures that for bridge balancing, the high linearity, energized portion of the potentiometers will be utilized.

The $1/r$ potentiometers must also be protected to prevent damage during bridge balancing when the quantities $1/r_3 - 1/r_1$ or $1/r_2 - 1/r_1$ momentarily become negative, or in case the operator forgets to use the operational rule $r_1 > r_2 > r_3$. This can be accomplished by using 20 turn center-tapped rheostats with 1/2 of the windings dummied.

In the bridge circuit, shown in Figure 3-3, voltages proportional to each side of equation II-4 are generated by multiplying the reciprocals of the denominators by their respective numerators. The reciprocals of the denominators are taken by means of linear rheostats driven by shafts representing the quantities whose reciprocals are desired. The numerators are taken by linear potentiometers as shown. At null the bridge balance condition is:

$$\frac{R_P' R_T' K_2' \phi_2'}{\left[R_T' + R_P'\right]\left[K_1'(\phi_1' - \phi_0') + \frac{R_T' R_P'}{R_T' + R_P'}\right] R_P'} \cdot E_{BB} = \frac{R_P R_T K_2 \phi_2}{\left[R_T + R_P\right]\left[K_1(\phi_1 - \phi_0) + \frac{R_T R_P}{R_T + R_P}\right] R_P} \cdot E_{BB} \qquad \text{III-1}$$

corresponding to:

$$\frac{\cos(\theta_2 - \theta_P) - \cos(\theta_1 - \theta_P)}{\frac{1}{r_2} - \frac{1}{r_1}} = \frac{\cos(\theta_3 - \theta_P) - \cos(\theta_1 - \theta_P)}{\frac{1}{r_3} - \frac{1}{r_1}} \qquad \text{III-2}$$

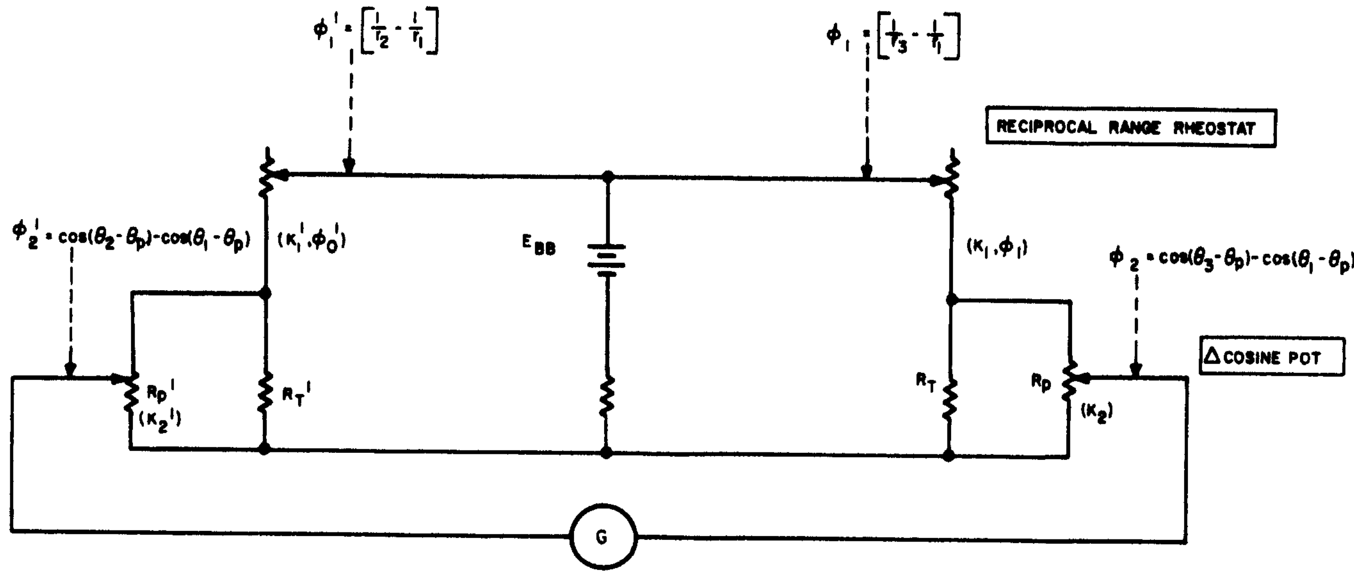

SYMBOLS AND DEFINITIONS

Rp = POT RESISTANCE, OHMS, RIGHT SIDE OF BRIDGE
Rp' = POT RESISTANCE, OHMS, LEFT SIDE OF BRIDGE
R_T = TRIM RESISTOR, OHMS, RIGHT SIDE OF BRIDGE
R_T' = TRIM RESISTOR, OHMS, LEFT SIDE OF BRIDGE
K_2 = GRADIENT, OHMS/DEGREE, RIGHT SIDE OF BRIDGE
K_2' = GRADIENT, OHMS/DEGREE, LEFT SIDE OF BRIDGE
K_1 = RHEOSTAT GRADIENT, OHMS/DEGREE, RIGHT SIDE OF BRIDGE
K_1' = RHEOSTAT GRADIENT, OHMS/DEGREE, LEFT SIDE OF BRIDGE
E_{BB} = BATTERY VOLTAGE
$\phi_1, \phi_1', \phi_2, \phi_2'$ = FUNCTIONAL SHAFT INPUT POSITIONS AS SHOWN
ϕ_0 = SHAFT PHASE ANGLE, IN DEGREES, AT ZERO FOR RIGHT RHEOSTAT
ϕ_0' = SAME FOR LEFT RHEOSTAT

FIGURE 3-3 BRIDGE CIRCUIT

In trimming the bridge it is necessary to set the shaft phase angles of the rheostats so that the denominators of Equation III-1 are linear representations of the denominators of Equation III-2. This may be accomplished by adjusting the values of the trim resistors such that

$$K_1 \phi_0 = \frac{R_T R_P}{R_T + R_P} \quad \text{and} \quad K_1' \phi_0' = \frac{R_T' R_P'}{R_T' + R_P'}$$

If, for example, the phase angle of the right rheostat is set to ϕ_0, its output will be

$$E_0 = \frac{R_P R_T}{(R_P + R_T) K_1 \phi_1} \cdot E_{BB} \qquad \text{III-3}$$

because the terms $K_1\phi_0$ and $\frac{R_T R_P}{R_T + R_P}$ in Equation III-1 cancel. This provides a rheostat output proportional to the reciprocal of the input, as desired. However, it is also necessary to insure that the net gradients of the two sides of the bridge are absolutely equivalent. This can be accomplished without requiring tight absolute linearities on the potentiometers and rheostats, by the following procedure.

First calculate the proper value of ϕ_0 to linearize the denominator of Equation III-1 using an appropriate value of R_T.

$$\phi_0 = \frac{R_T R_P}{K_1 (R_T + R_P)}$$

III-4

At balance, the following bridge condition will exist if both ϕ_0 and ϕ_0' have been properly set to provide linear outputs over their range.

$$\frac{R_T' K_2'}{(R_T' + R_P') K_1'} \cdot \frac{\phi_2'}{\phi_1'} = \frac{R_T K_2}{(R_T + R_P) K_1} \cdot \frac{\phi_2}{\phi_1}$$

III-5

Next, calling the lumped constants of Equation III-5, C and C' gives

$$C' \frac{\phi_2'}{\phi_1'} = C \frac{\phi_2}{\phi_1} \qquad \text{III-6}$$

The proper value of R_T' is then computed by equating

$$C' = C = \frac{R_T' K_2'}{K_1'(R_T' + R_P')} \qquad \text{III-7}$$

and solving for R_T'

$$R_T' = \frac{K_1' R_P' C}{K_2' - K_1' C} \qquad \text{III-8}$$

From this, the proper value of ϕ_o' is computed as

$$\phi_o' = \frac{R_T' R_P'}{(R_T' + R_P') K_1'} \qquad \text{III-9}$$

The trim resistors R_T and R_T' are installed first. Then the phase angles ϕ_o and ϕ_o' are set. This is accomplished by setting the $1/r_3$ and $1/r_2$ counters to their maximum readings (.99999) and the $1/r_1$ counter to the proper value corresponding to $1/ra_{hyperbolic}$, based on the roller chart scaling which was tentatively selected as r_{min}/r.

Next the shafting to the rheostats is disconnected and the wipers are rotated back from their zero ohm positions through angles corresponding to ϕ_o and ϕ_o'. The shafting to the rheostats is reconnected and the procedure is complete. ϕ_o and ϕ_o' represent the minimum shaft positions for which valid bridge balancing can be obtained. The zero point on the rheostat will now correspond to r_a hyperbolic plus a minimum radius slightly larger than the originally selected r_{min} (by the factor ϕ_o shown in Figure 3-2). This may be satisfactory or it may simply mean that a new initial value or r_{min} be chosen and the procedure starting with the rheostat phase adjustment be repeated until a satisfactory r_{min} is achieved. The final value of r_{min} is then used to calibrate the roller chart discussed in Section 3.5. The total of the four adjustments R_T, ϕ_o, R_T' and ϕ_o' insures that when ϕ_2/ϕ_1 is set equal to ϕ_2'/ϕ_1' by means of the input counters and dials, the bridge will balance. The cosine potentiometers are set up in a straightforward fashion such that minimum resistance corresponds to a cosine difference of +2 and the maximum resistance instrumented to 0.

The same low-voltage battery supplies both sides of the circuit, and while an extreme decrease in battery voltage will reduce the galvanometer sensitivity, it will not bias the null indication in either direction.

The output voltages are compared by a zero center galvanometer. It will be desirable to provide a four scale sensitivity setting, from "High" to "Low", rather than the two scale version shown in Figure 2-5. This topic is further developed in Section 3.4.

3.4 Component Capability

Component accuracy capabilities for the manual computer have been assessed and are tabulated in Figure 3-4. All major errors by component, source, maximum value or spread relative to 1 speed have been included. Each error is related to a specific ϵ No. in the error equations of Section 4. In addition, each is assigned a reference letter showing its location on computer schematic, Figure 3-5. The 1 σ errors have been computed on the basis of the maximum values assuming independent rectangular distributions for each error. In the following discussion it may be helpful to refer also to Figure 3-1.

For the gear trains and differentials, backlash is considered the major and only significant source of error. Precision 3 meshes or anti-backlash gearing has been used for the trains. Backlash in the Θ and $1/r$ precision differentials has been taken as 10 minutes of arc between end gears

NO.	COMPONENT	ERROR SOURCE	MAXIMUM VALUE REFERRED TO 1X	1σ VALUE	ϵ NO. IN STEP EQUATION FIG. 4.7	REFERENCE POINT ON SCHEMATIC FIGURE 3-5
1	θ_1 INPUT DIALS AND GEARING	DIAL READOUT AND GEAR BACKLASH	±5 SEC.	±2.89 SEC.	5	A
2	θ_2 INPUT DIALS AND GEARING	DIAL READOUT AND GEAR BACKLASH	±5 SEC.	±2.89 SEC.	13	B
3	θ_3 INPUT DIALS AND GEARING	DIAL READOUT AND GEAR BACKLASH	±5 SEC.	±2.89 SEC.	3	C
4	θ_p INPUT DIALS AND GEARING	DIAL READOUT AND GEAR BACKLASH	±5 SEC.	±2.89 SEC.	3 • 5 • 13	D
5	$(\theta_1-\theta_p)$ DIFFERENTIAL	BACKLASH	17 SEC. *	±5.20 SEC.	5	E
6	$(\theta_2-\theta_p)$ DIFFERENTIAL	BACKLASH	17 SEC.	±5.20 SEC.	13	F
7	$(\theta_3-\theta_p)$ DIFFERENTIAL	BACKLASH	17 SEC.	±5.20 SEC.	3	G
8	$(\theta_1-\theta_p)$ REDUCTION GEARING TO COS MECH	BACKLASH	2 MIN. *	±34.64 SEC.	5	H
9	$(\theta_2-\theta_p)$ REDUCTION GEARING TO COS MECH	BACKLASH	2 MIN.	±34.64 SEC.	13	I
10	$(\theta_3-\theta_p)$ REDUCTION GEARING TO COS MECH	BACKLASH	2 MIN.	±34.64 SEC.	3	J
11	$(\theta_1-\theta_p)$ COSINE MECHANISM	BEARING, PIN, SLOT ECCENTRICITIES AND PLAY	± 1/6000	±.0000962	6	K
12	$(\theta_2-\theta_p)$ COSINE MECHANISM	BEARING, PIN, SLOT ECCENTRICITIES AND PLAY	± 1/6000	±.0000962	16	L
13	$(\theta_3-\theta_p)$ COSINE MECHANISM	BEARING, PIN, SLOT ECCENTRICITIES AND PLAY	± 1/6000	±.0000962	6 • 16	M
14	$\cos(\theta_3-\theta_p)-\cos(\theta_1-\theta_p)$ DIFFERENTIAL	BACKLASH	± 1/4000	±.0001443	6	N
15	$\cos(\theta_2-\theta_p)-\cos(\theta_1-\theta_p)$ DIFFERENTIAL	BACKLASH	± 1/4000	±.0001443	16	O
16	$\cos(\theta_3-\theta_p)-\cos(\theta_1-\theta_p)$ POT DRIVE GEARING	BACKLASH	1/6000 *	±.0000481	6	P
17	$\cos(\theta_2-\theta_p)-\cos(\theta_1-\theta_p)$ POT DRIVE GEARING	BACKLASH	1/6000	±.0000481	16	Q
18	$\cos(\theta_3-\theta_p)-\cos(\theta_1-\theta_p)$ POTENTIOMETER	NON-LINEARITY	± 1/5000	±.0001155	6	R
19	$\cos(\theta_3-\theta_p)-\cos(\theta_1-\theta_p)$ POTENTIOMETER	NON-LINEARITY	± 1/5000	±.0001155	16	S
20	$1/r_1$ INPUT COUNTER AND GEARING	COUNTER READOUT AND GEAR BACKLASH	± 1/40,000	±.0000144	10 • 20	T
21	$1/r_2$ INPUT COUNTER AND GEARING	COUNTER READOUT AND GEAR BACKLASH	± 1/40,000	±.0000144	20	U
22	$1/r_3$ INPUT COUNTER AND GEARING	COUNTER READOUT AND GEAR BACKLASH	± 1/40,000	±.0000144	10	V
23	$(1/r_3-1/r_1)$ DIFFERENTIAL	BACKLASH	1/60,000 *	±.0000048	10	W
24	$(1/r_2-1/r_1)$ DIFFERENTIAL	BACKLASH	1/60,000	±.0000048	20	X
25	$(1/r_3-1/r_1)$ RHEOSTAT DRIVE GEARING	BACKLASH	1/6000 *	±.0000481	10	Y
26	$(1/r_2-1/r_1)$ RHEOSTAT DRIVE GEARING	BACKLASH	1/6000	±.0000481	20	Z
27	$(1/r_3-1/r_1)$ RHEOSTAT	NON-LINEARITY	± 1/5000	±.0001155	10	AA
28	$(1/r_2-1/r_1)$ RHEOSTAT	NON-LINEARITY	± 1/5000	±.0001155	20	BB
29	BRIDGE	TRIMMING ERROR DUE TO TRIM RESISTOR	± 1/6000	±.0000962	1	CC
30	GALVANOMETER	SENSITIVITY AND READOUT	± 1/100	———	30	DD

* TOTAL SPREAD.

FIGURE 3-4 MANUAL SPACE COMPUTER - COMPONENT ACCURACY EVALUATION

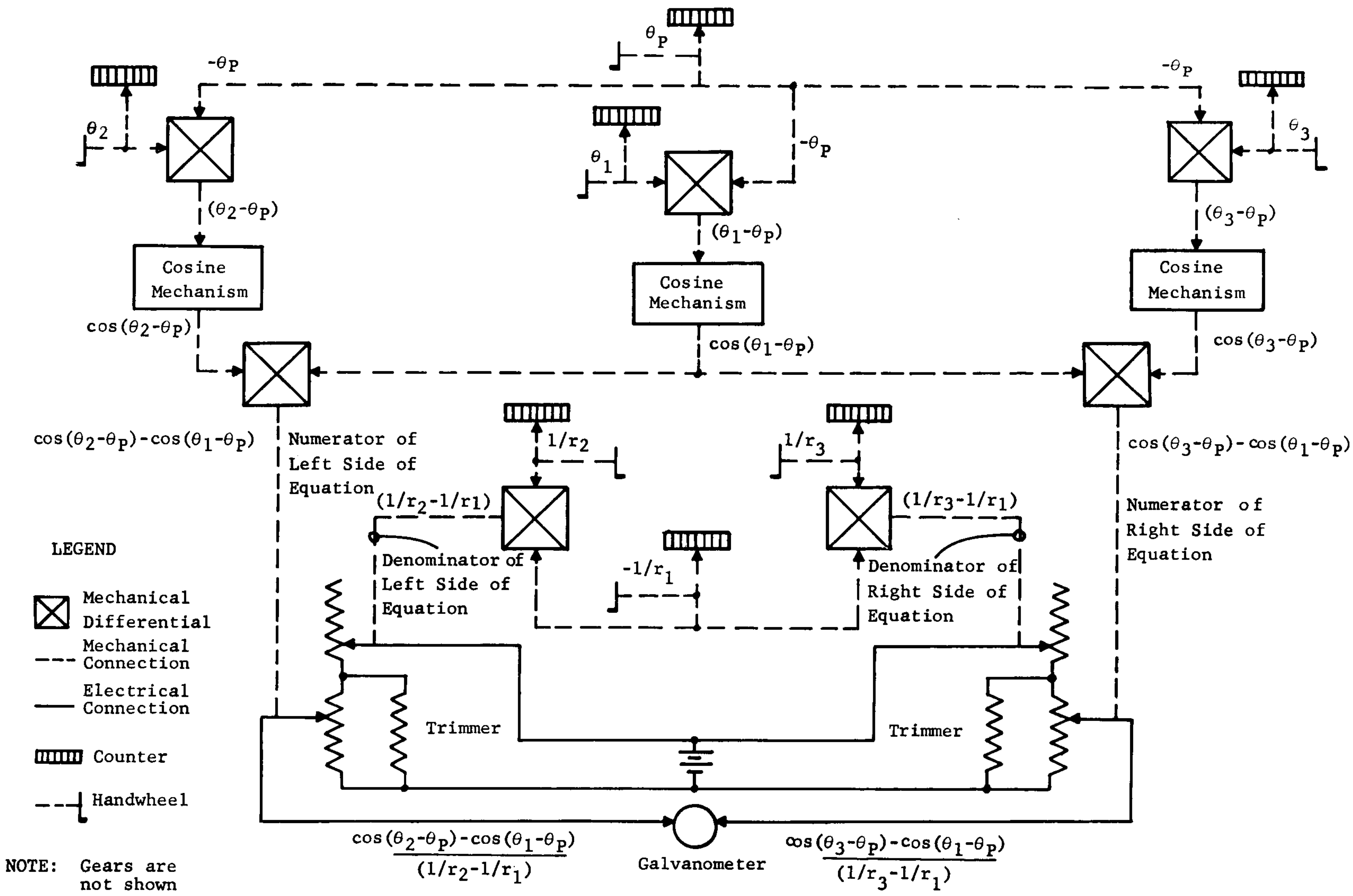

FIGURE 3-5.- COMPUTER SCHEMATIC DIAGRAM.

and related to the IX shafting. In general, for the critical gear train meshes, a total backlash of .001 inches has been specified in arriving at the maximum errors listed. The total backlash is attributable to center distance changes resulting from total composite error, pitch diameter tolerances, shaft and bearing eccentricities, etc.

Errors in the cosine mechanisms are caused primarily by bearing, pin, slot eccentricities, play and compliance under load. The error assigned of ±1/6000 is based on maintaining a tolerance of ±.001 inch over the full carriage travel of 6 inches (±3 inches). These errors are bias type errors relative to 2 corresponding to the full range of the cosine mechanisms.

Errors in the precision rack differentials of ±1/4000 are based on a backlash specification of ±.00075 inches over the 0 to +3 inch carriage travel of these devices. Again these are bias type error corresponding to the full functional range of 0 to +2 in the differential cosine functions which results from observing the operational rule $r_1 > r_2 > r_3$.

The linearity of the rheostats and potentiometers is specified as ±.02% of full range. The rheostats and potentiometers are assumed to have total ohmic values in excess of 1000 ohms, which makes a ±.02% linearity feasible since, in general, tighter linearities can be obtained in the higher resistance units. Resolution is assumed to be essentially infinite. Errors Nos. 20-28 are bias taken relative to $1/r_p$ (or 1/6430 KM) for this study, based on the maximum functional values and range of the $1/r_i$ and $1/r_j - 1/r_k$ functions. Again limiting the range of $1/r_j - 1/r_k$ to $1/r_p$ is a result of employing the operational rule described above.

The error of ±5 arc seconds assigned to the Θ input dials and gearing assumed that a vernier was used on the Θ input dial. However, since the results of the study show that this source of error is one of the least critical, a relaxation in accuracy of dial readout to 15 arc seconds or so can certainly be tolerated without significant effect on the overall accuracy.

The ±1/40,000 error listed for the 1/r input counters and gearing is compatible with the use of a four digit (.0000 to .9999) counter having a high speed dial with four graduations between each significant fourth decimal figure. Here again, results of the study indicated that this is a permissible accuracy degradation from the five digit, or 1/100,000 counter described in Section 3.3.

The tolerance on the trim resistor R_T', discussed under Section 3.2 above, is related as follows to the specified value for the scaling error listed as error No. 29 in Figure 3-4.

$$C(1 \pm \epsilon_1) = C' \qquad \text{III-10}$$

$$(R_T' \pm \Delta_{RT}') = \frac{K_1' R_p' C(1 \pm \epsilon_1)}{K_2' - K_1' C(1 \pm \epsilon_1)} \qquad \text{III-11}$$

$$\text{Allowable Tolerance, } \pm \Delta_{RT}' = \frac{K_1' R_p C(1 \pm \epsilon_1)}{K_2' - K_1 C(1 \pm \epsilon_1)} - R_T' \qquad \text{III-12}$$

For the galvanometer a microammeter with a sensitivity and readout accuracy of ±1% will be sufficient for any desired nulling accuracy. Errors in the bridge, resulting from galvanometer error, can be made as small as necessary by proper selection of shunt resistances and other circuit parameters. From the results of the study, it appears feasible to incorporate the following four sensitivity settings for the galvanometer in terms of the minimum discernable error in Γp, step 2, versus the full scale values:

Sensitivity Setting	Γp Corresponding to Minimum Discernable Galvanometer Signal	Γp Corresponding to Full Scale
High 1	±0.1 KM	±10 KM
2	±10 KM	±1000 KM
3	±1000 KM	±100,000 KM
Low 4	±100,000 KM	±10,000,000 KM

The corresponding minimum discernable signal in Θp on the High scale for step 1 would be less than 10 arc seconds. The other settings on step 1 would scale out proportionately.

4. METHOD OF ACCURACY ANALYSIS

4.1 Approach to Accuracy Analysis

The approach used in the accuracy analysis of the manual computer is shown in Figure 4-1. The final result, total errors in perigee radius and angle, with maneuver, represents the RSS combination of errors in two categories: (1) total errors assuming no maneuver; (i.e., only computing the vacuum perigee) and (2) the incremental errors due to the corrective maneuver computation. (i.e., computing the required change in velocity direction to alter the vacuum perigee) In turn, each of these subtotals consists of an RSS combination of hardware errors and errors in concept. Concept errors for the "no maneuver" category are incurred because of the simplifying assumptions of two body theory and a spherical earth in the manual computer formulation. The concept errors for the corrective maneuver computation are the result of assuming a parabolic trajectory for these calculations. Hardware errors in each category are composed of inaccuracies in the mechanical and electrical components of the manual computer and in the input observational data. Inaccuracies in the observational data is due primarily to inaccuracies in the measuring equipment and is therefore included in the hardware classification. The RSS summary results of the error analyses performed in this study are presented in Section 5.

4.2 Notation and Geometry

The notation and geometry used in the accuracy analyses of the manual computer is presented in Figures 4-2 and 4-3. These figures should be consulted when necessary in the further discussions of this section.

4.3 Trajectory Input Data and Computations

Trajectory input data for this program was obtained from a NASA Ames simulation which provided a series of 14 abort trajectories returning to earth from abort way stations separated in time by about four hours on a translunar trajectory. Each of these abort trajectories took into account the gravitational attraction of the sun, moon and earth, including earth oblateness effects. In addition, each trajectory had been precalculated by Ames to attain a perigee of 6430 kilometers including these effects. From this set of data, twenty-four problems for the manual computer accuracy analysis were formulated. These problems are in two groups, each group containing twelve problems. Four representative abort trajectories were used. These were trajectories numbers 1,2,5 and 14. In each group three problems were prepared for each of the four trajectories.

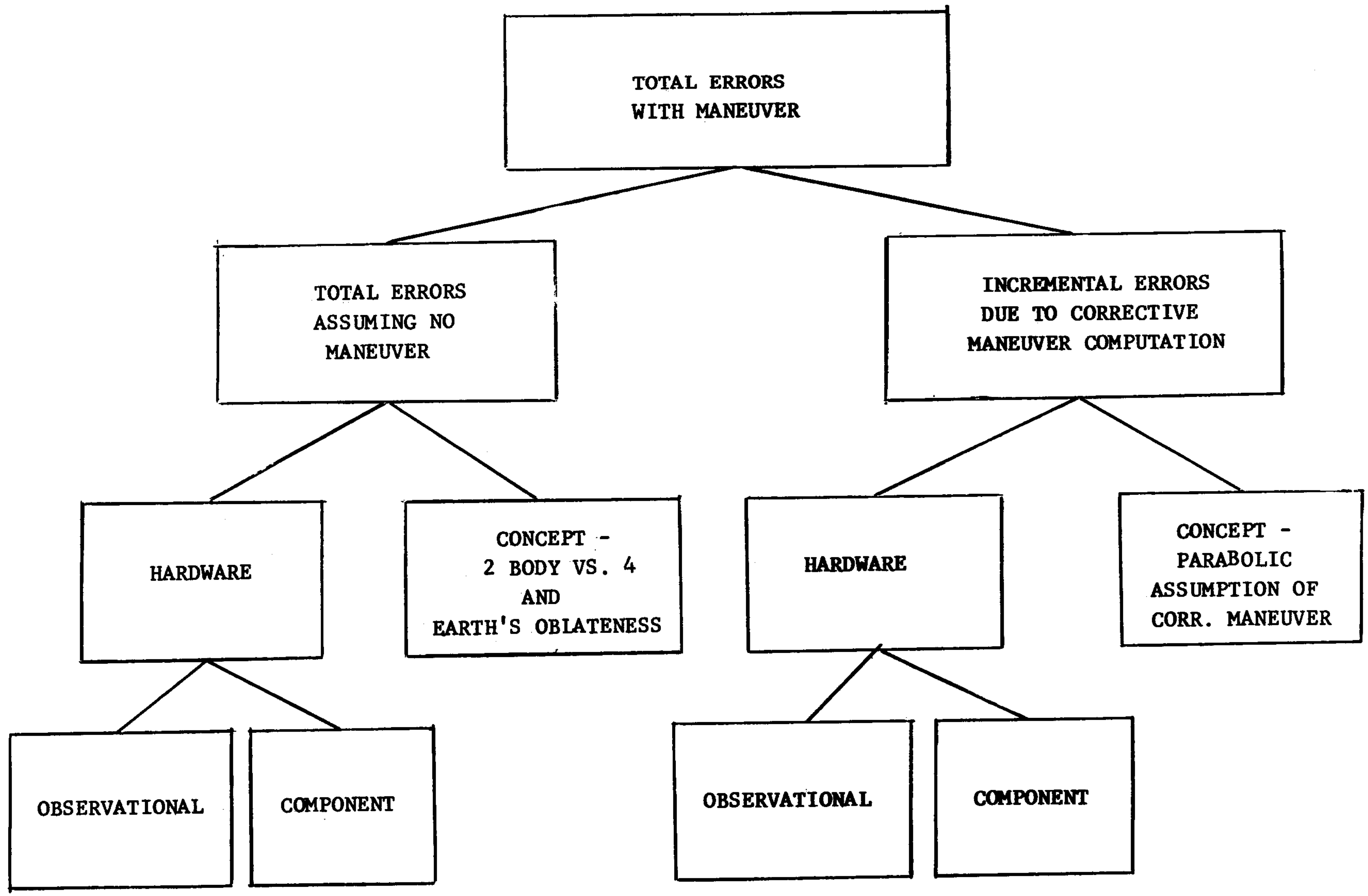

FIGURE 4-1 - Approach to Accuracy Analysis

SUBSCRIPTS

a	=	Apogee
c	=	Corrective maneuver point
P	=	Perigee
1,2,3,4	=	Successive Observation Points
N	=	Nominal (without error)
E	=	With error
D	=	Desired
S1,S2,etc	=	Step 1, Step 2, etc. of the Step Equations
H	=	Horizontal component
R	=	Radial component
PAB	=	Parabolic

SUPERSCRIPTS

No Prime	=	A computed quantity prior to the corrective maneuver based on the pure conic solution of Manual Computer.
'	=	Prime. A computed or desired quantity for the corrective maneuver based on a pure conic solution by the Manual Computer.
"	=	Double Prime. Used in connection with data and other quantities involving the NASA Abort Trajectories (for an exact perigee of 6430.--KM including four body and earth oblateness effects).
"'	=	Triple Prime. Used in connection with a corrective maneuver based on parabolic assumptions.

PARAMETERS AND CONSTANTS

r	=	The distance, in kilometers, from a given point in space to the center of the earth.
θ	=	Theta. The angle measured at the earth's center, in degrees, CCW (as seen generally from a point above the Northern Hemisphere) from the datum line between the earth's center and the reference star, to a given point in space. In this program the reference star is assumed to be on the radial from the earth's center which passes through the NASA data perigee for each trajectory.
X, Y, Z	=	Cartesian coordinates of a special point in a geocentric equatorial coordinate system.
β	=	Beta. The angle, in degrees, subtended by the earth as seen by an observer in space. $\sin \beta/2 = re/r$
re	=	The mean radius of the International spheroid $re = \dfrac{2X \text{ Equatorial Radius} + \text{Polar Radius}}{3}$ $= 6,371.229$ KM
$\theta j - \theta p$	=	The angle, in degrees, measured at the earth's center CCW in the plane of the orbit to the point in question.
ϕc PAB	=	The path angle, in degrees, between the radius and velocity vectors of a parabola passing through the point C and perigee.
ϕc	=	The angle less than 90°, measured (+) CCW from the normal to the radius vector at point C to the velocity vector, V_c, of the elliptical orbit. Since the corrective maneuver will always be performed in the third or fourth quadrants, the sign of ϕ_c will always be taken as positive.
ε	=	Epsilon. An error quantity.
Δ	=	Delta. A correction or increment deliberately introduced.
εrp, $\varepsilon\theta p$	=	Errors in kilometers and degrees, of perigee radius and angle, due to errors in the observations and in the instrumentation of the manual computer. They are the differences between r_{PES2} and r_{PNS2} and between θ_{PES1} and θ_{PNS1}
$\varepsilon rp'$, $\varepsilon\theta p'$	=	Errors in kilometers and degrees, corresponding to a change in perigee with error (instrumentation or observational) and a change without error. They are the differences between r'_{PES6} and r'_{PNS6} (the latter is simply r'_{PD}) and between θ'_{PES5} and θ'_{PNS5}.
$\varepsilon rp''$, $\varepsilon\theta p''$	=	Errors in kilometers and degrees, of perigee radius and angle, due to two body assumptions and a spherical earth. They are the differences between the desired perigee of the NASA data ($r_p'' = r'_{pD} =$ 6430.-- and $\theta_p'' = 0$) and the nominal solutions for r_p and θ_p, steps 2 and 1.
$\varepsilon rp'''$, $\varepsilon\theta p'''$	=	Errors in kilometers and degrees, of perigee radius and angle, due to the simplifying assumptions of a parabolic trajectory for the corrective maneuver. They are the differences between r_p''' and r'_{pN}; and θ_p''' and θ'_{PN}.
ΔrpD	=	Desired change in perigee radius, in kilometers introduced into step 5. It is the difference between the r'_{pD} of 6430.-- and r_{PES2}, the computed perigee radius of step 2 with error. Δr_{PDN} is simply the difference between 6430.-- and the nominal value of r_p from step 2.
ΔrpE	=	An interim value, computed in step 6, relative to the nominal value of r_p, used in computing εrp.
a	=	Semi-major axis of ellipse, in kilometers.
e	=	Eccentricity of orbit
μ	=	Gravitational constant of the earth, 3.986135×10^5 KM ^{3}/Sec.^{2}
V	=	Velocity in KM/Sec.
ΔV	=	Velocity increment in KM/Sec. based on parabolic assumptions for the corrective maneuver.
$\Delta\phi$	=	Change in flight path angle, in radians, based on parabolic assumptions.
h	=	Angular momentum in KM ^{2}/Sec.
ℓ	=	Semi-latus rectum in KM.

FIGURE 4-2 NOTATION

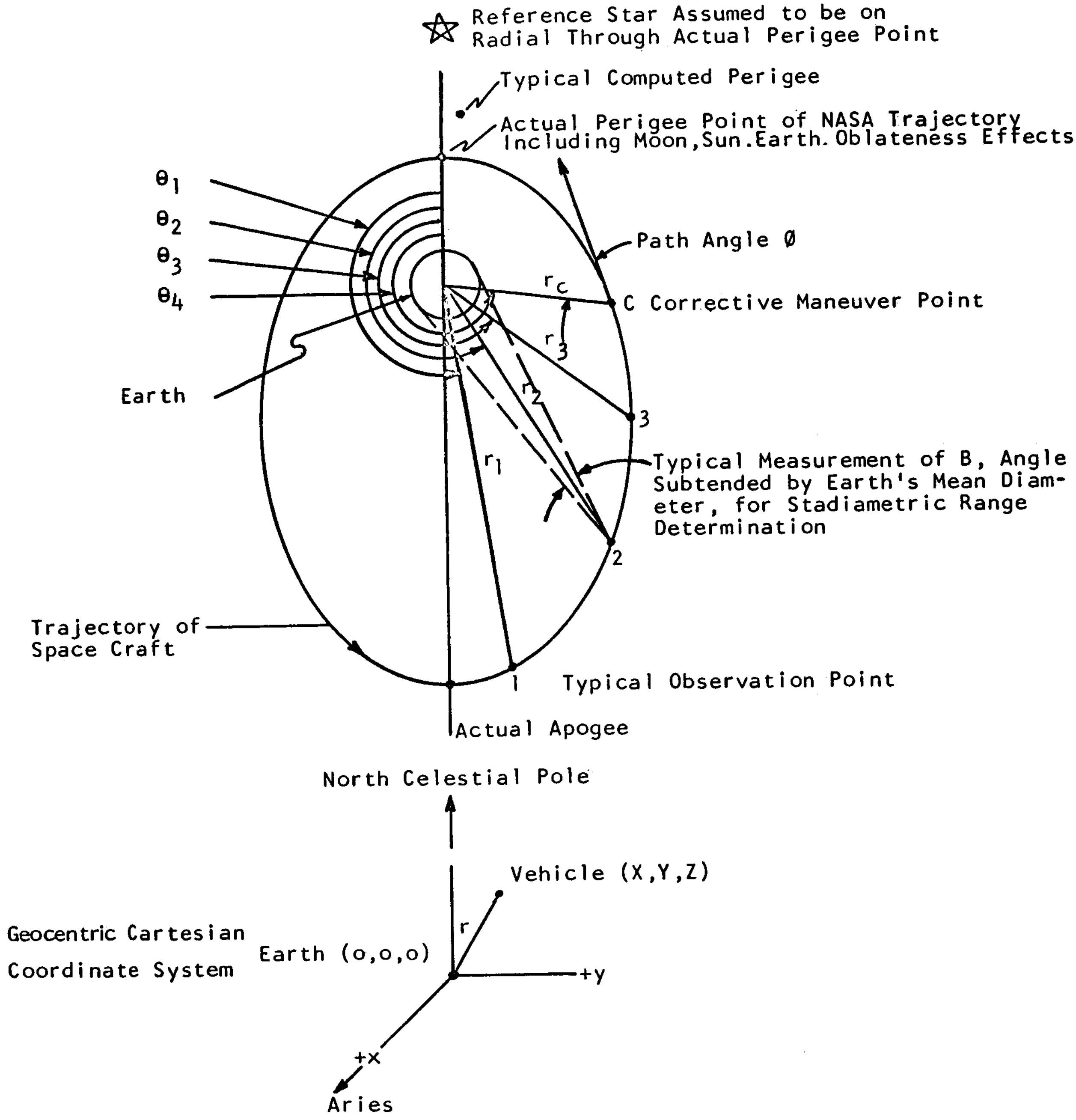

Figure 4 - 3 Geometry for Manual Space Computer Simulation

The first group contains problems with a fixed corrective maneuver point which occurs approximately 1/2 hour before perigee. The third observation point is also fired and occurs about 1 hour before perigee. In this group the first observation point is varied. For problem No. 1, the first observation is taken as the first or second point listed following the abort maneuver. There is one exception in the case of the 14th trajectory where the first measurement was arbitrarily limited to be within 200,000 KM of the earth. For problems 2 and 3, the first observation occurs successively closer to perigee. The second point is taken so that it divides the angle between the first and third observations about in half.

The second group contains problems with a fixed first observation point and a variable corrective maneuver point. The first observation is always taken at the first or second listed point following the abort maneuver, except in the case of the 14th trajectory as explained above. The first problem for each trajectory in Group 2 corresponds to the first problem in Group 1. Problems 2 and 3 of the second group represent situations where the corrective maneuver and third observation occur earlier. Again the second point is chosen to bisect approximately, the angle between the first and third observations.

A problem number is assigned to each of the twenty-four problems or cases. The first digit indicates the NASA abort trajectory number, 1 to 14. The second digit is the group number, 1 or 2 and the third digit is the problem number, 1 to 3. For example, problem number 1..2.3 means the third problem of the first trajectory in group 2.

Figure 4-4 presents the input data for the 24 problems. There are four points listed in X, Y, Z, r coordinates for each problem. The first three points represent the three selected observational positions while the radius to the fourth point represents the chosen radius for the corrective maneuver. The desired perigee is taken from the NASA data for each trajectory. Figure 4-4 also gives the θ and β angles, which are defined in Figure 4-2. The θ angles are computed from the cartesian coordinates of the NASA data by means of the following conversion

$$\cos(\theta_i - \theta_p) = \frac{X_i X_p + Y_i Y_p + Z_i Z_p}{r_i \, r_p} \qquad \text{IV-1}$$

where the subscript i corresponds to a given point, 1-4, of the NASA data and the subscript p corresponds to the desired perigee taken from the same data. In this program a ficticious reference star is assumed to be located on the radius vector from the earth's center through the perigee point actually attained on each orbit. This makes θ_p in equation. IV-1 zero and facilitates computation of the θ_i's. The computation for β is indicated in Figure 4-2.

Also indicated in Figure 4-4 are the approximate angular differences between the θ angles, the initial eccentrity of the orbit, the approximate radius of apogee if an apogee occurs on that trajectory, and the time differences between perigee and the third observation and between perigee and the corrective maneuver.

Figure 4-5 is a sample sheet for a typical problem showing the program inputs and results of input computations.

4.4 Analysis of Hardware Errors

The simulation sequence matrix and step equations utilized to determine the effect of hardware errors in this program are indicated in Figures 4-6 and 4-7.

It will be recalled that the relationship of the ϵ numbers of the step equations to specific 1σ hardware errors is spelled out in Figure 3-5. A similar relationship between errors in the observations and the ϵ numbers is provided in Figure 4-8. The 1σ error in sextant measurements has been taken as ± 10 arc seconds. Figure 4-8 indicates the steps on which the observational errors are introduced or removed from the error equations. This is different from the program used for component errors which are left in for all steps. Also noted in Figure 4-8 is the computation utilized in the program to translate a sextant error, $\epsilon\beta$, into the equivalent range error,

Only one error at a time is evaluated by means of the step equations. For steps 1-6, the computed value of the unknown, containing any accumulated errors is carried forward as an insert in the next step.

Although not all the ϵ numbers given in the step equations had a counterpart in terms of an error in the manual computer, all were programmed

PROBLEM NUMBER	POINT NUMBER	COORDINATES					ANGULAR DIFF: (DEG)				INITIAL ECCENTRICITY OF ORBIT	APPROXIMATE RADIUS OF APOGEE (KM)	TIME OF PERIGEE MINUS TIME OF THIRD OBSERVATION (HOURS)	TIME OF PERIGEE MINUS TIME OF CORRECTIVE MANEUVER, POINT NUMBER 4 (HOURS)
		X(KM)	Y(KM)	Z(KM)	R(KM)	Θ (DEG)	$\theta_2-\theta_1$	$\theta_3-\theta_2$	$\theta_3-\theta_1$	β (DEG)				
1.1.1	1 2 3 4	-25348.98 - 1244.625 -13981.04 -11564.65	-24617.55 -49471.34 -15954.10 - 4893.234	-18707.11 -23336.87 - 3406.16 - 1039.930	40000.35 54713.55 21484.99 12600.25	151.9204 191.4733 235.0675 264.3124	39	44	83	18.33013 13.37419 34.50019 60.74807	0.8	60000	1.048	0.474
1.1.2	1 2 3 4	-23544.21 6907.380 13981.04 11564.65	-39033.97 -41744.36 -15954.10 - 4893.234	-24873.81 -17412.74 - 3406.216 - 1039.929	51929.64 45754.86 21484.99 12600.25	164.8879 201.7934 235.0675 264.3124	37	33	70	14.0947 16.00856 34.50019 60.74807	0.8	60000	1.048	0.474
1.1.3	1 2 3 4	-17206.15 6907.380 13981.04 11564.65	-48555.69 -41744.36 -15954.10 - 4893.234	-27482.34 -17412.74 - 3406.216 1039.929	58386.52 45754.86 21484.99 12600.25	175.0937 201.7933 235.0675 264.3124	27	33	60	12.52936 16.00856 34.50019 60.74807	0.8	60000	1.048	0.474
Desired Perigee		1381.560	5536.093	2964.434	6430.000	0								
2.1.1	1 2 3 4	-34899.68 12468.53 15749.71 11910.58	-70968.21 -56274.26 -16079.63 - 4447.700	-42959.61 -22555.58 - 2947.825 - 1352.499	90000.01 61895.16 22700.17 12785.66	168.6179 204.2517 238.0388 266.5166	35	34	69	8.118890 11.81651 32.60025 59.77657	0.88	102000	1.043	0.457
2.1.2	1 2 3 4	27794.29 13315.79 15749.71 11910.58	-84860.42 -53498.81 -16079.63 - 4447.700	-47377.08 -21023.58 - 2947.825 1352.499	101086.1 59003.59 22700.17 12785.66	175.7324 205.7227 238.0388 266.5166	30	32	62	7.227238 12.39781 32.60025 59.77657	0.88	102000	1.043	0.457
2.1.3	1 2 3 4	-16754.35 13315.79 15749.71 11910.58	-89662.21 -53498.81 -16079.63 - 4447.700	-46442.94 -21023.58 - 2947.825 1352.499	102357.0 59003.59 22700.17 12785.66	182.5002 205.7227 238.0389 266.5166	23	32	55	7.137382 12.39781 32.60025 59.77657	0.88	None	1.043	0.457
Desired Perigee		1319.623	5555.760	2955.845	6430.000	0								
5.1.1	1 2 3 4	-38244.07 17421.28 15746.40 12525.57	-154716.6 -53713.20 -14883.17 - 5751.192	-82807.22 -19849.11 - 2329.790 969.7538	179602.0 59854.79 21791.87 13816.89	181.3799 211.6146 242.4483 263.7270	31	30	61	4.065892 12.22082 33.99945 54.91865	0.93	None	0.943	0.498
5.1.2	1 2 3 4	-27787.15 17944.09 15746.40 12525.57	-151517.8 -47565.06 -14883.17 - 5751.192	78308.07 -16846.45 - 2329.790 969.7538	172806.0 53555.84 21791.87 13816.89	184.5275 214.3701 242.4484 263.7270	29	28	57	4.225863 13.66466 33.99945 54.91865	0.93	None	0.943	0.498
5.1.3	1 2 3 4	- 1680.609 17944.09 15746.40 12525.57	-119356.7 -47565.06 -14883.17 - 5751.192	-55832.00 -16846.45 - 2329.790 969.7538	131780.04 53555.84 21791.87 13816.89	193.3424 214.3700 242.4484 263.7270	21	28	49	5.542356 13.66466 33.99945 54.91865	0.93	None	0.943	0.498
Desired Perigee		1515.177	5490.849	2983.239	6430.000	0								
14.1.1	1 2 3 4	10273.29 21816.61 16288.58 11819.87	-178648.4 -51878.56 -15816.37 - 4869.385	-75837.11 -14060.09 - 215.7669 3807.990	194350.4 58008.93 22705.10 13088.35	195.9770 216.5012 242.9808 268.1585	21	26	47	3.757235 12.61125 32.59297 58.25913	0.99	None	0.962	0.447
14.1.2	1 2 3 4	16989.22 21816.61 16288.58 11819.87	-13808.24 -51878.56 -15816.37 - 4869.385	-54781.71 -14060.09 - 215.7669 + 3807.990	149520.6 58008.93 22705.10 13088.35	199.7254 216.5012 242.9808 268.1585	17	26	43	4.884344 12.61125 32.59297 58.25913	0.99	None	0.962	0.447
14.1.3	1 2 3 4	20991.37 20145.84 16288.58 11819.87	-100550.5 -34062.12 -15816.37 - 4869.385	-36246.84 - 6772.448 - 215.7669 + 2807.990	108926.0 40149.08 22705.10 13088.35	204.6507 225.2625 242.9808 268.1585	20	18	38	6.706440 18.26165 32.59297 58.25913	0.99	None	0.962	0.447
Desired Perigee		1329.481	5515.188	3029.796	6430.286	0								

FIGURE 4 - 4 - OBSERVATIONAL DATA

(Manual Computer Inputs and Trajectory Parameters Based on NASA Abort Trajectories)

PROBLEM NUMBER	POINT NUMBER	COORDINATES X(KM)	Y(KM)	Z(KM)	R(KM)	θ (DEG)	ANGULAR DIFF. (DEG) $\theta_2-\theta_1$	$\theta_3-\theta_2$	$\theta_3-\theta_1$	β (DEG)	INITIAL ECCENTRICITY OF ORBIT	APPROXIMATE RADIUS OF APOGEE (KM)	TIME OF PERIGEE MINUS TIME OF THIRD OBSERVATION (HOURS)	TIME OF PERIGEE MINUS TIME OF CORRECTIVE MANEUVER, POINT NUMBER 4 (HOURS
1.2.1	1	-25348.98	-24647.55	-18707.11	40000.35	151.9204	39.5529	43.5942	83.1471	18.33013	0.8	60000	1.048	0.474
	2	- 1244.625	-49471.34	-23336.87	54713.55	191.4733				13.37419				
	3	13981.04	-15954.10	- 3406.216	21484.99	235.0675				34.50019				
	4	11564.65	- 4893.234	1039.930	12600.25	264.3124				60.74807				
1.2.2	1	-25348.98	-24647.55	-18707.11	40000.35	151.9204	29.2170	35.1097	64.3267	18.33013	0.8	60000	2.021	1.048
	2	-11600.87	-51301.14	-27152.63	59191.66	181.1374				12.35826				
	3	12689.01	-28829.09	- 9757.242	32974.70	216.2471				28.28101				
	4	13981.04	-15954.10	- 3406.216	21484.99	235.0676				34.50019				
1.2.3	1	-25348.98	-24647.55	-18707.11	40000.35	151.9204	28.4668	28.7317	57.1985	18.33013	0.8	60000	2.677	1.165
	2	-12343.90	-51113.26	-27278.12	59237.09	180.3872				12.34875				
	3	10582.58	-35071.13	-13260.21	38959.06	209.1189				18.82445				
	4	14038.88	-17819.74	- 4256.323	23081.37	231.7539				32.04722				
Desired Perigee		1381.560	5536.093	2964.434	6430.000	0								
2.2.1	1	-34899.68	-70968.21	-42959.61	90000.01	168.6179	35.6338	33.7871	69.4209	8.11889	0.88	102000	1.043	0.457
	2	12468.53	-56274.26	-22555.58	61895.16	204.2517				11.81651				
	3	15749.71	-16079.63	- 2947.825	22700.17	238.0388				32.60025				
	4	11910.58	- 4447.70	1352.499	12785.66	266.5166				59.77657				
2.2.2	1	-34899.68	-70968.21	-42959.61	90000.01	168.6179	24.8820	28.7049	53.5869	8.11889	0.88	102000	1.934	0.868
	2	1818.08	-77520.48	-35477.76	85272.52	193.4999				8.569819				
	3	16881.64	-29289.62	-87577.91	34922.35	222.2048				21.02381				
	4	15048.74	-12920.46	- 1681.823	19505.56	243.6073				37.33466				
2.2.3	1	-34899.68	-70968.21	-42959.61	90000.01	168.6179	23.9788	21.0334	45.0122	8.11889	0.88	102000	2.895	1.489
	2	529.023	-79152.65	-36605.52	87208.87	192.5967				8.379195				
	3	16095.63	-40270.04	-14082.60	45596.77	213.6301				16.06443				
	4	16675.59	-23171.09	- 5975.462	29166.43	288.4501				25.23530				
Desired Perigee		1319.623	5555.76	2955.845	6430.000	0								
5.2.1	1	-38244.07	-154716.6	-83807.22	179602.00	181.3799	30.2347	30.8337	61.0684	4.065892	0.93	None	0.943	0.498
	2	17421.28	-53713.20	-19849.11	59854.79	211.6146				12.22082				
	3	15746.40	-14883.17	- 2329.79	21791.87	242.4483				33.99945				
	4	12525.57	- 5751.192	969.7538	13816.89	263.7270				54.91865				
5.2.2	1	-39582.14	-154654.5	-83163.26	180002.4	180.9573	23.5826	23.4039	46.9865	4.056842	0.93	None	1.669	0.943
	2	14194.34	-73831.02	-30114.44	80989.98	204.5399				9.023883				
	3	17751.04	-26799.98	- 7273.724	32958.24	227.9438				22.29228				
	4	15746.40	-14883.17	- 2329.79	21791.87	242.4484				33.99945				
5.2.3	1	-39582.14	-154654.5	-83163.26	180002.4	180.9573	18.8975	22.4122	41.3097	4.056842	0.93	None	2.185	1.060
	2	9672.834	-91086.27	-39428.14	99723.87	199.8548				7.326096				
	3	18202.95	-33907.01	-10438.08	39874.63	222.2670				18.38843				
	4	16246.93	-17008.53	- 3170.028	23733.99	239.1612				31.14330				
Desired Perigee		1515.177	5490.849	2983.239	6430.000	0								
14.2.1	1	10273.29	-178648.4	-75837.11	194350.40	195.9770	20.5242	26.4796	47.0038	3.757235	0.99	None	0.962	0.447
	2	21816.61	-51878.56	-14060.09	58008.93	216.5012				12.61125				
	3	16288.58	-15816.37	- 215.7669	22705.10	242.9808				32.59297				
	4	11819.87	- 4869.385	2807.99	13088.35	268.1585				58.25913				
14.2.2	1	10273.29	-178648.40	-75837.11	194350.40	195.9770	17.0708	17.3374	34.4082	3.757235	0.99	None	1.619	0.768
	2	22186.50	-62096.03	-18487.99	68483.30	213.0478				10.67627				
	3	19009.14	-27088.19	- 4123.734	33348.50	230.3852				22.02813				
	4	15225.91	-12594.49	780.8634	19775.22	248.3355				37.58993				
14.2.3	1	10273.29	-178648.4	-75837.11	194350.40	195.9770	11.3869	17.8956	29.2855	3.757235	0.99	None	2.087	0.962
	2	21877.57	-85387.15	-29068.59	92814.74	207.3639				7.87228				
	3	20145.84	-34062.12	- 6772.448	40149.08	225.2625				18.26165				
	4	16288.58	-15816.37	- 215.7669	22705.10	242.9808				32.59297				
Desired Perigee		1323.481	5515.188	3029.796	6430.286	0								

FIGURE 4 - 4 - CONCLUDED

MANUAL SPACE COMPUTER ERROR ANALYSIS

PRCBLEM NUMBER 1.1.2

X (KM)	Y (KM)	Z (KM)	R (KM)	THETA (CEG)	COS THETA	BETA (DEG)
-C.2354421E 05	-0.39C3397E C5	-C.2487381E 05	0.5192964E 05	0.1648879E 03	-0.9654174E 00	0.1409471E 02
0.69C738CE 04	-0.4174436E C5	-C.1741274E 05	0.4575486E 05	0.2017934E 03	-C.9285289E 00	C.16C0856E 02
0.1398iC4E 05	-0.1595410E C5	-C.3406216E 04	0.2148499E 05	0.2350675E 03	-0.5726105E 00	C.3450019E 02
0.1156465E 05	-C.4893234E C4	C.1039929E 04	0.1260025E 05	0.2643124E 03	-0.9910359E-01	C.6074807E 02

CESIRED PERIGEE POSITICN FOLLOWS

C.1381560E 04	C.5536C93E C4	0.2964434E 04	0.643000CE 04

FIGURE 4-5

SAMPLE TABULATION - PROGRAM INPUTS

Step No.	Operational Procedure/Computer Simulation	θ_1	r_1	θ_2	r_2	θ_3	r_3	θ_p	$\Delta\phi$	Unknown
1	Given θ_1, r_1, θ_2, r_2, θ_3, r_3. Solve for θ_p	G	G	G	G	G	G	X_1	0	$X_1 = \theta_p$
2	Substitute θ_p for θ_3. Solve for r_p	G	G	G	G	X_1	X_2	X_1	0	$X_2 = r_p$
3	Insert the desired radius for the corrective maneuver, r_c for r_2. Solve for θ_c	G	G	X_3	r_c	X_1	X_2	X_1	0	$X_3 = \theta_c$
4	Substitute $\theta_p + 180^o = \theta_a$ for θ_1. Solve for apogee radius	X_1+180^o	X_4	X_3	r_c	X_1	X_2	X_1	0	X_4 = ra
5	Lock $\theta_3-\theta_p) = (X_1-X_1) = 0^o$. Lock $(\theta_1-\theta_p) = X_1+180^o-X_1 = 180^o$ Insert desired correction to perigee Δr_p desired = r_p desired of 6430... $-r_p$ computed Step 2. Change apogee radius accordingly $(r_a-\Delta r_p)$ maintaining size of major axis and energy of orbit. Solve for θ_p'.	X_1+180^o	$X_4-\Delta r_p$	X_3	r_c	X_1	$X_2+\Delta r_p$	X_5 in cos $(\theta_2-\theta_p)$	$\Delta\phi$	$X_5 = \theta_p'$
6	Not an operational step. The simulation uses θ_p' from step 5 to solve ror the corresponding r_p'									r_p'

The symbol "G" stands for "Given".

Figure 4-6 - Simulation Sequence Matrix

Step 1 (solve for $\theta\rho$)

Bridge Equation

$$0 = (1+\epsilon_1)\ \frac{[(1+\epsilon_2)\cos\ (\theta_3-\theta\rho+\epsilon_3)-1+\epsilon_4)\cos\ (\theta_1-\theta\rho+\epsilon_5)]+\epsilon_6}{(1+\epsilon_7)[\frac{1}{r_3+\epsilon_8} - \frac{1}{r_1+\epsilon_9}] + \epsilon_{10}} - 1+\epsilon_{11})\ \frac{[(1+\epsilon_{12})\cos\ (\theta_2-\theta\rho+\epsilon_{13})-(1+\epsilon_4)\cos(\theta_1-\theta\rho+\epsilon_5)]+\epsilon_{16}}{(1+\epsilon_{17})[\frac{1}{r_2+\epsilon_{18}} - \frac{1}{r_1+\epsilon_9}] + \epsilon_{20}} + \epsilon_{30}$$

Explicit Solution

$$\tan\theta\rho = \frac{\epsilon_6'' + [1+\epsilon_2\cos\ (\theta_3+\epsilon_3)-(1+\epsilon_4)\cos\ (\theta_1+\epsilon_5)] - K_1\ \ \epsilon_{16}'' + [(1+\epsilon_{12})\cos(\theta_2+\epsilon_{13})-(1+\epsilon_4)\cos\ (\theta_1+\epsilon_5)]}{K_1[(1+\epsilon_{12})\sin\ (\theta_2+\epsilon_{13})-(1+\epsilon_{14})\sin\ (\theta_1+\epsilon_{15})] - [(1+\epsilon_2)\sin\ (\theta_3+\epsilon_3) - (1+\epsilon_4)\sin(\theta_1+\epsilon_5)]}$$

where: $$K_1 = \frac{\frac{(1+\epsilon_7)}{(1+\epsilon_1)}\ \frac{r_1+\epsilon_9-r_3-\epsilon_8}{(r_3+\epsilon_9)(r_1+\epsilon_9} + \frac{\epsilon_{10}}{(1+\epsilon_1)}}{\frac{(1+\epsilon_{17})}{(1+\epsilon_{11})}\ .\frac{r_1+\epsilon_9-r_2-\epsilon_{18}}{(r_1+\epsilon_{19})(r_{12}+\epsilon_{18})} + \frac{\epsilon_{20}}{(1+\epsilon_{11})}},\quad \epsilon_6'' = \frac{\epsilon_6}{\cos\ \ \theta\rho},\quad \epsilon_{16}'' = \frac{\epsilon_{16}}{\cos\ \theta\rho}$$

NOTE: 1. For $\theta\rho$ small, $\epsilon_6 = \epsilon_6''$ and $\epsilon_{16} = \epsilon_{16}''$

2. For steps 1-6, the computed value of the unknown containing any accumulated errors, is carried forward as an insert in the next step.

FIGURE 4-7. STEP EQUATIONS

Step 2 (subsitute $\theta\rho$ for θ_3, $r\rho$ for r_3, solve for $r\rho$)

Bridge Equation

$$0 = (1+\epsilon_1)\frac{[(1+\epsilon_2)\cos\epsilon_3 - (1+\epsilon_4)\cos(\theta_1-\theta\rho+\epsilon_5)]+\epsilon_6}{(1+\epsilon_7)\left[\frac{1}{r\rho+\epsilon_8} - \frac{1}{r_1+\epsilon_9}\right] + \epsilon_{10}} - (1+\epsilon_{11})\frac{[(1+\epsilon_{12})\cos(\theta_2-\theta\rho+\epsilon_{13}) - (1+\epsilon_4)\cos(\theta_1-\theta\rho+\epsilon_5)]+\epsilon_{16}}{(1+\epsilon_{17})\left[\frac{1}{r_2+\epsilon_{18}} - \frac{1}{r_1+\epsilon_9}\right] + \epsilon_{20}} + \epsilon_{30}$$

Explicit Solution

$$r\rho = -\epsilon_8 + \frac{K_2\,(1+\epsilon_7)\,(r_1+\epsilon_9)}{(r_1+\epsilon_9)\,(1+\epsilon_7) + K_2\,(1+\epsilon_7 - \epsilon_{10}\,r_1 - \epsilon_{10}\,\epsilon_9)}$$

where $$K_2 = (1+\epsilon_7)\frac{(1+\epsilon_{11})\,[(1+\epsilon_{12})\cos(\theta_2+\epsilon_{13}-\theta\rho) - (1+\epsilon_4)\cos(\theta_1+\epsilon_5-\theta\rho) + \epsilon_{16}]}{(1+\epsilon_{17})(1+\epsilon_1)\left\{\left[\frac{1}{r_2+\epsilon_{18}} - \frac{1}{r_1+\epsilon_{19}}\right] + \frac{\epsilon_{20}}{(1+\epsilon_{17})}\right\}[(1+\epsilon_2)\cos\epsilon_3 - (1+\epsilon_4)\cos(\theta_1+\epsilon_5-\theta\rho) + \epsilon_6]}$$

NOTE: 1. ϵ_6 and ϵ_{16} may be obtained from Step 1 after solution of $\theta\rho$; ie $\epsilon_6 = \epsilon_6'' \cos\theta\rho$ and $\epsilon_{16} = \epsilon_{16}'' \cos\theta\rho$. See Note 1 of Step 1.

FIGURE 4-7. (continued)

Step 3 (substitute $r_c = r_2$, $\theta_c = \theta_c^2$, solve for θ_c)

Bridge Equation

$$0 = (1+\epsilon_1)\frac{[(1+\epsilon_2)\cos\epsilon_3 - (1+\epsilon_4)\cos(\theta_1-\theta\rho+\epsilon_5)]+\epsilon_6}{(1+\epsilon_7)\left[\frac{1}{r\rho+\epsilon_8} - \frac{1}{r_1\epsilon_9}\right] + \epsilon_{10}} - (1+\epsilon_{11})\frac{[(1+\epsilon_{12})\cos(\theta_c-\theta\rho+\epsilon_{13})-(1+\epsilon_4)\cos(\theta_1-\theta\rho+\epsilon_5)]\epsilon_{16}}{(1+\epsilon_{17})\left[\frac{1}{r_c+\epsilon_{18}} - \frac{1}{r_1+\epsilon_{19}}\right] + \epsilon_{20}} + \epsilon_{30}$$

Explicit Solution

$$\cos(\theta_c + \epsilon_{13} - \theta\rho) = \frac{[(1+\epsilon_2)\cos\epsilon_3 - (1+\epsilon_4)\cos(\theta_1+\epsilon_5-\theta\rho)] + \epsilon_6}{K_1\,(1+\epsilon_{12})} + \frac{(1+\epsilon_{14})}{1+\epsilon_{12}}\cos(\theta_1 + \epsilon_5 - \theta\rho) - \epsilon_{16}$$

$$\sin(\theta_c + \epsilon_{13} - \theta\rho) = [1 - \cos^2(\theta_c + \epsilon_{13} - \theta\rho)]^{1/2}$$

$$\theta_c = \arctan\frac{\sin(\theta_c + \epsilon_{13} - \theta\rho)}{\cos(\theta_c + \epsilon_{13} - \theta\rho)} - \epsilon_{13} + \theta\rho$$

NOTE: 1. Obtain K_1 from Step 1 with $r\rho = r_3$.

FIGURE 4-7. (continued)

Step 4 (substitute $\theta_1 = \theta_a = \theta_\rho + 180^o$, $r_1 = r_a$, solve for r_a)

Bridge Equation

$$0 = (1+\epsilon_1) \frac{[(1+\epsilon_2) \cos \epsilon_3 - (1+\epsilon_4) \cos (180^o+\epsilon_5)] + \epsilon_6}{(1+\epsilon_7) \quad [\frac{1}{r_\rho+\epsilon_8} - \frac{1}{r_a+\epsilon_9}] + \epsilon_{10}} - (1+\epsilon_{11}) \frac{[(1+\epsilon_{12})\cos (\theta_c - \theta_\rho + \epsilon_{13}) - (1+\epsilon_4)\cos (180^o+\epsilon_5)]\epsilon_{16}}{(1+\epsilon_{17}) \; [\frac{1}{r_c+\epsilon_{18}} - \frac{}{r_a+\epsilon_{19}}] + \epsilon_{20}} + \epsilon_{30}$$

Explicit Solution

$$r_a = \frac{K3 \; (1 + \epsilon_7) - (1 + \epsilon_{17})}{\epsilon_{10} \; K3 - \epsilon_{20} + K3 \frac{(1 + \epsilon_{17})}{r_\rho + \epsilon_8} - \frac{(1 + \epsilon_{17})}{r_c + \epsilon_8}} - \epsilon_9$$

where $$K_2 = \frac{(1 + \epsilon_{11}) \; [(1 + \epsilon_{12}) \cos (\theta_c + \epsilon_{13} - \theta \;) - (1 + \epsilon_4) \cos (180^o + \epsilon_{15}) + \epsilon_{16} \;]}{(1 + \epsilon_1) \;\; [(1 + \epsilon_2) \;\; \cos \;\; \epsilon_3 - (1 + \epsilon_4) \cos (180^o + \epsilon_5) + \epsilon_6 \;]}$$

FIGURE 4-7.(continued)

Step 5 - (change perigee and apogee by $\Delta r\rho$, solve for $\theta\rho'$)

Bridge Equation

$$0 = (1+\epsilon_1)\frac{[(1+\epsilon_2)\cos\epsilon_3 - (1+\epsilon_4)\cos(180^\circ+\epsilon_5)]+\epsilon_6}{(1+\epsilon_7)\left[\frac{1}{r\rho+\Delta r\rho+\epsilon_8} - \frac{1}{r_a-\Delta r\rho+\epsilon_9}\right] + \epsilon_{10}} - (1+\epsilon_{11})\frac{[(1+\epsilon_{12})\cos(\theta_c-\theta\rho'+\epsilon_{13})-(1+\epsilon_4)\cos(180^\circ+\epsilon_5)] + \epsilon_{16}}{(1+\epsilon_{17})\left[\frac{1}{r_c+\epsilon_{13}} - \frac{1}{r_a - \Delta r\rho + \epsilon_9}\right] + \epsilon_{20}} + \epsilon_{30}$$

Explicit Solution

$$\cos(\theta_c+\epsilon_{13}-\theta\rho') = \frac{\dfrac{(1+\epsilon_{17})}{(1+\epsilon_7)} \circ \dfrac{\left[\frac{1}{r_c+\epsilon_{18}} - \frac{1}{r_a-\Delta r\rho+\epsilon_9}\right]+\epsilon_{20}}{\left[\frac{1}{r\rho+\Delta r\rho+\epsilon_8} - \frac{1}{r_a-\Delta r\rho+\epsilon_9}\right]+\epsilon_{10}} \cdot \dfrac{(1+\epsilon_1)}{(1+\epsilon_{11})} \cdot [(1+\epsilon_2)\cos\epsilon_3-(1+\epsilon_4)\cos(180^\circ+\epsilon_5)+\epsilon_6]+(1+\epsilon_4)\cos(180^\circ+\epsilon_5)-\epsilon_{16}}{(1+\epsilon_{12})}$$

$$\sin(\theta_c + \epsilon_{13} - \theta\rho') = [1 - \cos^2(\theta_c + \epsilon_{13} - \theta\rho')]^{1/2}$$

$$\theta\rho' = \arctan\frac{\sin(\theta_c + \epsilon_3 - \theta\rho')}{\cos(\theta_c + \epsilon_{13} - \theta\rho')} - \theta_c - \epsilon_{13}$$

FIGURE 4-7.(continued)

Step 6a. (Remove all sources of error except $\theta\rho'$ from Step 5, solve for $\Delta r\rho$. All other quantities are the nominal computed values.)

Bridge Representation

$$\frac{2}{\dfrac{1}{r\rho + \Delta r\rho} - \dfrac{1}{r_2 - \Delta r\rho}} = \frac{\cos(\theta_c - \theta\rho') + 1}{\dfrac{1}{r_c} - \dfrac{1}{r_a - \Delta r\rho}}$$

Explicit Solution (see Note 1)

$$\Delta r\rho = -\frac{[r\rho - r_a + r_c(1 - 2K_4)]}{2} \pm \frac{1}{2}\left[\left[r\rho - r_a + r_c(1 - 2K_4)\right]^2 + 4r\rho(r_a - r_c) - 4K_4 r_c(r_a - r\rho)\right]^{1/2}$$

where $K_4 = \dfrac{\cos(\theta_c - \theta\rho') + 1}{2}$

Step 6b. (When $r_a > 100 \times 10^6$ KM, as in parabola)

Bridge Representation

$$\frac{2}{\dfrac{1}{r\rho + \Delta r\rho}} = \frac{\cos(\theta_c - \theta\rho') + 1}{\dfrac{1}{r_c}}$$

Explicit Solution

$$\Delta r\rho = K_4 r_c - r\rho$$

NOTE: 1. The (-) Sign of the second term in 6a applies for this study, since the corrective maneuver is initiated subsequent to passing the minor axis of the ellipse.

2. This step is utilized for error analysis only and has no counterpart in the actual manual computer operation.

FIGURE 4-7. (continued)

Step 7. Galvanometer Range and Sensitivity Investigation.

Step 7a. (Bridge Condition - Step 2 with all error sources removed and nominal values inserted. Vary $\Delta\theta\rho$, obtain the variation in n)

$$n = \frac{r_1\, r\rho\, [1 - \cos(\theta_1 - \theta\rho - \Delta\theta\rho)]}{r_1 - r\rho} - \frac{r_1\, r_2\, [\cos(\theta_2 - \theta\rho - \Delta\theta\rho) - \cos(\theta_1 - \theta\rho - \Delta\theta\rho)]}{r_1 - r_2}$$

Step 7b. (Bridge Condition - Step 2 with all error sources removed and nominal values inserted. Vary $\Delta r\rho = \epsilon_8$ and obtain the variation in ϵ_{30})

$$\epsilon_{30} = - \frac{(r\rho + \epsilon_8)\, r_1\, [1 - \cos(\theta_1 - \theta\rho)]}{r_1 - r\rho - \epsilon_8} + \frac{r_1\, r_2\, [\cos(\theta_2 - \theta\rho) - \cos(\theta_1 - \theta\rho)]}{r_1 - r_2}$$

Step 7c. (Bridge Condition - Step 1 with all error sources removed and nominal values inserted. Vary $\Delta\theta\rho$, obtain variation in ϵ_{30}.)

$$\epsilon_{30} = r_1\, r_2\, \frac{[\cos(\theta_2 - \theta\rho - \Delta\theta\rho) - \cos(\theta_1 - \theta\rho - \Delta\theta\rho)}{r_1 - r_2} - \frac{r_1\, r_3 [\cos(\theta_3 - \theta\rho - \Delta\theta\rho) - \cos(\theta_1 - \theta\rho - \Delta\theta\rho)]}{r_1 - r_3}$$

NOTE: 1. Values of $\Delta\theta\rho$ utilized were $\pm \frac{10}{3600}$ deg., $\pm \frac{60}{3600}$ deg. $\pm \frac{300}{3600}$ deg., $\pm \frac{1}{2}$ deg., ± 2 deg., ± 5 deg., ± 10 deg., ± 20 deg.

Values of $\Delta r\rho$ utilized were ± 1 KM, ± 5 KM, ± 10 KM, ± 20 KM, ± 50 KM, ± 100 KM, ± 150 KM, ± 1000 KM.

FIGURE 4-7. (Concluded)

Observation	Error Designation	1σ Value (Note 1)	Reference ϵ	Affects Bridge Equations Steps (Note 2)
θ_1	$\epsilon\theta_1$	± 10 sec	ϵ_5	1, 2, 3 only
θ_2	$\epsilon\theta_2$	"	ϵ_{13}	1, 2 only
θ_3	$\epsilon\theta_3$	"	ϵ_3	1 only
r_1	ϵr_1	$\epsilon\beta = \pm 10$ sec	ϵ_9	1, 2, 3 only
r_2	ϵr_2	"	ϵ_{18}	1, 2 only
r_3	ϵr_3	"	ϵ_8	1 only
r_c	ϵr_c	"	ϵ_{18}	3, 4, 5 only

NOTES: 1. $\epsilon\beta$ is the sextant error in measuring β, the angle subtended by the earth from the point concerned. $\epsilon r = -\epsilon\beta \cdot \frac{r}{2} \operatorname{ctn} \beta/_2$.

2. Bridge equations and steps are presented in Figure 4-7.

FIGURE 4-8 - Manual Space Computer Schedule of Observational Errors using nominal error source values for backup purposes or possible future reference. This was the case for many of the scale type errors having the form $(1+\epsilon)$.

In the program, Θp and rp are obtained from steps 1 and 2 and the errors $\epsilon\Theta p$ and ϵrp are calculated as the difference between the nominal values of Θp and rp and those obtained with error. $\Theta p'$ and rp' are obtained from steps 5 and 6 of the sequence and the errors $\epsilon\Theta p'$ and $\epsilon rp'$ are taken relative to the nominal (perfect) solutions for $\Theta p'$ and rp'. It is noted that step 6 is used for purposes of error analysis only and has no counterpart in the actual manual computer operation. From step 6 the error in perigee radius corresponding to a change in perigee with error versus a change without error is obtained. The signs of the errors as printed out are governed by rules which provide an insight into the relationship of the erroneous solutions relative to the nominal ones. For example, a negative value for ϵrp indicates that the erroneous solution for rp resulted in a perigee below (in altitude) that of the nominal solution. Also, for example, a positive value for $\epsilon\Theta p$ indicates that the erroneous solution for Θp resulted in a perigee ccw from the nominal one (see notation for Θp, Figure 4-2). This sign convention also applies to the printout of the two body vs. four and earth oblateness errors, $\epsilon rp''$ and $\epsilon\Theta p''$, relative to the NASA data (i.e. the desired perigee) and to the errors due to the parabolic assumption of corrective maneuver, $\epsilon rp'''$ and $\epsilon\Theta p'''$, taken relative to rp' and $\Theta p'$.

Figures 4-9 and 4-10 are sample sheets showing the program outputs for the nominal solution, indicated by EP(O, O), and for typical error source inputs. The first number in the parenthesis following the EP stands for a J number which corresponds to a given ϵ number. A table, not shown, is needed to relate all the J numbers to the equivalent ϵ numbers in the step equations. However, in the cases shown, J1, 2, 6 and 7 do correspond to $\epsilon 1$, 2, 6 and 7. The second number in the parenthesis stands for a K number which is a specific numerical value of the error source input. Each numerical input was evaluated first for its (+) value and then for its (-) value to test for linearity. This test was supplemented, generally, by introducing relatively large (+) and (-) error values for the K9 and 10 inputs. For example, K9 and 10 of $\epsilon 1$ correspond to a ±1.15% variation in the bridge trim parameter $(1+\epsilon 1)$. The results indicate good linearity even for this rather large error. The same thing is evident for K9 and 10 of $\epsilon 6$ which corresponds to a bias of ±0.0058 in the $(\Theta_3 - \Theta p)$ cosine mechanism. Satisfactory linearity in the results was obtained for all source errors and problems programmed.

MANUAL SPACE COMPUTER ERROR ANALYSIS

PROBLEM NUMBER 1.1.2 PAGE 2

ERROR	THETA(P) E(THP)PP	R(F) E(RP)PP	THETA(C) E(THC)PP	R(A) E(TP)	THETA(P)P E(RP)	+DELTA R(P) E(THP)P	-DELTA R(P) E(RP)P
EP(0, 0)	0.3599435E 03 -0.5647542E-01	0.6433447E 04 0.3446899E 01	0.2643151E 03 0.2622793E-02	0.5924613E 05 0.	0.3599743E 03 0.	0.5157360E 05 0.	-0.3446533E 01 0.3662109E-03
EP(1, 1)	0.3599431E 03 -0.5647542E-01	0.6433545E 04 0.3446899E 01	0.2643203E 03 0.2622793E-02	0.5924406E 05 -0.3893208E-03	0.3599748E 03 0.9808350E-01	0.5157355E 05 0.4883585E-03	-0.3501221E 01 -0.5432129E-01
EP(1, 2)	0.3599439E 03 -0.5647542E-01	0.6433348E 04 0.3446899E 01	0.2643098E 03 0.2622793E-02	0.5924819E 05 0.3893208E-03	0.3599738E 03 -0.9918213E-01	0.5157366E 05 -0.4986038E-03	-0.3390625E 01 0.5627441E-01
EP(1, 3)	0.3599412E 03 -0.5647542E-01	0.6434052E 04 0.3446899E 01	0.2643466E 03 0.2622793E-02	0.5923382E 05 -0.2346170E-02	0.3599773E 03 0.6051025E 00	0.5157328E 05 0.3073585E-02	-0.3790771E 01 -0.3438721E-00
EP(1, 4)	0.3599459E 03 -0.5647542E-01	0.6432846E 04 0.3446899E 01	0.2642836E 03 0.2622793E-02	0.5925841E 05 0.2342755E-02	0.3599712E 03 -0.6012573E 00	0.5157393E 05 -0.3036019E-02	-0.3106201E 01 0.3406982E-00
EP(1, 5)	0.3599318E 03 -0.5647542E-01	0.6436459E 04 0.3446899E 01	0.2644725E 03 0.2622793E-02	0.5918495E 05 -0.1172743E-01	0.3599896E 03 0.3011902E 01	0.5157197E 05 0.1530304E-01	-0.5161377E 01 -0.1714477E 01
EP(1, 6)	0.3599552E 03 -0.5647542E-01	0.6430439E 04 0.3446899E 01	0.2641578E 03 0.2622793E-02	0.5930788E 05 0.1171377E-01	0.3599591E 03 -0.3008240E 01	0.5157522E 05 -0.1514253E-01	-0.1749756E 01 0.1697144E 01
EP(1, 7)	0.3599200E 03 -0.5647542E-01	0.6439469E 04 0.3446899E 01	0.2646300E 03 0.2622793E-02	0.5912431E 05 -0.2346511E-01	0.5003113E-02 0.6021728E 01	0.5157032E 05 0.3071878E-01	-0.6889404E 01 -0.3442505E 01
EP(1, 8)	0.3599669E 03 -0.5647542E-01	0.6427433E 04 0.3446899E 01	0.2640006E 03 0.2622793E-02	0.5937018E 05 0.2341389E-01	0.3599441E 03 -0.6014160E 01	0.5157682E 05 -0.3013821E-01	-0.6933594E-01 0.3377563E 01
EP(1, 9)	0.3598965E 03 -0.5647542E-01	0.6445505E 04 0.3446899E 01	0.2649455E 03 0.2622793E-02	0.5900459E 05 -0.4698487E-01	0.3636393E-01 0.1205835E 02	0.5156698E 05 0.6207959E-01	-0.1040405E 02 -0.6957153E 01
EP(1,10)	0.3599903E 03 -0.5647542E-01	0.6421434E 04 0.3446899E 01	0.2636867E 03 0.2622793E-02	0.5949644E 05 0.4677313E-01	0.3599146E 03 -0.1201288E 02	0.5157997E 05 -0.5963780E-01	0.3235840E 01 0.6682739E 01
EP(2, 1)	0.3599441E 03 -0.5647542E-01	0.6432239E 04 0.3446899E 01	0.2643074E 03 0.2622793E-02	0.5924813E 05 0.5669057E-03	0.3599641E 03 -0.1208496E 01	0.5157470E 05 -0.1021796E-01	-0.2301514E 01 0.1145386E 01
EP(2, 2)	0.3599429E 03 -0.5647542E-01	0.6434655E 04 0.3446899E 01	0.2643227E 03 0.2622793E-02	0.5924412E 05 -0.5669057E-03	0.3599845E 03 0.1207519E 01	0.5157251E 05 0.1020772E-01	-0.4590332E 01 -0.1143433E 01
EP(2, 3)	0.3599469E 03 -0.5647542E-01	0.6426200E 04 0.3446899E 01	0.2642694E 03 0.2622793E-02	0.5925822E 05 0.3401434E-02	0.3599130E 03 -0.7247131E 01	0.5158015E 05 -0.6128046E-01	0.3419922E 01 0.6866821E 01
EP(2, 4)	0.3599401E 03 -0.5647542E-01	0.6440695E 04 0.3446899E 01	0.2643607E 03 0.2622793E-02	0.5923403E 05 -0.3401434E-02	0.3554772E-01 0.7247986E 01	0.5156706E 05 0.6126338E-01	-0.1031250E 02 -0.6865600E 01
EP(2, 5)	0.3599605E 03 -0.5647542E-01	0.6397210E 04 0.3446899E 01	0.2640865E 03 0.2622793E-02	0.5930705E 05 0.1702083E-01	0.3596676E 03 -0.3623657E 02	0.5160638E 05 -0.3066413E-00	0.3090234E 02 0.3434924E 02
EP(2, 6)	0.3599265E 03 -0.5647542E-01	0.6469706E 04 0.3446899E 01	0.2645433E 03 0.2622793E-02	0.5918599E 05 -0.1700717E-01	0.2805329E-00 0.3625940E 02	0.5154093E 05 0.3062486E-00	-0.3777710E 02 -0.3433020E 02

FIGURE 4-9 SAMPLE TABULATION - PROGRAM OUTPUTS FOR NOMINAL SOLUTION

MANUAL SPACE COMPUTER ERROR ANALYSIS

PROBLEM NUMBER 1.1.2 PAGE 5

ERROR	THETA(P) E(THP)PP	R(P) E(RP)PP	THETA(C) E(THC)PP	R(A) E(THP)	THETA(P)P E(RP)	+DELTA R(P) E(THP)P	-DELTA R(P) E(RP)P
EP(6, 1)	0.3599415E 03	0.6436156E 04	C.2643417E 03	C.5923908E 05	C.3599965E 03	0.5157123E 05	-0.5933594E 01
	-0.5647542E-C1	0.3446899E C1	C.2622793E-02	-0.1984170E-02	C.27C8679E 01	0.2219470E-01	-0.2486694E 01
EP(6, 2)	0.3599455E 03	C.6430736E 04	C.2642884E 03	C.5925319E 05	C.3599521E 03	0.5157598E 05	-0.9582520E 00
	-0.5647542E-C1	0.3446899E C1	C.2622793E-02	0.1984170E-02	-0.271C632E 01	-C.222C494E-01	0.2488647E 01
EP(6, 3)	0.3599405E C3	0.6437509E 04	C.2643550E 03	0.5923555E 05	0.7574680E-02	0.5157005E 05	-0.7177490E 01
	-0.5647542E-C1	0.3446899E 01	C.2622793E-02	-0.2974547E-02	0.4C62378E 01	0.3329034E-01	-0.3730591E 01
EP(6, 4)	0.3599465E C3	C.6429382E 04	C.2642751E 03	0.5925674E 05	0.359941CE 03	0.5157716E 05	0.2854004E-00
	-C.5647542E-C1	0.3446899E C1	C.2622793E-02	0.2974547E-02	-C.4C65369E 01	-C.333040CE-01	0.3732300E 01
EP(6, 5)	C.3599425E C3	0.6434800E 04	C.2643284E 03	C.5924259E 05	C.3599854E C3	0.5157242E 05	-0.4688721E 01
	-C.5647542E-C1	C.3446899E C1	C.2622793E-02	-C.9903774E-03	C.1352661E 01	0.110854CE-01	-0.1241821E 01
EP(6, 6)	C.3599445E C3	C.6432093E 04	C.2643018E 03	0.5924966E 05	C.3599632E 03	C.5157479E 05	-0.2203613E 01
	-C.5647542E-C1	0.3446899E 01	C.2622793E-02	C.9903774E-03	-C.1353943E C1	-0.1109223E-01	0.1243286E 01
EP(6, 7)	C.3599411E C3	0.6436703E 04	C.2643471E 03	C.5923764E 05	C.963C567E-03	C.5157075E 05	-0.6436768E 01
	-C.5647542E-C1	C.3446899E C1	C.2622793E-02	-C.2383736E-02	C.3255676E C1	C.2667872E-01	-0.2989868E 01
EP(6, 8)	C.3599459E C3	C.643C188E C4	C.2642830E 03	0.5925460E 05	C.3599476E 03	0.5157646E 05	-0.4545898E-00
	-C.5647542E-C1	C.3446899E 01	C.2622793E-02	C.2383736E-02	-C.3259155E 01	-C.2669921E-01	0.2992310E 01
EP(6, 9)	C.3598840E C3	C.6514358E 04	C.2651134E 03	C.5903895E 05	C.6394457E CC	C.515C272E 05	-0.7804175E 02
	-C.5647542E-C1	0.3446899E C1	C.2622793E-02	-0.5951144E-01	C.8C91101E 02	0.6651614E 0C	-0.7459485E 02
EP(6,1C)	C.3C374138E-C2	C.6351729E C4	C.2635153E 03	C.5946246E 05	C.3593069E C3	C.516450CE 05	0.7128101E 02
	-C.5647542E-C1	C.3446899E 01	C.2622793E-02	C.5951445E-01	-C.8171832E C2	-C.6674153E 00	0.7472790E 02
EP(7, 1)	C.3599439E C3	C.6433348E C4	C.2643098E 03	C.5924815E 05	C.3599738E 03	C.5157366E 05	-0.3390625E 01
	-C.5647542E-C1	0.3446899E C1	C.2622793E-02	0.3893208E-03	-0.9936523E-01	-C.4986C38E-03	0.5627441E-01
EP(7, 2)	C.3599431E C3	C.6433545E 04	C.2643203E 03	C.5924406E 05	C.3599748E 03	C.5157355E 05	-0.3500732E 01
	-C.5647542E-C1	C.3446899E 01	C.2622793E-02	-C.3893208E-03	C.9796143E-01	0.4849434E-03	-0.5383301E-01
EP(7, 3)	C.3599459E C3	C.6432844E 04	C.2642836E 03	C.5925841E 05	0.3599712E C3	C.5157393E 05	-0.3104248E 01
	-C.5647542E-C1	0.3446899E C1	C.2622793E-02	0.2342755E-02	-C.6C32104E 00	-0.3053C94E-02	0.3426514E-00
EP(7, 4)	C.3599412E C3	C.6434C50E 04	C.2643466E 03	C.5923382E 05	C.3599773E 03	C.5157328E 05	-0.3788818E 01
	-C.5647542E-C1	0.3446899E C1	C.2622793E-02	-0.2346170E-02	C.6C31494E 0C	C.3C5651CE-02	-0.3419189E-00
EP(7, 5)	C.3599552E C3	0.643C446E 04	C.2641582E 03	0.5930766E 05	0.3599592E 03	C.5157522E 05	-0.1753418E 01
	-C.5647542E-C1	0.3446899E 01	C.2622793E-02	0.1167962E-01	-C.3C0C671E 01	-0.1510838E-01	0.1693481E 01
EP(7, 6)	C.3599318E C3	0.6436467E C4	C.2644729E 03	0.5918477E 05	C.3599896E 03	0.5157197E 05	-0.5165527E 01
	-C.5647542E-01	0.3446899E 01	C.2622793E-02	-0.1176158E-01	0.3C2C203E 01	0.1534060E-01	-0.1718628E 01
EP(7, 7)	C.3599668E 03	0.6427465E 04	C.2640024E 03	C.5936944E 05	0.3599443E 03	0.5157681E 05	-0.8666992E-01
	-C.5647542E-C1	0.3446899E C1	C.2622793E-02	0.2328070E-01	-0.5981628E 01	-0.2998453E-01	0.3360229E 01

FIGURE 4-10 SAMPLE TABULATION - TYPICAL ERROR SOURCE INPUTS

4.5 Two Body vs. Four Body and Earth Oblateness Effects

Since the NASA abort trajectories contain the four body and earth oblateness effects, $\epsilon rp''$ and $\epsilon \Theta p''$ are obtained simply by taking the difference between perigee (rp'' and $\Theta p''$) for those results, and the nominal perigee (rp and Θp) solution, steps 1 and 2, by the manual computer. Referring to Figure 4-9, it can be seen that these errors are printed out as the first two errors on the second line. The error $\epsilon \Theta_c''$, representing the difference between Θ_c'' of the NASA data and Θ_c of the manual computer is also printed out although it has no direct use in the program.

4.6 Errors Due to Parabolic Assumption of Corrective Maneuver

As described in Section 2, the computation of the velocity increment and vehicle orientation for its application is based on the simplifying assumptions of a parabolic trajectory for the corrective maneuver. The manual computer corrective maneuver computation uses the incremental change in perigee angle, $\Delta \Theta p$, which is generated after inserting a desired change in perigee radius, Δrp, in the general conic equation. The velocity increment $\Delta V = V_{PAB} \times \Delta \phi$ is then applied perpendicular to an assumed parabolic flight path at the selected corrective point. From this it is assumed that the direction but not the magnitude of velocity vector is changed, preserving the same level of orbital energy. The simplifying assumptions made are

a. $\Delta \phi = \dfrac{\Delta \Theta}{2}$, which is true only if the trajectory is a parabola.

b. The vehicle has parabolic (escape) velocity at the correction point.

c. That it is satisfactory to apply the velocity increment normal to an assumed parabolic trajectory.

The program determines the errors due to these assumptions for each problem by first calculating the actual perigee (rp''' and $\Theta p'''$) that would result under two body theory from the application of the computed velocity increment to the existing nominally computed orbit at the correction point. These results are then compared with the simulated nominal manual computer solutions for revised perigee (rp' and $\Theta p'$).

$$\epsilon\Theta p''' = \Theta p''' - \Theta p' = (\Theta c - \Theta p') - (\Theta c - \Theta p''') \qquad \text{IV-2}$$

$$\epsilon rp''' = rp''' - rp' \qquad \text{IV-3}$$

The geometry involved in these error determinations is given in Figure 4-11.

Inputs to this portion of the program are obtained from the nominal computed problem solutions. Inputs are Θp, rp, Θ_a, ra, Θ_c, rc, $\Theta p'$ and rp'. The following input calculations are performed:

$$\Delta rp = rp' - r_p = rp'_D - rp_N \qquad \text{IV-4}$$

$$a = \frac{ra + rp}{2} \qquad \text{IV-5}$$

$$e = \frac{ra - rp}{ra + rp} \qquad \text{IV-6}$$

$$\Delta\Theta p = \Theta p' - \Theta p \qquad \text{IV-7}$$

$$\Delta\Theta = \frac{\Delta\Theta p}{2} \quad \text{radians} \qquad \text{IV-8}$$

Next the velocity on the ellipse at the point c is determined by means of the following equations. This velocity is resolved into its horizontal and vertical components (refer to Figure 4-12).

$$\cos \phi_c = (+) \left[\frac{1 + e \cos (\Theta_c - \Theta p)}{2 - rc/a}\right]^{1/2} \qquad \text{IV-9}$$

$$\sin \phi_c = \left[1 - \cos^2 \phi c\right]^{1/2} \qquad \text{IV-10}$$

$$Vc = (+) \left[\mu \left(\frac{2}{r_c} - \frac{1}{a}\right)\right]^{1/2} \qquad \text{IV-11}$$

$$V_{RC} = Vc \sin \phi c \qquad \text{IV-12}$$

$$V_{HC} = Vc \cos \phi c \qquad \text{IV-13}$$

$$\phi c = (+) \tan^{-1} \left[\frac{\sin \phi c}{\cos \phi c}\right] \qquad \text{IV-14}$$

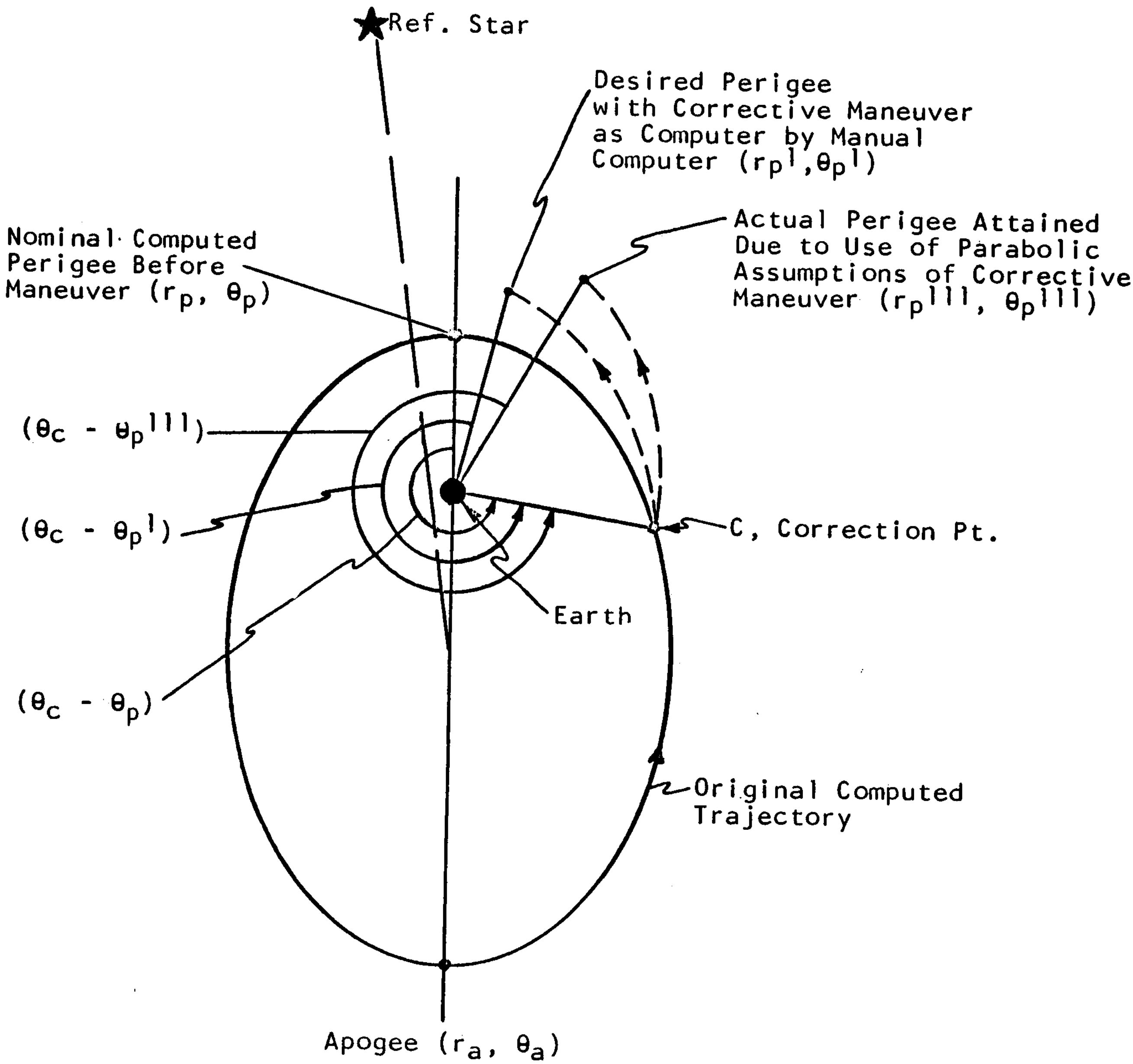

Figure 4 - 11

Geometry for Error Determination
Due to Parabolic Assumption of Corrective Maneuver

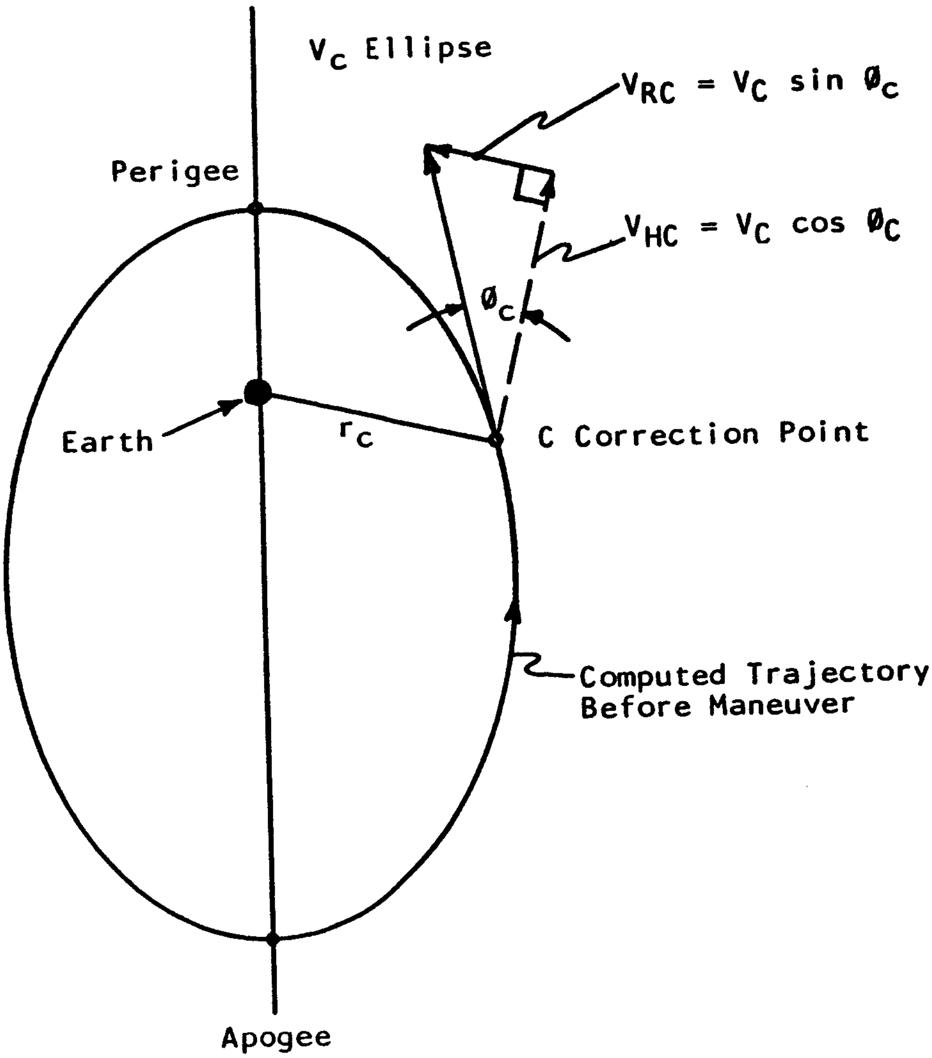

Figure 4 - 12

Resolution of Present Velocity
into Radial and Horizontal Components
for Error Determination of Parabolic Assumption
of Corrective Maneuver

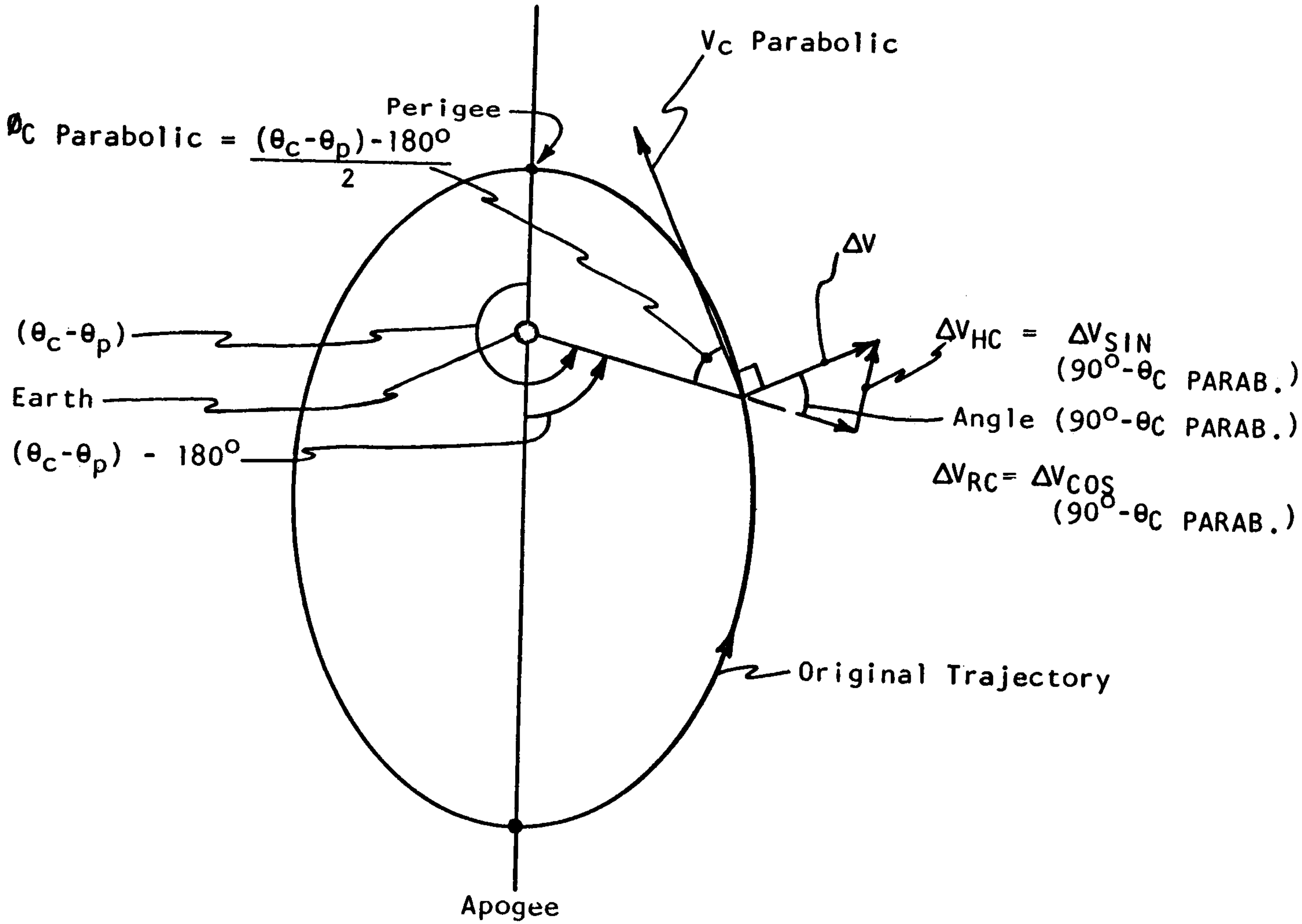

Figure 4 - 13

Resolution of Velocity Increment
for Error Determination of Parabolic Assumption

Next the magnitude of ΔV is computed:

$$V_{PAB} = \left[\frac{2\mu}{r_c}\right]^{1/2} \qquad \text{IV-15}$$

$$\Delta V = (+)\ (V_{PAB})\ (\Delta\phi) \qquad \text{IV-16}$$

where to avoid ambiguity the sign of ΔV is always taken as positive. The horizontal and radial components of ΔV are computed (refer to Figure 4-13):

$$\Delta V_{RC} = \Delta V \ \cos \ (90° - \phi_{C\ PAB}) \qquad \text{IV-17}$$

$$\Delta V_{HC} = \Delta V \ \sin \ (90° - \phi_{C\ PAB}) \qquad \text{IV-18}$$

Then the new velocity at point c in radial and horizontal components is

$$V_{RC}''' = V_{RC} \mp \Delta V_{RC} \qquad \text{IV-19}$$

$$V_{HC}''' = V_{HC} \pm \Delta V_{HC} \qquad \text{IV-20}$$

where the sign of the ΔV terms is taken relative to the signs $\pm$ of Δrp (see IV-4).

V_C''' is obtained.

$$V_C''' = \left[(V_{RC}''')^2 + (V_{HC}'''^2\right]^{1/2} \qquad \text{IV-21}$$

Now since all the trajectories encountered are elliptical, the following set of equations are utilized to obtain $(\Theta c - \Theta p''')$ and rp'''.

$$h''' = (rc)\ (V_{HC}''') \qquad \text{IV-22}$$

$$a''' = \frac{(rc)\ (\mu\ )}{2\mu - (V_C''')^2 r_c} \qquad \text{IV-23}$$

$$e''' = 1 - \frac{(h''')^2}{(\mu)\ (a''')}\ \ 1/2 \qquad \text{IV-24}$$

$$l''' = (a''')\ \ 1 - (e''')^2 \qquad \text{IV-25}$$

$$(\Theta c - \Theta p''') = \cos^{-1}\left[\frac{1''' - rc}{(rc)\ e'''}\right] \qquad \text{IV-26}$$

$$rp''' = a'''\,(1 - e''') \qquad \text{IV-27}$$

The results of equations IV-26 and 27 are utilized in equations IV-2 and 3 to obtain the error sought.

A sample sheet showing program inputs and outputs for the parabolic assumption analysis is given by Figure 4-14.

4.7 Galvanometer Range and Sensitivity Investigation

In order to obtain an insight into the percentage variation in the bridge null difference versus percentage variations in the quantities Θp and rp, the investigation indicated as step 7 of Figure 4-7 was programmed. Of particular interest are steps 7b and 7c. In step 7b, variations in ϵ_{30} (the null quantity) are obtained versus variations in rp according to note 1. In step 7c variations in ϵ_{30} are obtained versus variations in Θp according to note 1. The information obtained enables one to determine the minimum discernable error in rp and Θp vs. any desired scale range in these quantities for a given galvanometer sensitity (say 1%). Figure 4-15 is a sample sheet showing the program outputs for step 7, at the bottom. The top two lines of sixteen numbers correspond to the outputs of step 7a for the sixteen indicated values of $\Delta\Theta p$ in note 1, in the order stated. The third and fourth lines of 16 numbers for ϵ_{30} correspond to step 7b and the noted variations in Δrp. The same applies for the fifth and sixth lines and step 7c.

4.8 Alternate Counter Investigation

As part of this study, the feasibility of increasing accuracy by includi[ng] alternate counters at the output of the $(\Theta_3 - \Theta p)$ differential or at the output of the $(\Theta_3 - \Theta p)$ cosine mechanism was investigated. The idea was to minimize error by bypassing these components on step 2 when Θ_3 is matched to Θp. Similar counters were investigated for the operations of step 4 where Θ_1 is equated to $\Theta a = \Theta p + 180°$. However, since it was found that no improvement in accuracy could be obtained (due to the fact that the cosine function is insensiti[ve] to errors around zero and 180° anyway), details and results of this investigation have been omitted in this report.

MANUAL SPACE COMPUTER ERROR ANALYSIS

PROBLEM NUMBER 1.1.2 PAGE 19

INPUT SUMMARY

R(A) KM	R(C) KM	R(P) KM	R(P)P KM	THETA(A) DEG	THETA(C) DEG	THETA(P) DEG	THETA(P)P DEG
0.5924613E 05	0.1260025E 05	0.6433447E 04	0.6430000E 04	0.1799435E 03	0.2643151E 03	0.3599435E 03	0.3599743E 03

INPUT CALCULATIONS AND CONSTANTS

DELTA R(P) KM	A KM	E	MU KM3/SEC2	DELTA PHI RAD	DELTA THETA(P) DEG
-0.3446899E 01	0.3283979E 05	0.8040960E 00	0.3986135E 06	0.2684295E-03	0.3075976E-01

OUTPUT SUMMARY

COS(PHI(C))	SIN(PHI(C))	PHI(C) DEG	PHI(C)PAB DEG	THETA(CP)PPP DEG	E(THETA(P)PPP DEG
0.7549175E 00	0.6558198E 00	0.4098184E 02	0.4218577E 02	0.2643333E 03	0.7465363E-02

VC KM/SEC	VCPPP KM/SEC	VHC KM/SEC	VHCPPP KM/SEC	VRC KM/SEC	VRCPPP KM/SEC	VPAB KM/SEC	DELV KM/SEC
0.7150705E 01	0.7150518E 01	0.5358192E 01	0.5396610E 01	0.4689573E 01	0.4691007E 01	0.7954288E 01	0.2135166E-02

APPP KM	EPPP	HPPP KM2/SEC	LPPP	R(P)PPP KM	E(R(P))PPP KM
0.3282997E 05	0.8041591E 00	0.6799866E 05	0.1159975E 05	0.6429451E 04	-0.5493774E 00

FIGURE 4-14

SAMPLE TABULATION - PROGRAM FOR PARABOLIC ASSUMPTION OF CORRECTIVE MANEUVER

MANUAL SPACE COMPUTER ERROR ANALYSIS

PROBLEM NUMBER 1.1.2

ERROR	THETA(P) E(THP)PP	R(P) E(RP)PP	THETA(C) E(THC)PP	R(A) E(THP)	THETA(P)P E(RP)	+DELTA R(P) E(THP)P	-DELTA R(P) E(RP)P
EP(2E, 2)	0.3599427E 03	0.6433447E 04	0.2643151E 03	0.5924608E 05	0.3599735E 03	0.5157369E 05	-0.3356689E 01
	-0.5647542E-01	0.3446899E 01	0.2622793E-02	-0.8025472E-03	0.	-0.8025472E-03	0.9020996E-01
EP(2E, 3)	0.3599450E 03	0.6433449E 04	0.2643151E 03	0.5924609E 05	0.3599757E 03	0.5157345E 05	-0.3610352E 01
	-0.5647542E-01	0.3446899E 01	0.2622793E-02	0.1441170E-02	0.2197266E-02	0.1461660E-02	-0.1634521E-00
EP(2E, 4)	0.3599421E 03	0.6433447E 04	0.2643151E 03	0.5924608E 05	0.3599728E 03	0.5157376E 05	-0.3284668E 01
	-0.5647542E-01	0.3446899E 01	0.2622793E-02	-0.1444585E-02	0.	-0.1444585E-02	0.1622314E-00
EP(2E, 5)	0.3599531E 03	0.6433447E 04	0.2643151E 03	0.5924608E 05	0.3599839E 03	0.5157258E 05	-0.4524902E 01
	-0.5647542E-01	0.3446899E 01	0.2622793E-02	0.9623736E-02	0.	0.9623736E-02	-0.1078003E 01
EP(2E, 6)	0.3599339E 03	0.6433449E 04	0.2643151E 03	0.5924608E 05	0.3599647E 03	0.5157463E 05	-0.2369873E 01
	-0.5647542E-01	0.3446899E 01	0.2622793E-02	-0.9627151E-02	0.2258301E-02	-0.9606661E-02	0.1077026E 01
EP(2E, 7)	0.3599550E 03	0.6433449E 04	0.2643151E 03	0.5924608E 05	0.3599858E 03	0.5157237E 05	-0.4740234E 01
	-0.5647542E-01	0.3446899E 01	0.2622793E-02	0.1152594E-01	0.2258301E-02	0.1154643E-01	-0.1293335E 01
EP(2E, 8)	0.3599320E 03	0.6433447E 04	0.2643151E 03	0.5924608E 05	0.3599627E 03	0.5157484E 05	-0.2154541E 01
	-0.5647542E-01	0.3446899E 01	0.2622793E-02	-0.1152936E-01	0.	-0.1152936E-01	0.1292358E 01
EP(2E, 9)	0.3599916E 03	0.6433450E 04	0.2643151E 03	0.5924601E 05	0.2242009E-01	0.5156846E 05	-0.8841309E 01
	-0.5647542E-01	0.3446899E 01	0.2622793E-02	0.4810844E-01	0.3234863E-02	0.4813576E-01	-0.5394409E 01
EP(2E,10)	0.3598954E 03	0.6433448E 04	0.2643151E 03	0.5924600E 05	0.3599262E 03	0.5157874E 05	0.1943359E 01
	-0.5647542E-01	0.3446899E 01	0.2622793E-02	-0.4811185E-01	0.9765625E-03	-0.4810161E-01	0.5390259E 01
0.1169372E 02	-0.1169641E 02	0.7017934E 02	-0.7017896E 02	0.3508976E 03	-0.3508865E 03	0.2105621E 04	-0.2105066E 04
0.8424246E 04	-0.8415302E 04	0.2105495E 05	-0.2099906E 05	0.4200554E 05	-0.4178242E 05	0.8295788E 05	-0.8207219E 05
-0.2561035E 01	0.2500669E 01	-0.1280591E 02	0.1250310E 02	-0.2561461E 02	0.2560327E 02	-0.5124060E 02	0.5119543E 02
-0.1281856E 03	0.1279041E 03	-0.2566538E 03	0.2555280E 03	-0.3854053E 03	0.3828721E 03	-0.2618449E 04	0.2505819E 04
-0.9842773E 01	0.9893677E 01	-0.5919397E 02	0.5924304E 02	-0.2960669E 03	0.2961167E 03	-0.1776529E 04	0.1776581E 04
-0.7104844E 04	0.7104697E 04	-0.1774322E 05	0.1774327E 05	-0.3535143E 05	0.3535149E 05	-0.6962876E 05	0.6962881E 05

FIGURE 4-15

SAMPLE TABULATION - PROGRAM OUTPUTS FOR GALVANOMETER RANGE AND SENSITIVITY INVESTIGATION

5. RESULTS OF ACCURACY ANALYSIS

The results of the accuracy analysis for the twenty-four cases studied are presented in Figures 5-1 to 5-24. All computations and combinations of the errors presented have been accomplished in the manner described in Section 4. All results are based on 1 values.

These twenty-four sets of results are based on four representative trajectories chosen from a group of 14 translunar abort trajectories simulated by NASA, Ames. The trajectories chosen are numbers 1, 2, 5 and 14 with initial abort eccentricities and radial distances from the earth, respectively of 0.80, 0.88, 0.93, 0.99; 40,000 km, 90,000 km, 180,000 km, 355,000 km. Results from trajectory number 1 are given in Figures 5-1 to 5-3 and 5-13 to 5-15; those from trajectory number 2 are given in Figures 5-4 to 5-6 and 5-16 to 5-18; those from number 5 in Figures 5-7 to 5-9 and 5-19 to 5-21; and those from number 14 in Figures 5-10 to 5-12 and 5-22 to 5-24. A three digit identification has been assigned to each problem. The first digit of the problem number indicates the number of the abort trajectory.

The results are presented in two groups as indicated by the second digit of the problem number. Group 1 results are contained in Figures 5-1 to 5-12 and group 2 in Figures 5-13 to 5-24. Each group contains three cases from each of the four trajectories. The group 1 problems have fixed corrective maneuver and third observation points for each trajectory while the first and second observation points are varied. For group 2, the first observation point is fixed for each trajectory, while the second and third observation points and the corrective maneuver point are varied. For each trajectory, the first case presented from group 1 is identical to the first group 2 problem and therefore there are really only 20 different cases presented on figures 5-1 through 5-24. The location of the various observational and corrective maneuver points for all cases is given on Figure 4-4 in Section 4.

The data in Figures 5-1 to 5-24 are presented in three categories of perigee errors. The first column contains the errors assuming no corrective maneuver computation. The second column gives the incremental errors due to the computation of the corrective maneuver. The third column gives the RSS combination of the first two columns and represents the total error with a maneuver computation.

Four types of errors are presented, two of which are due to errors in concept and two of which are hardware type errors. The concept errors are (1) the two body vs. four body and earth oblateness effects and (2) the error due to the parabolic assumption for the corrective maneuver. The hardware errors are divided into errors in the observations and the instrumentation errors. The seven listed observational errors are based on the schedule of errors given in Figure 4-8. The sources and magnitudes of the thirty instrumentation errors are given in Section 3, Figure 3-4.

	ERROR SOURCE	ERRORS IN PERIGEE: ASSUMING NO MANEUVER RADIUS (KM)	ASSUMING NO MANEUVER ANGLE (DEG)	INCREMENT DUE TO MANEUVER COMP. RADIUS (KM)	INCREMENT DUE TO MANEUVER COMP. ANGLE (DEG)	TOTAL WITH MANEUVER RADIUS (KM)	TOTAL WITH MANEUVER ANGLE (DEG)
1.	TWO BODY VS. FOUR BODY AND EARTH OBLATENESS	3.74	0.0581	NOT APPLICABLE		3.74	0.0581
2.	OBSERVATIONAL ERRORS						
2.1	UNCERTAINTY IN MEASUREMENT OF θ(1)	0.26	0.0016	0.08	0.0007		
2.2	UNCERTAINTY IN MEASUREMENT OF θ(2)	0.19	0.0005	0.13	0.0012		
2.3	UNCERTAINTY IN MEASUREMENT OF θ(3)	0.45	0.0007	0.52	0.0046		
2.4	UNCERTAINTY IN MEASUREMENT OF R(1)	0.61	0.0038	0.19	0.0016		
2.5	UNCERTAINTY IN MEASUREMENT OF R(2)	1.07	0.0029	0.74	0.0066		
2.6	UNCERTAINTY IN MEASUREMENT OF R(3)	0.59	0.0009	0.69	0.0061		
2.7	UNCERTAINTY IN MEASUREMENT OF R(C)	NOT APPLICABLE		0.31	0.0027		
	RSS	1.47	0.0052	1.20	0.0107	1.90	0.0119
3.	INSTRUMENTATION ERRORS						
3.1	UNCERTAINTY IN θ(1) INPUT GEARING AND DIAL READING	0.07	0.0005	0.02	0.0002		
3.2	UNCERTAINTY IN θ(2) INPUT GEARING AND DIAL READING	0.05	0.0002	0.04	0.0003		
3.3	UNCERTAINTY IN θ(3) INPUT GEARING AND DIAL READING	0.13	0.0002	0.15	0.0013		
3.4	UNCERTAINTY IN θ(P) INPUT GEARING AND DIAL READING	0.00	0.0008	0.09	0.0008		
3.5	UNCERTAINTY IN (θ(1)-θ(P)) DIFFERENTIAL	0.13	0.0008	0.04	0.0004		
3.6	UNCERTAINTY IN (θ(2)-θ(P)) DIFFERENTIAL	0.10	0.0003	0.07	0.0006		
3.7	UNCERTAINTY IN (θ(3)-θ(P)) DIFFERENTIAL	0.23	0.0003	0.27	0.0024		
3.8	UNCERTAINTY IN (θ(1)-θ(P)) REDUCTION GEARING TO COS MECHANISM	0.89	0.0055	0.27	0.0024		
3.9	UNCERTAINTY IN (θ(2)-θ(P)) REDUCTION GEARING TO COS MECHANISM	0.66	0.0018	0.46	0.0041		
3.10	UNCERTAINTY IN (θ(3)-θ(P)) REDUCTION GEARING TO COS MECHANISM	1.55	0.0023	1.81	0.0161		
3.11	UNCERTAINTY IN (θ(1)-θ(P)) COSINE MECHANISM	2.17	0.0135	0.66	0.0058		
3.12	UNCERTAINTY IN (θ(2)-θ(P)) COSINE MECHANISM	3.78	0.0103	2.63	0.0234		
3.13	UNCERTAINTY IN (θ(3)-θ(P)) COSINE MECHANISM	1.61	0.0032	1.97	0.0176		
3.14	UNCERTAINTY IN COS(θ(3)-θ(P))-COS(θ(1)-θ(P)) DIFFERENTIAL	2.42	0.0048	2.96	0.0264		
3.15	UNCERTAINTY IN COS(θ(2)-θ(P))-COS(θ(1)-θ(P)) DIFFERENTIAL	5.66	0.0154	3.94	0.0351		
3.16	UNCERTAINTY IN COS(θ(3)-θ(P))-COS(θ(1)-θ(P)) POT DRIVE GEARING	0.60	0.0016	0.98	0.0088		
3.17	UNCERTAINTY IN COS(θ(2)-θ(P))-COS(θ(1)-θ(P)) POT DRIVE GEARING	1.89	0.0051	1.31	0.0117		
3.18	COS(θ(3)-θ(P))-COS(θ(1)-θ(P)) POT NON-LINEARITY	1.93	0.0039	2.37	0.0211		
3.19	COS(θ(2)-θ(P))-COS(θ(1)-θ(P)) POT NON-LINEARITY	4.54	0.0123	3.15	0.0281		
3.20	UNCERTAINTY IN 1/R(1) INPUT GEARING AND DIAL READING	0.37	0.0023	0.11	0.0010		
3.21	UNCERTAINTY IN 1/R(2) INPUT GEARING AND DIAL READING	0.64	0.0017	0.44	0.0039		
3.22	UNCERTAINTY IN 1/R(3) INPUT GEARING AND DIAL READING	0.27	0.0005	0.33	0.0030		
3.23	UNCERTAINTY IN (1/R(3)-1/R(1)) DIFFERENTIAL	0.09	0.0002	0.11	0.0010		
3.24	UNCERTAINTY IN (1/R(2)-1/R(1)) DIFFERENTIAL	0.21	0.0006	0.15	0.0013		
3.25	UNCERTAINTY IN (1/R(3)-1/R(1)) RHEOSTAT DRIVE GEARING	0.90	0.0018	1.11	0.0099		
3.26	UNCERTAINTY IN (1/R(2)-1/R(1)) RHEOSTAT DRIVE GEARING	2.12	0.0058	1.47	0.0132		
3.27	(1/R(3)-1/R(1)) RHEOSTAT NON-LINEARITY	2.17	0.0043	2.65	0.0237		
3.28	(1/R(2)-1/R(1)) RHEOSTAT NON-LINEARITY	5.09	0.0139	3.54	0.0316		
3.29	BRIDGE TRIMMING ERROR	0.18	0.0005	0.13	0.0011		
3.30	GALVANOMETER BIAS ERROR	NIL	NIL	NIL	NIL		
	RSS	11.43	0.0329	9.06	0.0809	14.58	0.0873
4.	ERRORS DUE TO PARABOLIC ASSUMPTION OF CORRECTIVE MANEUVER	NOT APPLICABLE		0.60	0.0081	0.60	0.0081
	TOTAL RSS ERRORS	12.11	0.0670	9.90	0.1005	15.64	0.1207

NOTE 1. SOURCE ERRORS UTILIZED ARE 1 SIGMA VALUES BASED ON MAXIMUM VALUES LISTED IN FIGURE NO. 3-4

MANUAL SPACE COMPUTER ERROR ANALYSIS • PROBLEM NUMBER 1.1.1

Figure 5-1

	ERROR SOURCE	ERRORS IN PERIGEE: ASSUMING NO MANEUVER, RADIUS (KM)	ASSUMING NO MANEUVER, ANGLE (DEG)	INCREMENT DUE TO MANEUVER COMP., RADIUS (KM)	INCREMENT DUE TO MANEUVER COMP., ANGLE (DEG)	TOTAL WITH MANEUVER, RADIUS (KM)	TOTAL WITH MANEUVER, ANGLE (DEG)
1.	TWO BODY VS. FOUR BODY AND EARTH OBLATENESS	3.45	0.0565	NOT APPLICABLE		3.45	0.0565
2.	OBSERVATIONAL ERRORS						
2.1	UNCERTAINTY IN MEASUREMENT OF θ(1)	0.17	0.0012	0.03	0.0003		
2.2	UNCERTAINTY IN MEASUREMENT OF θ(2)	0.50	0.0020	0.28	0.0025		
2.3	UNCERTAINTY IN MEASUREMENT OF θ(3)	0.67	0.0004	0.63	0.0056		
2.4	UNCERTAINTY IN MEASUREMENT OF R(1)	0.75	0.0053	0.15	0.0013		
2.5	UNCERTAINTY IN MEASUREMENT OF R(2)	1.51	0.0059	0.85	0.0076		
2.6	UNCERTAINTY IN MEASUREMENT OF R(3)	0.89	0.0005	0.83	0.0074		
2.7	UNCERTAINTY IN MEASUREMENT OF R(C)	NOT APPLICABLE		0.31	0.0027		
	RSS	2.09	0.0083	1.41	0.0126	2.52	0.0151
3.	INSTRUMENTATION ERRORS						
3.1	UNCERTAINTY IN θ(1) INPUT GEARING AND DIAL READING	0.05	0.0004	0.01	0.0001		
3.2	UNCERTAINTY IN θ(2) INPUT GEARING AND DIAL READING	0.14	0.0006	0.08	0.0007		
3.3	UNCERTAINTY IN θ(3) INPUT GEARING AND DIAL READING	0.20	0.0001	0.18	0.0016		
3.4	UNCERTAINTY IN θ(P) INPUT GEARING AND DIAL READING	0.00	0.0008	0.09	0.0008		
3.5	UNCERTAINTY IN (θ(1)-θ(P)) DIFFERENTIAL	0.09	0.0006	0.02	0.0002		
3.6	UNCERTAINTY IN (θ(2)-θ(P)) DIFFERENTIAL	0.26	0.0010	0.15	0.0013		
3.7	UNCERTAINTY IN (θ(3)-θ(P)) DIFFERENTIAL	0.35	0.0002	0.32	0.0029		
3.8	UNCERTAINTY IN (θ(1)-θ(P)) REDUCTION GEARING TO COS MECHANISM	0.60	0.0043	0.12	0.0011		
3.9	UNCERTAINTY IN (θ(2)-θ(P)) REDUCTION GEARING TO COS MECHANISM	1.74	0.0058	0.98	0.0087		
3.10	UNCERTAINTY IN (θ(3)-θ(P)) REDUCTION GEARING TO COS MECHANISM	2.33	0.0034	2.18	0.0194		
3.11	UNCERTAINTY IN (θ(1)-θ(P)) COSINE MECHANISM	2.64	0.0189	0.53	0.0047		
3.12	UNCERTAINTY IN (θ(2)-θ(P)) COSINE MECHANISM	5.35	0.0208	3.02	0.0269		
3.13	UNCERTAINTY IN (θ(3)-θ(P)) COSINE MECHANISM	2.71	0.0020	2.49	0.0222		
3.14	UNCERTAINTY IN COS(θ(3)-θ(P))-COS(θ(1)-θ(P)) DIFFERENTIAL	4.06	0.0030	3.73	0.0333		
3.15	UNCERTAINTY IN COS(θ(2)-θ(P))-COS(θ(1)-θ(P)) DIFFERENTIAL	8.03	0.0312	4.53	0.0404		
3.16	UNCERTAINTY IN COS(θ(3)-θ(P))-COS(θ(1)-θ(P)) POT DRIVE GEARING	1.35	0.0010	1.24	0.0111		
3.17	UNCERTAINTY IN COS(θ(2)-θ(P))-COS(θ(1)-θ(P)) POT DRIVE GEARING	2.67	0.0104	1.51	0.0134		
3.18	COS(θ(3)-θ(P))-COS(θ(1)-θ(P)) POT NON-LINEARITY	3.26	0.0024	2.99	0.0267		
3.19	COS(θ(2)-θ(P))-COS(θ(1)-θ(P)) POT NON-LINEARITY	6.42	0.0250	3.62	0.0323		
3.20	UNCERTAINTY IN 1/R(1) INPUT GEARING AND DIAL READING	0.45	0.0032	0.09	0.0008		
3.21	UNCERTAINTY IN 1/R(2) INPUT GEARING AND DIAL READING	0.90	0.0035	0.50	0.0045		
3.22	UNCERTAINTY IN 1/R(3) INPUT GEARING AND DIAL READING	0.46	0.0003	0.42	0.0038		
3.23	UNCERTAINTY IN (1/R(3)-1/R(1)) DIFFERENTIAL	0.15	0.0001	0.14	0.0012		
3.24	UNCERTAINTY IN (1/R(2)-1/R(1)) DIFFERENTIAL	0.30	0.0012	0.17	0.0015		
3.25	UNCERTAINTY IN (1/R(3)-1/R(1)) RHEOSTAT DRIVE GEARING	1.52	0.0011	1.40	0.0125		
3.26	UNCERTAINTY IN (1/R(2)-1/R(1)) RHEOSTAT DRIVE GEARING	3.00	0.0117	1.69	0.0151		
3.27	(1/R(3)-1/R(1)) RHEOSTAT NON-LINEARITY	3.65	0.0027	3.35	0.0299		
3.28	(1/R(2)-1/R(1)) RHEOSTAT NON-LINEARITY	7.21	0.0281	4.07	0.0363		
3.29	BRIDGE TRIMMING ERROR	0.10	0.0004	0.05	0.0005		
3.30	GALVANOMETER BIAS ERROR	NIL	NIL	NIL	NIL		
	RSS	16.62	0.0601	10.81	0.0964	19.82	0.1136
4.	ERRORS DUE TO PARABOLIC ASSUMPTION OF CORRECTIVE MANEUVER	NOT APPLICABLE		0.55	0.0075	0.55	0.0075
	TOTAL RSS ERRORS	17.10	0.0829	11.44	0.1127	20.58	0.1399

NOTE 1. SOURCE ERRORS UTILIZED ARE 1 SIGMA VALUES BASED ON MAXIMUM VALUES LISTED IN FIGURE NO. 3-4

MANUAL SPACE COMPUTER ERROR ANALYSIS • PROBLEM NUMBER 1.1.2

Figure 5-2

	ERROR SOURCE	ERRORS IN PERIGEE: ASSUMING NO MANEUVER RADIUS (KM)	ASSUMING NO MANEUVER ANGLE (DEG)	INCREMENT DUE TO MANEUVER COMP. RADIUS (KM)	INCREMENT DUE TO MANEUVER COMP. ANGLE (DEG)	TOTAL WITH MANEUVER RADIUS (KM)	TOTAL WITH MANEUVER ANGLE (DEG)
1.	TWO BODY VS. FOUR BODY AND EARTH OBLATENESS	3.29	0.0555	NOT APPLICABLE		3.29	0.0555
2.	OBSERVATIONAL ERRORS						
2.1	UNCERTAINTY IN MEASUREMENT OF θ(1)	0.09	0.0006	0.02	0.0002		
2.2	UNCERTAINTY IN MEASUREMENT OF θ(2)	0.69	0.0033	0.32	0.0029		
2.3	UNCERTAINTY IN MEASUREMENT OF θ(3)	0.78	0.0012	0.65	0.0058		
2.4	UNCERTAINTY IN MEASUREMENT OF R(1)	1.18	0.0084	0.23	0.0021		
2.5	UNCERTAINTY IN MEASUREMENT OF R(2)	2.09	0.0100	0.97	0.0086		
2.6	UNCERTAINTY IN MEASUREMENT OF R(3)	1.03	0.0016	0.86	0.0076		
2.7	UNCERTAINTY IN MEASUREMENT OF R(C)	NOT APPLICABLE		0.31	0.0027		
	RSS	2.81	0.0137	1.53	0.0137	3.20	0.0193
3.	INSTRUMENTATION ERRORS						
3.1	UNCERTAINTY IN θ(1) INPUT GEARING AND DIAL READING	0.03	0.0002	0.00	0.0000		
3.2	UNCERTAINTY IN θ(2) INPUT GEARING AND DIAL READING	0.20	0.0010	0.09	0.0008		
3.3	UNCERTAINTY IN θ(3) INPUT GEARING AND DIAL READING	0.23	0.0003	0.19	0.0017		
3.4	UNCERTAINTY IN θ(P) INPUT GEARING AND DIAL READING	0.00	0.0008	0.09	0.0008		
3.5	UNCERTAINTY IN (θ(1)-θ(P)) DIFFERENTIAL	0.05	0.0003	0.01	0.0001		
3.6	UNCERTAINTY IN (θ(2)-θ(P)) DIFFERENTIAL	0.36	0.0017	0.17	0.0015		
3.7	UNCERTAINTY IN (θ(3)-θ(P)) DIFFERENTIAL	0.41	0.0006	0.34	0.0030		
3.8	UNCERTAINTY IN (θ(1)-θ(P)) REDUCTION GEARING TO COS MECHANISM	0.31	0.0022	0.06	0.0005		
3.9	UNCERTAINTY IN (θ(2)-θ(P)) REDUCTION GEARING TO COS MECHANISM	2.40	0.0115	1.11	0.0099		
3.10	UNCERTAINTY IN (θ(3)-θ(P)) REDUCTION GEARING TO COS MECHANISM	2.71	0.0041	2.25	0.0201		
3.11	UNCERTAINTY IN (θ(1)-θ(P)) COSINE MECHANISM	4.16	0.0297	0.83	0.0074		
3.12	UNCERTAINTY IN (θ(2)-θ(P)) COSINE MECHANISM	7.40	0.0354	3.43	0.0306		
3.13	UNCERTAINTY IN (θ(3)-θ(P)) COSINE MECHANISM	3.23	0.0057	2.59	0.0232		
3.14	UNCERTAINTY IN COS(θ(3)-θ(P))-COS(θ(1)-θ(P)) DIFFERENTIAL	4.84	0.0085	3.89	0.0347		
3.15	UNCERTAINTY IN COS(θ(2)-θ(P))-COS(θ(1)-θ(P)) DIFFERENTIAL	11.09	0.0531	5.14	0.0458		
3.16	UNCERTAINTY IN COS(θ(3)-θ(P))-COS(θ(1)-θ(P)) POT DRIVE GEARING	1.61	0.0028	1.30	0.0116		
3.17	UNCERTAINTY IN COS(θ(2)-θ(P))-COS(θ(1)-θ(P)) POT DRIVE GEARING	3.69	0.0177	1.71	0.0153		
3.18	COS(θ(3)-θ(P))-COS(θ(1)-θ(P)) POT NON-LINEARITY	3.88	0.0068	3.11	0.0278		
3.19	COS(θ(2)-θ(P))-COS(θ(1)-θ(P)) POT NON-LINEARITY	8.88	0.0425	4.11	0.0367		
3.20	UNCERTAINTY IN 1/R(1) INPUT GEARING AND DIAL READING	0.70	0.0050	0.14	0.0013		
3.21	UNCERTAINTY IN 1/R(2) INPUT GEARING AND DIAL READING	1.25	0.0060	0.58	0.0052		
3.22	UNCERTAINTY IN 1/R(3) INPUT GEARING AND DIAL READING	0.54	0.0010	0.44	0.0039		
3.23	UNCERTAINTY IN (1/R(3)-1/R(1)) DIFFERENTIAL	0.18	0.0003	0.14	0.0013		
3.24	UNCERTAINTY IN (1/R(2)-1/R(1)) DIFFERENTIAL	0.42	0.0020	0.19	0.0017		
3.25	UNCERTAINTY IN (1/R(3)-1/R(1)) RHEOSTAT DRIVE GEARING	1.81	0.0032	1.46	0.0130		
3.26	UNCERTAINTY IN (1/R(2)-1/R(1)) RHEOSTAT DRIVE GEARING	4.15	0.0199	1.92	0.0172		
3.27	(1/R(3)-1/R(1)) RHEOSTAT NON-LINEARITY	4.35	0.0077	3.49	0.0311		
3.28	(1/R(2)-1/R(1)) RHEOSTAT NON-LINEARITY	9.97	0.0478	4.62	0.0412		
3.29	BRIDGE TRIMMING ERROR	0.25	0.0012	0.12	0.0010		
3.30	GALVANOMETER BIAS ERROR	NIL	NIL	NIL	NIL		
	RSS	22.40	0.1020	11.86	0.1058	25.35	0.1470
4.	ERRORS DUE TO PARABOLIC ASSUMPTION OF CORRECTIVE MANEUVER	NOT APPLICABLE		0.52	0.0071	0.52	0.0071
	TOTAL RSS ERRORS	22.82	0.1169	12.41	0.1205	25.57	0.1679

NOTE 1. SOURCE ERRORS UTILIZED ARE 1 SIGMA VALUES BASED ON MAXIMUM VALUES LISTED IN FIGURE NO.3-4

MANUAL SPACE COMPUTER ERROR ANALYSIS • PROBLEM NUMBER 1.1.3

Figure 5-3

	ERROR SOURCE	Assuming No Maneuver: Radius (KM)	Assuming No Maneuver: Angle (DEG)	Increment Due to Maneuver Comp.: Radius (KM)	Increment Due to Maneuver Comp.: Angle (DEG)	Total With Maneuver: Radius (KM)	Total With Maneuver: Angle (DEG)
1.	TWO BODY VS. FOUR BODY AND EARTH OBLATENESS	4.58	0.0626	NOT APPLICABLE		4.58	0.0626
2.	OBSERVATIONAL ERRORS						
2.1	UNCERTAINTY IN MEASUREMENT OF θ(1)	0.14	0.0010	0.02	0.0002		
2.2	UNCERTAINTY IN MEASUREMENT OF θ(2)	0.59	0.0026	0.30	0.0027		
2.3	UNCERTAINTY IN MEASUREMENT OF θ(3)	0.73	0.0008	0.64	0.0057		
2.4	UNCERTAINTY IN MEASUREMENT OF R(1)	0.77	0.0056	0.14	0.0012		
2.5	UNCERTAINTY IN MEASUREMENT OF R(2)	1.54	0.0066	0.79	0.0070		
2.6	UNCERTAINTY IN MEASUREMENT OF R(3)	0.89	0.0010	0.78	0.0069		
2.7	UNCERTAINTY IN MEASUREMENT OF R(C)	NOT APPLICABLE		0.29	0.0026		
	RSS	2.15	0.0092	1.35	0.0121	2.54	0.0152
3.	INSTRUMENTATION ERRORS						
3.1	UNCERTAINTY IN θ(1) INPUT GEARING AND DIAL READING	0.04	0.0003	0.01	0.0001		
3.2	UNCERTAINTY IN θ(2) INPUT GEARING AND DIAL READING	0.17	0.0007	0.05	0.0008		
3.3	UNCERTAINTY IN θ(3) INPUT GEARING AND DIAL READING	0.21	0.0002	0.18	0.0016		
3.4	UNCERTAINTY IN θ(P) INPUT GEARING AND DIAL READING	0.00	0.0008	0.09	0.0008		
3.5	UNCERTAINTY IN (θ(1)-θ(P)) DIFFERENTIAL	0.07	0.0005	0.01	0.0001		
3.6	UNCERTAINTY IN (θ(2)-θ(P)) DIFFERENTIAL	0.31	0.0013	0.16	0.0014		
3.7	UNCERTAINTY IN (θ(3)-θ(P)) DIFFERENTIAL	0.38	0.0004	0.33	0.0030		
3.8	UNCERTAINTY IN (θ(1)-θ(P)) REDUCTION GEARING TO COS MECHANISM	0.49	0.0036	0.09	0.0008		
3.9	UNCERTAINTY IN (θ(2)-θ(P)) REDUCTION GEARING TO COS MECHANISM	2.04	0.0088	1.05	0.0093		
3.10	UNCERTAINTY IN (θ(3)-θ(P)) REDUCTION GEARING TO COS MECHANISM	2.53	0.0028	2.21	0.0197		
3.11	UNCERTAINTY IN (θ(1)-θ(P)) COSINE MECHANISM	2.85	0.0209	0.51	0.0045		
3.12	UNCERTAINTY IN (θ(2)-θ(P)) COSINE MECHANISM	5.68	0.0246	2.92	0.0260		
3.13	UNCERTAINTY IN (θ(3)-θ(P)) COSINE MECHANISM	2.83	0.0038	2.41	0.0215		
3.14	UNCERTAINTY IN COS(θ(3)-θ(P))-COS(θ(1)-θ(P)) DIFFERENTIAL	4.25	0.0057	3.61	0.0322		
3.15	UNCERTAINTY IN COS(θ(2)-θ(P))-COS(θ(1)-θ(P)) DIFFERENTIAL	8.52	0.0369	4.37	0.0390		
3.16	UNCERTAINTY IN COS(θ(3)-θ(P))-COS(θ(1)-θ(P)) PCT DRIVE GEARING	1.41	0.0019	1.20	0.0107		
3.17	UNCERTAINTY IN COS(θ(2)-θ(P))-COS(θ(1)-θ(P)) PCT DRIVE GEARING	2.83	0.0123	1.46	0.0130		
3.18	COS(θ(3)-θ(P))-COS(θ(1)-θ(P)) PCT NON-LINEARITY	3.40	0.0045	2.89	0.0258		
3.19	COS(θ(2)-θ(P))-COS(θ(1)-θ(P)) PCT NON-LINEARITY	6.82	0.0295	3.50	0.0312		
3.20	UNCERTAINTY IN 1/R(1) INPUT GEARING AND DIAL READING	0.46	0.0033	0.08	0.0007		
3.21	UNCERTAINTY IN 1/R(2) INPUT GEARING AND DIAL READING	0.91	0.0039	0.47	0.0042		
3.22	UNCERTAINTY IN 1/R(3) INPUT GEARING AND DIAL READING	0.45	0.0006	0.38	0.0034		
3.23	UNCERTAINTY IN (1/R(3)-1/R(1)) DIFFERENTIAL	0.15	0.0002	0.13	0.0012		
3.24	UNCERTAINTY IN (1/R(2)-1/R(1)) DIFFERENTIAL	0.30	0.0013	0.16	0.0014		
3.25	UNCERTAINTY IN (1/R(3)-1/R(1)) RHEOSTAT DRIVE GEARING	1.51	0.0020	1.29	0.0115		
3.26	UNCERTAINTY IN (1/R(2)-1/R(1)) RHEOSTAT DRIVE GEARING	3.03	0.0131	1.56	0.0139		
3.27	(1/R(3)-1/R(1)) RHEOSTAT NON-LINEARITY	3.62	0.0048	3.08	0.0275		
3.28	(1/R(2)-1/R(1)) RHEOSTAT NON-LINEARITY	7.28	0.0315	3.74	0.0333		
3.29	BRIDGE TRIMMING ERROR	0.20	0.0009	0.10	0.0009		
3.30	GALVANOMETER BIAS ERROR	NIL	NIL	NIL	NIL		
	RSS	17.37	0.0701	10.34	0.0921	20.22	0.1157
4.	ERRORS DUE TO PARABOLIC ASSUMPTION OF CORRECTIVE MANEUVER	NOT APPLICABLE		0.43	0.0054	0.43	0.0054
	TOTAL RSS ERRORS	18.09	0.0944	11.40	0.1121	21.38	0.1466

NOTE 1. SOURCE ERRORS UTILIZED ARE 1 SIGMA VALUES BASED ON MAXIMUM VALUES LISTED IN FIGURE NO. 3-4

MANUAL SPACE COMPUTER ERROR ANALYSIS • PROBLEM NUMBER 2.1.1

Figure 5-4

	ERROR SOURCE	ERRORS IN PERIGEE: ASSUMING NO MANEUVER RADIUS (KM)	ASSUMING NO MANEUVER ANGLE (DEG)	INCREMENT DUE TO MANEUVER COMP. RADIUS (KM)	INCREMENT DUE TO MANEUVER COMP. ANGLE (DEG)	TOTAL WITH MANEUVER RADIUS (KM)	TOTAL WITH MANEUVER ANGLE (DEG)
1.	TWO BODY VS. FOUR BODY AND EARTH OBLATENESS	3.81	0.0571	NOT APPLICABLE		3.81	0.0571
2.	OBSERVATIONAL ERRORS						
2.1	UNCERTAINTY IN MEASUREMENT OF θ(1)	0.07	0.0005	0.01	0.0001		
2.2	UNCERTAINTY IN MEASUREMENT OF θ(2)	0.77	0.0038	0.34	0.0031		
2.3	UNCERTAINTY IN MEASUREMENT OF θ(3)	0.84	0.0015	0.67	0.0060		
2.4	UNCERTAINTY IN MEASUREMENT OF R(1)	1.00	0.0075	0.16	0.0015		
2.5	UNCERTAINTY IN MEASUREMENT OF R(2)	1.90	0.0094	0.85	0.0076		
2.6	UNCERTAINTY IN MEASUREMENT OF R(3)	1.02	0.0019	0.81	0.0072		
2.7	UNCERTAINTY IN MEASUREMENT OF R(C)	NOT APPLICABLE		0.29	0.0026		
	RSS	2.64	0.0128	1.44	0.0128	3.00	0.0181
3.	INSTRUMENTATION ERRORS						
3.1	UNCERTAINTY IN θ(1) INPUT GEARING AND DIAL READING	0.02	0.0001	0.00	0.0000		
3.2	UNCERTAINTY IN θ(2) INPUT GEARING AND DIAL READING	0.22	0.0011	0.10	0.0009		
3.3	UNCERTAINTY IN θ(3) INPUT GEARING AND DIAL READING	0.24	0.0004	0.19	0.0017		
3.4	UNCERTAINTY IN θ(P) INPUT GEARING AND DIAL READING	0.00	0.0008	0.09	0.0008		
3.5	UNCERTAINTY IN (θ(1)-θ(P)) DIFFERENTIAL	0.03	0.0003	0.01	0.0000		
3.6	UNCERTAINTY IN (θ(2)-θ(P)) DIFFERENTIAL	0.40	0.0020	0.18	0.0016		
3.7	UNCERTAINTY IN (θ(3)-θ(P)) DIFFERENTIAL	0.44	0.0008	0.35	0.0031		
3.8	UNCERTAINTY IN (θ(1)-θ(P)) REDUCTION GEARING TO COS MECHANISM	0.24	0.0018	0.04	0.0003		
3.9	UNCERTAINTY IN (θ(2)-θ(P)) REDUCTION GEARING TO COS MECHANISM	2.67	0.0132	1.19	0.0106		
3.10	UNCERTAINTY IN (θ(3)-θ(P)) REDUCTION GEARING TO COS MECHANISM	2.91	0.0053	2.31	0.0206		
3.11	UNCERTAINTY IN (θ(1)-θ(P)) COSINE MECHANISM	3.70	0.0275	0.61	0.0054		
3.12	UNCERTAINTY IN (θ(2)-θ(P)) COSINE MECHANISM	7.05	0.0347	3.15	0.0281		
3.13	UNCERTAINTY IN (θ(3)-θ(P)) COSINE MECHANISM	3.35	0.0072	2.54	0.0227		
3.14	UNCERTAINTY IN COS(θ(3)-θ(P))-COS(θ(1)-θ(P)) DIFFERENTIAL	5.02	0.0107	3.81	0.0340		
3.15	UNCERTAINTY IN COS(θ(2)-θ(P))-COS(θ(1)-θ(P)) DIFFERENTIAL	10.56	0.0520	4.72	0.0421		
3.16	UNCERTAINTY IN COS(θ(3)-θ(P))-COS(θ(1)-θ(P)) PCT DRIVE GEARING	1.67	0.0036	1.27	0.0113		
3.17	UNCERTAINTY IN COS(θ(2)-θ(P))-COS(θ(1)-θ(P)) PCT DRIVE GEARING	3.52	0.0173	1.57	0.0140		
3.18	COS(θ(3)-θ(P))-COS(θ(1)-θ(P)) PCT NON-LINEARITY	4.02	0.0086	3.05	0.0272		
3.19	COS(θ(2)-θ(P))-COS(θ(1)-θ(P)) PCT NON-LINEARITY	8.46	0.0416	3.78	0.0337		
3.20	UNCERTAINTY IN 1/R(1) INPUT GEARING AND DIAL READING	0.59	0.0044	0.10	0.0009		
3.21	UNCERTAINTY IN 1/R(2) INPUT GEARING AND DIAL READING	1.13	0.0056	0.50	0.0045		
3.22	UNCERTAINTY IN 1/R(3) INPUT GEARING AND DIAL READING	0.53	0.0011	0.41	0.0036		
3.23	UNCERTAINTY IN (1/R(3)-1/R(1)) DIFFERENTIAL	0.18	0.0004	0.14	0.0012		
3.24	UNCERTAINTY IN (1/R(2)-1/R(1)) DIFFERENTIAL	0.38	0.0019	0.17	0.0015		
3.25	UNCERTAINTY IN (1/R(3)-1/R(1)) RHEOSTAT DRIVE GEARING	1.79	0.0038	1.36	0.0121		
3.26	UNCERTAINTY IN (1/R(2)-1/R(1)) RHEOSTAT DRIVE GEARING	3.76	0.0185	1.68	0.0150		
3.27	(1/R(3)-1/R(1)) RHEOSTAT NON-LINEARITY	4.28	0.0092	3.25	0.0290		
3.28	(1/R(2)-1/R(1)) RHEOSTAT NON-LINEARITY	9.03	0.0445	4.04	0.0360		
3.29	BRIDGE TRIMMING ERROR	0.34	0.0017	0.15	0.0014		
3.30	GALVANOMETER BIAS ERROR	NIL	NIL	NIL	NIL		
	RSS	21.36	0.0990	11.06	0.0985	24.06	0.1397
4.	ERRORS DUE TO PARABOLIC ASSUMPTION OF CORRECTIVE MANEUVER	NOT APPLICABLE		0.35	0.0045	0.35	0.0045
	TOTAL RSS ERRORS	21.86	0.1150	11.80	0.1147	24.84	0.1624

NOTE 1. SOURCE ERRORS UTILIZED ARE 1 SIGMA VALUES BASED ON MAXIMUM VALUES LISTED IN FIGURE NO.3-4

MANUAL SPACE COMPUTER ERROR ANALYSIS • PROBLEM NUMBER 2.1.2

Figure 5-5

	ERRCR SCURCE	ERRORS IN PERIGEE					
		ASSLMING NO MANEUVER		INCREMENT DUE TC MANEUVER CCMP.		TCTAL WITH MANEUVER	
		RADIUS (KM)	ANGLE (DEG)	RADIUS (KM)	ANGLE (DEG)	RADIUS (KM)	ANGLE (DEG)
1.	TWO BODY VS. FOUR BCDY ANC EARTH CBLATENESS	3.33	C.0535	NOT APPLICABLE		3.33	0.0535
2.	OBSERVATICNAL ERRORS						
2.1	UNCERTAINTY IN MEASUREMENT CF θ(1)	C.C6	C.CCC4	0.C1	C.CCC1		
2.2	UNCERTAINTY IN MEASUREMENT CF θ(2)	C.99	C.C054	0.38	C.CC34		
2.3	UNCERTAINTY IN MEASUREMENT CF θ(3)	C.93	C.CC22	0.68	C.CC61		
2.4	UNCERTAINTY IN MEASUREMENT CF R(1)	1.43	C.C10C	0.23	C.0C21		
2.5	UNCERTAINTY IN MEASUREMENT CF R(2)	2.44	C.C134	0.94	C.CC84		
2.6	UNCERTAINTY IN MEASUREMENT CF R(3)	1.14	C.CC27	0.83	C.CC74		
2.7	UNCERTAINTY IN MEASUREMENT CF R(C)	NOT APPLICABLE		0.29	C.CC26		
	RSS	3.34	C.C183	1.52	C.C136	3.67	0.0228
3.	INSTRUMENTATICN ERRORS						
3.1	UNCERTAINTY IN θ(1) INPUT GEARING ANC CIAL REACING	C.C2	C.CC01	0.CC	C.CCCC		
3.2	UNCERTAINTY IN θ(2) INPUT GEARING ANC CIAL REACING	C.28	C.CC16	0.11	C.CC1C		
3.3	UNCERTAINTY IN θ(3) INPUT GEARING ANC CIAL REACING	C.27	C.CCC6	0.2C	C.CC17		
3.4	UNCERTAINTY IN θ(P) INPUT GEARING ANC CIAL REACING	C.CC	C.CCC8	0.C9	C.CCC8		
3.5	UNCERTAINTY IN (θ(1)-θ(P)) CIFFERENTIAL	C.C3	C.CCC2	0.CC	C.CCCC		
3.6	UNCERTAINTY IN (θ(2)-θ(P)) DIFFERENTIAL	C.51	C.CC28	0.2C	C.CC18		
3.7	UNCERTAINTY IN (θ(3)-θ(P)) DIFFERENTIAL	C.48	C.CC12	0.35	C.CC32		
3.8	UNCERTAINTY IN (θ(1)-θ(P)) REDUCTICN GEARING TC CCS MECHANISM	C.2C	C.CC15	0.C3	C.CCC3		
3.9	UNCERTAINTY IN (θ(2)-θ(P)) REDUCTICN GEARING TC CCS MECHANISM	3.44	C.C189	1.32	C.C118		
3.10	UNCERTAINTY IN (θ(3)-θ(P)) REDUCTICN GEARING TC CCS MECHANISM	3.23	C.CC77	2.37	C.C211		
3.11	UNCERTAINTY IN (θ(1)-θ(P)) CCSINE MECHANISM	5.28	C.C393	0.87	C.CC77		
3.12	UNCERTAINTY IN (θ(2)-θ(P)) CCSINE MECHANISM	9.C6	C.C497	3.48	C.C31C		
3.13	UNCERTAINTY IN (θ(3)-θ(P)) CCSINE MECHANISM	3.78	C.C104	2.61	C.C233		
3.14	UNCERTAINTY IN CCS(θ(3)-θ(P))-CCS(θ(1)-θ(P)) CIFFERENTIAL	5.67	C.C156	3.92	C.C349		
3.15	UNCERTAINTY IN CCS(θ(2)-θ(P))-CCS(θ(1)-θ(P)) CIFFERENTIAL	13.59	C.C745	5.22	C.C465		
3.16	UNCERTAINTY IN CCS(θ(3)-θ(P))-CCS(θ(1)-θ(P)) PCT CRIVE GEARING	1.89	C.CC52	1.3C	C.C116		
3.17	UNCERTAINTY IN CCS(θ(2)-θ(P))-CCS(θ(1)-θ(P)) PCT CRIVE GEARING	4.52	C.C248	1.74	C.C155		
3.18	CCS(θ(3)-θ(P))-CCS(θ(1)-θ(P)) PCT NCN-LINEARITY	4.54	C.C125	3.14	C.C279		
3.19	CCS(θ(2)-θ(P))-CCS(θ(1)-θ(P)) PCT NCN-LINEARITY	1C.88	C.C597	4.18	C.C372		
3.20	UNCERTAINTY IN 1/R(1) INPUT GEARING ANC CIAL REACING	C.84	C.CC63	0.14	C.CC12		
3.21	UNCERTAINTY IN 1/R(2) INPUT GEARING ANC CIAL REACING	1.45	C.008C	0.56	C.CC5C		
3.22	UNCERTAINTY IN 1/R(3) INPUT GEARING ANC CIAL REACING	C.61	C.0017	0.42	C.CC37		
3.23	UNCERTAINTY IN (1/R(3)-1/R(1)) CIFFERENTIAL	C.2C	C.CCC6	0.14	C.CC12		
3.24	UNCERTAINTY IN (1/R(2)-1/R(1)) CIFFERENTIAL	C.48	C.CC27	0.18	C.CC17		
3.25	UNCERTAINTY IN (1/R(3)-1/R(1)) RHECSTAT CRIVE GEARING	2.C2	C.CC55	1.39	C.C124		
3.26	UNCERTAINTY IN (1/R(2)-1/R(1)) RHECSTAT CRIVE GEARING	4.83	C.C265	1.86	C.C165		
3.27	(1/R(3)-1/R(1)) RHECSTAT NCN-LINEARITY	4.84	C.C133	3.34	C.C298		
3.28	(1/R(2)-1/R(1)) RHECSTAT NCN-LINEARITY	11.61	C.C637	4.46	C.C397		
3.29	BRICGE TRIMMING ERRCR	C.45	C.CC24	0.17	C.CC15		
3.30	GALVANCMETER BIAS ERRCR	NIL	NIL	NIL	NIL		
	RSS	26.97	C.1419	11.89	C.1C59	29.47	0.1770
4.	ERRORS CUE TO PARABCLIC ASSUMPTICN CF CCRRECTIVE MANEUVER	NOT APPLICABLE		0.31	C.CC4C	C.31	0.004C
	TOTAL RSS ERRCRS	27.38	C.1527	12.44	C.1195	30.C7	0.1939

NOTE 1. SOURCE ERRCRS UTILIZEC ARE 1 SIGMA VALLES BASEC CN MAXIMUM VALUES LISTEC IN FIGURE NO. 3-4

MANUAL SPACE CCMPUTER ERRCR ANALYSIS * PRCBLEM NUMBER 2.1.3

Figure 5-6

	ERROR SOURCE	ERRORS IN PERIGEE: ASSUMING NO MANEUVER — RADIUS (KM)	ASSUMING NO MANEUVER — ANGLE (DEG)	INCREMENT DUE TO MANEUVER COMP. — RADIUS (KM)	INCREMENT DUE TO MANEUVER COMP. — ANGLE (DEG)	TOTAL WITH MANEUVER — RADIUS (KM)	TOTAL WITH MANEUVER — ANGLE (DEG)
1.	TWO BODY VS. FOUR BODY AND EARTH OBLATENESS	4.59	0.0618	NOT APPLICABLE		4.59	0.0618
2.	OBSERVATIONAL ERRORS						
2.1	UNCERTAINTY IN MEASUREMENT OF θ(1)	0.02	0.0002	0.00	0.		
2.2	UNCERTAINTY IN MEASUREMENT OF θ(2)	0.97	0.0056	0.30	0.0025		
2.3	UNCERTAINTY IN MEASUREMENT OF θ(3)	0.95	0.0026	0.63	0.0053		
2.4	UNCERTAINTY IN MEASUREMENT OF R(1)	0.98	0.0080	0.01	0.0000		
2.5	UNCERTAINTY IN MEASUREMENT OF R(2)	1.53	0.0111	0.59	0.0049		
2.6	UNCERTAINTY IN MEASUREMENT OF R(3)	1.07	0.0029	0.72	0.0059		
2.7	UNCERTAINTY IN MEASUREMENT OF R(C)	NOT APPLICABLE		0.31	0.0026		
	RSS	2.77	0.0153	1.21	0.0100	3.03	0.0183
3.	INSTRUMENTATION ERRORS						
3.1	UNCERTAINTY IN θ(1) INPUT GEARING AND DIAL READING	0.01	0.0001	0.00	0.0000		
3.2	UNCERTAINTY IN θ(2) INPUT GEARING AND DIAL READING	0.28	0.0016	0.09	0.0007		
3.3	UNCERTAINTY IN θ(3) INPUT GEARING AND DIAL READING	0.27	0.0007	0.18	0.0015		
3.4	UNCERTAINTY IN θ(P) INPUT GEARING AND DIAL READING	0.00	0.0008	0.10	0.0008		
3.5	UNCERTAINTY IN (θ(1)-θ(P)) DIFFERENTIAL	0.01	0.0001	0.00	0.0000		
3.6	UNCERTAINTY IN (θ(2)-θ(P)) DIFFERENTIAL	0.50	0.0025	0.16	0.0013		
3.7	UNCERTAINTY IN (θ(3)-θ(P)) DIFFERENTIAL	0.49	0.0013	0.33	0.0027		
3.8	UNCERTAINTY IN (θ(1)-θ(P)) REDUCTION GEARING TO COS MECHANISM	0.08	0.0007	0.00	0.0000		
3.9	UNCERTAINTY IN (θ(2)-θ(P)) REDUCTION GEARING TO COS MECHANISM	3.37	0.0153	1.04	0.0086		
3.10	UNCERTAINTY IN (θ(3)-θ(P)) REDUCTION GEARING TO COS MECHANISM	3.29	0.0090	2.20	0.0182		
3.11	UNCERTAINTY IN (θ(1)-θ(P)) COSINE MECHANISM	3.71	0.0305	0.02	0.0002		
3.12	UNCERTAINTY IN (θ(2)-θ(P)) COSINE MECHANISM	7.36	0.0421	2.27	0.0188		
3.13	UNCERTAINTY IN (θ(3)-θ(P)) COSINE MECHANISM	3.66	0.0116	2.25	0.0186		
3.14	UNCERTAINTY IN COS(θ(3)-θ(P))-COS(θ(1)-θ(P)) DIFFERENTIAL	5.48	0.0174	3.37	0.0279		
3.15	UNCERTAINTY IN COS(θ(2)-θ(P))-COS(θ(1)-θ(P)) DIFFERENTIAL	11.04	0.0631	3.41	0.0282		
3.16	UNCERTAINTY IN COS(θ(3)-θ(P))-COS(θ(1)-θ(P)) PCT DRIVE GEARING	1.62	0.0058	1.12	0.0093		
3.17	UNCERTAINTY IN COS(θ(2)-θ(P))-COS(θ(1)-θ(P)) PCT DRIVE GEARING	3.68	0.0210	1.13	0.0094		
3.18	COS(θ(3)-θ(P))-COS(θ(1)-θ(P)) PCT NON-LINEARITY	4.39	0.0140	2.70	0.0223		
3.19	COS(θ(2)-θ(P))-COS(θ(1)-θ(P)) PCT NON-LINEARITY	8.84	0.0505	2.73	0.0225		
3.20	UNCERTAINTY IN 1/R(1) INPUT GEARING AND DIAL READING	0.58	0.0047	0.00	0.0000		
3.21	UNCERTAINTY IN 1/R(2) INPUT GEARING AND DIAL READING	1.15	0.0066	0.35	0.0029		
3.22	UNCERTAINTY IN 1/R(3) INPUT GEARING AND DIAL READING	0.57	0.0018	0.35	0.0029		
3.23	UNCERTAINTY IN (1/R(3)-1/R(1)) DIFFERENTIAL	0.19	0.0006	0.12	0.0010		
3.24	UNCERTAINTY IN (1/R(2)-1/R(1)) DIFFERENTIAL	0.38	0.0022	0.12	0.0010		
3.25	UNCERTAINTY IN (1/R(3)-1/R(1)) RHEOSTAT DRIVE GEARING	1.90	0.0060	1.17	0.0097		
3.26	UNCERTAINTY IN (1/R(2)-1/R(1)) RHEOSTAT DRIVE GEARING	3.82	0.0219	1.18	0.0098		
3.27	(1/R(3)-1/R(1)) RHEOSTAT NON-LINEARITY	4.55	0.0145	2.80	0.0231		
3.28	(1/R(2)-1/R(1)) RHEOSTAT NON-LINEARITY	5.17	0.0525	2.83	0.0234		
3.29	BRIDGE TRIMMING ERROR	0.55	0.0031	0.17	0.0014		
3.30	GALVANOMETER BIAS ERROR	NIL	NIL	NIL	NIL		
	RSS	22.44	0.1209	8.77	0.0725	24.09	0.1410
4.	ERRORS DUE TO PARABOLIC ASSUMPTION OF CORRECTIVE MANEUVER	NOT APPLICABLE		0.24	0.0028	0.24	0.0028
	TOTAL RSS ERRORS	23.07	0.1366	9.98	0.0559	25.14	0.1669

NOTE 1. SOURCE ERRORS UTILIZED ARE 1 SIGMA VALUES BASED ON MAXIMUM VALUES LISTED IN FIGURE NO. 3-4

MANUAL SPACE COMPUTER ERROR ANALYSIS • PROBLEM NUMBER 5.1.1

Figure 5-7

	ERROR SOURCE	ERRORS IN PERIGEE: ASSUMING NO MANEUVER RADIUS (KM)	ASSUMING NO MANEUVER ANGLE (DEG)	INCREMENT DUE TO MANEUVER COMP. RADIUS (KM)	INCREMENT DUE TO MANEUVER COMP. ANGLE (DEG)	TOTAL WITH MANEUVER RADIUS (KM)	TOTAL WITH MANEUVER ANGLE (DEG)
1.	TWO BODY VS. FOUR BODY AND EARTH OBLATENESS	3.75	0.0550	NOT APPLICABLE		3.75	0.0550
2.	OBSERVATIONAL ERRORS						
2.1	UNCERTAINTY IN MEASUREMENT OF θ(1)	0.08	0.0007	0.00	0.0000		
2.2	UNCERTAINTY IN MEASUREMENT OF θ(2)	1.16	0.0069	0.32	0.0027		
2.3	UNCERTAINTY IN MEASUREMENT OF θ(3)	1.08	0.0035	0.66	0.0055		
2.4	UNCERTAINTY IN MEASUREMENT OF R(1)	1.03	0.0087	0.02	0.0002		
2.5	UNCERTAINTY IN MEASUREMENT OF R(2)	2.14	0.0128	0.59	0.0049		
2.6	UNCERTAINTY IN MEASUREMENT OF R(3)	1.22	0.0040	0.75	0.0062		
2.7	UNCERTAINTY IN MEASUREMENT OF R(0)	NOT APPLICABLE		0.31	0.0026		
	RSS	3.11	0.0178	1.24	0.0103	3.35	0.0205
3.	INSTRUMENTATION ERRORS						
3.1	UNCERTAINTY IN θ(1) INPUT GEARING AND DIAL READING	0.02	0.0002	0.00	0.0000		
3.2	UNCERTAINTY IN θ(2) INPUT GEARING AND DIAL READING	0.34	0.0020	0.09	0.0008		
3.3	UNCERTAINTY IN θ(3) INPUT GEARING AND DIAL READING	0.31	0.0030	0.19	0.0016		
3.4	UNCERTAINTY IN θ(P) INPUT GEARING AND DIAL READING	0.00	0.0008	0.09	0.0008		
3.5	UNCERTAINTY IN (θ(1)-θ(P)) DIFFERENTIAL	0.04	0.0003	0.00	0.0000		
3.6	UNCERTAINTY IN (θ(2)-θ(P)) DIFFERENTIAL	0.61	0.0036	0.17	0.0014		
3.7	UNCERTAINTY IN (θ(3)-θ(P)) DIFFERENTIAL	0.56	0.0018	0.34	0.0028		
3.8	UNCERTAINTY IN (θ(1)-θ(P)) REDUCTION GEARING TO COS MECHANISM	0.27	0.0023	0.01	0.0001		
3.9	UNCERTAINTY IN (θ(2)-θ(P)) REDUCTION GEARING TO COS MECHANISM	4.03	0.0241	1.12	0.0092		
3.10	UNCERTAINTY IN (θ(3)-θ(P)) REDUCTION GEARING TO COS MECHANISM	3.76	0.0121	2.29	0.0189		
3.11	UNCERTAINTY IN (θ(1)-θ(P)) COSINE MECHANISM	3.91	0.0331	0.09	0.0008		
3.12	UNCERTAINTY IN (θ(2)-θ(P)) COSINE MECHANISM	8.17	0.0488	2.27	0.0188		
3.13	UNCERTAINTY IN (θ(3)-θ(P)) COSINE MECHANISM	4.25	0.0157	2.36	0.0195		
3.14	UNCERTAINTY IN COS(θ(3)-θ(P))-COS(θ(1)-θ(P)) DIFFERENTIAL	6.38	0.0235	3.54	0.0293		
3.15	UNCERTAINTY IN COS(θ(2)-θ(P))-COS(θ(1)-θ(P)) DIFFERENTIAL	12.24	0.0731	3.41	0.0282		
3.16	UNCERTAINTY IN COS(θ(3)-θ(P))-COS(θ(1)-θ(P)) POT DRIVE GEARING	2.12	0.0078	1.18	0.0097		
3.17	UNCERTAINTY IN COS(θ(2)-θ(P))-COS(θ(1)-θ(P)) POT DRIVE GEARING	4.08	0.0244	1.13	0.0094		
3.18	COS(θ(3)-θ(P))-COS(θ(1)-θ(P)) POT NON-LINEARITY	5.10	0.0188	2.83	0.0234		
3.19	COS(θ(2)-θ(P))-COS(θ(1)-θ(P)) POT NON-LINEARITY	9.80	0.0585	2.73	0.0225		
3.20	UNCERTAINTY IN 1/R(1) INPUT GEARING AND DIAL READING	0.61	0.0051	0.02	0.0001		
3.21	UNCERTAINTY IN 1/R(2) INPUT GEARING AND DIAL READING	1.27	0.0076	0.35	0.0029		
3.22	UNCERTAINTY IN 1/R(3) INPUT GEARING AND DIAL READING	0.66	0.0024	0.37	0.0030		
3.23	UNCERTAINTY IN (1/R(3)-1/R(1)) DIFFERENTIAL	0.22	0.0008	0.12	0.0010		
3.24	UNCERTAINTY IN (1/R(2)-1/R(1)) DIFFERENTIAL	0.42	0.0025	0.12	0.0010		
3.25	UNCERTAINTY IN (1/R(3)-1/R(1)) RHEOSTAT DRIVE GEARING	2.21	0.0091	1.22	0.0101		
3.26	UNCERTAINTY IN (1/R(2)-1/R(1)) RHEOSTAT DRIVE GEARING	4.24	0.0253	1.18	0.0097		
3.27	(1/R(3)-1/R(1)) RHEOSTAT NON-LINEARITY	5.29	0.0195	2.93	0.0243		
3.28	(1/R(2)-1/R(1)) RHEOSTAT NON-LINEARITY	10.17	0.0608	2.83	0.0234		
3.29	BRIDGE TRIMMING ERROR	0.70	0.0042	0.19	0.0016		
3.30	GALVANOMETER BIAS ERROR	NIL	NIL	NIL	NIL		
	RSS	25.15	0.1415	9.00	0.0744	26.71	0.1599
4.	ERRORS DUE TO PARABOLIC ASSUMPTION OF CORRECTIVE MANEUVER	NOT APPLICABLE		0.19	0.0023	0.19	0.0023
	TOTAL RSS ERRORS	25.62	0.1529	9.83	0.0932	27.44	0.1790

NOTE 1. SOURCE ERRORS UTILIZED ARE 1 SIGMA VALUES BASED ON MAXIMUM VALUES LISTED IN FIGURE NO. 3-4

MANUAL SPACE COMPUTER ERROR ANALYSIS • PROBLEM NUMBER 5.1.2

Figure 5-8

	ERROR SOURCE	ERRORS IN PERIGEE: ASSUMING NO MANEUVER, RADIUS (KM)	ASSUMING NO MANEUVER, ANGLE (DEG)	INCREMENT DUE TO MANEUVER COMP., RADIUS (KM)	INCREMENT DUE TO MANEUVER COMP., ANGLE (DEG)	TOTAL WITH MANEUVER, RADIUS (KM)	TOTAL WITH MANEUVER, ANGLE (DEG)
1.	TWO BODY VS. FOUR BODY AND EARTH OBLATENESS	3.01	0.0488	NOT APPLICABLE		3.01	0.0488
2.	OBSERVATIONAL ERRORS						
2.1	UNCERTAINTY IN MEASUREMENT OF θ(1)	0.38	0.0032	0.01	0.0001		
2.2	UNCERTAINTY IN MEASUREMENT OF θ(2)	1.63	0.0109	0.31	0.0026		
2.3	UNCERTAINTY IN MEASUREMENT OF θ(3)	1.26	0.0050	0.66	0.0054		
2.4	UNCERTAINTY IN MEASUREMENT OF R(1)	1.69	0.0143	0.04	0.0003		
2.5	UNCERTAINTY IN MEASUREMENT OF R(2)	3.00	0.0201	0.57	0.0047		
2.6	UNCERTAINTY IN MEASUREMENT OF R(3)	1.42	0.0056	0.74	0.0061		
2.7	UNCERTAINTY IN MEASUREMENT OF R(C)	NOT APPLICABLE		0.31	0.0026		
	RSS	4.27	0.0282	1.23	0.0102	4.45	0.0299
3.	INSTRUMENTATION ERRORS						
3.1	UNCERTAINTY IN θ(1) INPUT GEARING AND DIAL READING	0.11	0.0009	0.00	0.0000		
3.2	UNCERTAINTY IN θ(2) INPUT GEARING AND DIAL READING	0.47	0.0031	0.09	0.0007		
3.3	UNCERTAINTY IN θ(3) INPUT GEARING AND DIAL READING	0.36	0.0014	0.19	0.0016		
3.4	UNCERTAINTY IN θ(P) INPUT GEARING AND DIAL READING	0.00	0.0008	0.10	0.0008		
3.5	UNCERTAINTY IN (θ(1)-θ(P)) DIFFERENTIAL	0.20	0.0017	0.01	0.0000		
3.6	UNCERTAINTY IN (θ(2)-θ(P)) DIFFERENTIAL	0.84	0.0057	0.16	0.0013		
3.7	UNCERTAINTY IN (θ(3)-θ(P)) DIFFERENTIAL	0.65	0.0026	0.34	0.0028		
3.8	UNCERTAINTY IN (θ(1)-θ(P)) REDUCTION GEARING TO COS MECHANISM	1.30	0.0110	0.03	0.0002		
3.9	UNCERTAINTY IN (θ(2)-θ(P)) REDUCTION GEARING TO COS MECHANISM	5.64	0.0378	1.08	0.0089		
3.10	UNCERTAINTY IN (θ(3)-θ(P)) REDUCTION GEARING TO COS MECHANISM	4.35	0.0172	2.27	0.0188		
3.11	UNCERTAINTY IN (θ(1)-θ(P)) COSINE MECHANISM	6.43	0.0544	0.15	0.0012		
3.12	UNCERTAINTY IN (θ(2)-θ(P)) COSINE MECHANISM	11.46	0.0766	2.19	0.0181		
3.13	UNCERTAINTY IN (θ(3)-θ(P)) COSINE MECHANISM	5.02	0.0222	2.34	0.0194		
3.14	UNCERTAINTY IN COS(θ(3)-θ(P))-COS(θ(1)-θ(P)) DIFFERENTIAL	7.53	0.0332	3.51	0.0290		
3.15	UNCERTAINTY IN COS(θ(2)-θ(P))-COS(θ(1)-θ(P)) DIFFERENTIAL	17.17	0.1148	3.29	0.0272		
3.16	UNCERTAINTY IN COS(θ(3)-θ(P))-COS(θ(1)-θ(P)) POT DRIVE GEARING	2.51	0.0111	1.17	0.0097		
3.17	UNCERTAINTY IN COS(θ(2)-θ(P))-COS(θ(1)-θ(P)) POT DRIVE GEARING	5.72	0.0382	1.10	0.0090		
3.18	COS(θ(3)-θ(P))-COS(θ(1)-θ(P)) POT NON-LINEARITY	6.03	0.0266	2.81	0.0232		
3.19	COS(θ(2)-θ(P))-COS(θ(1)-θ(P)) POT NON-LINEARITY	13.75	0.0919	2.63	0.0218		
3.20	UNCERTAINTY IN 1/R(1) INPUT GEARING AND DIAL READING	1.00	0.0085	0.02	0.0002		
3.21	UNCERTAINTY IN 1/R(2) INPUT GEARING AND DIAL READING	1.78	0.0119	0.34	0.0028		
3.22	UNCERTAINTY IN 1/R(3) INPUT GEARING AND DIAL READING	0.78	0.0034	0.37	0.0030		
3.23	UNCERTAINTY IN (1/R(3)-1/R(1)) DIFFERENTIAL	0.26	0.0011	0.12	0.0010		
3.24	UNCERTAINTY IN (1/R(2)-1/R(1)) DIFFERENTIAL	0.59	0.0040	0.11	0.0009		
3.25	UNCERTAINTY IN (1/R(3)-1/R(1)) RHEOSTAT DRIVE GEARING	2.60	0.0115	1.21	0.0100		
3.26	UNCERTAINTY IN (1/R(2)-1/R(1)) RHEOSTAT DRIVE GEARING	5.94	0.0398	1.14	0.0094		
3.27	(1/R(3)-1/R(1)) RHEOSTAT NON-LINEARITY	6.24	0.0275	2.91	0.0241		
3.28	(1/R(2)-1/R(1)) RHEOSTAT NON-LINEARITY	14.27	0.0955	2.73	0.0226		
3.29	BRIDGE TRIMMING ERROR	0.85	0.0057	0.16	0.0013		
3.30	GALVANOMETER BIAS ERROR	NIL	NIL	NIL	NIL		
	RSS	34.30	0.2212	8.83	0.0730	35.42	0.2329
4.	ERRORS DUE TO PARABOLIC ASSUMPTION OF CORRECTIVE MANEUVER	NOT APPLICABLE		0.15	0.0018	0.15	0.0018
	TOTAL RSS ERRORS	34.70	0.2282	9.41	0.0884	35.95	0.2447

NOTE 1. SOURCE ERRORS UTILIZED ARE 1 SIGMA VALUES BASED ON MAXIMUM VALUES LISTED IN FIGURE NO. 3-4

MANUAL SPACE COMPUTER ERROR ANALYSIS • PROBLEM NUMBER 5.1.3

Figure 5-9

	ERROR SOURCE	ASSUMING NO MANEUVER RADIUS (KM)	ASSUMING NO MANEUVER ANGLE (DEG)	ERRORS IN PERIGEE INCREMENT DUE TO MANEUVER COMP. RADIUS (KM)	ERRORS IN PERIGEE INCREMENT DUE TO MANEUVER COMP. ANGLE (DEG)	TOTAL WITH MANEUVER RADIUS (KM)	TOTAL WITH MANEUVER ANGLE (DEG)
1.	TWO BODY VS. FOUR BODY AND EARTH OBLATENESS	4.76	0.0564	NOT APPLICABLE		4.76	0.0564
2.	OBSERVATIONAL ERRORS						
2.1	UNCERTAINTY IN MEASUREMENT OF θ(1)	0.48	0.0041	0.01	0.0001		
2.2	UNCERTAINTY IN MEASUREMENT OF θ(2)	1.89	0.0129	0.42	0.0037		
2.3	UNCERTAINTY IN MEASUREMENT OF θ(3)	1.41	0.0060	0.73	0.0063		
2.4	UNCERTAINTY IN MEASUREMENT OF R(1)	1.79	0.0153	0.05	0.0004		
2.5	UNCERTAINTY IN MEASUREMENT OF R(2)	3.24	0.0221	0.72	0.0063		
2.6	UNCERTAINTY IN MEASUREMENT OF R(3)	1.56	0.0066	0.80	0.0070		
2.7	UNCERTAINTY IN MEASUREMENT OF R(C)	NOT APPLICABLE		0.28	0.0025		
	RSS	4.69	0.0314	1.39	0.0122	4.89	0.0337
3.	INSTRUMENTATION ERRORS						
3.1	UNCERTAINTY IN θ(1) INPUT GEARING AND DIAL READING	0.14	0.0012	0.00	0.0000		
3.2	UNCERTAINTY IN θ(2) INPUT GEARING AND DIAL READING	0.55	0.0037	0.12	0.0011		
3.3	UNCERTAINTY IN θ(3) INPUT GEARING AND DIAL READING	0.41	0.0017	0.21	0.0018		
3.4	UNCERTAINTY IN θ(P) INPUT GEARING AND DIAL READING	0.00	0.0008	0.09	0.0008		
3.5	UNCERTAINTY IN (θ(1)-θ(P)) DIFFERENTIAL	0.25	0.0021	0.01	0.0001		
3.6	UNCERTAINTY IN (θ(2)-θ(P)) DIFFERENTIAL	0.59	0.0067	0.22	0.0019		
3.7	UNCERTAINTY IN (θ(3)-θ(P)) DIFFERENTIAL	0.73	0.0031	0.38	0.0033		
3.8	UNCERTAINTY IN (θ(1)-θ(P)) REDUCTION GEARING TO COS MECHANISM	1.68	0.0143	0.05	0.0004		
3.9	UNCERTAINTY IN (θ(2)-θ(P)) REDUCTION GEARING TO COS MECHANISM	6.56	0.0447	1.46	0.0128		
3.10	UNCERTAINTY IN (θ(3)-θ(P)) REDUCTION GEARING TO COS MECHANISM	4.89	0.0208	2.51	0.0220		
3.11	UNCERTAINTY IN (θ(1)-θ(P)) COSINE MECHANISM	6.96	0.0593	0.19	0.0016		
3.12	UNCERTAINTY IN (θ(2)-θ(P)) COSINE MECHANISM	12.64	0.0860	2.81	0.0246		
3.13	UNCERTAINTY IN (θ(3)-θ(P)) COSINE MECHANISM	5.68	0.0268	2.62	0.0229		
3.14	UNCERTAINTY IN COS(θ(3)-θ(P))-COS(θ(1)-θ(P)) DIFFERENTIAL	8.51	0.0401	3.93	0.0344		
3.15	UNCERTAINTY IN COS(θ(2)-θ(P))-COS(θ(1)-θ(P)) DIFFERENTIAL	18.94	0.1289	4.21	0.0368		
3.16	UNCERTAINTY IN COS(θ(3)-θ(P))-COS(θ(1)-θ(P)) POT DRIVE GEARING	2.83	0.0134	1.31	0.0114		
3.17	UNCERTAINTY IN COS(θ(2)-θ(P))-COS(θ(1)-θ(P)) POT DRIVE GEARING	6.31	0.0430	1.40	0.0123		
3.18	COS(θ(3)-θ(P))-COS(θ(1)-θ(P)) POT NON-LINEARITY	6.81	0.0321	3.15	0.0275		
3.19	COS(θ(2)-θ(P))-COS(θ(1)-θ(P)) POT NON-LINEARITY	15.17	0.1032	3.37	0.0295		
3.20	UNCERTAINTY IN 1/R(1) INPUT GEARING AND DIAL READING	1.06	0.0090	0.03	0.0002		
3.21	UNCERTAINTY IN 1/R(2) INPUT GEARING AND DIAL READING	1.92	0.0131	0.43	0.0037		
3.22	UNCERTAINTY IN 1/R(3) INPUT GEARING AND DIAL READING	0.86	0.0041	0.40	0.0035		
3.23	UNCERTAINTY IN (1/R(3)-1/R(1)) DIFFERENTIAL	0.29	0.0014	0.13	0.0012		
3.24	UNCERTAINTY IN (1/R(2)-1/R(1)) DIFFERENTIAL	0.64	0.0044	0.14	0.0012		
3.25	UNCERTAINTY IN (1/R(3)-1/R(1)) RHEOSTAT DRIVE GEARING	2.88	0.0136	1.33	0.0116		
3.26	UNCERTAINTY IN (1/R(2)-1/R(1)) RHEOSTAT DRIVE GEARING	6.41	0.0437	1.42	0.0125		
3.27	(1/R(3)-1/R(1)) RHEOSTAT NON-LINEARITY	6.90	0.0325	3.19	0.0279		
3.28	(1/R(2)-1/R(1)) RHEOSTAT NON-LINEARITY	15.41	0.1049	3.42	0.0300		
3.29	BRIDGE TRIMMING ERROR	1.00	0.0068	0.22	0.0019		
3.30	GALVANOMETER BIAS ERROR	NIL	NIL	NIL	NIL		
	RSS	37.83	0.2485	10.47	0.0916	39.25	0.2649
4.	ERRORS DUE TO PARABOLIC ASSUMPTION OF CORRECTIVE MANEUVER	NOT APPLICABLE		0.10	0.0012	0.10	0.0012
	TOTAL RSS ERRORS	38.42	0.2568	11.58	0.1082	40.12	0.2787

NOTE 1. SOURCE ERRORS UTILIZED ARE 1 SIGMA VALUES BASED ON MAXIMUM VALUES LISTED IN FIGURE NO. 3-4

MANUAL SPACE COMPUTER ERROR ANALYSIS • PROBLEM NUMBER 14.1.1

Figure 5-10

	ERROR SOURCE	ASSUMING NO MANEUVER RADIUS (KM)	ASSUMING NO MANEUVER ANGLE (DEG)	ERRORS IN PERIGEE INCREMENT DUE TO MANEUVER COMP. RADIUS (KM)	ERRORS IN PERIGEE INCREMENT DUE TO MANEUVER COMP. ANGLE (DEG)	TOTAL WITH MANEUVER RADIUS (KM)	TOTAL WITH MANEUVER ANGLE (DEG)
1.	TWO BODY VS. FOUR BODY AND EARTH OBLATENESS	3.68	0.0471	NOT APPLICABLE		3.68	0.0471
2.	OBSERVATIONAL ERRORS						
2.1	UNCERTAINTY IN MEASUREMENT OF E(1)	0.78	0.0067	0.02	0.0002		
2.2	UNCERTAINTY IN MEASUREMENT OF E(2)	2.30	0.0164	0.43	0.0038		
2.3	UNCERTAINTY IN MEASUREMENT OF E(3)	1.52	0.0069	0.73	0.0064		
2.4	UNCERTAINTY IN MEASUREMENT OF R(1)	2.37	0.0202	0.06	0.0005		
2.5	UNCERTAINTY IN MEASUREMENT OF R(2)	3.94	0.0280	0.74	0.0065		
2.6	UNCERTAINTY IN MEASUREMENT OF R(3)	1.68	0.0076	0.81	0.0070		
2.7	UNCERTAINTY IN MEASUREMENT OF R(C)	NOT APPLICABLE		0.28	0.0025		
	RSS	5.67	0.0401	1.41	0.0123	5.84	0.0420
3.	INSTRUMENTATION ERRORS						
3.1	UNCERTAINTY IN E(1) INPUT GEARING AND DIAL READING	0.22	0.0019	0.00	0.0000		
3.2	UNCERTAINTY IN E(2) INPUT GEARING AND DIAL READING	0.67	0.0047	0.13	0.0011		
3.3	UNCERTAINTY IN E(3) INPUT GEARING AND DIAL READING	0.44	0.0020	0.21	0.0018		
3.4	UNCERTAINTY IN E(P) INPUT GEARING AND DIAL READING	0.00	0.0008	0.09	0.0008		
3.5	UNCERTAINTY IN (E(1)-E(P)) DIFFERENTIAL	0.41	0.0035	0.01	0.0001		
3.6	UNCERTAINTY IN (E(2)-E(P)) DIFFERENTIAL	1.20	0.0085	0.23	0.0020		
3.7	UNCERTAINTY IN (E(3)-E(P)) DIFFERENTIAL	0.79	0.0036	0.38	0.0033		
3.8	UNCERTAINTY IN (E(1)-E(P)) REDUCTION GEARING TO COS MECHANISM	2.72	0.0232	0.07	0.0006		
3.9	UNCERTAINTY IN (E(2)-E(P)) REDUCTION GEARING TO COS MECHANISM	7.97	0.0567	1.50	0.0131		
3.10	UNCERTAINTY IN (E(3)-E(P)) REDUCTION GEARING TO COS MECHANISM	5.26	0.0240	2.52	0.0221		
3.11	UNCERTAINTY IN (E(1)-E(P)) COSINE MECHANISM	9.20	0.0783	0.25	0.0022		
3.12	UNCERTAINTY IN (E(2)-E(P)) COSINE MECHANISM	15.36	0.1092	2.88	0.0252		
3.13	UNCERTAINTY IN (E(3)-E(P)) COSINE MECHANISM	6.16	0.0308	2.63	0.0230		
3.14	UNCERTAINTY IN COS(E(3)-E(P))-COS(E(1)-E(P)) DIFFERENTIAL	9.22	0.0462	3.95	0.0345		
3.15	UNCERTAINTY IN COS(E(2)-E(P))-COS(E(1)-E(P)) DIFFERENTIAL	23.01	0.1636	4.32	0.0378		
3.16	UNCERTAINTY IN COS(E(3)-E(P))-COS(E(1)-E(P)) POT DRIVE GEARING	3.07	0.0154	1.31	0.0115		
3.17	UNCERTAINTY IN COS(E(2)-E(P))-COS(E(1)-E(P)) POT DRIVE GEARING	7.67	0.0545	1.44	0.0126		
3.18	COS(E(3)-E(P))-COS(E(1)-E(P)) POT NON-LINEARITY	7.39	0.0370	3.16	0.0277		
3.19	COS(E(2)-E(P))-COS(E(1)-E(P)) POT NON-LINEARITY	18.43	0.1310	3.46	0.0302		
3.20	UNCERTAINTY IN 1/R(1) INPUT GEARING AND DIAL READING	1.40	0.0119	0.04	0.0003		
3.21	UNCERTAINTY IN 1/R(2) INPUT GEARING AND DIAL READING	2.34	0.0166	0.44	0.0038		
3.22	UNCERTAINTY IN 1/R(3) INPUT GEARING AND DIAL READING	0.94	0.0047	0.40	0.0035		
3.23	UNCERTAINTY IN (1/R(3)-1/R(1)) DIFFERENTIAL	0.31	0.0016	0.14	0.0012		
3.24	UNCERTAINTY IN (1/R(2)-1/R(1)) DIFFERENTIAL	0.78	0.0055	0.14	0.0013		
3.25	UNCERTAINTY IN (1/R(3)-1/R(1)) RHEOSTAT DRIVE GEARING	3.12	0.0156	1.34	0.0117		
3.26	UNCERTAINTY IN (1/R(2)-1/R(1)) RHEOSTAT DRIVE GEARING	7.79	0.0554	1.46	0.0128		
3.27	(1/R(3)-1/R(1)) RHEOSTAT NON-LINEARITY	7.48	0.0375	3.20	0.0280		
3.28	(1/R(2)-1/R(1)) RHEOSTAT NON-LINEARITY	18.72	0.1332	3.51	0.0307		
3.29	BRIDGE TRIMMING ERROR	1.06	0.0075	0.20	0.0017		
3.30	GALVANOMETER BIAS ERROR	NIL	NIL	NIL	NIL		
	RSS	45.34	0.3141	10.63	0.0930	46.57	0.3276
4.	ERRORS DUE TO PARABOLIC ASSUMPTION OF CORRECTIVE MANEUVER	NOT APPLICABLE		0.08	0.0009	0.08	0.0009
	TOTAL RSS ERRORS	45.84	0.3202	11.34	0.1050	47.22	0.3370

NOTE 1. SOURCE ERRORS UTILIZED ARE 1 SIGMA VALUES BASED ON MAXIMUM VALUES LISTED IN FIGURE NO. 3-4

MANUAL SPACE COMPUTER ERROR ANALYSIS • PROBLEM NUMBER 14.1.2

Figure 5-11

	ERROR SOURCE	ERRORS IN PERIGEE: ASSUMING NO MANEUVER RADIUS (KM)	ANGLE (DEG)	INCREMENT DUE TO MANEUVER COMP. RADIUS (KM)	ANGLE (DEG)	TOTAL WITH MANEUVER RADIUS (KM)	ANGLE (DEG)
1.	TWO BODY VS. FOUR BODY AND EARTH OBLATENESS	2.76	0.0396	NOT APPLICABLE		2.76	0.0396
2.	OBSERVATIONAL ERRORS						
2.1	UNCERTAINTY IN MEASUREMENT OF E(1)	0.86	0.0080	0.05	0.0005		
2.2	UNCERTAINTY IN MEASUREMENT OF E(2)	3.30	0.0248	0.47	0.0041		
2.3	UNCERTAINTY IN MEASUREMENT OF E(3)	2.44	0.0140	0.84	0.0073		
2.4	UNCERTAINTY IN MEASUREMENT OF R(1)	2.11	0.0196	0.13	0.0012		
2.5	UNCERTAINTY IN MEASUREMENT OF R(2)	4.70	0.0353	0.67	0.0058		
2.6	UNCERTAINTY IN MEASUREMENT OF R(3)	2.69	0.0155	0.92	0.0081		
2.7	UNCERTAINTY IN MEASUREMENT OF R(C)	NOT APPLICABLE		0.28	0.0025		
	RSS	7.17	0.0524	1.52	0.0133	7.33	0.0541
3.	INSTRUMENTATION ERRORS						
3.1	UNCERTAINTY IN E(1) INPUT GEARING AND DIAL READING	0.25	0.0023	0.02	0.0001		
3.2	UNCERTAINTY IN E(2) INPUT GEARING AND DIAL READING	0.96	0.0072	0.14	0.0012		
3.3	UNCERTAINTY IN E(3) INPUT GEARING AND DIAL READING	0.70	0.0040	0.24	0.0021		
3.4	UNCERTAINTY IN E(P) INPUT GEARING AND DIAL READING	0.01	0.0008	0.09	0.0008		
3.5	UNCERTAINTY IN (E(1)-E(P)) DIFFERENTIAL	0.45	0.0042	0.03	0.0003		
3.6	UNCERTAINTY IN (E(2)-E(P)) DIFFERENTIAL	1.72	0.0129	0.24	0.0021		
3.7	UNCERTAINTY IN (E(3)-E(P)) DIFFERENTIAL	1.27	0.0073	0.43	0.0038		
3.8	UNCERTAINTY IN (E(1)-E(P)) REDUCTION GEARING TO COS MECHANISM	2.98	0.0278	0.19	0.0017		
3.9	UNCERTAINTY IN (E(2)-E(P)) REDUCTION GEARING TO COS MECHANISM	11.43	0.0859	1.62	0.0141		
3.10	UNCERTAINTY IN (E(3)-E(P)) REDUCTION GEARING TO COS MECHANISM	8.47	0.0487	2.91	0.0254		
3.11	UNCERTAINTY IN (E(1)-E(P)) COSINE MECHANISM	8.18	0.0761	0.52	0.0045		
3.12	UNCERTAINTY IN (E(2)-E(P)) COSINE MECHANISM	18.46	0.1387	2.61	0.0229		
3.13	UNCERTAINTY IN (E(3)-E(P)) COSINE MECHANISM	10.27	0.0626	3.13	0.0274		
3.14	UNCERTAINTY IN COS(E(3)-E(P))-COS(E(1)-E(P)) DIFFERENTIAL	15.40	0.0938	4.69	0.0410		
3.15	UNCERTAINTY IN COS(E(2)-E(P))-COS(E(1)-E(P)) DIFFERENTIAL	27.67	0.2078	3.92	0.0343		
3.16	UNCERTAINTY IN COS(E(3)-E(P))-COS(E(1)-E(P)) POT DRIVE GEARING	5.13	0.0312	1.56	0.0137		
3.17	UNCERTAINTY IN COS(E(2)-E(P))-COS(E(1)-E(P)) POT DRIVE GEARING	9.22	0.0692	1.30	0.0114		
3.18	COS(E(3)-E(P))-COS(E(1)-E(P)) POT NON-LINEARITY	12.33	0.0751	3.75	0.0328		
3.19	COS(E(2)-E(P))-COS(E(1)-E(P)) POT NON-LINEARITY	22.15	0.1664	3.13	0.0274		
3.20	UNCERTAINTY IN 1/R(1) INPUT GEARING AND DIAL READING	1.24	0.0116	0.08	0.0007		
3.21	UNCERTAINTY IN 1/R(2) INPUT GEARING AND DIAL READING	2.81	0.0211	0.40	0.0035		
3.22	UNCERTAINTY IN 1/R(3) INPUT GEARING AND DIAL READING	1.56	0.0095	0.48	0.0042		
3.23	UNCERTAINTY IN (1/R(3)-1/R(1)) DIFFERENTIAL	0.52	0.0032	0.16	0.0014		
3.24	UNCERTAINTY IN (1/R(2)-1/R(1)) DIFFERENTIAL	0.94	0.0070	0.13	0.0012		
3.25	UNCERTAINTY IN (1/R(3)-1/R(1)) RHEOSTAT DRIVE GEARING	5.21	0.0317	1.58	0.0139		
3.26	UNCERTAINTY IN (1/R(2)-1/R(1)) RHEOSTAT DRIVE GEARING	9.37	0.0704	1.33	0.0116		
3.27	(1/R(3)-1/R(1)) RHEOSTAT NON-LINEARITY	12.48	0.0760	3.80	0.0332		
3.28	(1/R(2)-1/R(1)) RHEOSTAT NON-LINEARITY	22.51	0.1692	3.18	0.0279		
3.29	BRIDGE TRIMMING ERROR	1.89	0.0142	0.27	0.0023		
3.30	GALVANOMETER BIAS ERROR	NIL	NIL	NIL	NIL		
	RSS	57.73	0.4182	11.20	0.0980	58.80	0.4295
4.	ERRORS DUE TO PARABOLIC ASSUMPTION OF CORRECTIVE MANEUVER	NOT APPLICABLE		0.06	0.0007	0.06	0.0007
	TOTAL RSS ERRORS	58.24	0.4233	11.63	0.1065	59.39	0.4365

NOTE 1. SOURCE ERRORS UTILIZED ARE 1 SIGMA VALUES BASED ON MAXIMUM VALUES LISTED IN FIGURE NO. 3-4

MANUAL SPACE COMPUTER ERROR ANALYSIS • PROBLEM NUMBER 14.1.3

Figure 5-12

	ERROR SOURCE	ERRORS IN PERIGEE: ASSUMING NO MANEUVER RADIUS (KM)	ASSUMING NO MANEUVER ANGLE (DEG)	INCREMENT DUE TO MANEUVER COMP. RADIUS (KM)	INCREMENT DUE TO MANEUVER COMP. ANGLE (DEG)	TOTAL WITH MANEUVER RADIUS (KM)	TOTAL WITH MANEUVER ANGLE (DEG)
1.	TWO BODY VS. FOUR BODY AND EARTH OBLATENESS	3.74	0.0581	NOT APPLICABLE		3.74	0.0581
2.	OBSERVATIONAL ERRORS						
2.1	UNCERTAINTY IN MEASUREMENT OF θ(1)	0.26	0.0016	0.08	0.0007		
2.2	UNCERTAINTY IN MEASUREMENT OF θ(2)	0.19	0.0005	0.13	0.0012		
2.3	UNCERTAINTY IN MEASUREMENT OF θ(3)	0.45	0.0007	0.52	0.0046		
2.4	UNCERTAINTY IN MEASUREMENT OF R(1)	0.61	0.0038	0.19	0.0016		
2.5	UNCERTAINTY IN MEASUREMENT OF R(2)	1.07	0.0029	0.74	0.0066		
2.6	UNCERTAINTY IN MEASUREMENT OF R(3)	0.59	0.0009	0.69	0.0061		
2.7	UNCERTAINTY IN MEASUREMENT OF R(C)	NOT APPLICABLE		0.31	0.0027		
	RSS	1.47	0.0052	1.20	0.0107	1.90	0.0119
3.	INSTRUMENTATION ERRORS						
3.1	UNCERTAINTY IN θ(1) INPUT GEARING AND DIAL READING	0.07	0.0005	0.02	0.0002		
3.2	UNCERTAINTY IN θ(2) INPUT GEARING AND DIAL READING	0.05	0.0002	0.04	0.0003		
3.3	UNCERTAINTY IN θ(3) INPUT GEARING AND DIAL READING	0.13	0.0002	0.15	0.0013		
3.4	UNCERTAINTY IN θ(P) INPUT GEARING AND DIAL READING	0.00	0.0008	0.09	0.0008		
3.5	UNCERTAINTY IN (θ(1)-θ(P)) DIFFERENTIAL	0.13	0.0008	0.04	0.0004		
3.6	UNCERTAINTY IN (θ(2)-θ(P)) DIFFERENTIAL	0.10	0.0003	0.07	0.0006		
3.7	UNCERTAINTY IN (θ(3)-θ(P)) DIFFERENTIAL	0.23	0.0003	0.27	0.0024		
3.8	UNCERTAINTY IN (θ(1)-θ(P)) REDUCTION GEARING TO COS MECHANISM	0.89	0.0055	0.27	0.0024		
3.9	UNCERTAINTY IN (θ(2)-θ(P)) REDUCTION GEARING TO COS MECHANISM	0.66	0.0018	0.46	0.0041		
3.10	UNCERTAINTY IN (θ(3)-θ(P)) REDUCTION GEARING TO COS MECHANISM	1.55	0.0023	1.81	0.0161		
3.11	UNCERTAINTY IN (θ(1)-θ(P)) COSINE MECHANISM	2.17	0.0135	0.66	0.0058		
3.12	UNCERTAINTY IN (θ(2)-θ(P)) COSINE MECHANISM	3.78	0.0103	2.63	0.0234		
3.13	UNCERTAINTY IN (θ(3)-θ(P)) COSINE MECHANISM	1.61	0.0032	1.97	0.0176		
3.14	UNCERTAINTY IN COS(θ(3)-θ(P))-COS(θ(1)-θ(P)) DIFFERENTIAL	2.42	0.0048	2.96	0.0264		
3.15	UNCERTAINTY IN COS(θ(2)-θ(P))-COS(θ(1)-θ(P)) DIFFERENTIAL	5.66	0.0154	3.94	0.0351		
3.16	UNCERTAINTY IN COS(θ(3)-θ(P))-COS(θ(1)-θ(P)) POT DRIVE GEARING	0.80	0.0016	0.98	0.0088		
3.17	UNCERTAINTY IN COS(θ(2)-θ(P))-COS(θ(1)-θ(P)) POT DRIVE GEARING	1.89	0.0051	1.31	0.0117		
3.18	COS(θ(3)-θ(P))-COS(θ(1)-θ(P)) POT NON-LINEARITY	1.93	0.0039	2.37	0.0211		
3.19	COS(θ(2)-θ(P))-COS(θ(1)-θ(P)) POT NON-LINEARITY	4.54	0.0123	3.15	0.0281		
3.20	UNCERTAINTY IN 1/R(1) INPUT GEARING AND DIAL READING	0.37	0.0023	0.11	0.0010		
3.21	UNCERTAINTY IN 1/R(2) INPUT GEARING AND DIAL READING	0.64	0.0017	0.44	0.0039		
3.22	UNCERTAINTY IN 1/R(3) INPUT GEARING AND DIAL READING	0.27	0.0005	0.33	0.0030		
3.23	UNCERTAINTY IN (1/R(3)-1/R(1)) DIFFERENTIAL	0.09	0.0002	0.11	0.0010		
3.24	UNCERTAINTY IN (1/R(2)-1/R(1)) DIFFERENTIAL	0.21	0.0006	0.15	0.0013		
3.25	UNCERTAINTY IN (1/R(3)-1/R(1)) RHEOSTAT DRIVE GEARING	0.90	0.0018	1.11	0.0099		
3.26	UNCERTAINTY IN (1/R(2)-1/R(1)) RHEOSTAT DRIVE GEARING	2.12	0.0058	1.47	0.0132		
3.27	(1/R(3)-1/R(1)) RHEOSTAT NON-LINEARITY	2.17	0.0043	2.65	0.0237		
3.28	(1/R(2)-1/R(1)) RHEOSTAT NON-LINEARITY	5.09	0.0139	3.54	0.0316		
3.29	BRIDGE TRIMMING ERROR	0.18	0.0005	0.13	0.0011		
3.30	GALVANOMETER BIAS ERROR	NIL	NIL	NIL	NIL		
	RSS	11.43	0.0329	9.06	0.0809	14.58	0.0873
4.	ERRORS DUE TO PARABOLIC ASSUMPTION OF CORRECTIVE MANEUVER	NOT APPLICABLE		0.60	0.0081	0.60	0.0081
	TOTAL RSS ERRORS	12.11	0.0670	9.90	0.1005	15.64	0.1207

NOTE 1. SOURCE ERRORS UTILIZED ARE 1 SIGMA VALUES BASED ON MAXIMUM VALUES LISTED IN FIGURE NO. 3-4

MANUAL SPACE COMPUTER ERROR ANALYSIS • PROBLEM NUMBER 1.2.1

Figure 5-13

	ERROR SOURCE	ERRORS IN PERIGEE: ASSUMING NO MANEUVER, RADIUS (KM)	ANGLE (DEG)	INCREMENT DUE TO MANEUVER COMP., RADIUS (KM)	ANGLE (DEG)	TOTAL WITH MANEUVER, RADIUS (KM)	ANGLE (DEG)
1.	TWO BODY VS. FOUR BODY AND EARTH OBLATENESS	4.15	0.0579	NOT APPLICABLE		4.15	0.0579
2.	OBSERVATIONAL ERRORS						
2.1	UNCERTAINTY IN MEASUREMENT OF θ(1)	0.46	0.0016	0.15	0.0007		
2.2	UNCERTAINTY IN MEASUREMENT OF θ(2)	0.04	0.0000	0.03	0.0001		
2.3	UNCERTAINTY IN MEASUREMENT OF θ(3)	0.50	0.0012	0.74	0.0037		
2.4	UNCERTAINTY IN MEASUREMENT OF R(1)	1.10	0.0037	0.36	0.0018		
2.5	UNCERTAINTY IN MEASUREMENT OF R(2)	1.90	0.0015	1.60	0.0080		
2.6	UNCERTAINTY IN MEASUREMENT OF R(3)	0.93	0.0022	1.38	0.0069		
2.7	UNCERTAINTY IN MEASUREMENT OF R(C)	NOT APPLICABLE		0.73	0.0037		
	RSS	2.48	0.0050	2.39	0.0119	3.44	0.0129
3.	INSTRUMENTATION ERRORS						
3.1	UNCERTAINTY IN θ(1) INPUT GEARING AND DIAL READING	0.13	0.0005	0.04	0.0002		
3.2	UNCERTAINTY IN θ(2) INPUT GEARING AND DIAL READING	0.01	0.0000	0.01	0.0000		
3.3	UNCERTAINTY IN θ(3) INPUT GEARING AND DIAL READING	0.14	0.0003	0.21	0.0011		
3.4	UNCERTAINTY IN θ(P) INPUT GEARING AND DIAL READING	0.00	0.0008	0.16	0.0008		
3.5	UNCERTAINTY IN (θ(1)-θ(P)) DIFFERENTIAL	0.24	0.0008	0.08	0.0004		
3.6	UNCERTAINTY IN (θ(2)-θ(P)) DIFFERENTIAL	0.02	0.0000	0.02	0.0001		
3.7	UNCERTAINTY IN (θ(3)-θ(P)) DIFFERENTIAL	0.26	0.0006	0.38	0.0019		
3.8	UNCERTAINTY IN (θ(1)-θ(P)) REDUCTION GEARING TO COS MECHANISM	1.60	0.0054	0.52	0.0026		
3.9	UNCERTAINTY IN (θ(2)-θ(P)) REDUCTION GEARING TO COS MECHANISM	0.12	0.0001	0.10	0.0005		
3.10	UNCERTAINTY IN (θ(3)-θ(P)) REDUCTION GEARING TO COS MECHANISM	1.72	0.0041	2.55	0.0127		
3.11	UNCERTAINTY IN (θ(1)-θ(P)) COSINE MECHANISM	3.91	0.0122	1.26	0.0063		
3.12	UNCERTAINTY IN (θ(2)-θ(P)) COSINE MECHANISM	6.69	0.0052	5.65	0.0283		
3.13	UNCERTAINTY IN (θ(3)-θ(P)) COSINE MECHANISM	2.78	0.0080	4.38	0.0219		
3.14	UNCERTAINTY IN COS(θ(3)-θ(P))-COS(θ(1)-θ(P)) DIFFERENTIAL	4.17	0.0119	6.56	0.0328		
3.15	UNCERTAINTY IN COS(θ(2)-θ(P))-COS(θ(1)-θ(P)) DIFFERENTIAL	10.03	0.0078	8.46	0.0422		
3.16	UNCERTAINTY IN COS(θ(3)-θ(P))-COS(θ(1)-θ(P)) POT DRIVE GEARING	1.39	0.0040	2.19	0.0109		
3.17	UNCERTAINTY IN COS(θ(2)-θ(P))-COS(θ(1)-θ(P)) POT DRIVE GEARING	3.34	0.0036	2.82	0.0140		
3.18	COS(θ(3)-θ(P))-COS(θ(1)-θ(P)) POT NON-LINEARITY	3.34	0.0096	5.25	0.0262		
3.19	COS(θ(2)-θ(P))-COS(θ(1)-θ(P)) POT NON-LINEARITY	8.03	0.0063	6.77	0.0338		
3.20	UNCERTAINTY IN 1/R(1) INPUT GEARING AND DIAL READING	0.66	0.0022	0.21	0.0011		
3.21	UNCERTAINTY IN 1/R(2) INPUT GEARING AND DIAL READING	1.13	0.0009	0.95	0.0047		
3.22	UNCERTAINTY IN 1/R(3) INPUT GEARING AND DIAL READING	0.47	0.0013	0.74	0.0037		
3.23	UNCERTAINTY IN (1/R(3)-1/R(1)) DIFFERENTIAL	0.16	0.0004	0.25	0.0012		
3.24	UNCERTAINTY IN (1/R(2)-1/R(1)) DIFFERENTIAL	0.38	0.0003	0.32	0.0016		
3.25	UNCERTAINTY IN (1/R(3)-1/R(1)) RHEOSTAT DRIVE GEARING	1.56	0.0045	2.46	0.0123		
3.26	UNCERTAINTY IN (1/R(2)-1/R(1)) RHEOSTAT DRIVE GEARING	3.75	0.0029	3.16	0.0158		
3.27	(1/R(3)-1/R(1)) RHEOSTAT NON-LINEARITY	3.74	0.0107	5.89	0.0294		
3.28	(1/R(2)-1/R(1)) RHEOSTAT NON-LINEARITY	9.02	0.0071	7.60	0.0379		
3.29	BRIDGE TRIMMING ERROR	0.39	0.0003	0.33	0.0016		
3.30	GALVANOMETER BIAS ERROR	NIL	NIL	NIL	NIL		
	RSS	20.01	0.0300	19.40	0.0968	27.87	0.1013
4.	ERRORS DUE TO PARABOLIC ASSUMPTION OF CORRECTIVE MANEUVER	NOT APPLICABLE		0.15	0.0035	0.15	0.0035
	TOTAL RSS ERRORS	20.59	0.0654	19.99	0.1135	28.69	0.1310

NOTE 1. SOURCE ERRORS UTILIZED ARE 1 SIGMA VALUES BASED ON MAXIMUM VALUES LISTED IN FIGURE NO. 3-4

MANUAL SPACE COMPUTER ERROR ANALYSIS • PROBLEM NUMBER 1.2.2

Figure 5-14

	ERROR SOURCE	ERRORS IN PERIGEE: ASSUMING NO MANEUVER RADIUS (KM)	ASSUMING NO MANEUVER ANGLE (DEG)	INCREMENT DUE TO MANEUVER COMP. RADIUS (KM)	INCREMENT DUE TO MANEUVER COMP. ANGLE (DEG)	TOTAL WITH MANEUVER RADIUS (KM)	TOTAL WITH MANEUVER ANGLE (DEG)
1.	TWO BODY VS. FOUR BODY AND EARTH OBLATENESS	4.29	0.0576	NOT APPLICABLE		4.29	0.0576
2.	OBSERVATIONAL ERRORS						
2.1	UNCERTAINTY IN MEASUREMENT OF θ(1)	0.54	0.0014	0.23	0.0011		
2.2	UNCERTAINTY IN MEASUREMENT OF θ(2)	0.02	0.	0.02	0.0001		
2.3	UNCERTAINTY IN MEASUREMENT OF θ(3)	0.55	0.0014	0.85	0.0039		
2.4	UNCERTAINTY IN MEASUREMENT OF R(1)	1.28	0.0034	0.55	0.0025		
2.5	UNCERTAINTY IN MEASUREMENT OF R(2)	2.41	0.0003	2.35	0.0109		
2.6	UNCERTAINTY IN MEASUREMENT OF R(3)	1.27	0.0031	1.95	0.0090		
2.7	UNCERTAINTY IN MEASUREMENT OF R(C)	NOT APPLICABLE		0.83	0.0038		
	RSS	3.11	0.0050	3.33	0.0154	4.55	0.0161
3.	INSTRUMENTATION ERRORS						
3.1	UNCERTAINTY IN θ(1) INPUT GEARING AND DIAL READING	0.16	0.0004	0.07	0.0003		
3.2	UNCERTAINTY IN θ(2) INPUT GEARING AND DIAL READING	0.01	0.	0.01	0.0000		
3.3	UNCERTAINTY IN θ(3) INPUT GEARING AND DIAL READING	0.16	0.0004	0.24	0.0011		
3.4	UNCERTAINTY IN θ(P) INPUT GEARING AND DIAL READING	0.00	0.0008	0.17	0.0008		
3.5	UNCERTAINTY IN (θ(1)-θ(P)) DIFFERENTIAL	0.28	0.0007	0.12	0.0006		
3.6	UNCERTAINTY IN (θ(2)-θ(P)) DIFFERENTIAL	0.01	0.	0.01	0.0000		
3.7	UNCERTAINTY IN (θ(3)-θ(P)) DIFFERENTIAL	0.29	0.0007	0.44	0.0020		
3.8	UNCERTAINTY IN (θ(1)-θ(P)) REDUCTION GEARING TO COS MECHANISM	1.86	0.0049	0.80	0.0037		
3.9	UNCERTAINTY IN (θ(2)-θ(P)) REDUCTION GEARING TO COS MECHANISM	0.06	0.0000	0.06	0.0003		
3.10	UNCERTAINTY IN (θ(3)-θ(P)) REDUCTION GEARING TO COS MECHANISM	1.92	0.0047	2.94	0.0135		
3.11	UNCERTAINTY IN (θ(1)-θ(P)) COSINE MECHANISM	4.54	0.0120	1.94	0.0090		
3.12	UNCERTAINTY IN (θ(2)-θ(P)) COSINE MECHANISM	8.50	0.0009	8.31	0.0383		
3.13	UNCERTAINTY IN (θ(3)-θ(P)) COSINE MECHANISM	3.96	0.0111	6.35	0.0293		
3.14	UNCERTAINTY IN COS(θ(3)-θ(P))-COS(θ(1)-θ(P)) DIFFERENTIAL	5.93	0.0166	9.52	0.0439		
3.15	UNCERTAINTY IN COS(θ(2)-θ(P))-COS(θ(1)-θ(P)) DIFFERENTIAL	12.74	0.0014	12.45	0.0574		
3.16	UNCERTAINTY IN COS(θ(3)-θ(P))-COS(θ(1)-θ(P)) POT DRIVE GEARING	1.58	0.0055	3.17	0.0146		
3.17	UNCERTAINTY IN COS(θ(2)-θ(P))-COS(θ(1)-θ(P)) POT DRIVE GEARING	4.24	0.0005	4.15	0.0191		
3.18	COS(θ(3)-θ(P))-COS(θ(1)-θ(P)) POT NON-LINEARITY	4.75	0.0133	7.63	0.0352		
3.19	COS(θ(2)-θ(P))-COS(θ(1)-θ(P)) POT NON-LINEARITY	10.20	0.0011	9.97	0.0459		
3.20	UNCERTAINTY IN 1/R(1) INPUT GEARING AND DIAL READING	0.75	0.0020	0.32	0.0015		
3.21	UNCERTAINTY IN 1/R(2) INPUT GEARING AND DIAL READING	1.43	0.0002	1.40	0.0064		
3.22	UNCERTAINTY IN 1/R(3) INPUT GEARING AND DIAL READING	0.67	0.0019	1.07	0.0049		
3.23	UNCERTAINTY IN (1/R(3)-1/R(1)) DIFFERENTIAL	0.22	0.0006	0.36	0.0016		
3.24	UNCERTAINTY IN (1/R(2)-1/R(1)) DIFFERENTIAL	0.48	0.0001	0.47	0.0021		
3.25	UNCERTAINTY IN (1/R(3)-1/R(1)) RHEOSTAT DRIVE GEARING	2.22	0.0062	3.57	0.0164		
3.26	UNCERTAINTY IN (1/R(2)-1/R(1)) RHEOSTAT DRIVE GEARING	4.77	0.0005	4.66	0.0215		
3.27	(1/R(3)-1/R(1)) RHEOSTAT NON-LINEARITY	5.32	0.0149	8.55	0.0394		
3.28	(1/R(2)-1/R(1)) RHEOSTAT NON-LINEARITY	11.46	0.0012	11.19	0.0516		
3.29	BRIDGE TRIMMING ERROR	0.50	0.0001	0.49	0.0022		
3.30	GALVANOMETER BIAS ERROR	NIL	NIL	NIL	NIL		
	RSS	25.74	0.0331	28.30	0.1305	38.25	0.1346
4.	ERRORS DUE TO PARABOLIC ASSUMPTION OF CORRECTIVE MANEUVER	NOT APPLICABLE		0.04	0.0030	0.04	0.0030
	TOTAL RSS ERRORS	26.27	0.0667	28.81	0.1435	38.59	0.1582

NOTE 1. SOURCE ERRORS UTILIZED ARE 1 SIGMA VALUES BASED ON MAXIMUM VALUES LISTED IN FIGURE NO. 3-4

MANUAL SPACE COMPUTER ERROR ANALYSIS * PROBLEM NUMBER 1.2.3

Figure 5-15

	ERROR SOURCE	ERRORS IN PERIGEE: ASSUMING NO MANEUVER RADIUS (KM)	ASSUMING NO MANEUVER ANGLE (DEG)	INCREMENT DUE TO MANEUVER COMP. RADIUS (KM)	INCREMENT DUE TO MANEUVER COMP. ANGLE (DEG)	TOTAL WITH MANEUVER RADIUS (KM)	TOTAL WITH MANEUVER ANGLE (DEG)
1.	TWO BODY VS. FOUR BODY AND EARTH OBLATENESS	4.58	0.0626	NOT APPLICABLE		4.58	0.0626
2.	OBSERVATIONAL ERRORS						
2.1	UNCERTAINTY IN MEASUREMENT OF E(1)	0.14	0.0010	0.02	0.0002		
2.2	UNCERTAINTY IN MEASUREMENT OF E(2)	0.59	0.0026	0.30	0.0027		
2.3	UNCERTAINTY IN MEASUREMENT OF E(3)	0.73	0.0008	0.64	0.0057		
2.4	UNCERTAINTY IN MEASUREMENT OF R(1)	0.77	0.0056	0.14	0.0012		
2.5	UNCERTAINTY IN MEASUREMENT OF R(2)	1.54	0.0066	0.79	0.0070		
2.6	UNCERTAINTY IN MEASUREMENT OF R(3)	0.89	0.0010	0.78	0.0069		
2.7	UNCERTAINTY IN MEASUREMENT OF R(C)	NOT APPLICABLE		0.29	0.0026		
	RSS	2.15	0.0092	1.35	0.0121	2.54	0.0152
3.	INSTRUMENTATION ERRORS						
3.1	UNCERTAINTY IN E(1) INPUT GEARING AND DIAL READING	0.04	0.0003	0.01	0.0001		
3.2	UNCERTAINTY IN E(2) INPUT GEARING AND DIAL READING	0.17	0.0007	0.09	0.0008		
3.3	UNCERTAINTY IN E(3) INPUT GEARING AND DIAL READING	0.21	0.0002	0.18	0.0016		
3.4	UNCERTAINTY IN E(P) INPUT GEARING AND DIAL READING	0.00	0.0006	0.09	0.0008		
3.5	UNCERTAINTY IN (E(1)-E(P)) DIFFERENTIAL	0.07	0.0005	0.01	0.0001		
3.6	UNCERTAINTY IN (E(2)-E(P)) DIFFERENTIAL	0.31	0.0013	0.16	0.0014		
3.7	UNCERTAINTY IN (E(3)-E(P)) DIFFERENTIAL	0.38	0.0004	0.33	0.0030		
3.8	UNCERTAINTY IN (E(1)-E(P)) REDUCTION GEARING TO COS MECHANISM	0.49	0.0036	0.09	0.0008		
3.9	UNCERTAINTY IN (E(2)-E(P)) REDUCTION GEARING TO COS MECHANISM	2.04	0.0088	1.05	0.0093		
3.10	UNCERTAINTY IN (E(3)-E(P)) REDUCTION GEARING TO COS MECHANISM	2.53	0.0022	2.21	0.0197		
3.11	UNCERTAINTY IN (E(1)-E(P)) COSINE MECHANISM	2.85	0.0209	0.51	0.0045		
3.12	UNCERTAINTY IN (E(2)-E(P)) COSINE MECHANISM	5.68	0.0246	2.92	0.0260		
3.13	UNCERTAINTY IN (E(3)-E(P)) COSINE MECHANISM	2.83	0.0038	2.41	0.0215		
3.14	UNCERTAINTY IN COS(E(3)-E(P))-COS(E(1)-E(P)) DIFFERENTIAL	4.25	0.0057	3.61	0.0322		
3.15	UNCERTAINTY IN COS(E(2)-E(P))-COS(E(1)-E(P)) DIFFERENTIAL	8.52	0.0369	4.37	0.0390		
3.16	UNCERTAINTY IN COS(E(3)-E(P))-COS(E(1)-E(P)) POT DRIVE GEARING	1.41	0.0019	1.20	0.0107		
3.17	UNCERTAINTY IN COS(E(2)-E(P))-COS(E(1)-E(P)) POT DRIVE GEARING	2.83	0.0123	1.46	0.0130		
3.18	COS(E(3)-E(P))-COS(E(1)-E(P)) POT NON-LINEARITY	3.40	0.0045	2.89	0.0258		
3.19	COS(E(2)-E(P))-COS(E(1)-E(P)) POT NON-LINEARITY	6.82	0.0295	3.50	0.0312		
3.20	UNCERTAINTY IN 1/R(1) INPUT GEARING AND DIAL READING	0.46	0.0033	0.08	0.0007		
3.21	UNCERTAINTY IN 1/R(2) INPUT GEARING AND DIAL READING	0.91	0.0039	0.47	0.0042		
3.22	UNCERTAINTY IN 1/R(3) INPUT GEARING AND DIAL READING	0.45	0.0006	0.38	0.0034		
3.23	UNCERTAINTY IN (1/R(3)-1/R(1)) DIFFERENTIAL	0.15	0.0002	0.13	0.0012		
3.24	UNCERTAINTY IN (1/R(2)-1/R(1)) DIFFERENTIAL	0.30	0.0013	0.16	0.0014		
3.25	UNCERTAINTY IN (1/R(3)-1/R(1)) RHEOSTAT DRIVE GEARING	1.51	0.0020	1.29	0.0115		
3.26	UNCERTAINTY IN (1/R(2)-1/R(1)) RHEOSTAT DRIVE GEARING	3.03	0.0131	1.56	0.0139		
3.27	(1/R(3)-1/R(1)) RHEOSTAT NON-LINEARITY	3.62	0.0048	3.08	0.0275		
3.28	(1/R(2)-1/R(1)) RHEOSTAT NON-LINEARITY	7.28	0.0315	3.74	0.0333		
3.29	BRIDGE TRIMMING ERROR	0.20	0.0009	0.10	0.0009		
3.30	GALVANOMETER BIAS ERROR	NIL	NIL	NIL	NIL		
	RSS	17.37	0.0701	10.34	0.0921	20.22	0.1157
4.	ERRORS DUE TO PARABOLIC ASSUMPTION OF CORRECTIVE MANEUVER	NOT APPLICABLE		0.43	0.0054	0.43	0.0054
	TOTAL RSS ERRORS	18.09	0.0944	11.40	0.1121	21.38	0.1466

NOTE 1. SOURCE ERRORS UTILIZED ARE 1 SIGMA VALUES BASED ON MAXIMUM VALUES LISTED IN FIGURE NO. 3-4

MANUAL SPACE COMPUTER ERROR ANALYSIS • PROBLEM NUMBER 2.2.1

Figure 5-16

	ERROR SOURCE	ERRORS IN PERIGEE: ASSUMING NO MANEUVER RADIUS (KM)	ANGLE (DEG)	INCREMENT DUE TO MANEUVER COMP. RADIUS (KM)	ANGLE (DEG)	TOTAL WITH MANEUVER RADIUS (KM)	ANGLE (DEG)
1.	TWO BODY VS. FOUR BODY AND EARTH OBLATENESS	6.14	0.0658	NOT APPLICABLE		6.14	0.0658
2.	OBSERVATIONAL ERRORS						
2.1	UNCERTAINTY IN MEASUREMENT OF θ(1)	0.28	0.0013	0.05	0.0003		
2.2	UNCERTAINTY IN MEASUREMENT OF θ(2)	0.61	0.0016	0.33	0.0019		
2.3	UNCERTAINTY IN MEASUREMENT OF θ(3)	0.87	0.0002	0.84	0.0049		
2.4	UNCERTAINTY IN MEASUREMENT OF R(1)	1.51	0.0072	0.28	0.0016		
2.5	UNCERTAINTY IN MEASUREMENT OF R(2)	2.73	0.0075	1.45	0.0085		
2.6	UNCERTAINTY IN MEASUREMENT OF R(3)	1.38	0.0003	1.33	0.0078		
2.7	UNCERTAINTY IN MEASUREMENT OF R(C)	NOT APPLICABLE		0.54	0.0032		
	RSS	3.58	0.0106	2.25	0.0131	4.23	0.0169
3.	INSTRUMENTATION ERRORS						
3.1	UNCERTAINTY IN θ(1) INPUT GEARING AND DIAL READING	0.08	0.0004	0.01	0.0001		
3.2	UNCERTAINTY IN θ(2) INPUT GEARING AND DIAL READING	0.18	0.0005	0.10	0.0006		
3.3	UNCERTAINTY IN θ(3) INPUT GEARING AND DIAL READING	0.24	0.0000	0.23	0.0013		
3.4	UNCERTAINTY IN θ(P) INPUT GEARING AND DIAL READING	0.01	0.0008	0.15	0.0009		
3.5	UNCERTAINTY IN (θ(1)-θ(P)) DIFFERENTIAL	0.14	0.0007	0.03	0.0002		
3.6	UNCERTAINTY IN (θ(2)-θ(P)) DIFFERENTIAL	0.31	0.0008	0.17	0.0010		
3.7	UNCERTAINTY IN (θ(3)-θ(P)) DIFFERENTIAL	0.45	0.0001	0.44	0.0026		
3.8	UNCERTAINTY IN (θ(1)-θ(P)) REDUCTION GEARING TO COS MECHANISM	0.95	0.0046	0.17	0.0010		
3.9	UNCERTAINTY IN (θ(2)-θ(P)) REDUCTION GEARING TO COS MECHANISM	2.07	0.0056	1.11	0.0065		
3.10	UNCERTAINTY IN (θ(3)-θ(P)) REDUCTION GEARING TO COS MECHANISM	3.01	0.0006	2.91	0.0170		
3.11	UNCERTAINTY IN (θ(1)-θ(P)) COSINE MECHANISM	5.55	0.0266	1.00	0.0058		
3.12	UNCERTAINTY IN (θ(2)-θ(P)) COSINE MECHANISM	10.11	0.0276	5.40	0.0315		
3.13	UNCERTAINTY IN (θ(3)-θ(P)) COSINE MECHANISM	4.54	0.0010	4.37	0.0255		
3.14	UNCERTAINTY IN COS(θ(3)-θ(P))-COS(θ(1)-θ(P)) DIFFERENTIAL	6.83	0.0015	6.58	0.0384		
3.15	UNCERTAINTY IN COS(θ(2)-θ(P))-COS(θ(1)-θ(P)) DIFFERENTIAL	15.15	0.0413	8.08	0.0472		
3.16	UNCERTAINTY IN COS(θ(3)-θ(P))-COS(θ(1)-θ(P)) POT DRIVE GEARING	2.26	0.0005	2.18	0.0127		
3.17	UNCERTAINTY IN COS(θ(2)-θ(P))-COS(θ(1)-θ(P)) POT DRIVE GEARING	5.06	0.0138	2.70	0.0158		
3.18	COS(θ(3)-θ(P))-COS(θ(1)-θ(P)) POT NON-LINEARITY	5.46	0.0012	5.26	0.0307		
3.19	COS(θ(2)-θ(P))-COS(θ(1)-θ(P)) POT NON-LINEARITY	12.14	0.0331	6.47	0.0378		
3.20	UNCERTAINTY IN 1/R(1) INPUT GEARING AND DIAL READING	0.88	0.0043	0.15	0.0009		
3.21	UNCERTAINTY IN 1/R(2) INPUT GEARING AND DIAL READING	1.60	0.0044	0.64	0.0049		
3.22	UNCERTAINTY IN 1/R(3) INPUT GEARING AND DIAL READING	0.74	0.0002	0.71	0.0041		
3.23	UNCERTAINTY IN (1/R(3)-1/R(1)) DIFFERENTIAL	0.26	0.0001	0.25	0.0015		
3.24	UNCERTAINTY IN (1/R(2)-1/R(1)) DIFFERENTIAL	0.53	0.0015	0.28	0.0016		
3.25	UNCERTAINTY IN (1/R(3)-1/R(1)) RHEOSTAT DRIVE GEARING	2.44	0.0005	2.36	0.0137		
3.26	UNCERTAINTY IN (1/R(2)-1/R(1)) RHEOSTAT DRIVE GEARING	5.37	0.0147	2.85	0.0166		
3.27	(1/R(3)-1/R(1)) RHEOSTAT NON-LINEARITY	5.83	0.0012	5.62	0.0328		
3.28	(1/R(2)-1/R(1)) RHEOSTAT NON-LINEARITY	12.94	0.0353	6.88	0.0402		
3.29	BRIDGE TRIMMING ERROR	0.04	0.0001	0.02	0.0001		
3.30	GALVANOMETER BIAS ERROR	NIL	NIL	NIL	NIL		
	RSS	30.09	0.0783	18.67	0.1090	35.41	0.1342
4.	ERRORS DUE TO PARABOLIC ASSUMPTION OF CORRECTIVE MANEUVER	NOT APPLICABLE		0.34	0.0040	0.34	0.0040
	TOTAL RSS ERRORS	30.92	0.1028	19.78	0.1280	36.71	0.1642

NOTE 1. SOURCE ERRORS UTILIZED ARE 1 SIGMA VALUES BASED ON MAXIMUM VALUES LISTED IN FIGURE NO.3-4

MANUAL SPACE COMPUTER ERROR ANALYSIS • PROBLEM NUMBER 2.2.2

Figure 5-17

	ERROR SOURCE	ERRORS IN PERIGEE					
		ASSUMING NO MANEUVER		INCREMENT DUE TO MANEUVER COMP.		TOTAL WITH MANEUVER	
		RADIUS (KM)	ANGLE (DEG)	RADIUS (KM)	ANGLE (DEG)	RADIUS (KM)	ANGLE (DEG)
1.	TWO BODY VS. FOUR BODY AND EARTH OBLATENESS	6.93	0.0661	NOT APPLICABLE		6.93	0.0661
2.	OBSERVATIONAL ERRORS						
2.1	UNCERTAINTY IN MEASUREMENT OF E(1)	0.35	0.0013	0.03	0.0001		
2.2	UNCERTAINTY IN MEASUREMENT OF E(2)	0.80	0.0016	0.43	0.0018		
2.3	UNCERTAINTY IN MEASUREMENT OF E(3)	1.15	0.0001	1.12	0.0047		
2.4	UNCERTAINTY IN MEASUREMENT OF R(1)	1.88	0.0074	0.12	0.0005		
2.5	UNCERTAINTY IN MEASUREMENT OF R(2)	3.94	0.0076	2.12	0.0089		
2.6	UNCERTAINTY IN MEASUREMENT OF R(3)	2.20	0.0002	2.15	0.0090		
2.7	UNCERTAINTY IN MEASUREMENT OF R(C)	NOT APPLICABLE		0.93	0.0039		
	RSS	5.10	0.0108	3.38	0.0142	6.12	0.0178
3.	INSTRUMENTATION ERRORS						
3.1	UNCERTAINTY IN E(1) INPUT GEARING AND DIAL READING	0.10	0.0004	0.01	0.0000		
3.2	UNCERTAINTY IN E(2) INPUT GEARING AND DIAL READING	0.22	0.0004	0.12	0.0005		
3.3	UNCERTAINTY IN E(3) INPUT GEARING AND DIAL READING	0.34	0.0000	0.33	0.0014		
3.4	UNCERTAINTY IN E(P) INPUT GEARING AND DIAL READING	0.01	0.0008	0.20	0.0008		
3.5	UNCERTAINTY IN (E(1)-E(P)) DIFFERENTIAL	0.17	0.0007	0.01	0.0000		
3.6	UNCERTAINTY IN (E(2)-E(P)) DIFFERENTIAL	0.42	0.0008	0.23	0.0010		
3.7	UNCERTAINTY IN (E(3)-E(P)) DIFFERENTIAL	0.60	0.0001	0.58	0.0025		
3.8	UNCERTAINTY IN (E(1)-E(P)) REDUCTION GEARING TO COS MECHANISM	1.21	0.0047	0.10	0.0004		
3.9	UNCERTAINTY IN (E(2)-E(P)) REDUCTION GEARING TO COS MECHANISM	2.80	0.0054	1.51	0.0063		
3.10	UNCERTAINTY IN (E(3)-E(P)) REDUCTION GEARING TO COS MECHANISM	3.96	0.0004	3.85	0.0162		
3.11	UNCERTAINTY IN (E(1)-E(P)) COSINE MECHANISM	6.97	0.0272	0.46	0.0019		
3.12	UNCERTAINTY IN (E(2)-E(P)) COSINE MECHANISM	14.59	0.0282	7.88	0.0331		
3.13	UNCERTAINTY IN (E(3)-E(P)) COSINE MECHANISM	7.62	0.0009	7.40	0.0311		
3.14	UNCERTAINTY IN COS(E(3)-E(P))-COS(E(1)-E(P)) DIFFERENTIAL	11.44	0.0014	11.10	0.0466		
3.15	UNCERTAINTY IN COS(E(2)-E(P))-COS(E(1)-E(P)) DIFFERENTIAL	21.88	0.0423	11.82	0.0496		
3.16	UNCERTAINTY IN COS(E(3)-E(P))-COS(E(1)-E(P)) PCT DRIVE GEARING	3.79	0.0005	3.68	0.0154		
3.17	UNCERTAINTY IN COS(E(2)-E(P))-COS(E(1)-E(P)) PCT DRIVE GEARING	7.31	0.0141	3.96	0.0166		
3.18	COS(E(3)-E(P))-COS(E(1)-E(P)) PCT NON-LINEARITY	9.17	0.0011	8.89	0.0373		
3.19	COS(E(2)-E(P))-COS(E(1)-E(P)) PCT NON-LINEARITY	17.53	0.0339	9.48	0.0398		
3.20	UNCERTAINTY IN 1/R(1) INPUT GEARING AND DIAL READING	1.12	0.0044	0.08	0.0003		
3.21	UNCERTAINTY IN 1/R(2) INPUT GEARING AND DIAL READING	2.32	0.0045	1.24	0.0052		
3.22	UNCERTAINTY IN 1/R(3) INPUT GEARING AND DIAL READING	1.25	0.0002	1.21	0.0051		
3.23	UNCERTAINTY IN (1/R(3)-1/R(1)) DIFFERENTIAL	0.42	0.0001	0.41	0.0017		
3.24	UNCERTAINTY IN (1/R(2)-1/R(1)) DIFFERENTIAL	0.77	0.0015	0.41	0.0017		
3.25	UNCERTAINTY IN (1/R(3)-1/R(1)) RHEOSTAT DRIVE GEARING	4.09	0.0005	3.96	0.0166		
3.26	UNCERTAINTY IN (1/R(2)-1/R(1)) RHEOSTAT DRIVE GEARING	7.79	0.0151	4.20	0.0176		
3.27	(1/R(3)-1/R(1)) RHEOSTAT NON-LINEARITY	9.76	0.0012	9.48	0.0398		
3.28	(1/R(2)-1/R(1)) RHEOSTAT NON-LINEARITY	18.72	0.0362	10.07	0.0423		
3.29	BRIDGE TRIMMING ERROR	0.03	0.0001	0.01	0.0000		
3.30	GALVANOMETER BIAS ERROR	NIL	NIL	NIL	NIL		
	RSS	44.41	0.0802	28.90	0.1213	52.98	0.1454
4.	ERRORS DUE TO PARABOLIC ASSUMPTION OF CORRECTIVE MANEUVER	NOT APPLICABLE		0.06	0.0018	0.06	0.0018
	TOTAL RSS ERRORS	45.24	0.1045	29.91	0.1389	54.23	0.1738

NOTE 1. SOURCE ERRORS UTILIZED ARE 1 SIGMA VALUES BASED ON MAXIMUM VALUES LISTED IN FIGURE NO.3-4

MANUAL SPACE COMPUTER ERROR ANALYSIS • PROBLEM NUMBER 2.2.3

Figure 5-18

	ERROR SOURCE	ERRORS IN PERIGEE: ASSUMING NO MANEUVER RADIUS (KM)	ASSUMING NO MANEUVER ANGLE (DEG)	INCREMENT DUE TO MANEUVER COMP. RADIUS (KM)	INCREMENT DUE TO MANEUVER COMP. ANGLE (DEG)	TOTAL WITH MANEUVER RADIUS (KM)	TOTAL WITH MANEUVER ANGLE (DEG)
1.	TWO BODY VS. FOUR BODY AND EARTH OBLATENESS	4.59	0.0618	NOT APPLICABLE		4.59	0.0618
2.	OBSERVATIONAL ERRORS						
2.1	UNCERTAINTY IN MEASUREMENT OF θ(1)	0.02	0.0002	0.00	0.		
2.2	UNCERTAINTY IN MEASUREMENT OF θ(2)	0.97	0.0056	0.30	0.0025		
2.3	UNCERTAINTY IN MEASUREMENT OF θ(3)	0.95	0.0026	0.63	0.0053		
2.4	UNCERTAINTY IN MEASUREMENT OF R(1)	0.98	0.0080	0.01	0.0000		
2.5	UNCERTAINTY IN MEASUREMENT OF R(2)	1.53	0.0111	0.59	0.0049		
2.6	UNCERTAINTY IN MEASUREMENT OF R(3)	1.07	0.0029	0.72	0.0059		
2.7	UNCERTAINTY IN MEASUREMENT OF R(C)	NOT APPLICABLE		0.31	0.0026		
	RSS	2.77	0.0153	1.21	0.0100	3.03	0.0183
3.	INSTRUMENTATION ERRORS						
3.1	UNCERTAINTY IN θ(1) INPUT GEARING AND DIAL READING	0.01	0.0001	0.00	0.0000		
3.2	UNCERTAINTY IN θ(2) INPUT GEARING AND DIAL READING	0.28	0.0016	0.09	0.0007		
3.3	UNCERTAINTY IN θ(3) INPUT GEARING AND DIAL READING	0.27	0.0007	0.18	0.0015		
3.4	UNCERTAINTY IN θ(P) INPUT GEARING AND DIAL READING	0.00	0.0008	0.10	0.0008		
3.5	UNCERTAINTY IN (θ(1)-θ(P)) DIFFERENTIAL	0.01	0.0001	0.00	0.0000		
3.6	UNCERTAINTY IN (θ(2)-θ(P)) DIFFERENTIAL	0.50	0.0029	0.16	0.0013		
3.7	UNCERTAINTY IN (θ(3)-θ(P)) DIFFERENTIAL	0.49	0.0013	0.33	0.0027		
3.8	UNCERTAINTY IN (θ(1)-θ(P)) REDUCTION GEARING TO COS MECHANISM	0.08	0.0007	0.00	0.0000		
3.9	UNCERTAINTY IN (θ(2)-θ(P)) REDUCTION GEARING TO COS MECHANISM	3.37	0.0193	1.04	0.0080		
3.10	UNCERTAINTY IN (θ(3)-θ(P)) REDUCTION GEARING TO COS MECHANISM	3.29	0.0090	2.20	0.0182		
3.11	UNCERTAINTY IN (θ(1)-θ(P)) COSINE MECHANISM	3.71	0.0305	0.02	0.0002		
3.12	UNCERTAINTY IN (θ(2)-θ(P)) COSINE MECHANISM	7.26	0.0421	2.27	0.0188		
3.13	UNCERTAINTY IN (θ(3)-θ(P)) COSINE MECHANISM	3.66	0.0116	2.25	0.0185		
3.14	UNCERTAINTY IN COS(θ(3)-θ(P))-COS(θ(1)-θ(P)) DIFFERENTIAL	5.48	0.0174	3.37	0.0279		
3.15	UNCERTAINTY IN COS(θ(2)-θ(P))-COS(θ(1)-θ(P)) DIFFERENTIAL	11.04	0.0631	3.41	0.0282		
3.16	UNCERTAINTY IN COS(θ(3)-θ(P))-COS(θ(1)-θ(P)) POT DRIVE GEARING	1.82	0.0038	1.12	0.0093		
3.17	UNCERTAINTY IN COS(θ(2)-θ(P))-COS(θ(1)-θ(P)) POT DRIVE GEARING	3.68	0.0210	1.13	0.0094		
3.18	COS(θ(3)-θ(P))-COS(θ(1)-θ(P)) POT NON-LINEARITY	4.39	0.0140	2.70	0.0223		
3.19	COS(θ(2)-θ(P))-COS(θ(1)-θ(P)) POT NON-LINEARITY	8.84	0.0505	2.73	0.0225		
3.20	UNCERTAINTY IN 1/R(1) INPUT GEARING AND DIAL READING	0.58	0.0047	0.00	0.0000		
3.21	UNCERTAINTY IN 1/R(2) INPUT GEARING AND DIAL READING	1.15	0.0066	0.35	0.0029		
3.22	UNCERTAINTY IN 1/R(3) INPUT GEARING AND DIAL READING	0.57	0.0018	0.35	0.0029		
3.23	UNCERTAINTY IN (1/R(3)-1/R(1)) DIFFERENTIAL	0.19	0.0006	0.12	0.0010		
3.24	UNCERTAINTY IN (1/R(2)-1/R(1)) DIFFERENTIAL	0.38	0.0022	0.12	0.0010		
3.25	UNCERTAINTY IN (1/R(3)-1/R(1)) RHEOSTAT DRIVE GEARING	1.90	0.0060	1.17	0.0097		
3.26	UNCERTAINTY IN (1/R(2)-1/R(1)) RHEOSTAT DRIVE GEARING	3.82	0.0219	1.18	0.0098		
3.27	(1/R(3)-1/R(1)) RHEOSTAT NON-LINEARITY	4.55	0.0145	2.80	0.0231		
3.28	(1/R(2)-1/R(1)) RHEOSTAT NON-LINEARITY	9.17	0.0525	2.83	0.0234		
3.29	BRIDGE TRIMMING ERROR	0.55	0.0031	0.17	0.0014		
3.30	GALVANOMETER BIAS ERROR	NIL	NIL	NIL	NIL		
	RSS	22.44	0.1209	8.77	0.0725	24.09	0.1410
4.	ERRORS DUE TO PARABOLIC ASSUMPTION OF CORRECTIVE MANEUVER	NOT APPLICABLE		0.24	0.0028	0.24	0.0028
	TOTAL RSS ERRORS	23.07	0.1366	9.98	0.0959	25.14	0.1669

NOTE 1. SOURCE ERRORS UTILIZED ARE 1 SIGMA VALUES BASED ON MAXIMUM VALUES LISTED IN FIGURE NO. 3-4

MANUAL SPACE COMPUTER ERROR ANALYSIS • PROBLEM NUMBER 5.2.1

Figure 5-19

	ERROR SOURCE	ERRORS IN PERIGEE: ASSUMING NO MANEUVER RADIUS (KM)	ASSUMING NO MANEUVER ANGLE (DEG)	INCREMENT DUE TO MANEUVER COMP. RADIUS (KM)	INCREMENT DUE TO MANEUVER COMP. ANGLE (DEG)	TOTAL WITH MANEUVER RADIUS (KM)	TOTAL WITH MANEUVER ANGLE (DEG)
1.	TWO BODY VS. FOUR BODY AND EARTH OBLATENESS	6.27	0.0680	NOT APPLICABLE		6.27	0.0680
2.	OBSERVATIONAL ERRORS						
2.1	UNCERTAINTY IN MEASUREMENT OF Θ(1)	0.03	0.0002	0.00	0.0000		
2.2	UNCERTAINTY IN MEASUREMENT OF Θ(2)	1.38	0.0058	0.34	0.0019		
2.3	UNCERTAINTY IN MEASUREMENT OF Θ(3)	1.35	0.0028	0.84	0.0047		
2.4	UNCERTAINTY IN MEASUREMENT OF R(1)	1.73	0.0106	0.17	0.0009		
2.5	UNCERTAINTY IN MEASUREMENT OF R(2)	3.47	0.0145	0.86	0.0048		
2.6	UNCERTAINTY IN MEASUREMENT OF R(3)	1.87	0.0039	1.17	0.0065		
2.7	UNCERTAINTY IN MEASUREMENT OF R(C)	NOT APPLICABLE		0.56	0.0031		
	RSS	4.71	0.0195	1.81	0.0101	5.05	0.0220
3.	INSTRUMENTATION ERRORS						
3.1	UNCERTAINTY IN Θ(1) INPUT GEARING AND DIAL READING	0.01	0.0001	0.00	0.		
3.2	UNCERTAINTY IN Θ(2) INPUT GEARING AND DIAL READING	0.40	0.0017	0.10	0.0005		
3.3	UNCERTAINTY IN Θ(3) INPUT GEARING AND DIAL READING	0.39	0.0008	0.24	0.0014		
3.4	UNCERTAINTY IN Θ(P) INPUT GEARING AND DIAL READING	0.00	0.0008	0.14	0.0008		
3.5	UNCERTAINTY IN (Θ(1)-Θ(P)) DIFFERENTIAL	0.02	0.0001	0.00	0.0000		
3.6	UNCERTAINTY IN (Θ(2)-Θ(P)) DIFFERENTIAL	0.71	0.0030	0.18	0.0010		
3.7	UNCERTAINTY IN (Θ(3)-Θ(P)) DIFFERENTIAL	0.70	0.0015	0.44	0.0025		
3.8	UNCERTAINTY IN (Θ(1)-Θ(P)) REDUCTION GEARING TO COS MECHANISM	0.10	0.0006	0.01	0.0001		
3.9	UNCERTAINTY IN (Θ(2)-Θ(P)) REDUCTION GEARING TO COS MECHANISM	4.78	0.0200	1.19	0.0066		
3.10	UNCERTAINTY IN (Θ(3)-Θ(P)) REDUCTION GEARING TO COS MECHANISM	4.68	0.0098	2.92	0.0163		
3.11	UNCERTAINTY IN (Θ(1)-Θ(P)) COSINE MECHANISM	6.55	0.0401	0.63	0.0035		
3.12	UNCERTAINTY IN (Θ(2)-Θ(P)) COSINE MECHANISM	13.17	0.0552	3.29	0.0183		
3.13	UNCERTAINTY IN (Θ(3)-Θ(P)) COSINE MECHANISM	5.62	0.0151	3.91	0.0218		
3.14	UNCERTAINTY IN COS(Θ(3)-Θ(P))-COS(Θ(1)-Θ(P)) DIFFERENTIAL	9.92	0.0227	5.86	0.0327		
3.15	UNCERTAINTY IN COS(Θ(2)-Θ(P))-COS(Θ(1)-Θ(P)) DIFFERENTIAL	19.74	0.0825	4.93	0.0275		
3.16	UNCERTAINTY IN COS(Θ(3)-Θ(P))-COS(Θ(1)-Θ(P)) POT DRIVE GEARING	3.31	0.0076	1.95	0.0109		
3.17	UNCERTAINTY IN COS(Θ(2)-Θ(P))-COS(Θ(1)-Θ(P)) POT DRIVE GEARING	6.57	0.0276	1.64	0.0091		
3.18	COS(Θ(3)-Θ(P))-COS(Θ(1)-Θ(P)) POT NON-LINEARITY	7.95	0.0182	4.69	0.0262		
3.19	COS(Θ(2)-Θ(P))-COS(Θ(1)-Θ(P)) POT NON-LINEARITY	15.80	0.0663	3.95	0.0220		
3.20	UNCERTAINTY IN 1/R(1) INPUT GEARING AND DIAL READING	1.02	0.0052	0.10	0.0005		
3.21	UNCERTAINTY IN 1/R(2) INPUT GEARING AND DIAL READING	2.05	0.0086	0.51	0.0029		
3.22	UNCERTAINTY IN 1/R(3) INPUT GEARING AND DIAL READING	1.03	0.0024	0.61	0.0034		
3.23	UNCERTAINTY IN (1/R(3)-1/R(1)) DIFFERENTIAL	0.34	0.0008	0.20	0.0011		
3.24	UNCERTAINTY IN (1/R(2)-1/R(1)) DIFFERENTIAL	0.88	0.0029	0.17	0.0010		
3.25	UNCERTAINTY IN (1/R(3)-1/R(1)) RHEOSTAT DRIVE GEARING	3.43	0.0078	2.03	0.0113		
3.26	UNCERTAINTY IN (1/R(2)-1/R(1)) RHEOSTAT DRIVE GEARING	6.84	0.0287	1.70	0.0095		
3.27	(1/R(3)-1/R(1)) RHEOSTAT NON-LINEARITY	8.23	0.0188	4.86	0.0272		
3.28	(1/R(2)-1/R(1)) RHEOSTAT NON-LINEARITY	16.43	0.0689	4.09	0.0228		
3.29	BRIDGE TRIMMING ERROR	0.60	0.0025	0.15	0.0008		
3.30	GALVANOMETER BIAS ERROR	NIL	NIL	NIL	NIL		
	RSS	39.84	0.1575	13.81	0.0772	42.16	0.1754
4.	ERRORS DUE TO PARABOLIC ASSUMPTION OF CORRECTIVE MANEUVER	NOT APPLICABLE		0.19	0.0021	0.19	0.0021
	TOTAL RSS ERRORS	40.60	0.1726	15.28	0.1034	43.38	0.2012

NOTE 1. SOURCE ERRORS UTILIZED ARE 1 SIGMA VALUES BASED ON MAXIMUM VALUES LISTED IN FIGURE NO. 3-4

MANUAL SPACE COMPUTER ERROR ANALYSIS • PROBLEM NUMBER 5.2.2

Figure 5-20

	ERROR SOURCE	ERRORS IN PERIGEE: ASSUMING NO MANEUVER RADIUS (KM)	ANGLE (DEG)	INCREMENT DUE TO MANEUVER COMP. RADIUS (KM)	ANGLE (DEG)	TOTAL WITH MANEUVER RADIUS (KM)	ANGLE (DEG)
1.	TWO BODY VS. FOUR BODY AND EARTH OBLATENESS	7.73	0.0725	NOT APPLICABLE		7.73	0.0725
2.	OBSERVATIONAL ERRORS						
2.1	UNCERTAINTY IN MEASUREMENT OF θ(1)	0.04	0.0002	0.00	0.0000		
2.2	UNCERTAINTY IN MEASUREMENT OF θ(2)	1.50	0.0055	0.45	0.0024		
2.3	UNCERTAINTY IN MEASUREMENT OF θ(3)	1.46	0.0025	0.58	0.0051		
2.4	UNCERTAINTY IN MEASUREMENT OF R(1)	2.50	0.0130	0.02	0.0001		
2.5	UNCERTAINTY IN MEASUREMENT OF R(2)	4.60	0.0168	1.38	0.0072		
2.6	UNCERTAINTY IN MEASUREMENT OF R(3)	2.24	0.0038	1.51	0.0079		
2.7	UNCERTAINTY IN MEASUREMENT OF R(C)	NOT APPLICABLE		0.63	0.0033		
	RSS	6.07	0.0224	2.39	0.0125	6.52	0.0257
3.	INSTRUMENTATION ERRORS						
3.1	UNCERTAINTY IN θ(1) INPUT GEARING AND DIAL READING	0.01	0.0001	0.00	0.0000		
3.2	UNCERTAINTY IN θ(2) INPUT GEARING AND DIAL READING	0.43	0.0016	0.13	0.0007		
3.3	UNCERTAINTY IN θ(3) INPUT GEARING AND DIAL READING	0.42	0.0007	0.28	0.0015		
3.4	UNCERTAINTY IN θ(P) INPUT GEARING AND DIAL READING	0.00	0.0008	0.15	0.0008		
3.5	UNCERTAINTY IN (θ(1)-θ(P)) DIFFERENTIAL	0.02	0.0001	0.00	0.		
3.6	UNCERTAINTY IN (θ(2)-θ(P)) DIFFERENTIAL	0.78	0.0028	0.24	0.0012		
3.7	UNCERTAINTY IN (θ(3)-θ(P)) DIFFERENTIAL	0.76	0.0013	0.51	0.0027		
3.8	UNCERTAINTY IN (θ(1)-θ(P)) REDUCTION GEARING TO COS MECHANISM	0.15	0.0008	0.00	0.0000		
3.9	UNCERTAINTY IN (θ(2)-θ(P)) REDUCTION GEARING TO COS MECHANISM	5.19	0.0190	1.56	0.0081		
3.10	UNCERTAINTY IN (θ(3)-θ(P)) REDUCTION GEARING TO COS MECHANISM	5.05	0.0086	3.40	0.0178		
3.11	UNCERTAINTY IN (θ(1)-θ(P)) COSINE MECHANISM	9.48	0.0492	0.06	0.0003		
3.12	UNCERTAINTY IN (θ(2)-θ(P)) COSINE MECHANISM	17.47	0.0639	5.26	0.0275		
3.13	UNCERTAINTY IN (θ(3)-θ(P)) COSINE MECHANISM	7.99	0.0146	5.18	0.0271		
3.14	UNCERTAINTY IN COS(θ(3)-θ(P))-COS(θ(1)-θ(P)) DIFFERENTIAL	11.97	0.0219	7.77	0.0406		
3.15	UNCERTAINTY IN COS(θ(2)-θ(P))-COS(θ(1)-θ(P)) DIFFERENTIAL	26.19	0.0957	7.89	0.0412		
3.16	UNCERTAINTY IN COS(θ(3)-θ(P))-COS(θ(1)-θ(P)) POT DRIVE GEARING	3.99	0.0073	2.55	0.0135		
3.17	UNCERTAINTY IN COS(θ(2)-θ(P))-COS(θ(1)-θ(P)) POT DRIVE GEARING	8.72	0.0319	2.62	0.0137		
3.18	COS(θ(3)-θ(P))-COS(θ(1)-θ(P)) POT NON-LINEARITY	5.58	0.0176	6.22	0.0325		
3.19	COS(θ(2)-θ(P))-COS(θ(1)-θ(P)) POT NON-LINEARITY	20.97	0.0766	6.31	0.0330		
3.20	UNCERTAINTY IN 1/R(1) INPUT GEARING AND DIAL READING	1.48	0.0077	0.01	0.0000		
3.21	UNCERTAINTY IN 1/R(2) INPUT GEARING AND DIAL READING	2.72	0.0099	0.81	0.0043		
3.22	UNCERTAINTY IN 1/R(3) INPUT GEARING AND DIAL READING	1.24	0.0023	0.81	0.0042		
3.23	UNCERTAINTY IN (1/R(3)-1/R(1)) DIFFERENTIAL	0.41	0.0008	0.27	0.0014		
3.24	UNCERTAINTY IN (1/R(2)-1/R(1)) DIFFERENTIAL	0.91	0.0033	0.27	0.0014		
3.25	UNCERTAINTY IN (1/R(3)-1/R(1)) RHEOSTAT DRIVE GEARING	4.14	0.0076	2.69	0.0141		
3.26	UNCERTAINTY IN (1/R(2)-1/R(1)) RHEOSTAT DRIVE GEARING	9.07	0.0332	2.72	0.0142		
3.27	(1/R(3)-1/R(1)) RHEOSTAT NON-LINEARITY	9.93	0.0182	6.45	0.0337		
3.28	(1/R(2)-1/R(1)) RHEOSTAT NON-LINEARITY	21.61	0.0798	6.54	0.0342		
3.29	BRIDGE TRIMMING ERROR	0.52	0.0019	0.16	0.0008		
3.30	GALVANOMETER BIAS ERROR	NIL	NIL	NIL	NIL		
	RSS	51.85	0.1806	19.74	0.1032	55.48	0.2080
4.	ERRORS DUE TO PARABOLIC ASSUMPTION OF CORRECTIVE MANEUVER	NOT APPLICABLE		0.19	0.0022	0.15	0.0022
	TOTAL RSS ERRORS	52.77	0.1959	21.34	0.1268	56.92	0.2333

NOTE 1. SOURCE ERRORS UTILIZED ARE 1 SIGMA VALUES BASED ON MAXIMUM VALUES LISTED IN FIGURE NO.3-4

MANUAL SPACE COMPUTER ERROR ANALYSIS - PROBLEM NUMBER 5.2.3

Figure 5-21

	ERROR SOURCE	ASSUMING NO MANEUVER RADIUS (KM)	ASSUMING NO MANEUVER ANGLE (DEG)	ERRORS IN PERIGEE INCREMENT DUE TO MANEUVER COMP. RADIUS (KM)	ERRORS IN PERIGEE INCREMENT DUE TO MANEUVER COMP. ANGLE (DEG)	TOTAL WITH MANEUVER RADIUS (KM)	TOTAL WITH MANEUVER ANGLE (DEG)
1.	TWO BODY VS. FOUR BODY AND EARTH OBLATENESS	4.76	0.0564	NOT APPLICABLE		4.76	0.0564
2.	OBSERVATIONAL ERRORS						
2.1	UNCERTAINTY IN MEASUREMENT OF E(1)	0.48	0.0041	0.01	0.0001		
2.2	UNCERTAINTY IN MEASUREMENT OF E(2)	1.89	0.0129	0.42	0.0037		
2.3	UNCERTAINTY IN MEASUREMENT OF E(3)	1.41	0.0060	0.73	0.0063		
2.4	UNCERTAINTY IN MEASUREMENT OF R(1)	1.79	0.0153	0.05	0.0004		
2.5	UNCERTAINTY IN MEASUREMENT OF R(2)	3.24	0.0221	0.72	0.0063		
2.6	UNCERTAINTY IN MEASUREMENT OF R(3)	1.56	0.0066	0.80	0.0070		
2.7	UNCERTAINTY IN MEASUREMENT OF R(C)	NOT APPLICABLE		0.28	0.0025		
	RSS	4.69	0.0314	1.39	0.0122	4.89	0.0337
3.	INSTRUMENTATION ERRORS						
3.1	UNCERTAINTY IN E(1) INPUT GEARING AND DIAL READING	0.14	0.0012	0.00	0.0000		
3.2	UNCERTAINTY IN E(2) INPUT GEARING AND DIAL READING	0.55	0.0037	0.12	0.0011		
3.3	UNCERTAINTY IN E(3) INPUT GEARING AND DIAL READING	0.41	0.0017	0.21	0.0018		
3.4	UNCERTAINTY IN E(P) INPUT GEARING AND DIAL READING	0.00	0.0008	0.09	0.0008		
3.5	UNCERTAINTY IN (E(1)-E(P)) DIFFERENTIAL	0.25	0.0021	0.01	0.0001		
3.6	UNCERTAINTY IN (E(2)-E(P)) DIFFERENTIAL	0.99	0.0067	0.22	0.0019		
3.7	UNCERTAINTY IN (E(3)-E(P)) DIFFERENTIAL	0.73	0.0031	0.38	0.0033		
3.8	UNCERTAINTY IN (E(1)-E(P)) REDUCTION GEARING TO COS MECHANISM	1.68	0.0143	0.05	0.0004		
3.9	UNCERTAINTY IN (E(2)-E(P)) REDUCTION GEARING TO COS MECHANISM	6.56	0.0447	1.46	0.0128		
3.10	UNCERTAINTY IN (E(3)-E(P)) REDUCTION GEARING TO COS MECHANISM	4.89	0.0208	2.51	0.0220		
3.11	UNCERTAINTY IN (E(1)-E(P)) COSINE MECHANISM	6.96	0.0593	0.19	0.0016		
3.12	UNCERTAINTY IN (E(2)-E(P)) COSINE MECHANISM	12.64	0.0860	2.81	0.0246		
3.13	UNCERTAINTY IN (E(3)-E(P)) COSINE MECHANISM	5.68	0.0268	2.62	0.0229		
3.14	UNCERTAINTY IN COS(E(3)-E(P))-COS(E(1)-E(P)) DIFFERENTIAL	8.51	0.0401	3.93	0.0344		
3.15	UNCERTAINTY IN COS(E(2)-E(P))-COS(E(1)-E(P)) DIFFERENTIAL	18.94	0.1289	4.21	0.0368		
3.16	UNCERTAINTY IN COS(E(3)-E(P))-COS(E(1)-E(P)) POT DRIVE GEARING	2.83	0.0134	1.31	0.0114		
3.17	UNCERTAINTY IN COS(E(2)-E(P))-COS(E(1)-E(P)) POT DRIVE GEARING	6.31	0.0430	1.40	0.0123		
3.18	COS(E(3)-E(P))-COS(E(1)-E(P)) POT NON-LINEARITY	6.81	0.0321	3.15	0.0275		
3.19	COS(E(2)-E(P))-COS(E(1)-E(P)) POT NON-LINEARITY	15.17	0.1032	3.37	0.0295		
3.20	UNCERTAINTY IN 1/R(1) INPUT GEARING AND DIAL READING	1.06	0.0090	0.03	0.0002		
3.21	UNCERTAINTY IN 1/R(2) INPUT GEARING AND DIAL READING	1.92	0.0131	0.43	0.0037		
3.22	UNCERTAINTY IN 1/R(3) INPUT GEARING AND DIAL READING	0.86	0.0041	0.40	0.0035		
3.23	UNCERTAINTY IN (1/R(3)-1/R(1)) DIFFERENTIAL	0.29	0.0014	0.13	0.0012		
3.24	UNCERTAINTY IN (1/R(2)-1/R(1)) DIFFERENTIAL	0.64	0.0044	0.14	0.0012		
3.25	UNCERTAINTY IN (1/R(3)-1/R(1)) RHEOSTAT DRIVE GEARING	2.88	0.0136	1.33	0.0116		
3.26	UNCERTAINTY IN (1/R(2)-1/R(1)) RHEOSTAT DRIVE GEARING	6.41	0.0437	1.42	0.0125		
3.27	(1/R(3)-1/R(1)) RHEOSTAT NON-LINEARITY	6.90	0.0325	3.19	0.0279		
3.28	(1/R(2)-1/R(1)) RHEOSTAT NON-LINEARITY	15.41	0.1049	3.42	0.0300		
3.29	BRIDGE TRIMMING ERROR	1.00	0.0068	0.22	0.0019		
3.30	GALVANOMETER BIAS ERROR	NIL	NIL	NIL	NIL		
	RSS	37.83	0.2485	10.47	0.0916	39.25	0.2649
4.	ERRORS DUE TO PARABOLIC ASSUMPTION OF CORRECTIVE MANEUVER	NOT APPLICABLE		0.10	0.0012	0.10	0.0012
	TOTAL RSS ERRORS	38.42	0.2568	11.58	0.1082	40.12	0.2787

NOTE 1. SOURCE ERRORS UTILIZED ARE 1 SIGMA VALUES BASED ON MAXIMUM VALUES LISTED IN FIGURE NO.3-4

MANUAL SPACE COMPUTER ERROR ANALYSIS • PROBLEM NUMBER 14.2.1

Figure 5-22

	ERROR SOURCE	ERRORS IN PERIGEE: ASSUMING NO MANEUVER RADIUS (KM)	ASSUMING NO MANEUVER ANGLE (DEG)	INCREMENT DUE TO MANEUVER COMP. RADIUS (KM)	INCREMENT DUE TO MANEUVER COMP. ANGLE (DEG)	TOTAL WITH MANEUVER RADIUS (KM)	TOTAL WITH MANEUVER ANGLE (DEG)
1.	TWO BODY VS. FOUR BODY AND EARTH OBLATENESS	6.43	0.0642	NOT APPLICABLE		6.43	0.0642
2.	OBSERVATIONAL ERRORS						
2.1	UNCERTAINTY IN MEASUREMENT OF E(1)	0.84	0.0058	0.11	0.0007		
2.2	UNCERTAINTY IN MEASUREMENT OF E(2)	3.36	0.0186	0.34	0.0020		
2.3	UNCERTAINTY IN MEASUREMENT OF E(3)	2.52	0.0100	0.89	0.0055		
2.4	UNCERTAINTY IN MEASUREMENT OF R(1)	3.11	0.0216	0.40	0.0025		
2.5	UNCERTAINTY IN MEASUREMENT OF R(2)	6.29	0.0348	0.62	0.0038		
2.6	UNCERTAINTY IN MEASUREMENT OF R(3)	3.29	0.0130	1.17	0.0072		
2.7	UNCERTAINTY IN MEASUREMENT OF R(C)	NOT APPLICABLE		0.47	0.0029		
	RSS	8.86	0.0482	1.75	0.0107	9.03	0.0494
3.	INSTRUMENTATION ERRORS						
3.1	UNCERTAINTY IN E(1) INPUT GEARING AND DIAL READING	0.24	0.0017	0.03	0.0002		
3.2	UNCERTAINTY IN E(2) INPUT GEARING AND DIAL READING	0.97	0.0054	0.10	0.0006		
3.3	UNCERTAINTY IN E(3) INPUT GEARING AND DIAL READING	0.73	0.0029	0.26	0.0016		
3.4	UNCERTAINTY IN E(P) INPUT GEARING AND DIAL READING	0.00	0.0008	0.13	0.0008		
3.5	UNCERTAINTY IN (E(1)-E(P)) DIFFERENTIAL	0.44	0.0030	0.06	0.0003		
3.6	UNCERTAINTY IN (E(2)-E(P)) DIFFERENTIAL	1.75	0.0097	0.18	0.0011		
3.7	UNCERTAINTY IN (E(3)-E(P)) DIFFERENTIAL	1.31	0.0052	0.46	0.0029		
3.8	UNCERTAINTY IN (E(1)-E(P)) REDUCTION GEARING TO COS MECHANISM	2.91	0.0202	0.38	0.0023		
3.9	UNCERTAINTY IN (E(2)-E(P)) REDUCTION GEARING TO COS MECHANISM	11.64	0.0643	1.16	0.0071		
3.10	UNCERTAINTY IN (E(3)-E(P)) REDUCTION GEARING TO COS MECHANISM	6.76	0.0346	3.10	0.0191		
3.11	UNCERTAINTY IN (E(1)-E(P)) COSINE MECHANISM	12.07	0.0637	1.57	0.0097		
3.12	UNCERTAINTY IN (E(2)-E(P)) COSINE MECHANISM	24.47	0.1352	2.44	0.0150		
3.13	UNCERTAINTY IN (E(3)-E(P)) COSINE MECHANISM	12.39	0.0515	4.00	0.0246		
3.14	UNCERTAINTY IN COS(E(3)-E(P))-COS(E(1)-E(P)) DIFFERENTIAL	18.57	0.0771	6.00	0.0368		
3.15	UNCERTAINTY IN COS(E(2)-E(P))-COS(E(1)-E(P)) DIFFERENTIAL	36.67	0.2026	3.47	0.0225		
3.16	UNCERTAINTY IN COS(E(3)-E(P))-COS(E(1)-E(P)) POT DRIVE GEARING	6.19	0.0257	2.00	0.0123		
3.17	UNCERTAINTY IN COS(E(2)-E(P))-COS(E(1)-E(P)) POT DRIVE GEARING	12.22	0.0675	1.22	0.0075		
3.18	COS(E(3)-E(P))-COS(E(1)-E(P)) POT NON-LINEARITY	14.87	0.0617	4.80	0.0295		
3.19	COS(E(2)-E(P))-COS(E(1)-E(P)) POT NON-LINEARITY	29.37	0.1622	2.93	0.0180		
3.20	UNCERTAINTY IN 1/R(1) INPUT GEARING AND DIAL READING	1.24	0.0127	0.24	0.0015		
3.21	UNCERTAINTY IN 1/R(2) INPUT GEARING AND DIAL READING	3.72	0.0206	0.37	0.0023		
3.22	UNCERTAINTY IN 1/R(3) INPUT GEARING AND DIAL READING	1.89	0.0078	0.61	0.0037		
3.23	UNCERTAINTY IN (1/R(3)-1/R(1)) DIFFERENTIAL	0.63	0.0026	0.20	0.0012		
3.24	UNCERTAINTY IN (1/R(2)-1/R(1)) DIFFERENTIAL	1.24	0.0059	0.12	0.0008		
3.25	UNCERTAINTY IN (1/R(3)-1/R(1)) RHEOSTAT DRIVE GEARING	6.28	0.0261	2.03	0.0125		
3.26	UNCERTAINTY IN (1/R(2)-1/R(1)) RHEOSTAT DRIVE GEARING	12.43	0.0687	1.23	0.0076		
3.27	(1/R(3)-1/R(1)) RHEOSTAT NON-LINEARITY	15.05	0.0625	4.87	0.0299		
3.28	(1/R(2)-1/R(1)) RHEOSTAT NON-LINEARITY	29.90	0.1652	2.96	0.0182		
3.29	BRIDGE TRIMMING ERROR	1.51	0.0083	0.15	0.0009		
3.30	GALVANOMETER BIAS ERROR	NIL	NIL	NIL	NIL		
	RSS	74.19	0.3947	12.82	0.0786	75.29	0.4025
4.	ERRORS DUE TO PARABOLIC ASSUMPTION OF CORRECTIVE MANEUVER	NOT APPLICABLE		0.10	0.0010	0.10	0.0010
	TOTAL RSS ERRORS	75.00	0.4028	14.45	0.1021	76.38	0.4156

NOTE 1. SOURCE ERRORS UTILIZED ARE 1 SIGMA VALUES BASED ON MAXIMUM VALUES LISTED IN FIGURE NO. 3-4

MANUAL SPACE COMPUTER ERROR ANALYSIS • PROBLEM NUMBER 14.2.2

Figure 5-23

	ERROR SOURCE	ERRORS IN PERIGEE					
		ASSUMING NO MANEUVER		INCREMENT DUE TO MANEUVER COMP.		TOTAL WITH MANEUVER	
		RADIUS (KM)	ANGLE (DEG)	RADIUS (KM)	ANGLE (DEG)	RADIUS (KM)	ANGLE (DEG)
1.	TWO BODY VS. FOUR BODY AND EARTH OBLATENESS	8.99	0.0764	NOT APPLICABLE		8.99	0.0764
2.	OBSERVATIONAL ERRORS						
2.1	UNCERTAINTY IN MEASUREMENT OF θ(1)	1.52	0.0091	0.12	0.0007		
2.2	UNCERTAINTY IN MEASUREMENT OF θ(2)	4.19	0.0211	0.37	0.0021		
2.3	UNCERTAINTY IN MEASUREMENT OF θ(3)	2.68	0.0093	1.00	0.0055		
2.4	UNCERTAINTY IN MEASUREMENT OF R(1)	5.64	0.0337	0.45	0.0025		
2.5	UNCERTAINTY IN MEASUREMENT OF R(2)	9.33	0.0471	0.83	0.0046		
2.6	UNCERTAINTY IN MEASUREMENT OF R(3)	3.81	0.0132	1.42	0.0078		
2.7	UNCERTAINTY IN MEASUREMENT OF R(C)	NOT APPLICABLE		0.55	0.0031		
	RSS	12.67	0.0643	2.09	0.0115	12.84	0.0654
3.	INSTRUMENTATION ERRORS						
3.1	UNCERTAINTY IN θ(1) INPUT GEARING AND DIAL READING	0.44	0.0026	0.04	0.0002		
3.2	UNCERTAINTY IN θ(2) INPUT GEARING AND DIAL READING	1.21	0.0061	0.11	0.0006		
3.3	UNCERTAINTY IN θ(3) INPUT GEARING AND DIAL READING	0.77	0.0027	0.29	0.0016		
3.4	UNCERTAINTY IN θ(P) INPUT GEARING AND DIAL READING	0.00	0.0008	0.14	0.0008		
3.5	UNCERTAINTY IN (θ(1)-θ(P)) DIFFERENTIAL	0.79	0.0047	0.06	0.0003		
3.6	UNCERTAINTY IN (θ(2)-θ(P)) DIFFERENTIAL	2.18	0.0110	0.20	0.0011		
3.7	UNCERTAINTY IN (θ(3)-θ(P)) DIFFERENTIAL	1.39	0.0048	0.52	0.0029		
3.8	UNCERTAINTY IN (θ(1)-θ(P)) REDUCTION GEARING TO COS MECHANISM	5.28	0.0215	0.42	0.0023		
3.9	UNCERTAINTY IN (θ(2)-θ(P)) REDUCTION GEARING TO COS MECHANISM	14.52	0.0732	1.30	0.0072		
3.10	UNCERTAINTY IN (θ(3)-θ(P)) REDUCTION GEARING TO COS MECHANISM	9.29	0.0323	3.45	0.0191		
3.11	UNCERTAINTY IN (θ(1)-θ(P)) COSINE MECHANISM	21.85	0.1305	1.71	0.0095		
3.12	UNCERTAINTY IN (θ(2)-θ(P)) COSINE MECHANISM	26.19	0.1824	3.25	0.0180		
3.13	UNCERTAINTY IN (θ(3)-θ(P)) COSINE MECHANISM	14.34	0.0520	4.94	0.0274		
3.14	UNCERTAINTY IN COS(θ(3)-θ(P))-COS(θ(1)-θ(P)) DIFFERENTIAL	21.48	0.0779	7.41	0.0410		
3.15	UNCERTAINTY IN COS(θ(2)-θ(P))-COS(θ(1)-θ(P)) DIFFERENTIAL	54.25	0.2734	4.89	0.0271		
3.16	UNCERTAINTY IN COS(θ(3)-θ(P))-COS(θ(1)-θ(P)) POT DRIVE GEARING	7.16	0.0259	2.47	0.0137		
3.17	UNCERTAINTY IN COS(θ(2)-θ(P))-COS(θ(1)-θ(P)) POT DRIVE GEARING	18.07	0.0911	1.82	0.0089		
3.18	COS(θ(3)-θ(P))-COS(θ(1)-θ(P)) POT NON-LINEARITY	17.20	0.0623	5.93	0.0328		
3.19	COS(θ(2)-θ(P))-COS(θ(1)-θ(P)) POT NON-LINEARITY	43.44	0.2189	3.91	0.0216		
3.20	UNCERTAINTY IN 1/R(1) INPUT GEARING AND DIAL READING	3.33	0.0199	0.26	0.0015		
3.21	UNCERTAINTY IN 1/R(2) INPUT GEARING AND DIAL READING	5.51	0.0278	0.49	0.0027		
3.22	UNCERTAINTY IN 1/R(3) INPUT GEARING AND DIAL READING	2.18	0.0079	0.75	0.0042		
3.23	UNCERTAINTY IN (1/R(3)-1/R(1)) DIFFERENTIAL	0.73	0.0026	0.25	0.0014		
3.24	UNCERTAINTY IN (1/R(2)-1/R(1)) DIFFERENTIAL	1.84	0.0093	0.16	0.0009		
3.25	UNCERTAINTY IN (1/R(3)-1/R(1)) RHEOSTAT DRIVE GEARING	7.27	0.0263	2.51	0.0139		
3.26	UNCERTAINTY IN (1/R(2)-1/R(1)) RHEOSTAT DRIVE GEARING	18.41	0.0928	1.63	0.0091		
3.27	(1/R(3)-1/R(1)) RHEOSTAT NON-LINEARITY	17.41	0.0631	6.02	0.0333		
3.28	(1/R(2)-1/R(1)) RHEOSTAT NON-LINEARITY	44.34	0.2236	3.92	0.0217		
3.29	BRIDGE TRIMMING ERROR	1.33	0.0067	0.12	0.0007		
3.30	GALVANOMETER BIAS ERROR	NIL	NIL	NIL	NIL		
	RSS	105.67	0.5206	16.00	0.0886	106.87	0.5280
4.	ERRORS DUE TO PARABOLIC ASSUMPTION OF CORRECTIVE MANEUVER	NOT APPLICABLE		0.11	0.0011	0.11	0.0011
	TOTAL RSS ERRORS	106.80	0.5300	18.47	0.1175	108.39	0.5429

NOTE 1. SOURCE ERRORS UTILIZED ARE 1 SIGMA VALUES BASED ON MAXIMUM VALUES LISTED IN FIGURE NO. 3-4

MANUAL SPACE COMPUTER ERROR ANALYSIS • PROBLEM NUMBER 14.2.3

Figure 5-24

6. DISCUSSION OF THE ACCURACY ANALYSIS RESULTS

Graphs of the total errors in perigee for each problem of Section 5 versus the angular difference between the first and third observations ($\theta_3 - \theta_1$) are shown in Figures 6-1 to 6-4. Figures 6-1 and 6-2 are the plots for the Group 1 errors in perigee radius and angle, and 6-3 and 6-4 are those for Group 2. All data presented are based on 1 σ values.

The data for the Group 1 errors shown on Figures 6-1 and 6-2 indicate a very clear cut relationship between total error and the total sweep angle over which observations are made. These curves present the overall effect of starting to make the observations later on the trajectory with the locations of the last observation and the corrective maneuver fixed. It should be noted that all the points fall on a single curve very closely despite the facts that:

(a) the data was taken from four different trajectories whose eccentricities vary from 0.80 to 0.99 and

(b) the locations of the second or middle observations were, for the various cases, only approximately at the center of the sweep angle between the first and third observations.

Preliminary studies of accuracy had indicated that the optimum selection for the middle observation is at the sweep angle midpoint. Slight deviations of the location of this second observation from optimum has only a small second order influence on overall accuracy. In all the cases presented, the actual location of the second observation was generally only roughly at the angular midpoint between the first and third observation. (See Figure 4-4 in Section 4.)

The overall accuracy results for the first group of cases (Figures 6-1 and 6-2) clearly show that accuracy is significantly enhanced by making the first observation as soon as possible. Similarly, as shown on Figures 6-3 and 6-4, the data from the Group 2 errors clearly show that accuracy is significantly enhanced by making the third observation as late as possible. For this latter group, families of curves have been drawn on Figures 6-3 and 6-4, each curve corresponding to the data for each trajectory. With each trajectory, the first observation is kept fixed and the corrective maneuver point is altered with corresponding changes in the second and third observational points. For the purpose of comparison, the curves of Figures 6-1.

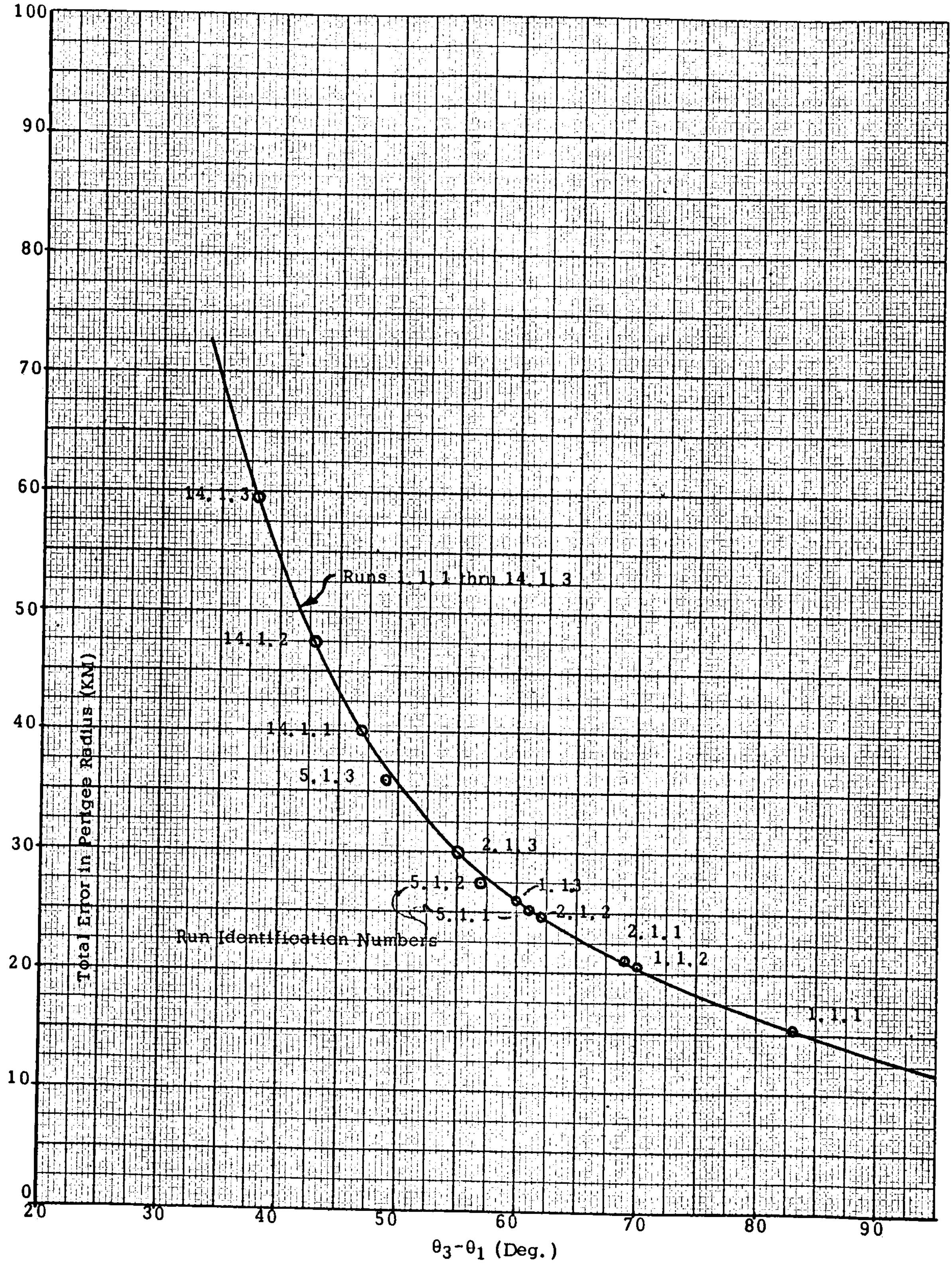

FIGURE 6-1 TOTAL ERROR IN PERIGEE RADIUS VS. $\theta_3 - \theta_1$ FOR GROUP 1

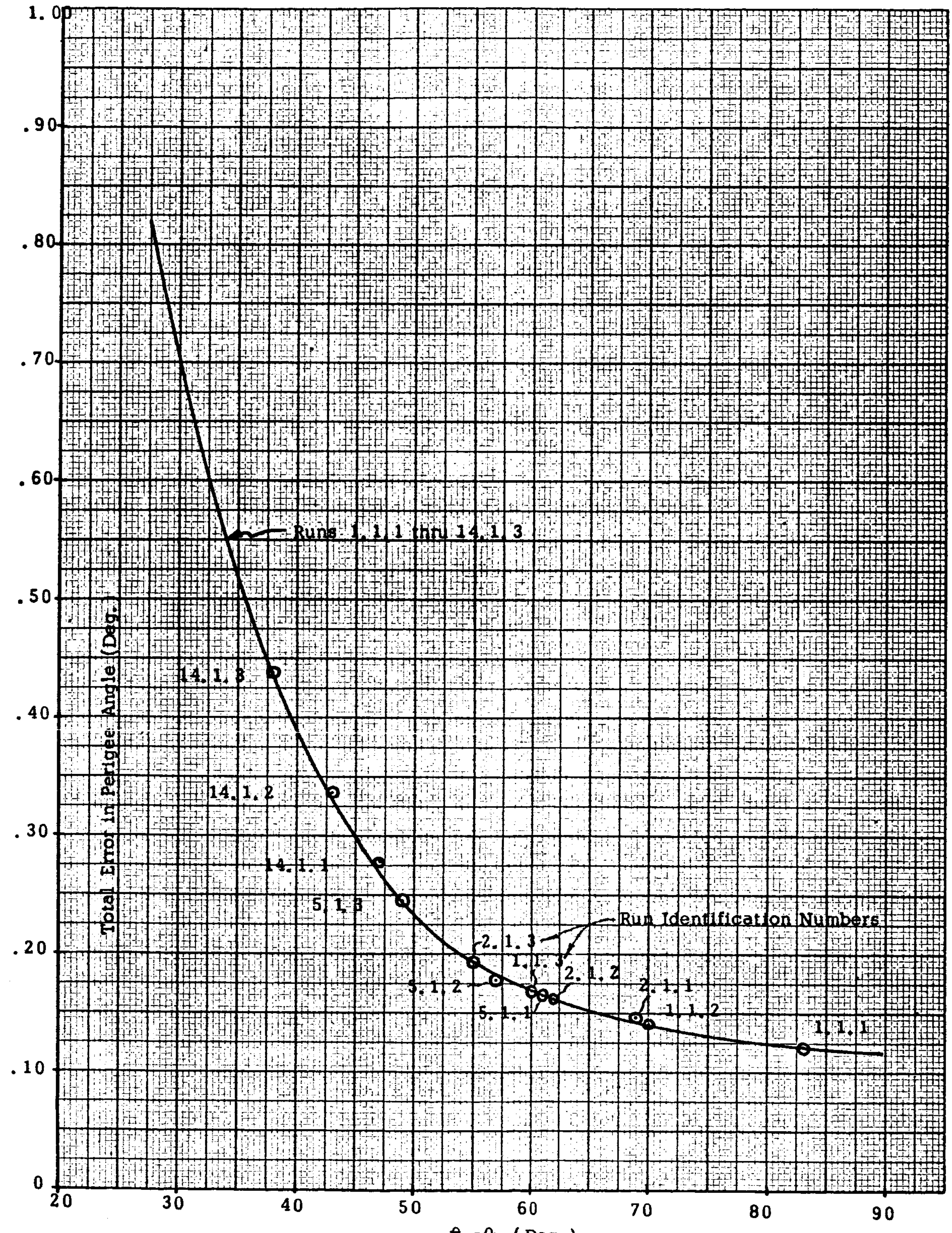

FIGURE 6-2 TOTALERROR IN PERIGEE ANGLE VS. $\theta_3-\theta_1$ FOR GROUP 1

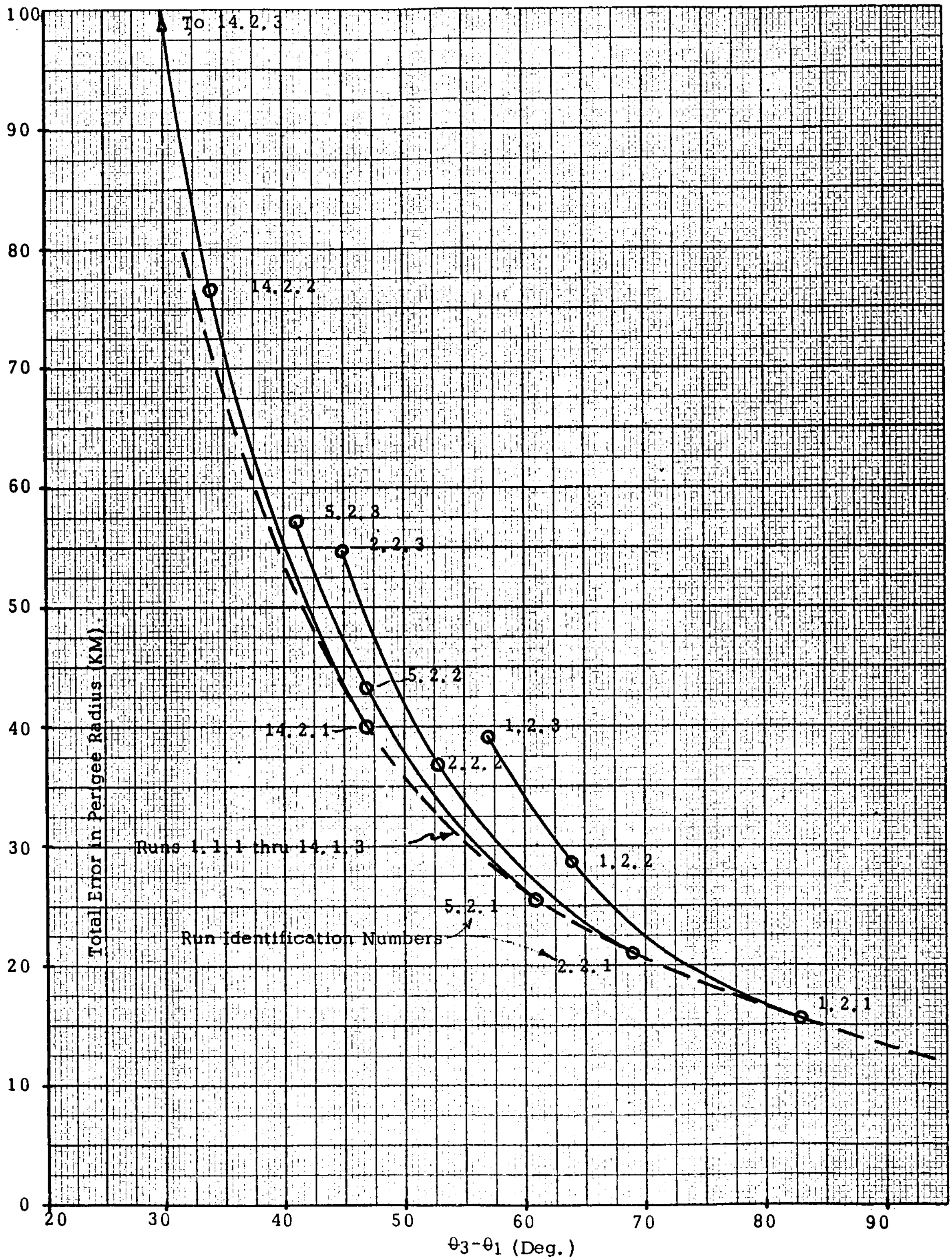

FIGURE 6-3 TOTAL ERROR IN PERIGEE RADIUS VS. $\theta_3 - \theta_1$ FOR GROUP 2

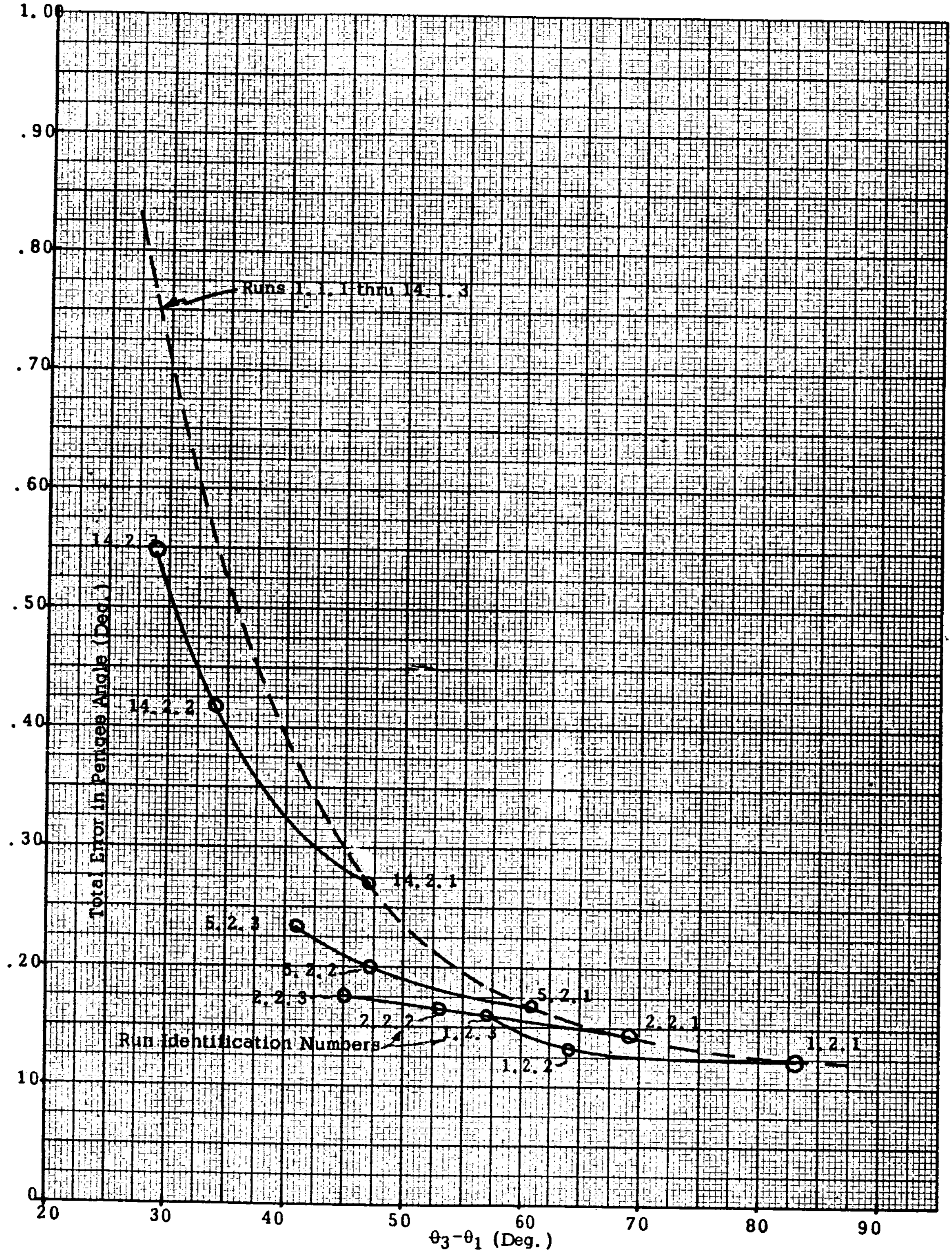

FIGURE 6-4 TOTAL ERROR IN PERIGEE ANGLE VS. $\theta_3-\theta_1$ FOR GROUP 2

and 6-2 are repeated on Figures 6-3 and 6-4 respectively as dashed lines.

Thus, as is shown on all these curves, while it is critically important to have the spread of observations over as large an angle as possible, accuracy of perigee radius is influenced even more by the location of the last observation than it is by the location of the first observation. Of course, choice in selecting the point for the third observation is very much limited by practical considerations governing the time required to prepare and execute the corrective maneuver, the amount of fuel available, and the time required to prepare for reentry. It seems reasonable to require a minimum of thirty minutes between the corrective maneuver and perigee and a similar minimum interval between the third observation and the corrective maneuver. These limits correspond to the points selected in Group 1.

It is obvious, from the Group 2 results, that accuracy is degraded considerably as the time for the corrective maneuver is made earlier. The degradation is the direct result, primarily, of having to move back the time of the third observation by a corresponding interval. This is clearly shown on Figure 6-5 which shows the relationships, for the four trajectories, between total error in perigee radius and the time between the last observation and perigee.

Certain general conclusions may be made regarding the overall accuracy capability of the manual computer. The accuracy is better with the lower eccentricity abort trajectories simply because it allows for a wider sweep angle for the observations. For $e \doteq 0.80$, the best overall perigee accuracy of about 16 km was obtained. The most nearly parabolic trajectory ($e \doteq 0.99$) gave an accuracy of about 40 km. For this trajectory, the first measurement was (arbitrarily) limited to be within 200,000 km of the earth which in turn resulted in only about 4.76 km error due to the two body theoretical basis for the computer. By allowing this latter error to be greater and therefore making the first measurement further from the earth (260,00 km), about four more degrees of total sweep angle would be obtained with near parabolic trajectories. This would improve the accuracy to about 35 km. (See Figure 6-1).

Thus, overall, accuracy of from 16 to 35 km in perigee radius is obtained. This is total error, including both perigee and maneuvering computations, both equipment and theoretical model errors and both input data and computer mechanization errors. Consider, for representative cases, the composition of the total error in perigee radius. For this purpose, take cases 1.1.1, 5.1.1, and 5.1.3. These are summarized on Figure 6-6.

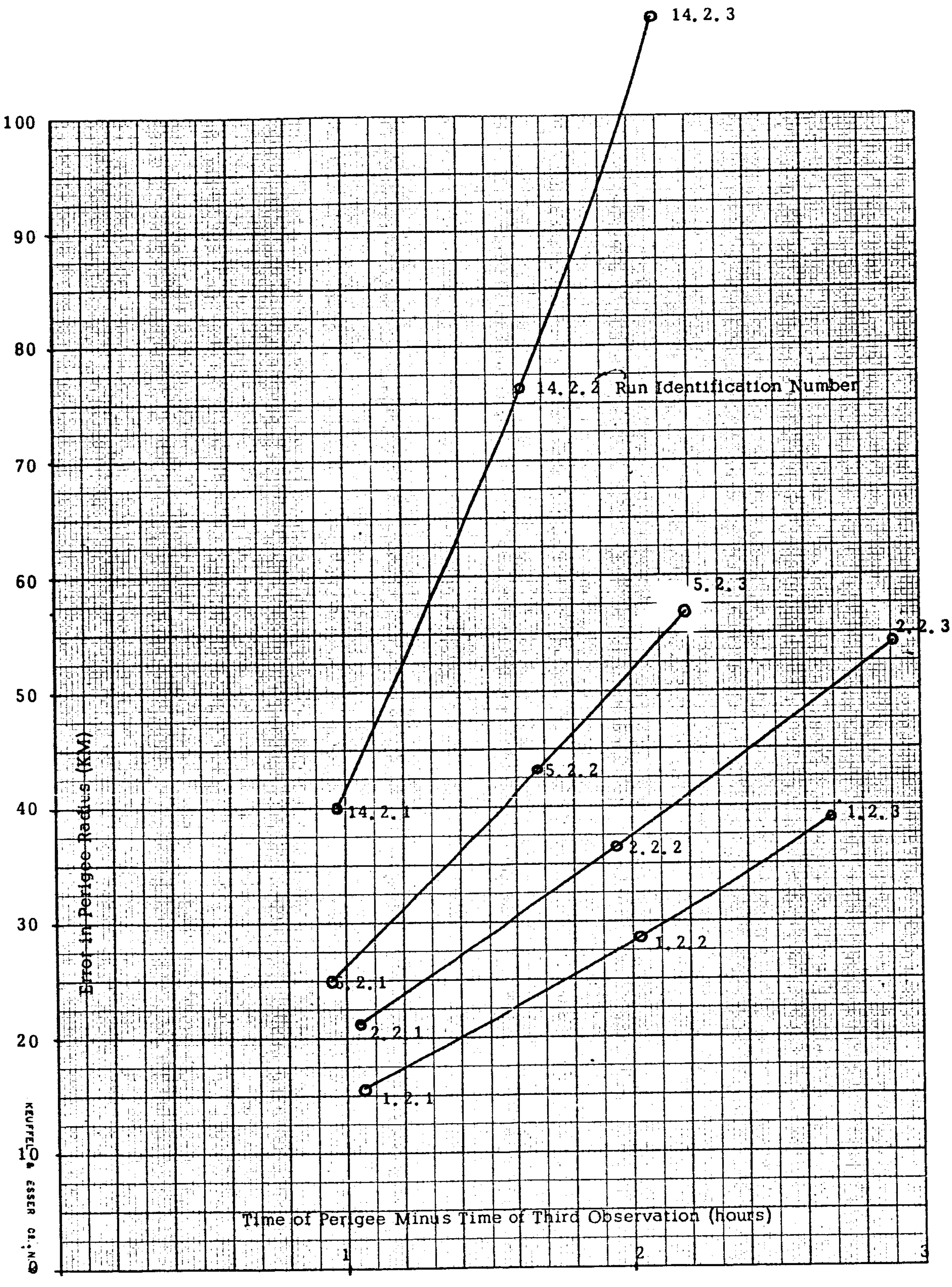

FIGURE 6-5 ERRORS IN PERIGEE VS. TIME OF THIRD OBSERVATION

Error Category		Error in Perigee Radius (Km)		
		Problem No.		
		1.1.1	5.1.1	5.1.3
Assuming no Maneuver	Two body vs four body and earth oblateness.	3.74	4.59	3.01
	Observational	1.47	2.77	4.27
	Instrumentation	11.43	22.44	34.30
	Total-no maneuver	12.11	23.07	34.70
Increment due to Maneuver Computation	Observational	1.20	1.21	1.23
	Instrumentation	9.06	8.77	8.83
	Parabolic Assumption of Corrective Maneuver	0.60	0.24	0.15
	Total-increment	9.90	9.98	9.41
With Maneuver	Observational	1.90	3.03	4.45
	Instrumentation	14.58	24.09	35.42
	Theoretical	3.79	4.60	3.01
	Total	15.64	25.14	35.95

Figure 6-6. Error Composition in Representative Problems

From an examination of Figure 6-6, some general facts are noted. The instrumentation errors of the manual computer are the dominant cause of perigee error. The instrumentation errors consistently cause about eight times as much error in perigee as do the errors in the observational input data.

The effects of the theoretical errors of the computer mechanization, i.e., the two body assumptions in computing the vacuum perigee and the parabolic assumption in computing the corrective maneuver, are consistently small, between 3 and 5 km. error in perigee. Besides, by means of pre-computed tables, these effects could, if necessary, be removed by the operator in using the manual computer.

The incremental total error in perigee radius due to the corrective maneuver computation is roughly the same for all cases, about 10 km. When added, RSS, to the perigee error assuming no maneuver, this affects overall accuracy by only a small amount. For the largest error case shown on Figure 6-6 (case 5.1.3), the net incremental increase due to the maneuver is from 34.7 km to about 36.0 km or about 4%.

A detailed examination of the instrumentation errors indicated on Figures 5-1 through 5-24 in Section 5 shows that error is significantly contributed by the various components, both mechanical and electrical, throughout the manual computer instrumentation. As would be expected, almost all of the error comes from the components operating at one speed; i.e, input dials and gearing operating at high gear ratios contribute very little error. By way of illustration, consider the instrumentation errors assumming no maneuver for case 5.1.3 shown on Figure 5-9. All 30 errors R.S.S. to a total error in perigee of 34.3 km. Four of the errors contribute more than 10 km each, two being mechanical components and two electrical components. These components contributing most to the total instrumentation error are: (1) a cosine mechanism; (2) a rack differential driven by two cosine mechanisms; (3) a potentiometer driven by a rack differential; and (4) a rheostat driven by the differential of two reciprocal ranges. This general breakdown of the instrumentation errors is quite typical of all 20 cases presented in Section 5.

It should be noted that all of the four largest contributors to the instrumentation errors discussed above are components that are used to process information taken at the second or middle observation. This is consistent with the breakdown of the effect of input data errors on the error in perigee radius. Generally, input data errors from the second observation have a greater effect than observational errors from the first and third readings.

APPENDIX A

Manual Space Computer Error Analysis Program

Introduction

Pages 4 thru 23 of this appendix comprise the Fortran program written to perform this Error Analysis. The following table describes briefly by page and Fortran statement numbers the execution of the program.

Pages	Statements	Function
1	Thru 215	Read Inputs or Observation Points, Errors, Run ID, etc.
1	From 215	Initialization
2	to 391	Compute Theta, Cos Theta, Beta,
2-4	37-123	Select Error Source and Value from Input Matrix
4-6	40-712	Compute Results Obtained by Manual Computer
6	72-766	Compute Perigee Radius of Corrective Maneuver
6	77-78	Compute Miscellaneous Error Terms
	779-8100	Save Those Results Needed for Summary Output Tabulation
7-8	290-311	Write Detailed Output Tape
8	132-135	Compute Galvanometer Range and Accuracy
8-9	5000-4145	Compute required Change in Velocity and direction to achieve desired perigee
9-10	4150-1590	Write Output Tape
10-20	13999-End	Write Summary Output Tape to Produce RSS Error Tabulation

Following the program are the operating instructions required to compile and execute the program.

APPENDIX A

Manual Space Computer Error Analysis Program

Operating Instructions

1. This program may be compiled and executed on any IBM 7090/7094 with a 32000 word storage capacity.

2. The program is written in the Fortran II language.

3. The program reads input data from logical tape 5 and writes output on logical tape 6 and on the on-line printer.

4. The END card of the program is followed immediately by a DATA card and then the following input information:

1st card	-	number of runs (1 to 99)
2nd thru 43rd cards	-	ten variations of each of twenty-one error sources
44th thru 47th cards	-	twenty variations to nominal perigee radius used to determine the accuracy of the galvanometer throughout its range.
48th thru 51st cards	-	twenty variations to nominal perigee angle used to establish the required range of the galvanometer.
52nd card	-	Problem identification (1st problem)
53rd card	-	x, y, z, r of 1st observation point (KM)
54th card	-	" 2nd " " "
55th card	-	" 3rd " " "
56th card	-	" corrective maneuver point (KM)
57th card	-	" desired perigee point (KM)
58th card	-	quadrant of first observation point
59th card	-	problem identification (2nd problem)
60th card	-	x, y, z, r of 1st observation point (KM)
61st card	-	" " 2nd " " "
etc.		

Successive runs may be made by simply adding a set of seven cards per run corresponding to cards 52 thru 58.

The field widths on these input cards are as specified by the format statements in the program. (See statements 199, 200, 201, 202, and 215)

5. The program has three sense switches to control the output as desired.

   5.1 Sense Switch 6 - When only this switch is down, just the RSS summary output is produced. (See figure 5.1).

   5.2 Sense Switch 5 - If only this switch is down, only the more detailed output from which the RSS summary was derived, is produced. (See figures 4.5, 4.9, and 4.14)

   5.3 If both switches 5 and 6 are down, both of the above types of output will be produced.

   5.4 Sense Switch 4 - Normally the computer will halt after each run to allow the operator to reset switches 5 and 6 for the next run. If switch 4 is down the computer will not halt between runs. If many runs are to be made with the same type output desired on each, switch 4 should be down.

6. When printing the output tape under program control, the printer should be under the control of a computer which will recognize the following carriage control characters in the first print wheel position.

1	Restore page before printing
Blank	Single space after printing
0	Double space after printing
+	No space after printing.

```
      ERR1F(A)=A/(3600.*57.2957795)
      ERR2F(A)=A/RP
      ERR3F(A,B,C)=-A*B/2.*COSF(C)/SINF(C)
      DIMENSION RERP(36),RETHP(36),RERPP(36),RETHPP(36),RSS(4)
      DIMENSION  BETA(4),R(5),THETA(4),X(5),Y(5),Z(5),COSTH(4),
     1EP(30,10),THETAD(4),EP22(16),EN(16),DTP(16),GAMMA(4),EP8(16)
      DIMENSION ALPHA(3),ERR1F(1),ERR2F(1),ERR3F(1),IDRUN(4)
      DIMENSION EP30(16),DELP(16)
      READ INPUT TAPE 5,215,NORUN
      READ INPUT TAPE 5,201,((EP(J,K),K=1,10),J=1,21),(EP8(I),I=1,20),
     1(DTP(I),I=1,20)
 1000 READ INPUT TAPE 5,199,IDRUN
      READ INPUT TAPE 5,200,(X(I),Y(I),Z(I),R(I),I=1,4),XP,YP,ZP,RP
      READ INPUT TAPE 5,202,NQUAD
  199 FORMAT (4A6)
  200 FORMAT (4E18.3)
  201 FORMAT (5E14.0)
  202 FORMAT (I1)
  203 FORMAT (66H1                                  MANUAL SPACE COMPUTER ERR
     1OR ANALYSIS)
  204 FORMAT (1H ,78X4A6,8X5HPAGE I3//)
  205 FORMAT(1H ,4E18.7)
  206 FORMAT (117H               X  (KM)          Y  (KM)          Z  (KM)
     1  R  (KM)      THETA (DEG)      COS THETA      BETA (DEG)          //)
  207 FORMAT(118H      ERROR          THETA(P)            R(P)          THETA(C
     1)          R(A)       THETA(P)P      +DELTA R(P)     -DELTA R(P)/ )
  208 FORMAT(6H          ,7E15.7//)
  209 FORMAT (117H                        E(THP)PP          E(RP)PP          E(THC
     1)PP          E(THP)          E(RP)          E(THP)P          E(RP)P    //)
  210 FORMAT(6H    EP(,I2,1H,,I2,4H)    ,7E15.7/15H               ,7E15.7/
     1/)
  212 FORMAT(8E15.7)
  213 FORMAT(38H        DESIRED PERIGEE POSITION FOLLOWS//)
  214 FORMAT (6X4E15.7)
  215 FORMAT (I2)
C     COMPUTE BETA, THE ANGLE SUBTENDED BY THE EARTH
    1 NPAGE=0
      M=1
      RSS(1)=0.
      RSS(2)=0.
      RSS(3)=0.
      RSS(4)=0.
      LINES=0
      E3=0
      E13=0
      E15=0
      E5=0
      DRP=0
      ERPP=0
      RNOM1=0
      THC=0
      THP=0
      THPP=0
      ETHPPP=0
      ETHCPP=0
```

```
      ETHP=0
      ETHPP=0
      RE=6371.229
      DO 10I=1,4
      GAMMA(I)= ATANF(RE/SQRTF(R(I)**2-RE**2))
      BETA(I)=2.*GAMMA(I)
      BETA(I)=57.2957795 * BETA(I)
C     COMPUTE THETA, THE ANGULAR COORDINATE OF THE VEHICLE
   10 THETA(I)=ATANF(SQRTF((R(I)*RP)**2-(X(I)*XP+Y(I)*YP+Z(I)*ZP)**2)/
     1(X(I)*XP+Y(I)*YP+Z(I)*ZP))
C     DETERMINE PROPER QUADRANT OF THETAS IF QUAD OF THETA(1) IS GIVEN
      I=1
   15 IF(THETA(I))16,20,20
   16 IF(NQUAD-3) 17,25,999
   17 THETA(I)=THETA(I)+3.14159265
      GO TO 30
   20 IF(NQUAD-3) 30,999,21
   21 THETA(I)=-THETA(I)+6.2831853
   25 THETA(I)=-THETA(I)+3.14159265
   30 DO 33 I=1,2
      ALPHA(I)=ATANF(SQRTF((R(I)*R(I+1))**2-(X(I)*X(I+1)+Y(I)*Y(I+1)
     1+Z(I)*Z(I+1))**2)/(X(I)*X(I+1)+Y(I)*Y(I+1)+Z(I)*Z(I+1)))
      IF (ALPHA(I))32,33,33
   32 ALPHA(I)=ALPHA(I)+3.14159265
   33 THETA(I+1)=THETA(I)+ALPHA(I)
      I=1
      IF (THETA(I+3))36,34,34
   34 THETA(I+3)=-THETA(I+3)+6.2831853
      GO TO 390
   36 THETA(I+3)=-THETA(I+3)+3.14159265
  390 DO 391 I=1,4
C     COMPUTE THE COSINES OF THE THETA ANGLES
   12 COSTH(I)=COSF(THETA(I))
  391 THETAD(I)=57.2957795*THETA(I)
      J=0
      K=0
      GO TO 40
   37 DO 128 J=1,28
   38 DO 128 K=1,10
      GO TO (100,101,102,103,104,105,106,107,108,109,110,111,112,
     1113,114,115,116,118,119,120,121,1211,1212,1213,1214,162,164,166),J
  100 E1=EP(J,K)
      GO TO 122
  101 E1=0
      E2=EP(J,K)
      GO TO 122
  102 E2=0
      E3=ERR1F(EP(J,K))
      GO TO 122
  103 E3=0
      E4=EP(J,K)
      E14=E4
      GO TO 122
  104 E4=0
      E14=0
      E5=ERR1F(EP(J,K))
```

```
      E15=E5
      GO TO 122
 105  E5=0
      E15=0
      E6=EP(J,K)
      GO TO 122
 106  E6=0
      E7=EP(J,K)
      GO TO 122
 107  E7=0
      E8=ERR1F(EP(J,K))
      E8=ERR3F(E8,R(3),GAMMA(3))
      SAVE1=E8
      GO TO 122
 108  E8=0
      E9=ERR1F(EP(J,K))
      E9=ERR3F(E9,R(1),GAMMA(1))
      SAVE2=E9
      E19=E9
      GO TO 122
 109  E9=0
      E19=0
      E10=ERR2F(EP(J,K))
      GO TO 122
 110  E10=0
      E11=EP(J,K)
      GO TO 122
 111  E11=0
      E12=EP(J,K)
      GO TO 122
 112  E12=0
      E13=ERR1F(EP(J,K))
      GO TO 122
 113  E13=0
      E3=ERR1F(EP(3,K))
      SENSE LIGHT 1
      GO TO 122
 114  E3=ERR1F(EP(3,K))
      E6=0
      SENSE LIGHT 2
      GO TO 122
 115  E3=0
      E6=0
      E16=EP(J,K)
      GO TO 122
 116  E16=0
      E17=EP(J,K)
      GO TO 122
 118  E17=0
      E18=ERR1F(EP(J,K))
      E18=ERR3F(E18,R(2),GAMMA(2))
      SAVE3=E18
      GO TO 122
 119  E18=0
      E20=ERR2F(EP(J,K))
      GO TO 122
```

```
 120 E5=ERR1F(EP(5,K))
     E15=E5
     E6=0.
     E16=0.
     E20=0
     SENSE LIGHT 4
     GO TO 122
 121 E5=ERR1F(EP(5,K))
     E15=E5
     E6=0
     E16=0
     SENSE LIGHT 3
     GO TO 122
1211 E5=0
     E15=0
     E18=0.
     NCB=1
     GO TO 40
1212 NCB=0
     E18=0
     E3=ERR1F(EP(8,K))
     GO TO 40
1213 E3=0
     E5=ERR1F(EP(8,K))
     E15=E5
     GO TO 40
1214 E5=0
     E15=0
     E13=ERR1F(EP(8,K))
     GO TO 40
 162 E6=EP(6,K)
     E16=E6
     E13=0
     GO TO 40
 164 E6=0
     E16=0
     E10=ERR2F(EP(10,K))
     E20=E10
     IF(E10) 40,128,40
 166 E10=0
     E20=0
     E3=ERR1F(EP(3,K))
     E5=E3
     E15=E3
     E13=E3
     GO TO 40
 122 IF(EP(J,K)) 40,123,40
 123 GO TO (128,128,128,128,128,128,128,128,128,128,128,128,128,40,
    140 ,128,128,128,128,40,40,40,40,40,40,40,40),J
C      COMPUTE THETA(P) THP WITH NO ERROR
  40 C=1.
     RR=(((C+E7)/(C+E1))*(R(1)+E9-R(3)-E8)/((R(3)+E8)*(R(1)+E9))+E10/
    1(C+E1))/(((C+E17)/(C+E11))*(R(1)+E19-R(2)-E18)/((R(1)+E19)*(R(2)+
    2E18))+E20/(C+E11))
     I=1
     THP=ATANF((E6+(C+E2)*COSF(THETA(I+2)+E3)-(C+E4)*COSF(THETA(I)+E5)-
```

```
     1RR*(E16+(C+E12)*COSF(THETA(I+1)+E13)-(C+E14)*COSF(THETA(I)+E15)))/
     2(RR*((C+E12)*SINF(THETA(I+1)+E13)-(C+E14)*SINF(THETA(I)+E15))-
     3(C+E2)*SINF(THETA(I+2)+E3)+(C+E4)*SINF(THETA(I)+E5)))
      E8=C
      IF (J-23) 410,409,410
  409 E3=0
  410 IF (THP) 411,41,41
  411 THP=THP+6.2831853
   41 IF(SENSE LIGHT 1) 43,42
   42 IF(SENSE LIGHT 2)44,45
   43 E3=ERR1F(EP(J,K))
      GC TO 45
   44 E3=C
      E6=ERR1F(EP(J,K))
C     SUBSTITUTE THP FOR THETA(3) AND SCLVE FOR RPC
   45 A=((C+E7)*(C+E11)*((C+E12)*COSF(THETA(I+1)+E13-THP)-(C+E14)*COSF
     1(THETA(I)+E15-THP)+E16*COSF(THP)))/((C+E17)*(C+E1)*(((R(1)+E19)-
     2(R(2)+E18))/((R(2)+E18)*(R(1)+E19))+E20/(C+E17))*((C+E2)*CCSF(E3)
     3-(C+E4)*COSF(THETA(I)+E5-THP)+E6*CCSF(THP)))
      RPC=-E8+((C+E7)*(R(1)+E9)*A)/((R(1)+E9)*(C+E7)+(C+E7-E10*R(1)
     1-E10*E9)*A)
      E18=0
      IF(NOB) 452,452,451
  451 E18=ERR1F(EP(18,K))
      E18=ERR3F(E18,R(4),GAMMA(4))
      SAVE4=E18
      IF(E18) 452,128,452
  452 IF(J-25) 455,454,455
  454 E13=0
  455 DRP=RP-RPC
C     COMPUTE ANGULAR PCSITICN OF CORRECTION POINT
      B=(((C+E7)/(C+E1))*((R(1)+E9-RPC-E8)/((RPC+E8)*(R(1)+E9)))+E10/
     1(C+E1))*(C+E12)/(((C+E17)/(C+E11))*((R(1)+E9-R(4)-E18)/((R(1)+E9)*
     2(R(4)+E18)))+E20/(C+E11))
      CTHC=((C+E2)*COSF(E3)-(C+E4)*COSF(THETA(I)+E5-THP)+E6*COSF(THP))/B
     1+(C+E14)*COSF(THETA(I)+E15-THP)/(C+E12)-E16*CCSF(THP)
      STHC=SQRTF(C-CTHC**2)
      THC=ATANF(STHC/CTHC)
      E9=0
      E19=0
      IF(J-24) 460,457,460
  457 E5=C
      E15=0
  460 IF(THC) 46,47,47
   46 THC=-THC+3.14159265
      GC TO 48
   47 THC=-THC+6.2831853
   48 THC=THC-E13+THP
      IF(THC-6.2831853) 52,50,50
   50 THC=THC-6.2831853
   52 IF(SENSE LIGHT 3)55,53
   53 IF(SENSE LIGHT 4)57,62
   55 E5=ERR1F(EP(J,K))
      E15=E5
      GC TO 62
   57 E5=C
```

```
      E15=0
      E16=ERR1F(EP(J,K))
      E6=E16
C     COMPUTE RADIUS OF APOGEE
   62 D=(C+E11)*((C+E12)*COSF(THC+E13-THP)-(C+E14)*COSF(3.14159265+E15)
     1+E16*COSF(THP))/((C+E1)*((C+E2)*COSF(E3)-(C+E4)*COSF(3.14159265+
     2E5)+E6*COSF(THP)))
      RA=(D*(C+E7)-(C+E17))/(E10*D-E20+D*(C+E7)/(RPC+E8)-(C+E17)/
     1(R(4)+E8))-E9
   64 IF(RA-10000000.) 65,67,67
C     CHANGE APOGEE AND PERIGEE BY DELTA R AND COMPUTE THPP
   65 F=((C+E17)*((RA-DRP    +E19-R(4)-E18)/((R(4)+E18)*(RA-DRP    +E19)))
     1+E20)/((C+E7)*((RA-DRP    +E9-RPC-DRP -E8)/((RPC+DRP+E8)*(RA-
     2DRP    +E9)))+E10)
      GO TO 69
   67 SENSE LIGHT 1
      GO TO 65
   69 CTHPP=(F*((C+E1)/(C+E11))*((C+E2)*COSF(E3)-(C+E4)*COSF(3.14159265
     1+E5)+E6*COSF(THP))+(C+E14)*COSF(3.14159265+E15)-E16*COSF(THP))
     2/(C+E12)
      STHPP=SQRTF(C-CTHPP**2)
      THPP=ATANF(STHPP/CTHPP)
      IF(THPP) 70,711,711
   70 THPP=THPP+3.14159265
      GO TO 711
  711 THPP=THPP+THC+E13
      IF(THPP-6.2831853) 72,712,712
  712 THPP=THPP-6.2831853
   72 IF(RNOM1)76,75,76
   75 RNOM1=RPC
      RNOM2=THC
      RNOM3=RA
      RNOM4=THPP
      RNOM=THP
C     COMPUTE CHANGE IN PERIGEE
   76 G=(COSF(RNOM2-THPP)+1.)/2.
      IF (SENSE LIGHT 1) 766,765
  765 BB=RNOM1-RNOM3+R(4)*(C-2.*G)
      CC=-(RNOM1*(RNOM3-R(4))-G*R(4)*(RNOM3-RNOM1))
      DRPMI=-BB/2.- SQRTF((BB)**2-4.*CC)/2.
      DRPPL=-BB/2.+ SQRTF((BB)**2-4.*CC)/2.
      GO TO 77
  766 DRPMI=R(4)*G-RPC
      DRPPL=C
C     MISCELLANEOUS CALCULATIONS
   77 IF(RNOM-3.14159265) 7711,7711,771
  771 ETHPPP=RNOM-6.2831853
      GO TO 772
 7711 ETHPPP=RNOM
  772 ERPPP=-RP+RNOM1
      I=1
      ETHCPP=RNOM2-THETA(I+3)
      ETHP=THP-RNOM
      IF(ETHP) 7721,773,7725
 7721 IF(ETHP+3.14159265) 7722,773,773
 7722 ETHP=ETHP+6.2831853
```

```
      GO TO 773
 7725 IF(ETHP-3.14159265) 773,773,7727
 7727 ETHP=ETHP-6.2831853
  773 ERP=RPC-RNOM1
      ETHPP=THPP-RNOM4
      IF(ETHPP) 774,778,776
  774 IF(ETHPP+3.14159265) 775,778,778
  775 ETHPP=6.2831853+ETHPP
      GO TO 778
  776 IF(ETHPP-3.14159265) 778,778,777
  777 ETHPP=ETHPP-6.2831853
  778 ERPP=DRPMI+ERPPP
   78 C1=57.2957795
      THC=C1*THC
      THP=C1*THP
      THPP=C1*THPP
      ETHPPP=C1*ETHPPP
      ETHCPP=C1*ETHCPP
      ETHP=C1*ETHP
      ETHPP=C1*ETHPP
      IF (SENSE SWITCH 6) 779,290
  779 IF (J) 780,8100,780
  780 GO TO (7800,8100,7820,8100,7840,7850,8100,7870,7880,7890,8100,
     18100,7920,8100,8100,7950,8100,7970,7980,8100,8100,8020,8030,8040,
     28050,8060,8070,8080),J
 7800 GO TO (8200,8100,8100,8100,8100,8100,8100,8100,8100,8100),K
 7820 GO TO (8200,8100,8200,8100,8200,8100,8100,8100,8100,8100),K
 7840 GO TO (8200,8100,8200,8100,8200,8100,8100,8100,8100,8100),K
 7850 GO TO (8200,8100,8200,8100,8200,8100,8200,8100,8100,8100),K
 7870 GO TO (8200,8100,8100,8100,8100,8100,8100,8100,8100,8100),K
 7880 GO TO (8200,8100,8100,8100,8100,8100,8100,8100,8100,8100),K
 7890 GO TO (8200,8100,8200,8100,8200,8100,8200,8100,8100,8100),K
 7920 GO TO (8200,8100,8200,8100,8200,8100,8100,8100,8100,8100),K
 7950 GO TO (8200,8100,8200,8100,8200,8100,8200,8100,8100,8100),K
 7970 GO TO (8200,8100,8100,8100,8100,8100,8100,8100,8100,8100),K
 7980 GO TO (8200,8100,8200,8100,8200,8100,8200,8100,8100,8100),K
 8020 GO TO (8200,8100,8100,8100,8100,8100,8100,8100,8100,8100),K
8030  GO TO (8200,8100,8100,8100,8100,8100,8100,8100,8100,8100),K
 8040 GO TO (8200,8100,8100,8100,8100,8100,8100,8100,8100,8100),K
 8050 GO TO (8200,8100,8100,8100,8100,8100,8100,8100,8100,8100),K
 8060 GO TO (8200,8100,8100,8100,8100,8100,8100,8100,8100,8100),K
 8070 GO TO (8200,8100,8100,8100,8100,8100,8100,8100,8100,8100),K
 8080 GO TO (8200,8100,8100,8100,8100,8100,8100,8100,8100,8100),K
 8200 RERP(M)=ERP
      RERPP(M)=ERPP
      RETHP(M)=ETHP
      RETHPP(M)=ETHPP
      M=M+1
 8100 IF (SENSE SWITCH 5) 290,80
  290 IF(LINES-2) 300,300,312
  300 NPAGE=NPAGE+1
      WRITE OUTPUT TAPE 6,203
      WRITE OUTPUT TAPE 6,204,IDRUN,NPAGE
      LINES=2
      IF(NPAGE-1)305,305,310
  305 WRITE OUTPUT TAPE 6,206
```

```
      WRITE OUTPUT TAPE 6,208,(X(I),Y(I),Z(I),R(I),THETAD(I),COSTH(I),
     1BETA(I),I=1,4)
      WRITE OUTPUT TAPE 6,213
      WRITE OUTPUT TAPE 6,214,XP,YP,ZP,RP
      GO TO 300
  310 LINES=LINES+2
      WRITE OUTPUT TAPE 6,207
      WRITE OUTPUT TAPE 6,209
  312 WRITE OUTPUT TAPE 6,210,J,K,THP,RPC,THC,RA,THPP,DRPPL,DRPMI,
     1ETHPPP,ERPPP,ETHCPP,ETHP,ERP,ETHPP,ERPP
      LINES=LINES+3
      IF(LINES-54)80,80,311
  311 LINES=0
   80 IF(J-1) 37,128,128
  128 CONTINUE
  999 GO TO 132
  132 DO 135 I=1,16
      J=1
      H=R(1)*R(2)*(COSF(THETA(J+1)-RNOM)-COSF(THETA(J)-RNOM))/(R(1)-
     1R(2))
      EP22(I)=H-(RNOM1+EP8(I))*R(1)*(C-COSF(THETA(J)-RNOM))/(R(1)-
     1RNOM1-EP8(I))
      DELP(I)=ERR1F(DTP(I))
      HP=R(1)*R(2)*(COSF(THETA(J+1)-RNOM-DELP(I))-COSF(THETA(J)-DELP(I)-
     1RNOM))/(R(1)-R(2))
      EP30(I)=HP-R(1)*R(3)*(COSF(THETA(J+2)-DELP(I)-RNOM)-COSF(THETA(J)-
     1DELP(I)-RNOM))/(R(1)-R(3))
  135 EN(I)=R(1)*RNOM1*(C-COSF(THETA(J)-RNOM-DELP(I)))/(R(1)-RNOM1)-R(1)
     1*R(2)*(COSF(THETA(J+1)-RNOM-DELP(I))-COSF(THETA(J)-RNOM-DELP(I)))/
     2(R(1)-R(2))
      RAD=57.2957795
      RA=RNOM3
      RC=R(4)
      RPP=RP
      RP=RNOM1
      THA=RNOM+3.14159265
 5000 IF (THA-6.2831853) 5200,5100,5100
 5100 THA=THA-6.2831853
      GO TO 5000
 5200 THAD=THA*RAD
      THC=RNOM2
      THCD=RNOM2*RAD
      THP=RNOM
      THPD=RNOM*RAD
      THPP=RNOM4
      THPPD=RNOM4*RAD
      SMU=.3986135E6
      DRP=RPP-RP
      DTHP=THPP-THP
      IF (DTHP) 5210,5230,5205
 5205 IF (DTHP-3.14159265) 5230,5230,5207
 5207 DTHP=DTHP-6.2831853
      GO TO 5230
 5210 IF (DTHP+3.14159265) 5220,5230,5230
 5220 DTHP=DTHP+6.2831853
 5230 DTHPD=DTHP*RAD
```

```
      DPHI=ABSF(.5*DTHP)
      AA=RA+RP
      A=.5*AA
      E=(RA-RP)/AA
      THCMP=THC-THP
 5240 IF (THCMP) 5250,5260,5260
 5250 THCMP=THCMP+6.2831853
      GO TO 5240
 5260 THCMPD=THCMP*RAD
      CSPC=SQRTF((1.+E*COSF(THCMP))/(2.-(RC/A)))
      SNPC=SQRTF(1.-CSPC*CSPC)
      PHIC=ATANF(SNPC/CSPC)
      PHICD=PHIC*RAD
      PCPBD=.5*(THCMPD-180.)
      VC=SQRTF(SMU*((2./RC)-(1./A)))
      VHC=VC*CSPC
      VRC=VC*SNPC
      VRCC=(90.-PCPBD)/RAD
      VPARB=SQRTF(2.*(SMU/RC))
      DELTAV=VPARB*DPHI
      IF(DRP) 2000,3000,3000
 2000 VRCPPP=VRC+(DELTAV*COSF(VRCC))
      VHCPPP=VHC-(DELTAV*(SINF(VRCC)))
      GO TO 4000
 3000 VRCPPP=VRC-(DELTAV*COSF(VRCC))
      VHCPPP=VHC+(DELTAV*SINF(VRCC))
 4000 VCPPP=SQRTF((VRCPPP*VRCPPP)+(VHCPPP*VHCPPP))
      HPPP=RC*VHCPPP
      APPP=(RC*SMU)/((2.*SMU)-(VCPPP*VCPPP*RC))
      EPPP=SQRTF(1.-((HPPP*HPPP)/(SMU*APPP)))
      RPPPP=APPP*(1.-EPPP)
      SLPPP=APPP*(1.-(EPPP*EPPP))
      ERPPPP=RPPPP-RPP
      TCPT=(SLPPP-RC)/(RC*EPPP)
      TCPPPP=RAD*(ATANF((SQRTF(1.-(TCPT*TCPT)))/TCPT))
   22 IF(TCPPPP) 23,24,24
   23 TCPPPP=-TCPPPP+180.
      GO TO 26
   24 TCPPPP=-TCPPPP+360.
   26 ETPPPP=THCD-THPPD
 4100 IF (ETPPPP) 4110,4120,4120
 4110 ETPPPP=ETPPPP+360.
      GO TO 4100
 4120 ETPPPP=ETPPPP-TCPPPP
      IF (ETPPPP) 4140,4150,4130
 4130 IF (ETPPPP-180.) 4150,4150,4135
 4135 ETPPPP=ETPPPP-360.
      GO TO 4150
 4140 IF (ETPPPP+180.) 4145,4150,4150
 4145 ETPPPP=ETPPPP+360.
 4150 NPAGE=NPAGE+1
      IF (SENSE SWITCH 6) 4152,4153
 4152 IF (SENSE SWITCH 5) 4153,13999
 4153 WRITE OUTPUT TAPE 6,212,(EN(I),I=1,16),(EP22(I),I=1,16),
     1(EP30(I),I=1,16)
      WRITE OUTPUT TAPE 6,203
```

```
      WRITE OUTPUT TAPE 6,204,IDRUN,NPAGE
      WRITE OUTPUT TAPE 6,216
      WRITE OUTPUT TAPE 6,220
      WRITE OUTPUT TAPE 6,225,RA,RC,RP,RPP,THAD,THCD,THPD,THPPD
      WRITE OUTPUT TAPE 6,230
      WRITE OUTPUT TAPE 6,240
      WRITE OUTPUT TAPE 6,245,DRP,A,E,SMU,DPHI,DTHPD
      WRITE OUTPUT TAPE 6,250
      WRITE OUTPUT TAPE 6,260
      WRITE OUTPUT TAPE 6,265,CSPC,SNPC,PHICD,PCPBD,TCPPPP,ETPPPP
      WRITE OUTPUT TAPE 6,270
      WRITE OUTPUT TAPE6,275,VC,VCPPP,VHC,VHCPPP,VRC,VRCPPP,VPARB,DELTAV
      WRITE OUTPUT TAPE 6,280
      WRITE OUTPUT TAPE 6,285,APPP,EPPP,HPPP,SLPPP,RPPPP,ERPPPP
  216 FORMAT(1H0,53X13HINPUT SUMMARY)
  220 FORMAT(1H0,119H    R(A) KM          R(C) KM          R(P) KM        R(P
     1)P KM        THETA(A) DEG    THETA(C) DEG    THETA(P) DEG   THETA(P)P D
     2EG)
  225 FORMAT(8E15.7)
  230 FORMAT(1H0,43X32HINPUT CALCULATIONS AND CONSTANTS)
  240 FORMAT(1H0,117H   DELTA R(P) KM                A KM                  E
     1               MU KM3/SEC2         DELTA PHI RAD    DELTA THETA(P) DEG
     2)
  245 FORMAT(E17.7,E19.7,4E20.7//)
  250 FORMAT(1H0,53X14HOUTPUT SUMMARY)
  260 FORMAT(1H0,117H  COS(PHI(C))              SIN(PHI(C))              PHI(C)
     1DEG          PHI(C)PAB DEG       THETA(CP)PPP DEG    E(THETA(P)PPP DEG
     2)
  265 FORMAT(E15.7,E21.7,2E20.7,E21.7,E19.7)
  270 FORMAT(1H0,118H   VC KM/SEC      VCPPP KM/SEC    VHC KM/SEC     VHCPP
     1P KM/SEC    VRC KM/SEC     VRCPPP KM/SEC    VPAB KM/SEC     DELV KM/SE
     2C)
  275 FORMAT(8E15.7)
  280 FORMAT(1H0,116H       APPP KM                  EPPP                HPPP KM2
     1/SEC             LPPP               R(P)PPP KM         E(R(P))PPP KM)
  285 FORMAT(E17.7,5E20.7)
      IF (SENSE SWITCH 5) 1590,1599
 1590 IF (SENSE SWITCH 6) 13999,1599
13999 WRITE OUTPUT TAPE 6,14000
14000 FORMAT(1H1,87X17HERRORS IN PERIGEE)
      WRITE OUTPUT TAPE 6,14100
14100 FORMAT(74X44HASSUMING NC   INCREMENT DUE TO   TOTAL WITH )
      WRITE OUTPUT TAPE 6,14101
14101 FORMAT(76X40HMANEUVER     MANEUVER COMP.     MANEUVER)
      WRITE OUTPUT TAPE 6,14200
14200 FORMAT(30X12HERROR SOURCE,31X45HRADIUS  ANGLE   RADIUS  ANGLE   RA
     1DIUS  ANGLE)
      WRITE OUTPUT TAPE 6,14201
14201 FORMAT(74X44H(KM)   (DEG)    (KM)   (DEG)    (KM)   (DEG))
31002 COL1 = ERPPP
      COL2=ETHPPP
      COL3=ERPPP
      COL4=ETHPPP
      COL1 = ABSF(COL1)
      COL2 = ABSF(COL2)
      COL5 = COL1
```

```
      COL6 = COL2
      WRITE OUTPUT TAPE 6,14300,COL1,COL2,COL5,COL6
14300 FORMAT(1H 71H1.     TWO BODY VS. FOUR BODY AND EARTH OBLATENESS
     1                     ,F7.2,F8.4,17H  NOT APPLICABLE ,F7.2,F8.4)
      WRITE OUTPUT TAPE 6,14400
14400 FORMAT(1H0,71H2.     OBSERVATIONAL ERRORS
     1                     )
      DO 18352 M=1,36
      GO TO (31004,31006,31008,31010,31012,31014,31016,31018,31020,
     131022,31024,31026,31028,31030,31032,31034,31036,31038,31040,31042,
     231044,31046,31048,31050,31052,31054,31056,31058,31060,31062,31064,
     331066,31068,31070,31072,31074),M
31004 COL1=RERP(32)
      COL2=RETHP(32)
      COL3=RERPP(32)
      COL4=RETHPP(32)
      COL1 = ABSF(COL1)
      COL2 = ABSF(COL2)
      COL3 = ABSF(COL3)
      COL4 = ABSF(COL4)
      WRITE OUTPUT TAPE 6,14500,COL1,COL2,COL3,COL4
14500 FORMAT(1H+,71H  2.1   UNCERTAINTY IN MEASUREMENT OF O(1)
     1                     ,F7.2,F8.4,F8.2,F8.4)
      WRITE OUTPUT TAPE 6,14450
14450 FORMAT(1H ,38X1H-)
      GO TO 18350
31006 COL1=RERP(33)
      COL2=RETHP(33)
      COL3=RERPP(33)
      COL4=RETHPP(33)
      COL1 = ABSF(COL1)
      COL2 = ABSF(COL2)
      COL3 = ABSF(COL3)
      COL4 = ABSF(COL4)
      WRITE OUTPUT TAPE 6,14600,COL1,COL2,COL3,COL4
14600 FORMAT(1H+,71H  2.2   UNCERTAINTY IN MEASUREMENT OF O(2)
     1                     ,F7.2,F8.4,F8.2,F8.4)
      WRITE OUTPUT TAPE 6,14450
      GO TO 18350
31008 COL1=RERP(31)
      COL2=RETHP(31)
      COL3=RERPP(31)
      COL4=RETHPP(31)
      COL1 = ABSF(COL1)
      COL2 = ABSF(COL2)
      COL3 = ABSF(COL3)
      COL4 = ABSF(COL4)
      WRITE OUTPUT TAPE 6,14700,COL1,COL2,COL3,COL4
14700 FORMAT(1H+,71H  2.3   UNCERTAINTY IN MEASUREMENT OF O(3)
     1                     ,F7.2,F8.4,F8.2,F8.4)
      WRITE OUTPUT TAPE 6,14450
      GO TO 18350
31010 COL1=RERP(13)
      COL2=RETHP(13)
      COL3=RERPP(13)
      COL4=RETHPP(13)
```

```
      CCL1 = ABSF(COL1)
      CCL2 = ABSF(COL2)
      COL3 = ABSF(COL3)
      CCL4 = ABSF(CCL4)
      WRITE OUTPUT TAPE 6,148CC,CCL1,CCL2,COL3,CCL4
1480C FCRMAT(1H ,71H  2.4   UNCERTAINTY IN MEASUREMENT CF R(1)
     1                      ,F7.2,F8.4,F8.2,F8.4)
      GC TO 18350
31012 COL1=RERP(25)
      CCL1 = ABSF(CCL1)
      CCL2=RETHP(25)
      CCL2 = ABSF(COL2)
      CCL3=RERPP(25)
      CCL3 = ABSF(COL3)
      CCL4=RETHPP(25)
      CCL4 = ABSF(CCL4)
      WRITE CUTPUT TAPE 6,149CC,CCL1,CCL2,CCL3,COL4
1490C FCRMAT(1H ,71H  2.5   UNCERTAINTY IN MEASUREMENT CF R(2)
     1                      ,F7.2,F8.4,F8.2,F8.4)
      GC TO 1835C
31014 CCL1=RERP(12)
      CCL1 = ABSF(COL1)
      COL2=RETHP(12)
      COL2 = ABSF(COL2)
      CCL3=RERPP(12)
      CCL3 = ABSF(COL3)
      CCL4=RETHPP(12)
      CCL4 = ABSF(CCL4)
      WRITE CUTPUT TAPE 6,150CC,CCL1,CCL2,CCL3,CCL4
150CC FCRMAT(1H ,71H  2.6   UNCERTAINTY IN MEASUREMENT CF R(3)
     1                      ,F7.2,F8.4,F8.2,F8.4)
      GC TO 1835C
31016 CCL1=RERP(3C)
      CCL1 = ABSF(COL1)
      CCL2=RETHP(3C)
      CCL2 = ABSF(CCL2)
      CCL3=RERPP(3C)
      CCL3 = ABSF(COL3)
      COL4=RETHPP(3C)
      CCL4 = ABSF(CCL4)
      WRITE OUTPUT TAPE 6,151CC,CCL3,CCL4
1510C FCRMAT(1H ,71H  2.7   UNCERTAINTY IN MEASUREMENT CF R(C)
     1                      ,15H NCT APPLICABLE,F8.2,F8.4)
      RSS(1)=COL1**2+RSS(1)
      RSS(2)=CCL2**2+RSS(2)
      RSS(3)=COL3**2+RSS(3)
      RSS(4)=COL4**2+RSS(4)
      CCL1 = SQRTF(RSS(1))
      CCL2 = SQRTF(RSS(2))
      CCL3 = SQRTF(RSS(3))
      CCL4 = SQRTF(RSS(4))
      RSS(1)=C.
      RSS(2)=C.
      RSS(3)=C.
      RSS(4)=C.
      SAVE1=CCL1
```

```
      SAVE2=COL2
      SAVE3=COL3
      SAVE4=COL4
      COL5 = SQRTF(COL1**2+COL3**2)
      COL6 = SQRTF(COL2**2+COL4**2)
      WRITE OUTPUT TAPE 6,15200,COL1,COL2,COL3,COL4,COL5,COL6
15200 FORMAT(1H0,71H         RSS
     1                   ,F7.2,F8.4,F8.2,F8.4,F8.2,F8.4)
      WRITE OUTPUT TAPE 6,15300
15300 FORMAT(1H0,71H3.     INSTRUMENTATION ERRORS
     1                   )
      GO TO 18350
31018 COL1=RERP(5 )
      COL1 = ABSF(COL1)
      COL2=RETHP(5 )
      COL2 = ABSF(COL2)
      COL3=RERPP(5 )
      COL3 = ABSF(COL3)
      COL4=RETHPP(5 )
      COL4 = ABSF(COL4)
      WRITE OUTPUT TAPE 6,15400,COL1,COL2,COL3,COL4
15400 FORMAT(1H+,71H  3.1   UNCERTAINTY IN O(1) INPUT GEARING AND DIAL R
     1EADING             ,F7.2,F8.4,F8.2,F8.4)
      WRITE OUTPUT TAPE 6,15350
15350 FORMAT(1H ,23X1H-)
      GO TO 18350
31020 COL1=RERP(18)
      COL1 = ABSF(COL1)
      COL2=RETHP(18)
      COL2 = ABSF(COL2)
      COL3=RERPP(18)
      COL3 = ABSF(COL3)
      COL4=RETHPP(18)
      COL4 = ABSF(COL4)
      WRITE OUTPUT TAPE 6,15500,COL1,COL2,COL3,COL4
15500 FORMAT(1H+,71H  3.2   UNCERTAINTY IN O(2) INPUT GEARING AND DIAL R
     1EADING             ,F7.2,F8.4,F8.2,F8.4)
      WRITE OUTPUT TAPE 6,15350
      GO TO 18350
31022 COL1=RERP( 2)
      COL1 = ABSF(COL1)
      COL2=RETHP(2 )
      COL2 = ABSF(COL2)
      COL3=RERPP(2 )
      COL3 = ABSF(COL3)
      COL4=RETHPP(2 )
      COL4 = ABSF(COL4)
      WRITE OUTPUT TAPE 6,15600,COL1,COL2,COL3,COL4
15600 FORMAT(1H+,71H  3.3   UNCERTAINTY IN O(3) INPUT GEARING AND DIAL R
     1EADING             ,F7.2,F8.4,F8.2,F8.4)
      WRITE OUTPUT TAPE 6,15350
      GO TO 18350
31024 COL1=RERP(36)
      COL1 = ABSF(COL1)
      COL2=RETHP(36)
      COL2 = ABSF(COL2)
```

```
      COL3=RERPP(36)
      COL3 = ABSF(COL3)
      COL4=RETHPP(36)
      COL4 = ABSF(COL4)
      WRITE OUTPUT TAPE 6,15700,COL1,COL2,COL3,COL4
15700 FORMAT(1H+,71H  3.4   UNCERTAINTY IN O(P) INPUT GEARING AND DIAL R
     1EADING                ,F7.2,F8.4,F8.2,F8.4)
      WRITE OUTPUT TAPE 6,15350
      GO TO 18350
31026 COL1=RERP( 6)
      COL1 = ABSF(COL1)
      COL2=RETHP(6 )
      COL2 = ABSF(COL2)
      COL3=RERPP(6 )
      COL3 = ABSF(COL3)
      COL4=RETHPP(6 )
      COL4 = ABSF(COL4)
      WRITE OUTPUT TAPE 6,15800,COL1,COL2,COL3,COL4
15800 FORMAT(1H+,71H  3.5   UNCERTAINTY IN (O(1)-O(P)) DIFFERENTIAL
     1                      ,F7.2,F8.4,F8.2,F8.4)
      WRITE OUTPUT TAPE 6,15750
15750 FORMAT(1H ,24X6H-     -)
      GO TO 18350
31028 COL1=RERP(19)
      COL1 = ABSF(COL1)
      COL2=RETHP(19)
      COL2 = ABSF(COL2)
      COL3=RERPP(19)
      COL3 = ABSF(COL3)
      COL4=RETHPP(19)
      COL4 = ABSF(COL4)
      WRITE OUTPUT TAPE 6,15900,COL1,COL2,COL3,COL4
15900 FORMAT(1H+,71H  3.6   UNCERTAINTY IN (O(2)-O(P)) DIFFERENTIAL
     1                      ,F7.2,F8.4,F8.2,F8.4)
      WRITE OUTPUT TAPE 6,15750
      GO TO 18350
31030 COL1=RERP( 3)
      COL1 = ABSF(COL1)
      COL2=RETHP(3 )
      COL2 = ABSF(COL2)
      COL3=RERPP(3 )
      COL3 = ABSF(COL3)
      COL4=RETHPP(3 )
      COL4 = ABSF(COL4)
      WRITE OUTPUT TAPE 6,16000,COL1,COL2,COL3,COL4
16000 FORMAT(1H+,71H  3.7   UNCERTAINTY IN (O(3)-O(P)) DIFFERENTIAL
     1                      ,F7.2,F8.4,F8.2,F8.4)
      WRITE OUTPUT TAPE 6,15750
      GO TO 18350
31032 COL1=RERP( 7)
      COL1 = ABSF(COL1)
      COL2=RETHP(7 )
      COL2 = ABSF(COL2)
      COL3=RERPP(7 )
      COL3 = ABSF(COL3)
      COL4=RETHPP(7 )
```

```
      COL4 = ABSF(COL4)
      WRITE OUTPUT TAPE 6,16100,COL1,COL2,COL3,COL4
16100 FORMAT(1H+,71H  3.8   UNCERTAINTY IN (O(1)-O(P)) REDUCTION GEARING
     1 TO COS MECHANISM  ,F7.2,F8.4,F8.2,F8.4)
      WRITE OUTPUT TAPE 6,15750
      GO TO 18350
31034 COL1=RERP(20)
      COL1 = ABSF(COL1)
      COL2=RETHP(20)
      COL2 = ABSF(COL2)
      COL3=RERPP(20)
      COL3 = ABSF(COL3)
      COL4=RETHPP(20)
      COL4 = ABSF(COL4)
      WRITE OUTPUT TAPE 6,16200,COL1,COL2,COL3,COL4
16200 FORMAT(1H+,71H  3.9   UNCERTAINTY IN (O(2)-O(P)) REDUCTION GEARING
     1 TO COS MECHANISM  ,F7.2,F8.4,F8.2,F8.4)
      WRITE OUTPUT TAPE 6,15750
      GO TO 18350
31036 COL1=RERP( 4)
      COL1 = ABSF(COL1)
      COL2=RETHP(4 )
      COL2 = ABSF(COL2)
      COL3=RERPP(4 )
      COL3 = ABSF(COL3)
      COL4=RETHPP(4 )
      COL4 = ABSF(COL4)
      WRITE OUTPUT TAPE 6,16300,COL1,COL2,COL3,COL4
16300 FORMAT(1H+,71H  3.10  UNCERTAINTY IN (O(3)-O(P)) REDUCTION GEARING
     1 TO COS MECHANISM  ,F7.2,F8.4,F8.2,F8.4)
      WRITE OUTPUT TAPE 6,15750
      GO TO 18350
31038 COL1=RERP(34)
      COL1 = ABSF(COL1)
      COL2=RETHP(34)
      COL2 = ABSF(COL2)
      COL3=RERPP(34)
      COL3 = ABSF(COL3)
      COL4=RETHPP(34)
      COL4 = ABSF(COL4)
      WRITE OUTPUT TAPE 6,16400,COL1,COL2,COL3,COL4
16400 FORMAT(1H+,71H  3.11  UNCERTAINTY IN (O(1)-O(P)) COSINE MECHANISM
     1                    ,F7.2,F8.4,F8.2,F8.4)
      WRITE OUTPUT TAPE 6,15750
      GO TO 18350
31040 COL1=RERP(21)
      COL1 = ABSF(COL1)
      COL2=RETHP(21)
      COL2 = ABSF(COL2)
      COL3=RERPP(21)
      COL3 = ABSF(COL3)
      COL4=RETHPP(21)
      COL4 = ABSF(COL4)
      WRITE OUTPUT TAPE 6,16500,COL1,COL2,COL3,COL4
16500 FORMAT(1H+,71H  3.12  UNCERTAINTY IN (O(2)-O(P)) COSINE MECHANISM
     1                    ,F7.2,F8.4,F8.2,F8.4)
```

```
      WRITE OUTPUT TAPE 6,15750
      GO TO 16350
31042 COL1=RERP( 8)
      COL1 = ABSF(COL1)
      COL2=RETHP( 8)
      COL2 = ABSF(COL2)
      COL3=RERPP(8 )
      COL3 = ABSF(COL3)
      COL4=RETHPP(8 )
      COL4 = ABSF(COL4)
      WRITE OUTPUT TAPE 6,16600,COL1,COL2,COL3,COL4
16600 FORMAT(1H+,71H  3.13  UNCERTAINTY IN (C(3)-O(P)) COSINE MECHANISM
     1                      ,F7.2,F8.4,F8.2,F8.4)
      WRITE OUTPUT TAPE 6,15750
      GO TO 16350
31044 COL1=RERP(9 )
      COL1 = ABSF(COL1)
      COL2=RETHP(9 )
      COL2 = ABSF(COL2)
      COL3=RERPP(9 )
      COL3 = ABSF(COL3)
      COL4=RETHPP(9 )
      COL4 = ABSF(COL4)
      WRITE OUTPUT TAPE 6,16700,COL1,COL2,COL3,COL4
16700 FORMAT(1H+,71H  3.14  UNCERTAINTY IN COS(C(3)-O(P))-COS(O(1)-O(P))
     1 DIFFERENTIAL       ,F7.2,F8.4,F8.2,F8.4)
      WRITE OUTPUT TAPE 6,16650
16650 FORMAT(1H ,27X21H-     -         -    -)
      GO TO 16350
31046 COL1=RERP(22)
      COL1 = ABSF(COL1)
      COL2=RETHP(22)
      COL2 = ABSF(COL2)
      COL3=RERPP(22)
      COL3 = ABSF(COL3)
      COL4=RETHPP(22)
      COL4 = ABSF(COL4)
      WRITE OUTPUT TAPE 6,16800,COL1,COL2,COL3,COL4
16800 FORMAT(1H+,71H  3.15  UNCERTAINTY IN COS(C(2)-O(P))-COS(O(1)-O(P))
     1 DIFFERENTIAL       ,F7.2,F8.4,F8.2,F8.4)
      WRITE OUTPUT TAPE 6,16650
      GO TO 16350
31048 COL1=RERP(10)
      COL1 = ABSF(COL1)
      COL2=RETHP(10)
      COL2 = ABSF(COL2)
      COL3=RERPP(10)
      COL3 = ABSF(COL3)
      COL4=RETHPP(10)
      COL4 = ABSF(COL4)
      WRITE OUTPUT TAPE 6,16900,COL1,COL2,COL3,COL4
16900 FORMAT(1H+,71H  3.16  UNCERTAINTY IN COS(C(3)-O(P))-COS(O(1)-O(P))
     1 POT DRIVE GEARING ,F7.2,F8.4,F8.2,F8.4)
      WRITE OUTPUT TAPE 6,16650
      GO TO 16350
31050 COL1=RERP(23)
```

```
      COL1 = ABSF(COL1)
      COL2=RETHP(23)
      COL2 = ABSF(COL2)
      COL3=RERPP(23)
      COL3 = ABSF(COL3)
      COL4=RETHPP(23)
      COL4 = ABSF(COL4)
      WRITE OUTPUT TAPE 6,17000,COL1,COL2,COL3,COL4
17000 FORMAT(1H+,71H  3.17  UNCERTAINTY IN COS(C(2)-O(P))-COS(O(1)-O(P))
     1 POT DRIVE GEARING ,F7.2,F8.4,F8.2,F8.4)
      WRITE OUTPUT TAPE 6,16650
      GO TO 18350
31052 COL1=RERP(11)
      COL1 = ABSF(COL1)
      COL2=RETHP(11)
      COL2 = ABSF(COL2)
      COL3=RERPP(11)
      COL3 = ABSF(COL3)
      COL4=RETHPP(11)
      COL4 = ABSF(COL4)
      WRITE OUTPUT TAPE 6,17100,COL1,COL2,COL3,COL4
17100 FORMAT(1H+,71H  3.18  COS(C(3)-C(P))-COS(C(1)-C(P)) PCT NON-LINEAR
     1ITY                     ,F7.2,F8.4,F8.2,F8.4)
      WRITE OUTPUT TAPE 6,17050
17050 FORMAT(1H ,12X21H-     -          -    -)
      GO TO 18350
31054 COL1=RERP(24)
      COL1 = ABSF(COL1)
      COL2=RETHP(24)
      COL2 = ABSF(COL2)
      COL3=RERPP(24)
      COL3 = ABSF(COL3)
      COL4=RETHPP(24)
      COL4 = ABSF(COL4)
      WRITE OUTPUT TAPE 6,17200,COL1,COL2,COL3,COL4
17200 FORMAT(1H+,71H  3.19  COS(C(2)-C(P))-COS(C(1)-O(P)) PCT NON-LINEAR
     1ITY                     ,F7.2,F8.4,F8.2,F8.4)
      WRITE OUTPUT TAPE 6,17050
      GO TO 18350
31056 COL1=RERP(35)
      COL1 = ABSF(COL1)
      COL2=RETHP(35)
      COL2 = ABSF(COL2)
      COL3=RERPP(35)
      COL3 = ABSF(COL3)
      COL4=RETHPP(35)
      COL4 = ABSF(COL4)
      WRITE OUTPUT TAPE 6,17300,COL1,COL2,COL3,COL4
17300 FORMAT(1H 71H  3.20  UNCERTAINTY IN 1/R(1) INPUT GEARING AND DIAL
     1READING                 ,F7.2,F8.4,F8.2,F8.4)
      GO TO 18350
31058 COL1=RERP(26)
      COL1 = ABSF(COL1)
      COL2=RETHP(26)
      COL2 = ABSF(COL2)
      COL3=RERPP(26)
```

```
      COL3 = ABSF(CCL3)
      CCL4=RETHPP(26)
      COL4 = ABSF(COL4)
      WRITE OUTPUT TAPE 6,17400,CCL1,COL2,COL3,CCL4
17400 FORMAT(1H ,71H  3.21  UNCERTAINTY IN 1/R(2) INPUT GEARING AND DIAL
     1 READING              ,F7.2,F8.4,F8.2,F8.4)
      GO TO 18350
31060 CCL1=RERP(14)
      CCL1 = ABSF(COL1)
      CCL2=RETHP(14)
      COL2 = ABSF(CCL2)
      CCL3=RERPP(14)
      COL3 = ABSF(COL3)
      CCL4=RETHPP(14)
      COL4 = ABSF(COL4)
      WRITE OUTPUT TAPE 6,17500,CCL1,COL2,CCL3,COL4
17500 FORMAT(1H ,71H  3.22  UNCERTAINTY IN 1/R(3) INPUT GEARING AND DIAL
     1 READING              ,F7.2,F8.4,F8.2,F8.4)
      GO TO 18350
31062 COL1=RERP(15)
      COL1 = ABSF(CCL1)
      COL2=RETHP(15)
      CCL2 = ABSF(COL2)
      CCL3=RERPP(15)
      CCL3 = ABSF(CCL3)
      COL4=RETHPP(15)
      CCL4 = ABSF(CCL4)
      WRITE OUTPUT TAPE 6,17600,CCL1,CCL2,CCL3,CCL4
17600 FORMAT(1H ,71H  3.23  UNCERTAINTY IN (1/R(3)-1/R(1)) DIFFERENTIAL
     1                      ,F7.2,F8.4,F8.2,F8.4)
      GO TO 18350
31064 CCL1=RERP(27)
      CCL1 = ABSF(COL1)
      CCL2=RETHP(27)
      CCL2 = ABSF(COL2)
      COL3=RERPP(27)
      COL3 = ABSF(COL3)
      CCL4=RETHPP(27)
      CCL4 = ABSF(COL4)
      WRITE OUTPUT TAPE 6,17700,CCL1,CCL2,COL3,CCL4
17700 FORMAT(1H ,71H  3.24  UNCERTAINTY IN (1/R(2)-1/R(1)) DIFFERENTIAL
     1                      ,F7.2,F8.4,F8.2,F8.4)
      GO TO 18350
31066 CCL1=RERP(16)
      CCL1 = ABSF(CCL1)
      CCL2=RETHP(16)
      CCL2 = ABSF(COL2)
      COL3=RERPP(16)
      COL3 = ABSF(COL3)
      CCL4=RETHPP(16)
      CCL4 = ABSF(CCL4)
      WRITE OUTPUT TAPE 6,17800,CCL1,COL2,CCL3,CCL4
17800 FORMAT(1H ,71H  3.25  UNCERTAINTY IN (1/R(3)-1/R(1)) RHEOSTAT DRIV
     1E GEARING             ,F7.2,F8.4,F8.2,F8.4)
      GO TO 18350
31068 CCL1=RERP(28)
```

```
      CCL1 = ABSF(CCL1)
      CCL2=RETHP(28)
      CCL2 = ABSF(COL2)
      COL3=RERPP(28)
      CCL3 = ABSF(COL3)
      COL4=RETHPP(28)
      COL4 = ABSF(COL4)
      WRITE OUTPUT TAPE 6,179CC,COL1,CCL2,CCL3,COL4
17900 FORMAT(1H ,71H  3.26  UNCERTAINTY IN (1/R(2)-1/R(1)) RHEOSTAT DRIV
     1E GEARING            ,F7.2,F8.4,F8.2,F8.4)
      GC TO 1835C
31070 COL1=RERP(17)
      COL1 = ABSF(COL1)
      CCL2=RETHP(17)
      CCL2 = ABSF(COL2)
      CCL3=RERPP(17)
      CCL3 = ABSF(CCL3)
      COL4=RETHPP(17)
      CCL4 = ABSF(COL4)
      WRITE OUTPUT TAPE 6,18CCC,CCL1,CCL2,COL3,COL4
18000 FORMAT(1H ,71H  3.27  (1/R(3)-1/R(1)) RHECSTAT NCN-LINEARITY
     1                     ,F7.2,F8.4,F8.2,F8.4)
      GC TO 1835C
31072 CCL1=RERP(29)
      COL1 = ABSF(CCL1)
      COL2=RETHP(29)
      CCL2 = ABSF(CCL2)
      CCL3=RERPP(29)
      CCL3 = ABSF(COL3)
      COL4=RETHPP(29)
      CCL4 = ABSF(COL4)
      WRITE OUTPUT TAPE 6,181CO,CCL1,CCL2,CCL3,COL4
18100 FORMAT(1H ,71H  3.28  (1/R(2)-1/R(1)) RHECSTAT NCN-LINEARITY
     1                     ,F7.2,F8.4,F8.2,F8.4)
      GC TO 1835C
31074 CCL1=RERP(1 )
      CCL1 = ABSF(CCL1)
      COL2=RETHP(1)
      CCL2 = ABSF(CCL2)
      CCL3=RERPP(1 )
      COL3 = ABSF(COL3)
      COL4=RETHPP(1)
      CCL4 = ABSF(CCL4)
      WRITE OUTPUT TAPE 6,1820C,CCL1,CCL2,COL3,COL4
18200 FORMAT(1H ,71H  3.29  BRIDGE TRIMMING ERRCR
     1                     ,F7.2,F8.4,F8.2,F8.4)
      WRITE CUTPUT TAPE 6,183CO
1830C FORMAT(1H ,31H  3.30  GALVANCMETER BIAS ERROR,44X3HNIL,5X3HNIL,
     15X3HNIL,5X3HNIL)
1835C RSS(1)=COL1**2+RSS(1)
      RSS(2)=COL2**2+RSS(2)
      RSS(3)=COL3**2+RSS(3)
18352 RSS(4)=COL4**2+RSS(4)
      CCL1 = SQRTF(RSS(1))
      CCL2 = SQRTF(RSS(2))
      CCL3 = SQRTF(RSS(3))
```

```
      CCL4 = SQRTF(RSS(4))
      CCL5 = SQRTF(COL1**2+CCL3**2)
      CCL6 = SQRTF(COL2**2+CCL4**2)
      WRITE OUTPUT TAPE 6,184CC,CCL1,CCL2,CCL3,COL4,COL5,COL6
1840C FCRMAT(1HC,71H          RSS
     1                     F7.2,F8.4,F8.2,F8.4,F8.2,F8.4)
      CCL3 = ABSF(ERPPPP)
      CCL4 = ABSF(ETPPPP)
      CCL5=COL3
      COL6=COL4
      WRITE OUTPUT TAPE 6,1850C,COL3,CCL4,CCL5,CCL6
18500 FCRMAT(1HC,71H4.     ERRCRS DUE TC PARABCLIC ASSUMPTICN CF CORRECT
     1IVE MANEUVER    *    ,15H NCT APPLICABLE,F8.2,F8.4,F8.2,F8.4)
      COL1=SQRTF(RSS(1)   +SAVE1**2+ERPPP**2)
      CCL2=SQRTF(RSS(2)   +SAVE2**2+ETHPPP**2)
      CCL3=SQRTF(RSS(3)   +SAVE3**2+ERPPP**2+ERPPPP**2)
      CCL4=SQRTF(RSS(4)   +SAVE4**2+ETHPPP**2+ETPPPP**2)
      CCL5 = SQRTF(CCL1**2+CCL3**2)
      CCL6 = SQRTF(CCL2**2+CCL4**2)
      WRITE OUTPUT TAPE 6,186CC,CCL1,CCL2,CCL3,CCL4,CCL5,CCL6
1860C FCRMAT(1HC,71H       TCTAL RSS ERRCRS
     1                     ,F7.2,F8.4,F8.2,F8.4,F8.2,F8.4)
      WRITE CUTPUT TAPE 6,187CC
1870C FCRMAT(1HC,94HNCTE 1. SCURCE ERRCRS UTILIZEC ARE 1 SIGMA VALUES BA
     1SED ON MAXIMUM VALUES LISTEC IN FIGURE NC.  )
      WRITE OUTPUT TAPE 6,189CC,ICRUN
1890C FCRMAT(1HC,29X39HMANUAL SPACE CCMPUTER ERRCR ANALYSIS * ,4A6)
      WRITE OUTPUT TAPE 6,19CCC
19CCC FCRMAT(1H ,51X1CHFIGURE NC.)
 1999 NORUN=NCRUN-1
      IF (SENSE SWITCH 4) 26CC2,24999
24999 PRINT 25CCC
25CCC FCRMAT(1H1,69HCPERATCR ACTICN PAUSE *** RESET SENSE SWITCHES 5 ANC
     1 6 ANC PUSH START)
      PRINT 26CCC,ICRUN
26CCC FCRMAT(1HC,5CHEND CF ARMA MANUAL SPACE CCMPUTER ERRCR ANALYSIS  ,4
     1A6)
      PAUSE
26CC2 IF (NCRUN) 16C,16C,1CCC
  16C PRINT 27CCC
27CCC FCRMAT (1H ,15HEND CF ARMA JCB///)
      CALL EXIT
      END(1,1,0,C,1,C,1,1,0,C,C,C,0,0,0)
```